

EVOLUTION OF LARGER BENTHIC FORAMINIFERA  
DURING THE PALEOCENE-EARLY EOCENE INTERVAL  
IN THE EAST TETHYS (INDUS BASIN, PAKISTAN)

Thesis submitted for the degree of

Doctor of Philosophy

at the University of Leicester

by

Jawad Afzal BSc (Hon), MSc (Peshawar)

Department of Geology

University of Leicester

September 2010

## **EVOLUTION OF LARGER BENTHIC FORAMINIFERA DURING THE PALEOCENE-EARLY EOCENE INTERVAL IN THE EAST TETHYS (INDUS BASIN, PAKISTAN)**

Jawad Afzal

### **Abstract**

Paleocene-Eocene stratigraphy of the Indus Basin is revised and a modern stratigraphic nomenclature is presented. Forty-five species of larger benthic foraminifera (LBF) are described from newly collected sections. Eight Tethyan foraminiferal biozones (SBZ1-SBZ8) and a stable carbon isotopic stratigraphy spanning the Paleocene to Early Eocene interval are established. The evolution of shallow marine communities (especially LBFs) in the east and comparison with west Tethys is discussed. In contrast to coralg-dominated west Tethys (particularly during the SBZ3 Biozone), the Late Paleocene carbonate biotas in the Indus Basin were dominated by LBFs, and corals are scarce. This difference is interpreted here as a product of local palaeoecological conditions and/or the Tethyan latitudinal temperature gradient. The responses of the shallow marine biota and ecosystem to earliest Eocene environmental changes in the east Tethys were remarkably different from those of west Tethys. The larger foraminifer turnover and rapid radiation of typical Eocene LBFs (e.g. *Alveolina*, *Nummulites*, *Orbitolites*) during this time were not observed in the east Tethys. During the earliest Eocene, inner ramp environments of the Indus Basin were still characterized by typical Late Paleocene LBF assemblages (mainly miscellanids, ranikothalids). Mid ramp settings were occupied by nutrient-tolerant heterotroph-dominated communities (mainly encrusting foraminifera) with very rare or no LBFs. These biotic differences were possibly created by the superimposition of initial India-Asia collision on PETM related stresses at the P-E boundary, generating biogeographical barriers and severe environmental conditions (increased continental run off, elevated temperatures) in the east. High sea temperatures (32°C to 33.5°C) and increased productivity/nutrient levels compared to the west Tethys are suggested by  $\delta^{18}\text{O}$  and  $\delta^{13}\text{C}$  isotope data from well-preserved carbonates. Later, in the Early Eocene (SBZ7-SBZ8 biozones), oligotrophic LBFs (nummulitids, orthopragminids) started to dominate ramp environments, indicating stable environmental conditions.

## Acknowledgements

First, I would like to express my gratitude to my supervisors, Dr. Mark Williams and Prof. Richard J. Aldridge for their expertise, understanding, patience and for allowing me the freedom to pursue my interests during my PhD studies. And to Asih, Mark's wife for helping me to adapt to life in England.

Many thanks also to my thesis chair Prof. David Siveter for his encouragement and scientific discussion.

I am grateful for the financial support of the National Centre of Excellence in Geology (NCEG), University of Peshawar, Pakistan for these studies. The Department of Geology, University of Leicester, UK and the British Geological Survey (BGS) palaeoclimates programme are thanked for their additional financial and laboratory support.

Professor M. Asif Khan and Dr. Mohammad Sayab (NCEG) are thanked for organizational support given during the entire course of these studies. I thank Prof. M. Tahir Shah, Prof. Irshad Ahmad, Dr Fazl Rabbi Khan, Liaqat Ali, Seema Anjum, Sohail Wahid and Syed Muntazir Abbas of the NCEG for their motivation and encouragement. Thanks also to other people in the NCEG for their help with field logistics and laboratory work: M. Saeed, Asif Majeed, Malka Saimeen Ozair, Riaz Ahmad Durrani, Farhidoon Sahar, Tasbeehullah, Naseer Khan, Hamid Gul, Bilal, Mir Alam, Barkat Ali, Ayub Masih, Javed Masih, Akhtar Ali, Razaq Hazara, Mohammad Younas, Abdul Qayyum Khan, Muhammad Khan, Mushtaq Ali Shah, Gul Muhammad, M. Fayaz and M. Tariq.

I am grateful to Dr. Abdul Salam, Aimal Khan Kasi and Ali Ahmad of the Centre of Excellence in Mineralogy and Dr. Akhtar M. Kassi and Mohibullah Mohibullah of the Geology Department, University of Balochistan, Pakistan for facilitating field studies in the Quetta region. Yousaf Haroon and M. Ashraf Khan of the GSP, Peshawar, for their assistance in fieldwork in the Kohat area and Hamid Afridi, Khan Zeb Jadoon (University of Peshawar) and Ishtiaq Noor (Hydrocarbon Development Institute of Pakistan, Islamabad) are thanked for providing literature.

Appreciation also goes out to all academic, clerical and technical staff members of the Department of Geology, University of Leicester for their assistance throughout my PhD program.

Dr. Ian Wilkinson and Dr. Michael H. Stephenson at the BGS are thanked for providing access to the BGS petrographic microscopy facilities and motivational discussion on my research work.

I am thankful to Prof. Melanie J. Leng (NERC Isotope Geosciences Laboratory, BGS, Keyworth, Nottingham) for her help with isotope analysis and technical discussion, which greatly improved my understanding of isotope geochemistry.

Dr. Giles Miller and Mr. Clive Jones of the Natural History Museum, London are thanked for providing access to foraminifer collection at the museum and useful literature.

I wish to thank Professor Robert Speijer (Katholieke University, Leuven, Belgium), Dr Matthew Wakefield (BG Group), Dr. Christian Scheibner (Bremen University) and Dr.

Willem Renema (Nationaal Natuurhistorisch Museum Naturalis, Netherlands) for constructive reviews of the papers that form the basis of chapters 2 and 3 in this thesis.

I must also acknowledge Dr. Paul Bown (University College London) and Dr. Appy Sluijs and Prof. Henk Brinkhuis (Utrecht University, Netherlands) who kindly processed my samples for dinoflagellate and calcareous nannofossils.

Prof. Aftab Ahmad Butt (Punjab University, Pakistan) is thanked for his discussion on larger foraminifera of the Indus Basin.

Antonino Briguglio (University of Vienna) and Dr. Massimo Di Carlo (Rome University) are thanked for providing literature and discussion on Paleogene larger foraminifera.

Prof. Lukas Hottinger (Museum of Natural History, Basel) is acknowledged for his advice on preparing larger foraminifera slides and identification.

I would like to thank other PhD students I have worked with in Leicester, who always encouraged and guided me in many ways whenever I needed: Dr. David Baines, Sam Cheyney, Dr. Peter Fitch, Dr. Pablo Dávila, Dr. Simon Jowitt, Stephen Grebby, Alex Lemon, David Riley, Dr. Nick Roberts, Dr. Steve Rippington, Dr. Andrew Shore, Alison Tasker, Chris Willcox, Dr. Joanne Tudge, Irfan Jan, Laurent Darras, Sam Matthews, Nina Jordan and Rebecca Williams.

For the continuous encouragement and discussion on my research work, I would like to say a big thank you to the people in the Palaeobiology Research Group, especially Dinah Smith, Dr. Xiaoya Ma, Dr. Carys Bennett, Mohibullah Mohibullah and Dr. Jan Zalasiewicz.

Special thanks go to my friends, who always believed in me and encouraged me to pursue a PhD: Nauman Zahid, Joanne Whelan, Irshad Ahmad, Muhammad Shahid (late), M. Imtiaz, Inayatullah, Sanaullah Khan, Zahid Iqbal, Amjid Ali, Malik Zia-u-Deen, Qasim Kakar, Azhar Israr and Nadir Sher.

Finally, a very special thank to my family for their never-ending support through my entire life. In particular to my father Said Afzal and my brother Sheher Yar, who even though they have no clue of what I am doing in my PhD, always encouraged discussion about my research and listen to me very carefully and have tried their best to understand.

**Contents**

Title	Page
<b>ABSTRACT</b>	i
<b>ACKNOWLEDGEMENTS</b>	ii
<b>CHAPTER 1: INTRODUCTION</b>	1
<b>Introduction</b>	2
<b>The Indus Basin of Pakistan</b>	5
<b>Materials and methods</b>	8
1) Palaeontological methods	8
2) Sedimentological methods	8
3) Geochemical methods	10
<b>Chapter summary</b>	10
Chapter 2	10
Chapter 3	11
Chapter 4	11
Chapter 5	11
Chapter 6	11
Chapter 7	12
<b>CHAPTER 2: REVISED STRATIGRAPHY OF THE LOWER CENOZOIC SUCCESSION OF THE GREATER INDUS BASIN IN PAKISTAN</b>	13
<b>Abstract</b>	14
<b>Introduction</b>	14
<b>Geological setting</b>	16
<b>Stratigraphy of the Greater Indus Basin in Pakistan</b>	18
<b>The Upper Indus Basin</b>	20
Sub-basins: Kohat area, Kala Chitta Range, Hazara Range, Salt Range, Surghar Range	20
<b>The Lower Indus Basin</b>	30
The Sulaiman Range and Kirthar Range	30
<b>Regional stratigraphical context</b>	34
<b>Conclusions</b>	41
<b>CHAPTER 3: PALEOCENE-EARLY EOCENE LARGER BENTHIC FORAMINIFERA OF THE INDUS BASIN, PAKISTAN: SYSTEMATIC PALAEOLOGY</b>	43
<b>Introduction</b>	44
<b>Stratigraphic setting</b>	47
<b>Studied sections</b>	49
Upper Indus Basin	51
Lower Indus Basin	51
<b>Systematic palaeontology</b>	55

Suborder ROTALIINA Loeblich & Tappan, 1987	55
Suborder MILIOLINA Delage & Herouard, 1896	98
Suborder TEXTULARIINA Delage & Herouard, 1896	111
<b>Larger foraminifera plates</b>	121
Plate 1 <i>Lockhartia, Sakesaria</i>	122
Plate 2 <i>Laffitteina, Kathina, Rotalia</i>	124
Plate 3 <i>Setia, Orbitosiphon, Daviesina</i>	126
Plate 4 <i>Miscellanea</i>	128
Plate 5 <i>Ranikothalia, Operculina</i>	130
Plate 6 <i>Assilina</i>	132
Plate 7 <i>Nummulites</i>	134
Plate 8 <i>Discocyclina</i>	136
Plate 9 <i>Discocyclina, Orbitoclypeus, Actinocyclina</i>	138
Plate 10 <i>Spiroloculina, Quinqueloculina, Triloculina, Idalina</i>	140
Plate 11 <i>Glomalveolina</i>	142
Plate 12 <i>Alveolina</i>	144
Plate 13 <i>Somalina, Opertorbitolites, Saudia, Keramosphaera</i>	146
Plate 14 <i>Fallotella, Karsella, Dictyoconus</i>	148
Plate 15 <i>Coskinon, Vania</i>	150
<b>CHAPTER 4: EVOLUTION OF PALEOCENE TO EARLY EOCENE LARGER BENTHIC FORAMINIFER ASSEMBLAGES OF THE INDUS BASIN, PAKISTAN</b>	152
<b>Abstract</b>	153
<b>Introduction</b>	154
<b>Geological setting</b>	157
<b>Stratigraphy</b>	158
<b>Materials, methods and studied sections</b>	159
Materials and methods	159
Studied sections in the Upper Indus Basin	161
Studied sections in the Lower Indus Basin	163
<b>Stable isotope stratigraphy</b>	165
<b>Larger benthic foraminifera (LBF) biostratigraphy</b>	168
<b>Comparison of LBF ranges with those in other regions of Tethys</b>	170
Paleocene LBFs	171
Early Eocene LBFs	176
<b>Evolution of Early Palaeogene LBFs in the east Tethys Ocean</b>	178
<b>LBFs and India-Asia Collision at the P-E boundary</b>	183
<b>Response of LBF assemblages to the PETM in east Tethys</b>	185
<b>Conclusions</b>	189
<b>CHAPTER 5: PALAEOENVIRONMENTAL EVOLUTION OF EAST TETHYS SHALLOW MARINE BENTHIC COMMUNITIES DURING LATE PALEOCENE - EARLY EOCENE CLIMATE AND OCEANOGRAPHIC CHANGE</b>	190
<b>Abstract</b>	191
<b>Introduction</b>	192
<b>Geological and stratigraphical setting</b>	195

<b>Materials and Methods</b>	195
<b>Microfacies and depositional environments</b>	196
Late Paleocene microfacies	197
Early Eocene microfacies	203
<b>Facies changes, biotic changes and palaeoenvironmental evolution</b>	209
Late Paleocene	209
Early Eocene	214
<b>Discussion</b>	219
Comparison of the shallow marine benthic biota of the Indus Basin with other Tethyan carbonate successions	219
Environmental changes and evolution of carbonate factories in the Indus Basin	221
Biotic and environmental changes through the Late Paleocene-Early Eocene	225
<b>Conclusions</b>	231
 <b>CHAPTER 6: STABLE ISOTOPE (<math>\delta^{18}\text{O}</math> AND <math>\delta^{13}\text{C}</math>) ANALYSIS OF LATEST PALEOCENE-EARLY EOCENE CARBONATES, INDUS BASIN, PAKISTAN</b>	233
 <b>Abstract</b>	234
<b>Introduction</b>	234
<b>Materials and methods</b>	236
<b>Microfacies</b>	237
<b>Petrographic assessment of the limestones</b>	237
Well preserved carbonates	237
Marine phreatic diagenesis	239
Meteoric diagenesis	239
Burial diagenesis	241
<b>Stable isotope results</b>	243
<b>Discussion</b>	244
Diagenetic overprint and isotopic interpretation	244
Palaeoenvironmental interpretation	247
<b>Conclusions</b>	252
 <b>CHAPTER 7: CONCLUSIONS</b>	255
 <b>APPENDICES</b>	261
 <b>Appendix 1</b> Samples data of the Kotal Pass section	262
<b>Appendix 2</b> Samples data of the Shakardara Well-1	262
<b>Appendix 3</b> Samples data of the Zranda section	262
<b>Appendix 4</b> Samples data of the Muree Brewery section	262
<b>Appendix 5</b> Samples data of the Hanna Lake section	262
<b>Appendix 6</b> Detailed microfacies description	262
<b>Appendix 7</b> Research paper published in the Journal of Micropaleontology	262
<b>Appendix 8</b> Research paper in press for Lethaia	262
<b>Appendix 9</b> British Geological Survey repository numbers	263

---

## Contents

---

<b>NOTE</b>	266
<b>REFERENCES</b>	267

---

---

# Chapter 1

---

## Introduction

---

## Chapter 1: Introduction

### Introduction

The early Palaeogene climate was marked by long-term global warming, beginning in the late Paleocene (Selandian, ~59 Ma) and terminating in the early Eocene (Ypresian, ~51 Ma) (Zachos *et al.* 2001). This overall trend was punctuated by the short-term climatic perturbation of the Paleocene-Eocene Thermal Maximum (PETM) at the Paleocene-Eocene (P-E) boundary and this had a significant impact on marine and terrestrial biota (Zachos *et al.* 2003). The PETM was associated with an abrupt negative carbon isotope excursion of ca  $-2.5$  to  $-4\%$  (CIE, Zachos *et al.* 2001, 2007), that most likely resulted from rapid dissociation of methane at the sea floor (Dickens *et al.* 1999; Bains *et al.* 2000). During the PETM, sea surface temperatures increased by  $5^{\circ}\text{C}$  in the tropics and by up to  $8^{\circ}\text{C}$  at higher latitudes. Open marine planktonic and benthic foraminifera, dinoflagellates and calcareous nannofossils display extinctions and diversifications through the P-E boundary (e.g., Pak & Miller 1992; Thomas 2007; Gibbs *et al.* 2006; Petrizzo 2007). The well-known benthic foraminifer extinction event (BEE; Pak & Miller 1992), resulted in the extinction of approximately 40% of all smaller benthic foraminifera in the deep sea. On land, major changes in floral communities and terrestrial vertebrates occurred in response to increased temperature and atmospheric  $\text{CO}_2$  (Harrington & Jaramillo 2007).

Shallow-sea larger benthic foraminifera (LBF) were common inhabitants of Paleocene-Early Eocene carbonate environments. However, only recently has the impact of the PETM on shallow marine biota been studied and a link between the PETM climatic perturbation and biotic events in carbonate environments suggested (e.g. Orue-Etxebarria *et al.* 2001; Scheibner *et al.* 2005; Scheibner & Speijer 2008a, 2008b;

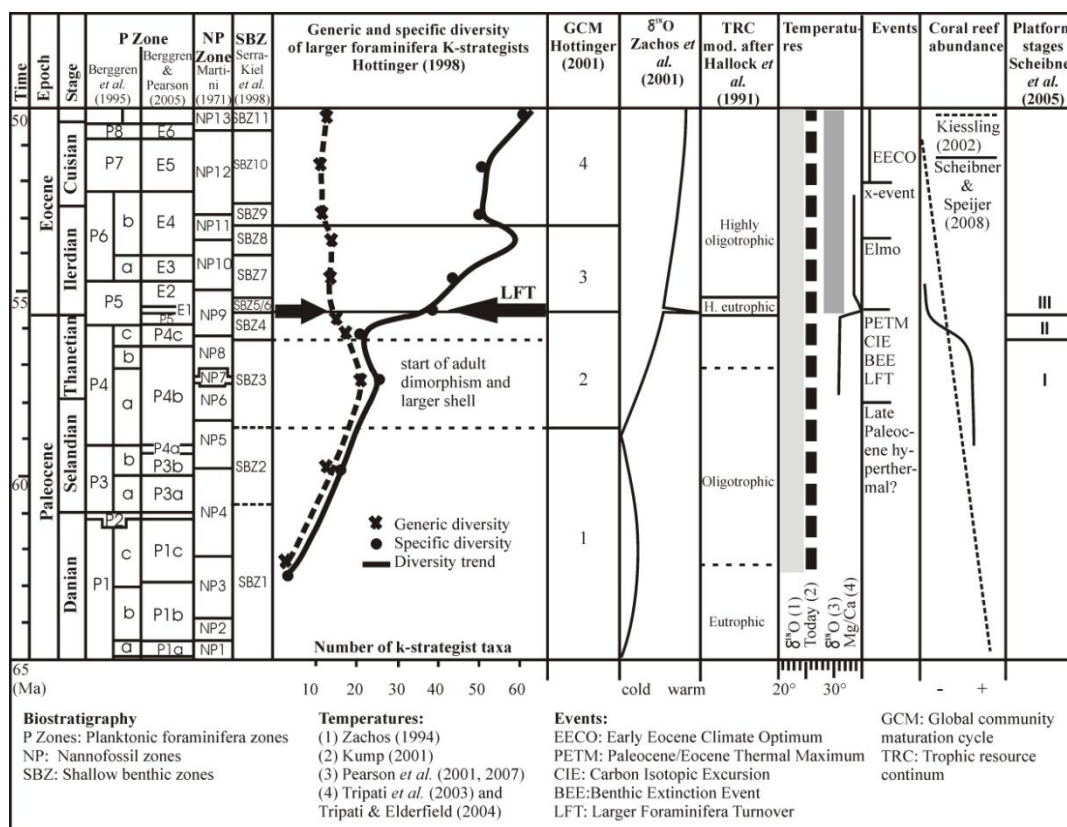


**Figure 1.** The Tethyan Paleocene to Early Eocene biostratigraphy, and comparison of trends in evolution of larger benthic foraminifera,  $\delta^{18}\text{O}$  isotopes, coral reef abundance, and trophic resource continuum (TRC: level of nutrients in ocean water) (after Scheibner & Speijer 2008a).

Pujalte *et al.* 2009b) (Fig. 1). Orue-Etxebarria *et al.* (2001) examined the P-E boundary succession in the Pyrenees (northern Tethys) and concluded that the impact of the PETM on the evolution of benthic faunas in shallow-water environments may have been greater than previously thought, but did not explain any possible causes for this relationship. Recently, Scheibner *et al.* (2005) and Scheibner & Speijer (2008a, 2008b, 2009) studied P-E sections in the western Tethys (Egypt). They suggested an interplay between rising temperatures and changes in the trophic resource regime and their effects on biota (especially corals and LBF), and long-term evolutionary changes in larger foraminifera were the main causes for the changes in shallow-water ecosystems (Fig.1).

The PETM climatic perturbation on shallow marine biota is well known from west Tethys, whereas data from east Tethys are scant or obscure. Therefore, detailed

analysis of Late Paleocene-Early Eocene shallow marine carbonates and biota from east Tethys is vital for understanding the severity and extent of the PETM.

The marine early Tertiary carbonate successions of the Indus Basin of Pakistan formed on the northwestern shelf margin of the Indian Plate in east Tethys, and have been studied since the 19<sup>th</sup> century (see Afzal *et al.* 2009, and Afzal *et al.* in press for references). These studies have, however, led to a highly variable application of stratigraphical names and conflicting stratigraphical and sedimentological interpretations (see Afzal *et al.* 2009, in press for a summary of problems). Moreover, the precise biostratigraphic position of the P-E boundary and the regional and global significance of shallow marine carbonates and their associated biota (especially larger foraminifera) from the Indus Basin of Pakistan through the P-E boundary was, prior to the present study, poorly known.

In order to address the above-mentioned problems, I have studied 5 outcrop sections and cores from a petroleum well from the Indus Basin of Pakistan (Figs 2, 3A-B). In this thesis I aim to: 1) review published and unpublished lithostratigraphical and biostratigraphical information on the Paleocene-Eocene of the Indus Basin in order to provide a modern stratigraphical nomenclature; 2) thoroughly appraise the systematic palaeontology of the Paleocene-Early Eocene LBFs; 3) establish a LBF biostratigraphic scheme together with a Carbon isotopic stratigraphy for the Paleocene-Early Eocene carbonate succession and discuss the evolution of LBFs in the Tethyan bioprovinces (east and west) and the roles of the India-Asia collision and the PETM on the evolutionary patterns of these foraminifera; 4) establish microfacies and describe palaeoecological assemblages (LBFs, algae and other biocomponents) from the Late Paleocene-Early Eocene in order to reconstruct palaeoenvironments and utilize these to examine the effects of the early Paleogene environmental changes (e.g. early Paleogene long-term and short-term PETM warming) and India-Asia collision on these shallow

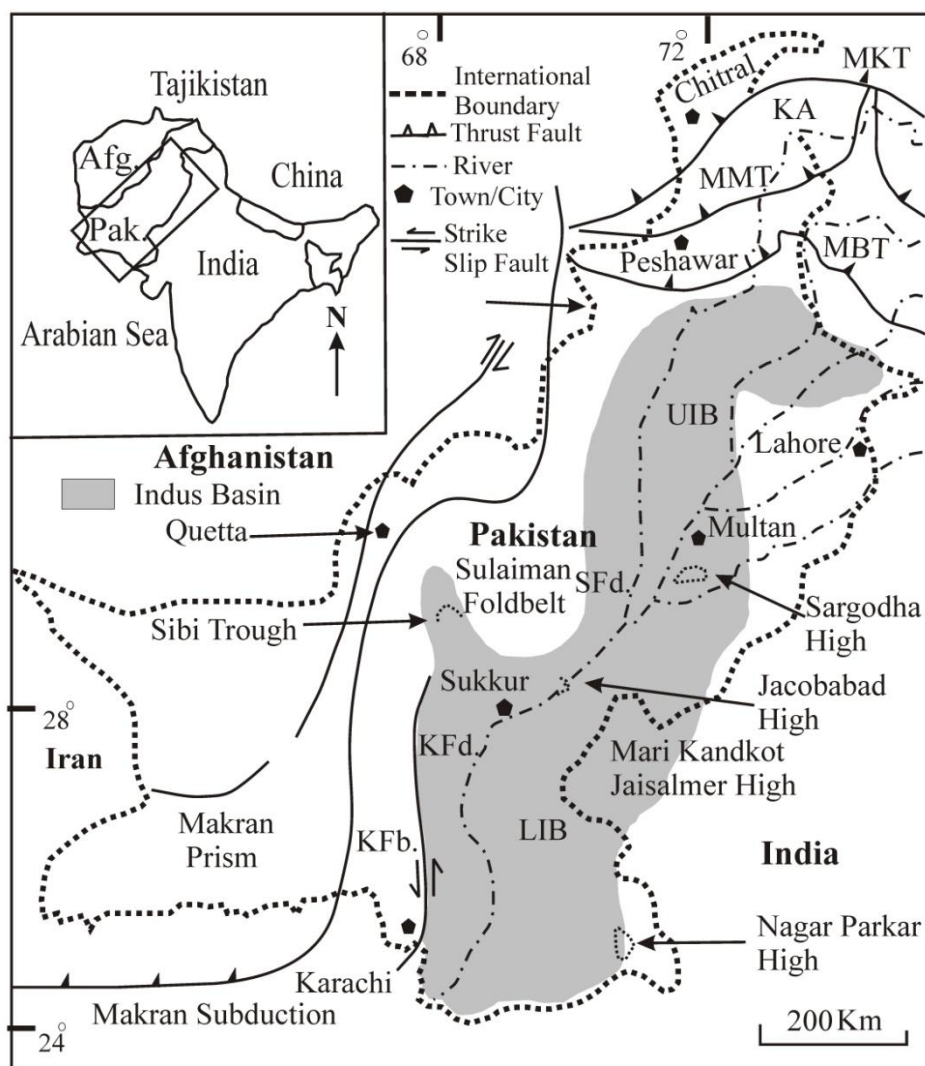


**Figure 2.** Map of Pakistan, showing position of the Greater Indus Basin and major tectonic units (modified after Wakefield & Monteil 2002). MKT, Main Kohistan Thrust; MMT, Main Mantle Thrust; MBT, Main Boundary Thrust; KFb., Kirthar Foldbelt; KFd., Kirthar Foredeep; SFd., Sulaiman Foredeep; KA, Kohistan Arc; UIB, Upper Indus Basin; LIB, Lower Indus Basin.

marine ecosystems and biota in the east Tethys; and finally 5) generate and examine stable carbon and oxygen isotope data from the latest Paleocene-Early Eocene carbonate microfacies in order to evaluate the impact of diagenetic alteration on isotopic variability and to reconstruct paleoenvironmental conditions where materials preserve a primary geochemical signal.

### The Indus Basin of Pakistan

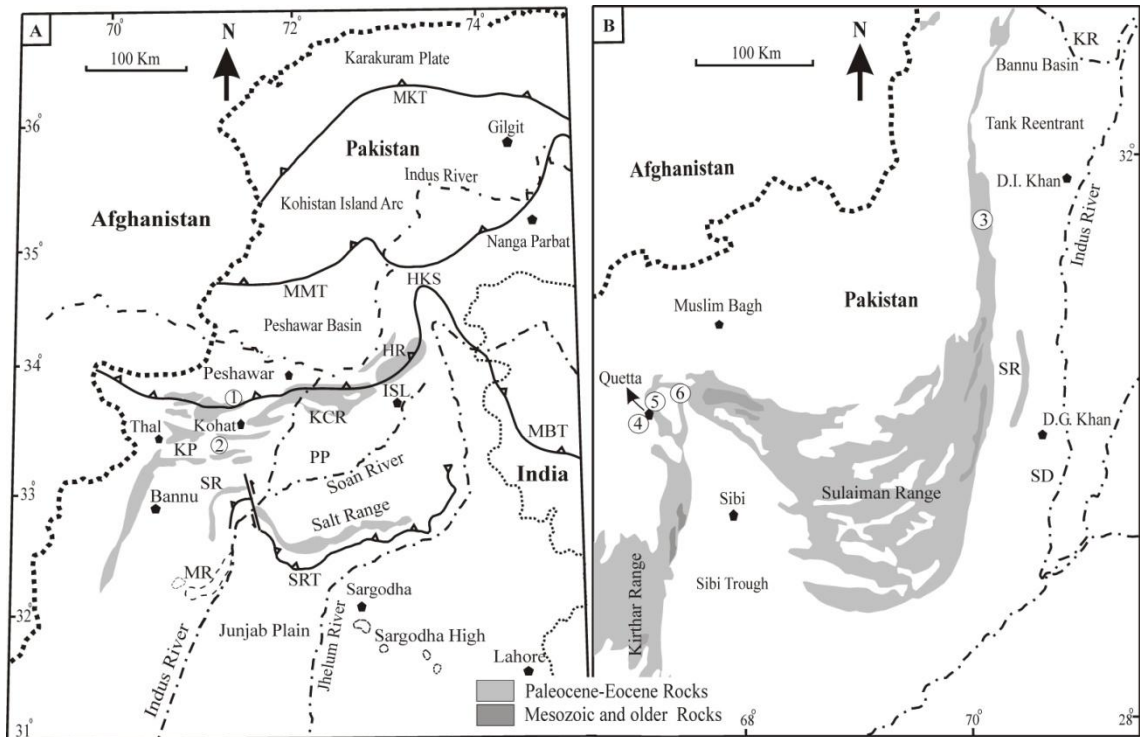


**Figure 3.** (A) Map of the Upper Indus Basin showing distribution of Paleocene-Eocene sedimentary rocks and studied stratigraphical sections (modified after Köthe *et al.* 1988). KP, Kohat Plateau; PP, Potwar Plateau; KCR, Kala Chitta Range; HR, Hazara Range; SR, Surghar Range; SRT, Salt Range Thrust; MR, Marwat Range; HKS, Hazara-Kashmir Syntaxis; ISL, Islamabad; 1, Kotal Pass section; 2, Shakardara Well-1. (B) Map of part of the Lower Indus Basin showing distribution of Paleocene-Eocene sedimentary rocks and studied stratigraphical sections (modified after Köthe *et al.* 1988). KR, Kurram River; SD, Sulaiman Depression; SR, Sulaiman Range; 3, Mughal Kot-Toi section; 4, Muree Brewery section; 5, Hanna Lake section; 6, Zranda section.

The lower Cenozoic succession of the Indus Basin was deposited on the northwestern continental shelf margin of the Indian Plate, in the east Tethys Ocean. The Indus Basin covers an area of about 873,000 km<sup>2</sup>, extending over most of eastern Pakistan and the westernmost parts of India (Fig. 2, in Afzal *et al.* 2009). The Indus Basin in Pakistan is traditionally divided into Lower and Upper basins, and consists of several sub-basins, ranges, plateaus and provinces (Figs 2-3). The lower Cenozoic succession of these basins is varied in lithology and thickness, but mainly consists of marine limestone and shale with subordinate sandstone and non-marine red beds, gypsum, anhydrite, salt and coal (Afzal *et al.* 2009).

The rock succession of the Upper Indus Basin is exposed at the surface along east-west trending fold and thrust belts of the Kohat, Hazara, Banu and Wazirestan areas and the Kala Chitta, Surghar and Salt ranges which form the northernmost element of the Indus Basin in Pakistan (Fig. 3A). The Upper Indus Basin is mainly represented by marine limestone and shale with subordinate sandstone and non-marine red beds, gypsum, anhydrite, salt and coal (Afzal *et al.* 2009). Material from the Upper Indus Basin is sourced from the Late Paleocene Lockhart Formation in the Kotal Pass section of the Kohat Hill Range and from the cores of Shakardara Well-1 in the Kohat Plateau (Afzal *et al.* in press, Fig. 3A).

The Sargodha High separates the Lower and Upper Indus basins, with the Lower Basin south of the Sargodha High (Fig. 3A). The lower Cenozoic rock succession of the Lower Indus Basin is exposed in the Sulaiman and Kirthar ranges (Fig. 3B), and consists dominantly of marine limestone and shale with minor non-marine sandstone, gypsum and coal (Afzal *et al.* 2009). The Paleocene-Early Eocene Dungan Formation has been collected from the following four outcrop sections in the Sulaiman Range (Fig. 3B): 1) Mughal Kot section in the north-eastern Sulaiman Range; 2) Zranda section in the Kach-Ziarat area of the western Sulaiman Range; and 3) and 4) Muree Brewery and Hanna Lake sections in the Quetta district of the westernmost Sulaiman Range. The Dungan Formation in these sections is composed of highly fossiliferous limestone.

The Paleocene-Early Eocene sedimentary succession of the Indus Basin was greatly influenced by India-Asia collisional tectonics (Afzal *et al.* 2009). The estimates of the timing of the initial collision vary from 65 Ma to 45 Ma (Beck *et al.* 1995; Rowley 1996; Hodges 2000; Afzal *et al.* 2009; Copley *et al.* 2010). However, a hiatus equivalent to planktonic foraminiferal biozones upper P5 to P7 in the Indus Basin has been related to the subduction and orogenic processes of the initial India-Asia collision at the P-E boundary (see Afzal *et al.* 2009). India-Asia tectonics interrupted carbonate

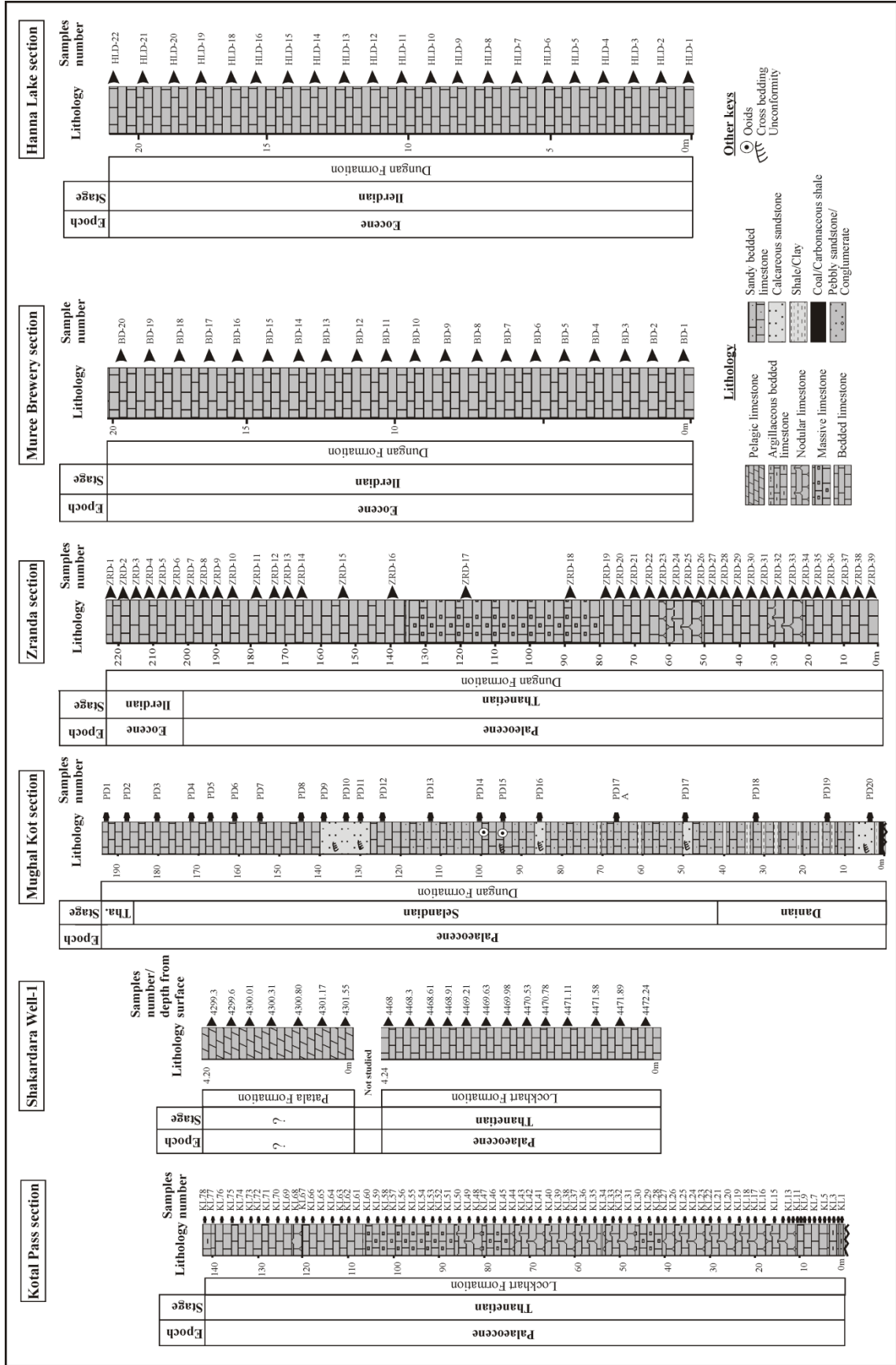
sedimentation through the P-E boundary in most of the Upper Indus Basin (see Afzal *et al.* 2009 for summary). However, the Dungan Formation in the Muree Brewery, Hanna Lake and Zranda sections provides a continuous record of shallow-marine carbonates through the Late Paleocene-Early Eocene.

### **Materials and methods**

A total of 200 limestone samples were collected from five outcrop sections and a petroleum well including, 78 samples from the Late Paleocene Lockhart Formation in the Kotal Pass section and 20 core samples from the Shakardara Well-1 in the Upper Indus Basin (Figs 3A, 4). In the Lower Indus Basin, all samples were collected from the Paleocene-Early Eocene Dungan Formation including, 21 samples from the Mughal Kot section, 39 samples from the Zranda section, 20 samples from the Muree Brewery section and 22 from the Hanna Lake section (Figs 3B, 4). The following methods were employed for palaeontological, sedimentological and geochemical analysis:

*1) Palaeontological methods:* The highly indurated carbonate rocks prohibit extraction of individual specimens, therefore I have prepared random and oriented thin sections for the identification of LBFs. Anatomical and morphological terms follow those used by Hottinger (1960, 2006, 2009) and Sirel (1997a, 1997b) and the classification proposed by Loeblich & Tappan (1988) was followed for the identification of LBF genera and species. The style of the Palaeontographical Society of London has been adopted for the systematic description of LBFs. Photographs of identified LBFs were taken in plane-polarized light with a digital camera on a Nikon petrographic microscope and scanning electron microscope (SEM) in the Department of Geology, University of Leicester.

*2) Sedimentological methods:* I have prepared standard limestone thin sections (2.5cm × 5cm and 2.5cm × 7cm) for carbonate microfacies analysis and for the study of palaeoecological assemblages, complimented by limestone slab and field data



**Figures 4.** Studied Paleocene-Early Eocene stratigraphic sections in the Indus Basin of Pakistan. For location of sections see Figure 3A-B. All samples of the present study are deposited in the British Geological Survey (BGS), Keyworth, Nottingham, England. For BGS repository numbers see Appendix 9.

(sedimentary structures, fossils and stratigraphic relationships). For the microfacies analysis the methods of Wilson (1975) and Flügel (1982, 2004) were followed, such as visual examination and quantitative-semi-quantitative analysis of lithology, grain types (biogenic or abiogenic), textures, fossil assemblages and bioclasts in thin sections.

Palaeoecological assemblages (with emphasis on LBFs and calcareous algae) in studied microfacies are compared with modern counterparts and known facies models (e.g. Hottinger 1983; Reiss & Hottinger 1984; Hallock & Glenn 1986; Hottinger 1997; Langer & Hottinger 2000; Hohenegger & Yordanova 2001).

3) *Geochemical methods:* For stable C and O isotope analysis, a total of 56 limestone samples were selected from the latest Paleocene-Early Eocene part of the Dungan Formation in the Zranda, Muree Brewery and Hanna Lake sections. Analytical procedures are given in Chapter 6.

### **Chapter summary**

*Chapter 2.* Long-standing stratigraphical problems in the Paleocene-Eocene stratigraphy of the Indus Basin are discussed in Chapter 2. The published biostratigraphical data (on dinoflagellate, nannofossil, planktonic foraminiferal and shallow benthonic foraminiferal) for the Greater Indus Basin in Pakistan are collated, reinterpreted (where necessary) and correlated with the early Paleogene global standard chronostratigraphy and biostratigraphy. The lithostratigraphy and physical stratigraphical relationships of the Paleogene succession of the Indus Basin in terms of the relationship between local tectonics (India-Asia collision) and global sea level change are discussed. A revised stratigraphical nomenclature for the Paleocene-Eocene rock units of the Indus Basin is

suggested. These results have been published (Afzal, J., Williams, M. & Aldridge, R.J. 2009). Revised stratigraphy of the lower Cenozoic succession of the Greater Indus Basin in Pakistan. *Journal of Micropalaeontology*, **28**, 7-23). See Appendix 7.

*Chapter 3.* Taxonomy for the Paleocene-Early Eocene LBFs from the newly collected sections is presented in chapter 3. A total of 45 species of LBFs are described and illustrated.

*Chapter 4.* The LBF biostratigraphy and stable carbon isotope stratigraphy for the Paleocene-Early Eocene carbonate successions of the Indus Basin is established. Eight Tethyan foraminiferal biozones (SBZ1-SBZ8) spanning the Paleocene to Early Eocene are identified. Faunal differences between east and west Tethys are discussed. The effects of the PETM and initial India-Asia collision on the evolution of LBFs in the Indus Basin have been evaluated. These results form a research paper in press for *Lethaia* (Afzal, J., Williams, M., Leng, M.J., Aldridge, R.J., Stephenson, M.H. Evolution of Paleocene to Early Eocene larger benthic foraminifer assemblages of the Indus Basin, Pakistan). See Appendix 8.

*Chapter 5.* In this chapter I have focused on palaeoenvironmental evolution of the Late Paleocene-Early Eocene shallow marine benthic communities in the Indus Basin. Both carbonate microfacies and palaeoecological assemblage analyses allowed the reconstruction of depositional models, depths, water energy, nutrients and light levels in carbonate environments. The environmental changes and related evolution of carbonate factories in the Indus Basin are discussed. A pan-Tethyan biotic and facies comparison is presented with discussion on the impact of environmental changes associated with early Paleogene climate change (i.e. long-term early Paleogene warming and the PETM perturbation) and India-Asia tectonics is presented.

*Chapter 6.* Stable carbon and oxygen isotope data through the latest Paleocene-Early Eocene carbonate facies of the Dungan Formation are presented. The diagenetic

alteration in carbonate microfacies and its impact on isotopic variability, and the relationship between the geochemical signal and depositional environments are discussed. Where possible, paleoenvironmental conditions are reconstructed, using the geochemical signal of pristine carbonate facies.

*Chapter 7.* The conclusions from all chapters are presented in this chapter.

With the exception of this chapter (Introduction) and Chapter 7 (Conclusions), each chapter of this thesis is written as a separate research paper and has either been published/in press in peer-reviewed journals (e.g. chapters 2 and 4) or will soon be submitted for publication.

---

## **Chapter 2**

---

Revised stratigraphy of the  
lower Cenozoic succession of  
the Greater Indus Basin in  
Pakistan

---

## **Chapter 2: Revised stratigraphy of the lower Cenozoic succession of the Greater Indus Basin in Pakistan**

### **Abstract**

A refined stratigraphy for the lower Cenozoic succession of the Greater Indus Basin in Pakistan is presented. This region preserves an important East Tethyan marine succession through the Paleocene-Eocene, but its interpretation in terms of regional (tectonic) and global (climatic) effects has been inhibited by poorly constrained stratigraphy. Established dinoflagellate, nannofossil, planktonic foraminiferal and shallow benthonic foraminiferal biostratigraphical data for the Greater Indus Basin in Pakistan are collated, reinterpreted (where necessary) and correlated with the global standard chronostratigraphy and biostratigraphy of the early Paleogene. Inter-regional stratigraphical correlations for the Upper Indus Basin and Lower Indus Basin are resolved. Age diagnostic larger benthonic foraminifera from the Late Paleocene Lockhart Formation are illustrated. These collective biostratigraphical data provide a means of interpreting the lithostratigraphy and physical stratigraphical relationships of the Paleogene succession in terms of the interplay between local tectonics (India-Asia collision) and global sea level change. The timing of the Tethys closure, initial and final contact of the Indian-Asian plates, and dispersal of land mammals on the Indian Plate are discussed and correlated using the stratigraphical record of the basin.

### **Introduction**

The stratigraphy of the fossiliferous lower Cenozoic sediments of the Greater Indus Basin as represented in Pakistan has been a subject of research since the late nineteenth century. The early studies, summarized in Table 1, led to a detailed record of

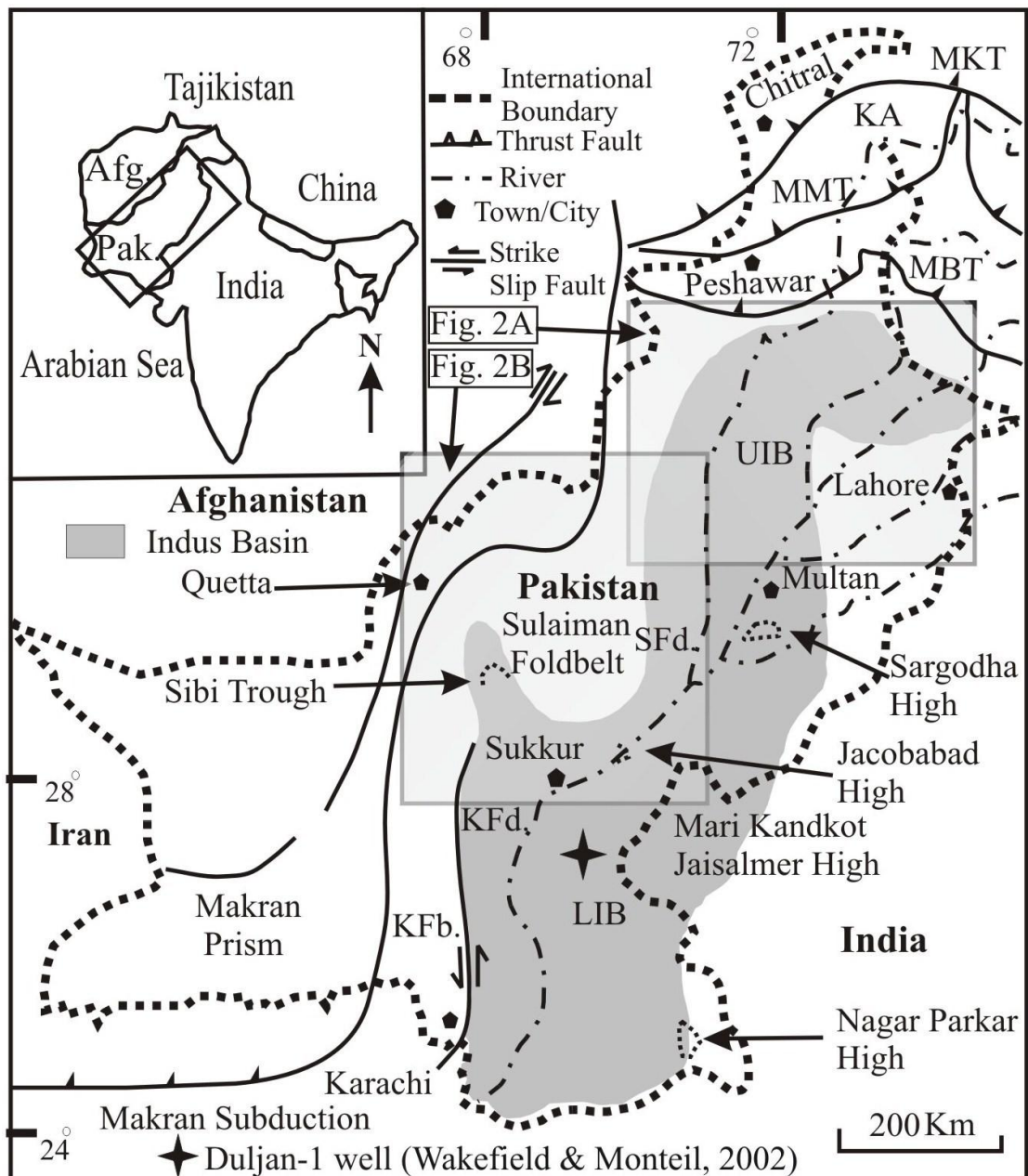


**Figure 1.** Map of Pakistan, showing position of the Greater Indus Basin and major tectonic units (modified after Wakefield & Monteil 2002). MKT, Main Kohistan Thrust; MMT, Main Mantle Thrust; MBT, Main Boundary Thrust; KfB., Kirthar Foldbelt; KFd., Kirthar Foredeep; SFd., Sulaiman Foredeep; KA, Kohistan Arc; UIB, Upper Indus Basin; LIB, Lower Indus Basin.

the lithology, biostratigraphy, and palaeoenvironments that was compiled and published by the Geological Survey of Pakistan (GSP) (Shah 1977). This publication incorporated well illustrated reference sections from parts of the Greater Indus Basin in Pakistan. Recent discoveries of new stratigraphical sections, combined with new published data

and information from extensive petroleum exploration in the region, have provided new insights into the lithostratigraphical and biostratigraphical framework. This wealth of data has, however, led to highly variable application of stratigraphical names and a variety of conflicting stratigraphical interpretations.

The aims of this paper are to: a) review published and unpublished lithostratigraphical and biostratigraphical information throughout the Greater Indus Basin in Pakistan; b) provide a modern stratigraphical nomenclature for the rock units published by the Geological Survey of Pakistan (Shah 1977) in the light of newly available evidence; and c) discuss the palaeogeography and depositional systems of these stratigraphical units in the light of this refined stratigraphical nomenclature.

### **Geological setting**

The lower Cenozoic succession of the Greater Indus Basin represents the northwestern continental shelf margin setting of the Indian Plate (Figs 1, 2). The basin extends over most of eastern Pakistan and the westernmost parts of India, covering an area of about 873,000 km<sup>2</sup> (Wandrey *et al.* 2004) and comprises several sub-basins, plateaus and ranges (e.g. Shah 1977). The sedimentary rock succession was deposited in the eastern part of the Tethyan Ocean. In this chapter I deal with the stratigraphy of the basin as it is represented in Pakistan. The Greater Indus Basin in Pakistan is traditionally divided into two sub-basins referred to as the Upper Indus Basin and the Lower Indus Basin (Figs 1, 2). The Upper Indus Basin, also known as the Kohat-Potwar Range, forms the northernmost element of the Greater Indus Basin in Pakistan and is bounded to the north by the Kala Chitta Range. The Salt Range composite orocline forms the southern limit (Figs 1, 2A), while the Kurram thrust fault marks its western limit. The Pezu wrench fault separates the Upper Indus Basin from the Lower Indus Basin. Lower Cenozoic

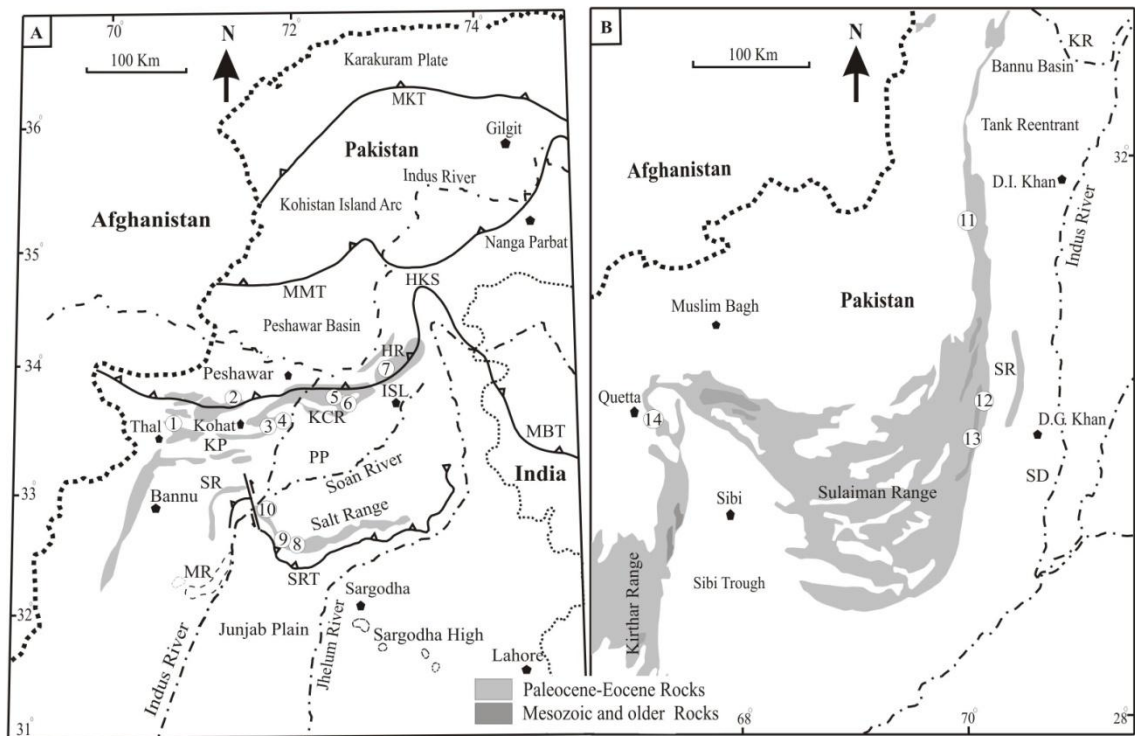


**Figure 2.** (A) Map of the Upper Indus Basin showing distribution of Paleocene-Eocene sedimentary rocks and key stratigraphical sections (modified after Köthe *et al.* 1988). KP, Kohat Plateau; PP, Potwar Plateau; KCR, Kala Chitta Range; HR, Hazara Range; SR, Surghar Range; SRT, Salt Range Thrust; MR, Marwat Range; HKS, Hazara-Kashmir Syntaxis; ISL, Islamabad; 1, North of Hangu section; 2, Kotal Pass section; 3, Tarkhobi section; 4, Panoba section; 5, Burjjanwala Laman; 6, Chak Dalla; 7, Bagnotar-Kuldana; 8, Patala Nala section; 9, Nammal Gorge section; 10, Khairabad section. (B) Map of part of the Lower Indus Basin showing distribution of Paleocene-Eocene sedimentary rocks and key stratigraphical sections (modified after Köthe *et al.* 1988). KR, Kurram River; SD, Sulaiman Depression; SR, Sulaiman Range; 11, Mughal Kot-Toi section; 12, Zinda Pir section; 13, Rakhi Nala section; 14, Muree Brewery section.

sediments of the Upper Indus Basin are exposed at surface along east-west trending fold and thrust belts of the Kohat, Hazara, Banu and Wazirestan areas and the Kala Chitta, Surghar and Salt ranges (Fig. 2A). The Lower Indus Basin is constrained by the Mari-Khandkot-Jaisalmer High to the east, and the Kirthar Fold Belt and Foredeep to the west (Figs 1, 2B), while the Jacobabad High is sometimes used to separate the Lower and Upper basins (e.g. Kemal *et al.* 1992), with the Upper Basin north of the Sargodha High. The tectonic history and stratigraphical framework of the region are strongly influenced by collision of the Indo-Pakistan and Asian plates (Butler 1995; Beck *et al.*

1995; Hodges 2000). Indeed, the lower Cenozoic stratigraphy of the Greater Indus Basin in Pakistan is critical in terms of assessing India-Asia collision, as estimates of the timing of the initial collision vary from 65 Ma to 45 Ma (Searle *et al.* 1987; Dewey *et al.* 1989; Le Pichon *et al.* 1992; Beck *et al.* 1995; Rowley 1996).

The Indo-Pakistan plate in the north and northwestern part of Pakistan was subject to subduction and orogenic processes at about 55 Ma near the Paleocene-Eocene boundary (de Sigoyer *et al.* 2000; Qayyum *et al.* 2001; Khan & Srivastava 2006). A combination of detailed age dating and palaeobathymetric determinations indicates significant basin uplift and erosion at end Cretaceous and end Eocene times, the latter coinciding with the closure of Neo-Tethys (Wakefield & Monteil 2002). During the collision, the existing Late Cretaceous Tethyan sediments accreted onto the eastern margin of the Indo-Pakistan plate and probably spilled over and spread across most of the Indo-Pakistan plate (Khan & Srivastava 2006). The Himalaya mountain chain is a direct result of this continental collision, during which the fold and thrust belts of western and north-western Pakistan were initiated (Le Fort 1996).

### **Stratigraphy of the Greater Indus Basin in Pakistan**

The rocks of lower Cenozoic age in the Greater Indus Basin in Pakistan are remarkably varied in lithology and thickness, but mainly consist of marine limestone and shale with subordinate sandstone and non-marine red beds, gypsum, anhydrite, salt and coal (Shah 1977). Terrestrial emergence at the end of the Paleocene, followed by marine submergence in the Early Eocene (Shah 1977), was succeeded by a short-lived regression at the close of late Early Eocene times, resulting in evaporites being deposited in the Kohat area (Nagappa 1959). Following evaporite formation a marine transgression at the start of the Middle Eocene affected a large area including the

Author	Research undertaken
Blanford 1879	Geology of western Sind
Davies & Pinfold 1937	The Eocene beds of the Salt Range
Davies 1927	The Ranikot beds at Thal
Eames 1952	The geology of standard sections in the western Punjab and in the Kohat District, Pakistan
Fatmi 1974	Lithostratigraphy of the Kohat-Potwar Province, Indus Basin
Haque 1956	Foraminifera of the Ranikot and the Laki of the Salt Range, Pakistan
Hemphill & Kidwai 1973	Stratigraphy of the Bannu and Dera Ismail Khan areas, Pakistan
Hunting Survey Corporation 1961	Geology of part of West Pakistan
Latif 1964	Pelagic foraminifera of the Paleocene-Eocene of Rakhi Nala, Pakistan
Latif 1970	Geology of Southeast Hazara, Pakistan
Latif 1976	Micropalaeontology of the Galis group of Hazara, Pakistan
Middlemiss 1896	Geology of the Hazara and the Black Mountain
Nagappa 1959	Foraminiferal biostratigraphy of the Cretaceous-Eocene succession in India-Pakistan
Waagen & Wynne 1872	Geology of the upper Punjab
Williams 1959	Stratigraphy of the Lower Indus Basin
Wynne 1874	Geology of Mari Hill Station, Punjab

**Table 1.** List of key authors who have presented stratigraphical information for the Greater Indus Basin, Pakistan.

western Kohat, the Lower Indus Basin, the Axial Belt and the Baluchistan Basin (Shah 1977). During Middle and Late Eocene times different parts of Pakistan became emergent and this resulted in unconformities of varying magnitude (Shah 1977).

A revised nomenclature for the stratigraphical units of the Greater Indus Basin in Pakistan was defined by the GSP, who compiled work from a number of authors (Shah 1977). Subsequently published biostratigraphical work on calcareous nannofossils, dinoflagellates, planktonic and benthonic foraminifera (e.g. Köthe *et al.*

1988; Butt 1991; Afzal & Daniels 1991; Weiss 1993; Afzal 1996; Jones 1997; Akhtar & Butt 1999; Afzal & Butt 2001; Raza 2001a & b; Wakefield & Monteil 2002; Ferrandez-Canadell 2002; Warraich *et al.* 2000; Warraich & Nishi 2003; Sameeni & Butt 2004; Afzal *et al.* 2005; Siddiqui 2006) is summarized here in order to update and, where necessary, modify lithostratigraphical and biostratigraphical designations for various stratigraphical units published by the GSP (Shah 1977): see figures 3 to 7.

### **The Upper Indus Basin**

The evolution of the lower Cenozoic stratigraphical nomenclature for the Upper Indus Basin is given in Table 2. An integrated dinoflagellate, nannofossil, shallow benthonic and planktonic foraminiferal biostratigraphy for the Upper Indus Basin, related to standard chronostratigraphy and biostratigraphy, is presented for the first time (Fig. 3). Biostratigraphical and lithostratigraphical evidence for the age of Paleocene-Eocene stratigraphical units from various parts of the Upper Indus Basin is shown in Figure 4 against global chronostratigraphy and biostratigraphy. The stratigraphical context for these units is discussed below.

### **Sub-basins: Kohat area, Kala Chitta Range, Hazara Range, Salt Range, Surghar Range**

The Kohat area represents the northwestern part of the Upper Indus Basin and exposes a succession of Cenozoic rocks (Fig. 2A). The Kala Chitta Range marks the northern edge of the Potwar Plateau and merges north-easterly into the Hazara Range, representing the north-eastern portion of the Upper Indus Basin (Fig. 2A). The Salt and Surghar ranges form the southern portion of the Upper Indus Basin. The Salt Range is an east-west trending narrow mountain belt bounded by the Jhelum River to the east and the Indus

River to the west (Fig. 2A). The Surghar Range is a north-south trending mountain range separated from the Salt Range to the west by the Indus River and the strike slip Kala Bagh Fault (Fig. 2A). Mesozoic and Cenozoic marine sediments of the Salt Range extend into the Surghar Range (Fig. 2A).

The Hangu Formation of Shah (1977) is the basal Cenozoic sedimentary unit in this region (Fig. 4). It comprises sandstone, siltstone and clays in the Kohat area, Kala Chitta and Hazara ranges (Shah 1977), with argillaceous limestone beds in the Salt Range and also a coal-bearing horizon in the Surghar Range (Shah 1977; Warwick *et al.* 1993). The formation unconformably overlies the Late Cretaceous Kawagarh Formation in most of the basin (Latif 1976; Shah 1977), but occasionally overlies Palaeozoic units in the Salt Range and Surghar Range (Shah 1977). The Hangu Formation is unfossiliferous in the Kohat area, Kala Chitta and Hazara ranges (Latif 1976; Shah 1977; Weiss 1993) and its chronostratigraphical position is based on regional geological context (Fig. 4). In the Salt Range upper parts of the formation yield age diagnostic foraminifera (Davies & Pinfold 1937; Haque 1956; Weiss 1993; Ferrandez-Canadell 2002), nannofossils (Köthe *et al.* 1988; Warwick *et al.* 1993) and dinoflagellates (Köthe *et al.* 1988), which are identical to biota reported from the overlying basal Lockhart Formation elsewhere in the basin (Fig. 4).

The Lockhart Formation consists of nodular limestone in the Kohat area, Kala Chitta and Hazara ranges (Latif 1970, 1976; Fatmi 1974; Shah 1977; Akhtar & Butt 1999) and limestone and marl in the Salt and Surghar ranges (Shah 1977). The Lockhart Formation yields abundant age diagnostic larger benthonic foraminifera in the Kohat area (Weiss 1993; present study), the Kala Chitta and Hazara ranges (Latif 1970, 1976; Akhtar & Butt 1999) and the Salt Range (Davies & Pinfold 1937; Haque 1956; Weiss 1993). These occurrences and newly reported *Miscellanea miscella*, *Ranikothalia*



**Figure 3.** Dinoflagellate, nannofossil, shallow benthonic foraminiferal and planktonic foraminiferal biozones for the Paleocene-Eocene of the Upper Indus Basin. Biostratigraphical data are compiled from various sections of the Kohat Basin (Shah 1977; Köthe *et al.* 1988; Weiss 1993; Afzal *et al.* 2005; present study), the Salt Range (Shah 1977; Köthe *et al.* 1988; Gibson 1990; Weiss 1993; Afzal & Butt 2000; Sameeni & Butt 2004) and the Kala Chitta Range (Afzal & Butt 1999, 2001). The Upper Indus Basin biostratigraphy corresponds to the shallow benthonic biozones (SBZ) of Serra-Kiel *et al.* (1998) and Scheibner *et al.* (2005), calcareous nannofossil biozones (CNZ) of Martini (1971), planktonic foraminiferal biozones (PFZ) of Berggren *et al.* (1995) and chronostratigraphy of Luterbacher *et al.* (2004). The Danian/Selandian boundary is after Arenillas *et al.* (2008). The dinoflagellate biozones and datum markers, which could not be correlated with the European zonal schemes, are those established for the Greater Indus Basin in Pakistan and correlated with the nannofossil biozones of Martini (1971) by Köthe *et al.* (1988). There are additional datum markers for nannofossil biozones by Köthe *et al.* (1988).

*sindensis*, *Lockhartia conditi*, *Lockhartia haimei* and *Operculina jiwani* from the Kotal Pass, Kohat area, support maximum stratigraphical ranges through foraminiferal shallow benthonic biozones SBZ3-SBZ4 (Serra-Kiel *et al.* 1998) (Pl. 1; figs 1-12). Planktonic foraminifera from the Kohat area (Afzal *et al.* 2005), dinoflagellates (equivalent to nannofossil biozones NP6-NP8 of Martini 1971) from the Salt Range (Köthe *et al.* 1988) and nannofossils from the Surghar Range (Warwick *et al.* 1993) also support this biostratigraphical range (Figs 3, 4).

The Lockhart Formation is succeeded by shale, sandstone and marly limestone of the Patala Formation (Shah 1977; Akhtar & Butt 1999). The occurrence of sandstone within the formation is restricted to the Salt and Surghar ranges (Shah 1977; Gibson 1990; Warwick *et al.* 1993) (Fig. 4). The Patala Formation in the Kala Chitta and Hazara ranges (Latif 1970, 1976; Akhtar & Butt 1999) and the Salt Range (Haque 1956; Weiss 1993; Sameeni & Butt 2004) contains late Thanetian to early Ilerdian larger benthonic foraminiferal species suggesting biozones SBZ4 to SBZ6 (Fig. 4). Age diagnostic planktonic foraminiferal species from the Hazara Range, e.g. *Globorotalia elongata* [= *Morozovella elongata*], and *Globigerina soldadoensis* [= *Muricoglobigerina soldadoensis*] (Latif 1976), and from the Salt Range (Weiss 1993),

indicate the *Morozovella velascoensis-Acarinina soldadoensis* Biozone (= P4c-P5 biozones of Berggren *et al.* 1995). Planktonic foraminiferal biozones P5-P6b from the Salt Range (Afzal & Butt 2000) and Kohat area (Weiss 1993) provide a stratigraphical range that extends across the Paleocene-Eocene boundary (Fig. 4). Identification of dinoflagellate biozones equivalent to NP8-NP11 from the Salt Range and nannofossil biozones NP8-NP12 from the Kohat area and the Salt Range (Köthe *et al.* 1988) support a late Thanetian-early Ypresian biostratigraphical age (Figs 3, 4). There have been inconsistencies in the logging and mapping of the Patala Formation and its boundaries have consequently been placed differently by various workers (Gibson 1990), leading to varying stratigraphical interpretations. However, the regional stratigraphic framework suggests a maximum age of late Thanetian-early Ypresian (Figs 4, 7).

The Patala Formation is separated by an unconformity (upper P5-P6a) from the overlying nodular limestone and marl/shale of the Margala Hill Formation in the Kala Chitta and Hazara ranges (Latif 1970, 1976; Shah 1977; Akhtar & Butt 1999, 2001) (Fig. 4). In most of the Kohat area the Patala Formation is conformably overlain by greenish shales of the Panoba Formation, but in the Salt and Surghar ranges it is followed conformably by the marl/shale and limestone of the Nammal Formation (Shah 1977) (Fig. 4).

The larger benthonic foraminifera from the Panoba Formation (Meissner *et al.* 1968 in Shah 1977) indicate an age of SBZ10 (Fig. 4). The Margala Hill Formation yields larger benthonic foraminifera (Latif 1970, 1976; Akhtar & Butt 1999, 2001), which support a biostratigraphical age through biozones SBZ8-SBZ11 (Fig. 4). The larger benthonic foraminifera and zonally important planktonic foraminiferal species from the Nammal Formation (Weiss 1993; Afzal & Butt 2000; Sameeni & Butt 2004) suggest a P7-P9 age (Figs 3, 4). Köthe *et al.* (1988) also recorded the same biostratigraphical age based on the recognition of nannofossil biozones NP11-NP12 and

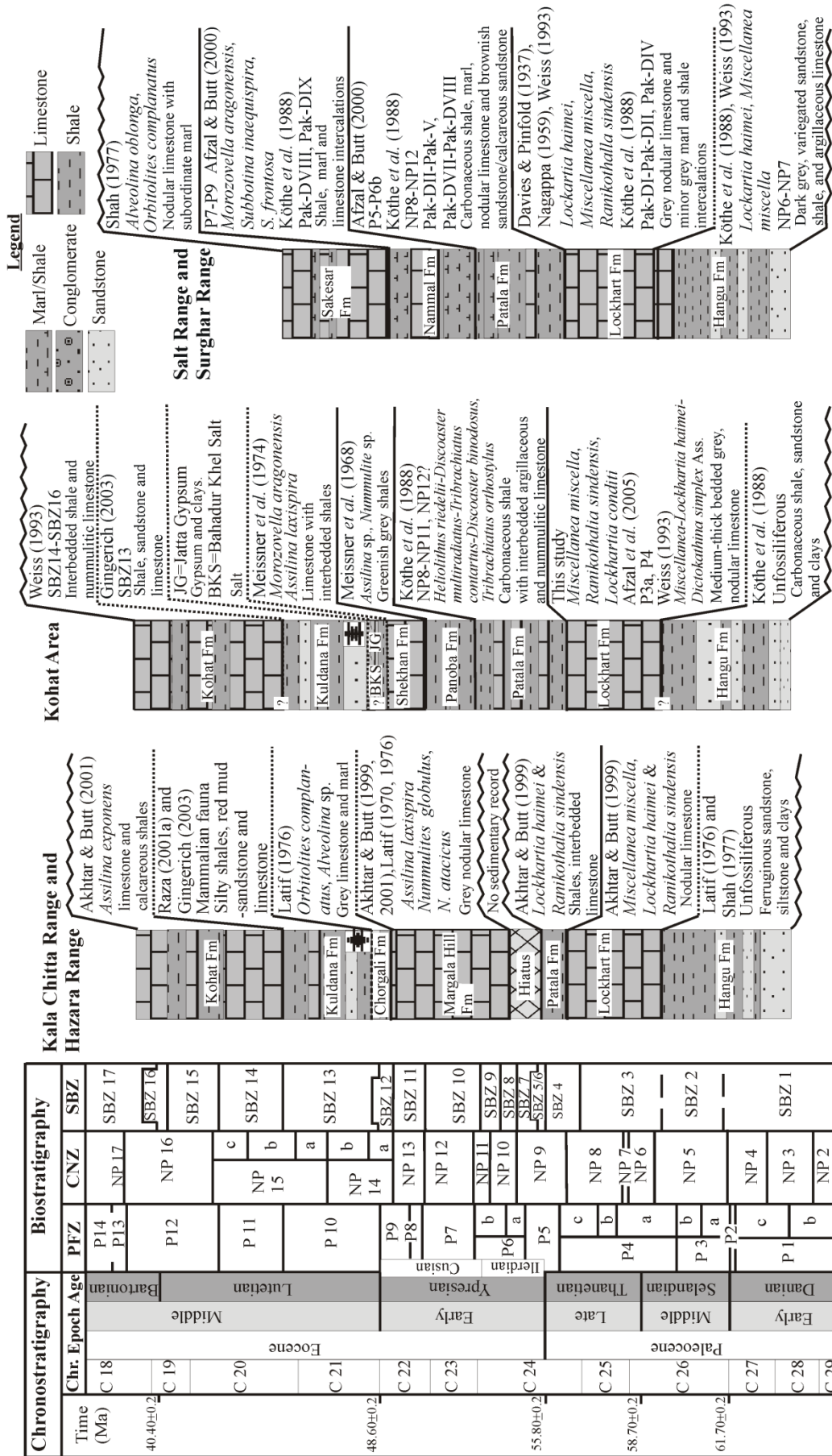


**Figure 4.** Summary of biostratigraphical and lithostratigraphical evidence for Paleocene-Eocene stratigraphical units from various parts of the Upper Indus Basin. Data for the Kohat area are from various sections, including Panoba (e.g. Meissner *et al.* 1968; Meissner *et al.* 1974; Shah 1977; Köthe *et al.* 1988; Weiss 1993; Gingerich 2003), Tarkhobi (Shah 1977; Köthe *et al.* 1988), Kotal Pass (Afzal *et al.* 2005; present study) and North of Hangu (Weiss 1993). Sources for the Kala Chitta Range-Hazara Range are Latif (1970, 1976), Shah (1977), and Akhtar & Butt (1999, 2001). Sources for the Salt Range-Surghar Range and adjoining areas are Davies & Pinfold (1937), Haque (1956), Shah (1977), Köthe *et al.* (1988), Gibson (1990), Weiss (1993), Afzal & Daniels (1991), Afzal & Butt (2000), Ferrandez-Canadell (2002) and Sameeni & Butt (2004).

of dinoflagellates equivalent to NP11-NP14.

The Panoba Formation is overlain by limestone and shale of the Shekhan Formation in the northern Kohat area, and by the Jatta Gypsum or Bahadur Khel Salt in the southwest Kohat area (Shah 1977) (Fig. 4). Limestone and marl of the Chorgali Formation overlie the Margala Hill Formation in the Kala Chitta and Hazara ranges and Sakesar Formation in the eastern Salt Range (Shah 1977). In the Surghar Range, limestone and marl of the Sakesar Formation conformably overlie the Nammal Formation and mark the end of marine deposition in this part of the basin, being overlain unconformably by non-marine molasse sediments of Miocene age (Shah 1977).

The Shekhan Formation is barren of nannofossils and dinoflagellates (Köthe *et al.* 1988). The larger benthonic foraminifera indicate a late Ypresian age (= SBZ 11) (Nagappa 1959; Pascoe 1963; Shah 1977; Weiss 1993). The occurrence of *Assilina laxispira* and the planktonic foraminifera *Morozovella aragonensis* and others is indicative of biozones P8-P9 (Meissner *et al.* 1974) (Figs 3, 4). The Shekhan Formation is overlain by unfossiliferous evaporitic deposits of the Bahadur Khel Salt and Jatta Gypsum (Meissner *et al.* 1974; Shah 1977) (Fig. 4).

The Chorgali Formation in the Kala Chitta, Hazara and eastern Salt ranges

Chronostratigraphy		Biostratigraphy			Dinoflagellates	Nannofossil zones and zonal markers	Larger foraminiferal assemblages and key species	Planktonic foraminiferal zones and zonal markers
Time (Ma)	Chr. Epoch	Age	PFZ	CNZ	SBZ	(after Köthe et al., 1988)		
37.20±0.1	Eocene	Late	P 17	NP 19-20	SBZ 20	<i>Calcidiscus protoamula</i>	<i>Ass. cancellata</i> - Nagappa (1959)	P16
C 15			P 16	NP 18	SBZ 19	<i>H. euphratis</i>	<i>N. beumonti</i> - Weiss (1993)	P15
40.40±0.2	Eocene	Middle	P 15	NP 17	SBZ 18	<i>Areosphaeridium</i> sp.	<i>Orbitolites complanatus</i> - Weiss (1993)	P14
C 19			P 14	NP 16	SBZ 17	<i>H. heezeni, H. intermedia</i>	<i>Alveolina elliptica</i> - Weiss (1993)	P13
C 20			P 13	NP 15	SBZ 16	<i>Sph. spingeri, Rhadospaera gladius</i>	<i>Ass. leymerei</i> - Weiss (1993)	P12
C 21			P 12	NP 14	SBZ 15	<i>H. heezeni, H. intermedia, Sph. spingeri</i>	<i>Alveolina sp.</i> - Assenblage - Nagappa (1959) and Akhtar & Butt (2000)	P11
48.60±0.2	Eocene	Early	P 11	NP 15	SBZ 14	<i>Distatodinium</i> sp.	<i>Ass. leymerei</i> - Weiss (1993)	P10
C 22			P 10	NP 14	SBZ 13	<i>D. subloedoensis</i>	<i>Ass. leymerei</i> - Weiss (1993)	P9
C 23			P 9	NP 13	SBZ 12	<i>Sph. editus</i>	<i>Ass. leymerei</i> - Weiss (1993)	P8
C 24			P 8	NP 12	SBZ 11	<i>D. loedoensis, D. kuepperi</i>	<i>Ass. leymerei</i> - Weiss (1993)	P7
55.80±0.2	Paleocene	Late	P 7	NP 11	SBZ 10	<i>Homotryblidium oceanicum</i>	<i>Ass. leymerei</i> - Weiss (1993)	P6
C 25			P 6	NP 10	SBZ 9	<i>F. tympamiformis</i>	<i>Ass. leymerei</i> - Weiss (1993)	P5
C 26			P 5	NP 9	SBZ 8	<i>Discoaster multiradiatus</i>	<i>Ass. leymerei</i> - Weiss (1993)	P4c
C 27			P 4	NP 8	SBZ 7	<i>Helolithus riedeli</i>	<i>Ass. leymerei</i> - Weiss (1993)	P4a
61.70±0.2	Paleocene	Middle	P 4	NP 7	SBZ 6	<i>Neochiastozygus digitatus</i>	<i>Ass. leymerei</i> - Weiss (1993)	P3b
C 28			P 3	NP 6	SBZ 5	<i>Tribrachiatus pertusus</i>	<i>Ass. leymerei</i> - Weiss (1993)	P3a
C 29			P 2	NP 5	SBZ 4	<i>Fasciculithus magnus</i>	<i>Ass. leymerei</i> - Weiss (1993)	P1b
65.50±0.3	Paleocene	Early	P 2	NP 4	SBZ 3	<i>Ellipsolithus macellus</i>	<i>Ass. leymerei</i> - Weiss (1993)	P1a
C 29			P 1	NP 3	SBZ 2	<i>Ellipsolithus macellus</i>	<i>Ass. leymerei</i> - Weiss (1993)	P1a

**Figure 5.** Dinoflagellate, nannofossil, shallow benthonic foraminiferal and planktonic foraminiferal biozones for Paleocene-Eocene stratigraphical units of the Lower Indus Basin. Biostratigraphical data are compiled from various sections of the Sulaiman and Kirthar ranges (Eames 1952; Nagappa 1959; Shah 1977; Köthe *et al.* 1988; Weiss 1993; Afzal 1996; Akhtar & Butt 2000; Warraich *et al.* 2000; Wakefield & Monteil 2002; Warraich & Nishi 2003). The Lower Indus Basin biostratigraphy corresponds to the standard shallow benthonic biozones (SBZ) of Serra-Kiel *et al.* (1998) and Scheibner *et al.* (2005), calcareous nannofossil biozones (CNZ) of Martini (1971), planktonic foraminiferal biozones (PFZ) of Berggren *et al.* (1995) and chronostratigraphy of Luterbacher *et al.* (2004). The dinoflagellate biozones and datum markers are established for the Greater Indus Basin in Pakistan and correlated with the nannofossils of Martini (1971) by Köthe *et al.* (1988). There are additional datum markers recognized for nannofossil biozones by Köthe *et al.* (1988).

yields age diagnostic larger benthonic foraminifera from biozones SBZ11-SBZ12 (Latif 1970, 1976; Shah 1977; Sameeni & Butt 2004) (Fig. 4).

The shale and marl succession of the Kuldana Formation, which yields fossil mammals (Raza 2001a), succeeds the Chorgali Formation in the Kala Chitta and Hazara ranges and the Bahadur Khel Salt and Jatta Gypsum in the Kohat area (Shah 1977). On the basis of larger benthonic foraminifera from the Kala Chitta and Hazara ranges (Latif 1970, 1976) and mammal faunas from different parts of the Kohat area and Kala Chitta Range (Raza 2001a; Gingerich 2003) the Kuldana Formation is assigned to Biozone SBZ13 or older (Fig. 4). The shale and nummulitic limestone succession of the Kohat Formation overlies the Kuldana Formation in most of the Kohat area, Kala Chitta and Hazara ranges (Shah 1977; Akhtar & Butt 1999, 2001).

The Kohat Formation marks the last episode of marine sedimentation in the Kohat area, Kala Chitta and Hazara ranges and is overlain by non-marine molasse sediments of the Miocene Murree Formation. The late Ypresian-Lutetian age assignment for the Kohat Formation given by Shah (1977) is based on molluscs (Eames 1952) and larger benthonic foraminifera (see Meissner *et al.* 1968). The same biostratigraphical ages can be extracted from the foraminifer record of Meissner *et al.*



**Figure 6.** Summary of biostratigraphical and lithostratigraphical evidence for Paleocene-Eocene stratigraphical units from various parts of the western Lower Indus Basin and Duljan-1 well of the eastern Lower Indus Basin (after Wakefield & Monteil 2002). Legend as for Figure 4.

(1974). Weiss (1993) reported larger benthonic foraminifera from the Kohat area of intermediate biostratigraphical age between biozones SBZ10 and SBZ17. Similarly, *Assilina exponens*, reported by Akhtar & Butt (2001), also ranges in age from biozones SBZ13 to SBZ17. These foraminiferal occurrences and the regional stratigraphic position imply a biostratigraphical range of SBZ14 to SBZ16 for the Kohat Formation (Fig. 4).

### **The Lower Indus Basin**

The early Paleogene sediments of the Lower Indus Basin were deposited on a broad shelf area of the passive continental margin of the Indo-Pakistan Plate (Bannert 1992). The history of stratigraphical nomenclature for the Lower Indus Basin is given in Table 3 and the biostratigraphic framework in Figures 5 and 6. A regional stratigraphical correlation with the Upper Indus Basin is given in Figure 7. Early Paleogene marine sediments are well exposed across the basin (Fig. 2B). The context for the different stratigraphical units from key sections is discussed below.

### **The Sulaiman Range and Kirthar Range**

The Sulaiman Range forms a lobate structure in the northern part of the Lower Indus Basin, while the Kirthar Range forms a North-South linear feature in the southern region (Figs 1, 2B). The succession in the Sulaiman and Kirthar ranges has been studied since the nineteenth century.

The Dungan Formation of Kazmi (1995) marks the basal lithological unit of the lower Tertiary and unconformably overlies Late Cretaceous units in most of the Lower Indus Basin. It equates to the Khadro, Bara, Lakhra and Dungan formations of Shah (1977). The lowermost sandstone, siltstone and shale portion (Khadro Formation of Shah 1977) of the formation is widely developed in the Kirthar Range, but rare or absent in the Sulaiman Range (e.g. Rakhi Nala). It has yielded planktonic foraminifera of Biozone P1 (Nagappa 1959) (Figs 5, 6). The overlying sandstone/siltstone unit (Bara Formation of Shah 1977) of the lower Dungan Formation is widely distributed in the Kirthar Range, but rare in the Sulaiman Range. It lacks age diagnostic fossils (Shah 1977; Afzal 1996; Wakefield & Monteil 2002). The upper Dungan Formation (the Lakhra and Dungan formations of Shah 1977 and Bara and Lakhra members of Wakefield & Monteil 2002) is dominantly limestone and shale, and is well developed in the Sulaiman and Kirthar ranges. Many biostratigraphically important larger benthonic foraminifera from the formation include *Miscellanea miscella*, *Discocyclina ranikotensis*, *D. dispansa*, *Lockhartia haimei*, *Alveolina* sp., *Ranikothalia nuttalli* and *Assilina dandotica* (in Shah 1977; Weiss 1993; Akhtar & Butt 2000; Wakefield & Monteil 2002) which suggest an age of late Thanetian to early Ilerdian. The nannofossil biozones NP4, NP7 and NP9 (Köthe *et al.* 1988) and planktonic foraminiferal biozones P7 (Afzal 1996) and P3-P7 (Jones 1997; Warraich *et al.* 2000) further support a Middle Paleocene-Early Eocene age. The upper contact of the formation with the overlying Ghazij Formation has been interpreted as conformable in most of the basin (Shah 1977, 1990; Kazmi 1995); however, Warraich *et al.* (2000) reported biozones P6-lower P7? to be missing, with a conglomeratic bed between these formations in the northwestern Sulaiman Range (Rakhi Nala and Zinda Pir areas) , suggesting the presence of an unconformity (Figs 6, 7).

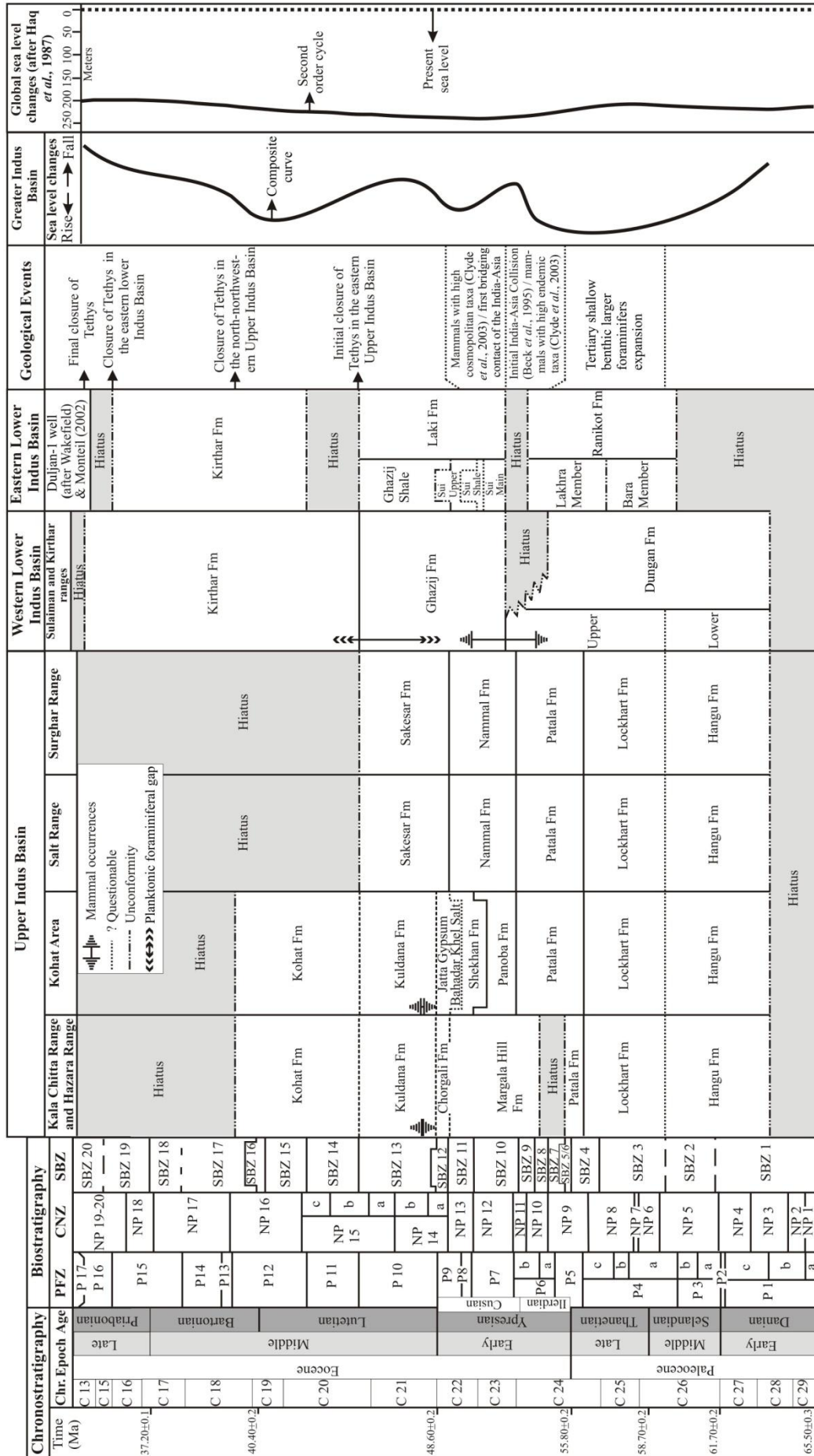


**Figure 7.** Regional stratigraphical correlation of the lower Cenozoic successions of the Greater Indus Basin, Pakistan, showing significant geological events and their correlation with basin stratigraphy and global sea level changes (2<sup>nd</sup> order cycle) of Haq *et al.* (1987).

The Ghazij Formation, as recognized here, corresponds to the Ghazij and Laki formations of Shah (1977), the Laki Formation of Wakefield & Monteil (2002) and the Ghazij Group of Shah (1990) and Kazmi (1995). It is dominantly shale with subordinate claystone, sandstone, limestone, coal and conglomerate. The formation is well-developed in the Sulaiman Range and parts of the Kirthar Range (Shah 1977). Early biostratigraphical ages determined from rich occurrences of larger benthonic foraminifera e.g. *Assilina leymeriei*, *A. pustulosa*, *Orbitolites complanatus*, *Nummulites globulus*, etc. (equivalent to biozones SBZ8-SBZ13) (Eames 1952; Nagappa 1959) were later confirmed by Weiss (1993) and Wakefield & Monteil (2002). Planktonic foraminiferal biostratigraphical ages were first investigated by Latif (1964) and Samantha (1973) and later by Afzal (1996), who supported an age range of biozones P7-P9. This assignment has recently been confirmed by the detailed work of Wakefield & Monteil (2002) and Warraich & Nishi (2003), who reported a continuous record of planktonic biozones P7 to P10? (Figs 5, 6). Planktonic foraminiferal studies also show a gap spanning upper P10? to P11 in the upper part of the Ghazij Formation to the lower part of the Kirthar Formation in the western Sulaiman Range (Warraich & Nishi 2003) (Figs 5, 6). However, Köthe *et al.* (1988) reported dinoflagellate Biozone Pak-DIX (equivalent to nannofossil biozones NP12- lower NP14) from the upper part of the formation and Pak-DX to Pak-DXI (equivalent to upper NP14-NP19/20) from the overlying Kirthar Formation of Shah (1977) (Figs 5, 6). These results suggest a conformable relationship between the Ghazij and Kirthar formations in the western Lower Indus Basin; however this relationship is unconformable in the eastern Lower

Indus Basin with a ~2my hiatus with Biozone P11 absent (Wakefield & Monteil 2002) (Figs 6, 7).

The Kirthar Formation consists of limestone and shale with minor marl (Shah 1977). The formation is widely distributed in the Sulaiman-Kirthar ranges and is richly fossiliferous with many age diagnostic fossils (Shah 1977). Based on the foraminiferal records of the Hunting Survey Corporation (1960), Shah (1977) assigned a broad stratigraphical range of Ypresian-Priabonian. However, other foraminiferal studies have given an age of late Lutetian-early Priabonian based on occurrences of planktonic foraminiferal species indicative of Biozone P14 (Latif 1964) and of biozones P12-13 and P15 to P17 (Samantha 1973). Warraich & Nishi (2003) and Wakefield & Monteil (2002) recently established the presence of a continuous record of biozones P12 to P15? (Figs 6, 7). The lower part of the Kirthar Formation is rich in larger benthonic foraminifera including *Assilina spinosa*, *A. exponens*, *A. cancellata*, *Nummulites beaumonti* and *Discocyclina sowerbyi*, equivalent to biozones SBZ13-SBZ18 (Eames 1952; Nagappa 1959; Weiss 1993), suggesting a shallow marine environment, which may account for the gap in the planktonic foraminiferal records. The Kirthar Formation is mostly overlain by Miocene-Pliocene age molasse sediments of the Siwalik Group (Shah 1977).

### **Regional stratigraphical context**

The lower Cenozoic succession of the Greater Indus Basin in Pakistan is characterized by considerable changes in lithologies and fauna. Inter-regional stratigraphical correlations for the Greater Indus Basin in Pakistan are given in Figure 7 and are related to global sea level variations and bio-chronostratigraphy.

The earliest marine Cenozoic sedimentation in the basin seems to have commenced with the Early Paleocene transgression (Haq *et al.* 1987). The continental-

near shore facies of the Hangu Formation initially dominated in the north-northwestern parts of the basin (Hazara Range, Kala Chitta Range and Kohat area) (Latif 1976; Köthe *et al.* 1988; Weiss 1993; Akhtar & Butt 1999). South-westwards, into the Surghar and Salt ranges, it extended into shallow marine-deltaic facies, with coal and marine fossils (Shah 1977; Warwick *et al.* 1993), and further south into the correlative planktonic and smaller benthonic foraminifera-bearing lower Dungan Formation (= *Cardita Beaumonti* Beds in Nagappa 1959) (figs 6, 7). This marine flooding was succeeded by widespread carbonate platform deposition of the Lockhart Formation in the Upper Indus Basin and upper Dungan Formation (= Bara and Lakhra members of Wakefield & Monteil 2002) in the Lower Indus Basin. The correlative planktonic foraminifer-bearing shales of the Dungan Formation in the northwestern Sulaiman Range (e.g. Rakhi Nala and Zinda Pir areas) were deposited in an open marine environment (Warraich *et al.* 2000). These carbonates recorded the first expansion of lower Cenozoic shallow benthonic larger foraminifera in the basin (Weiss 1993; Akhtar & Butt 1999; Warraich *et al.* 2000; Wakefield & Monteil 2002; Afzal *et al.* 2005); these preferentially flourished in oligotrophic conditions (Hottinger 1997) (Figs 4, 6). The carbonate platform was buried by deep marine clastics of the Patala Formation (= P4c-P6) in most of the Upper Indus Basin and by the shales of the Ghazij Formation (= P7-P10) in parts of the Lower Indus Basin. The hiatus equivalent to biozones upper P5-P6a in the northern Upper Indus Basin (Kala Chitta and Hazara ranges; Akhtar & Butt 1999, 2001) and P6-lower P7? in the western (Zinda Pir area; Warraich *et al.* 2000) and P6b-lower P7 in the eastern (Duljan-1 Well; Wakefield & Monteil 2002) parts of the Lower Indus Basin may have been caused by compression, uplift and erosion associated with India-Asia collision (around 55 Ma; Beck *et al.* 1995; Klootwijk *et al.* 1991; Warraich & Nishi 2003) (Fig. 7). These events were accompanied by highly significant stratigraphic

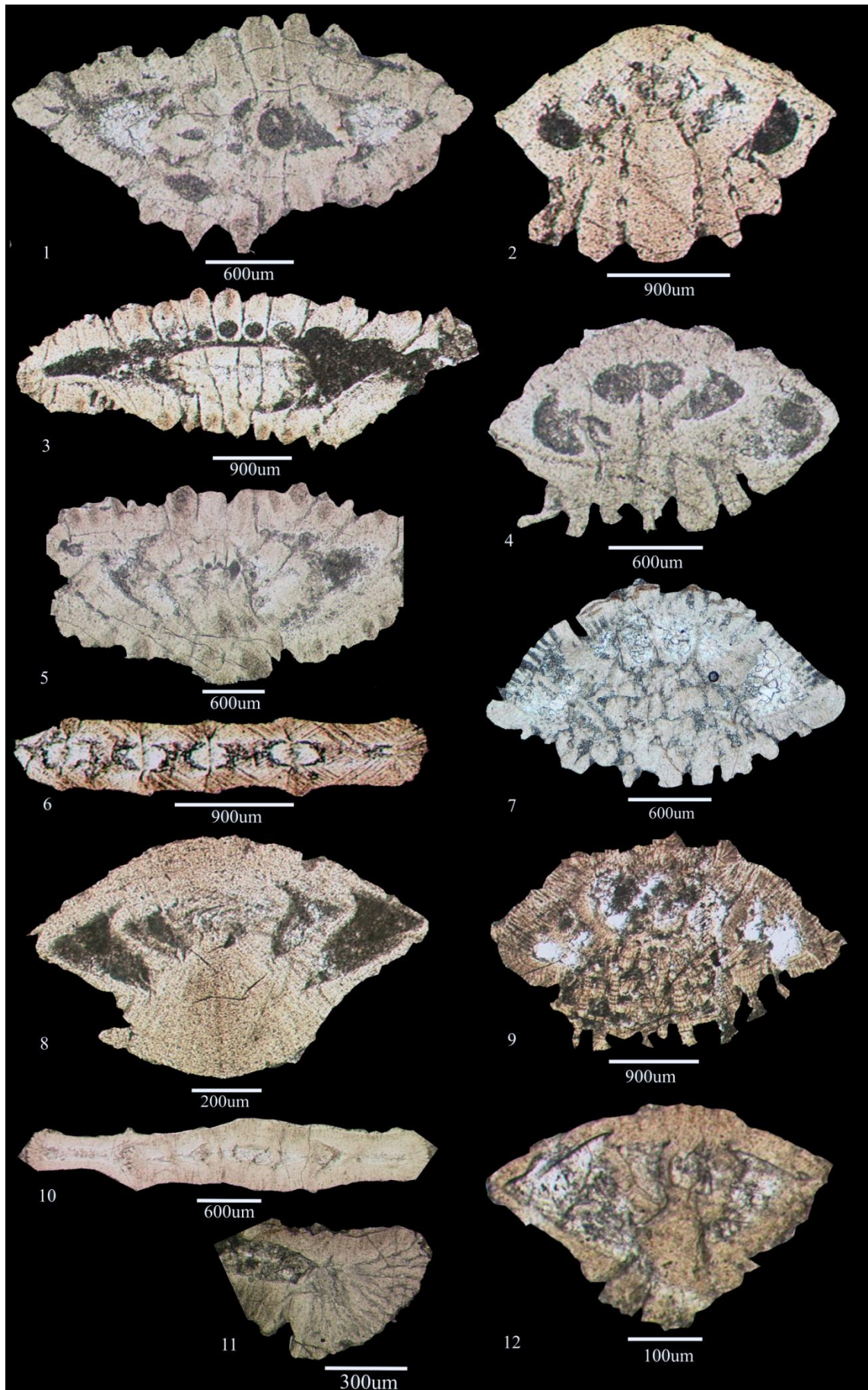


**Plate 1.** Biostratigraphically significant Thanetian shallow benthonic foraminifera of the Lockhart Formation from the Kotal Pass section of the Kohat area (Upper Indus Basin). 1, 3 & 5. *Miscellanea miscella* (d' Archiac & Haime), 1, 5, megalospheric form, axial section; 3, microspheric form, off centre axial section. 2 & 4. *Lockhartia conditi* (Nuttall), 2, 4, axial section. 6. *Operculina jiwani* Davies & Pinfold, off centre axial section. 7 & 9. *Lockhartia haimi* (Davies), axial section. 8. *Kathina selveri* Smout, axial section. 10 & 11. *Ranikothalia sindensis* (Davies), 10, microspheric form, axial section; 11, marginal cord, axial section. 12. *Rotalia trochidiformis* Lamarck, axial section.

changes in parts of the basin, for example, producing intermittent shallow and deep marine sediments (Weiss 1993; Afzal & Butt 1999; Warraich *et al.* 2000) and dramatic shifts from marine to continental deposits, the latter containing endemic mammal occurrences (Clyde *et al.* 2003). The Paleocene/Eocene boundary has been established in the basin through the identification of planktonic foraminiferal biozones P5/P6 (Afzal & Butt 2000; Warraich *et al.*, 2000), larger benthonic foraminifer assemblages (Weiss 1993; Akhtar & Butt 1999), and nannofossil biozones NP9/NP10 (Köthe *et al.* 1988) (Figs 3-6).

The open marine planktonic foraminifera of the lower Cenozoic successions of the Greater Indus Basin in Pakistan show abrupt changes in composition, for example there was an increase in tropical-subtropical species of the morozovellid group during P4-P5 biozones followed by a decrease of morozovellids and an increase of cooler water species of subbotinid group foraminifera during biozones P6-P7 (Afzal & Butt 2000; Warraich *et al.* 2000; Warraich & Nishi 2003). The shallow marine benthonic foraminiferal communities of the Greater Indus Basin in Pakistan experienced a significant diversification of species near the Paleocene-Eocene boundary; Thanetian-earliest Ilerdian (= SBZ4-SBZ6?) small species including *Miscellanea*, *Ranikothalia* and *Lockhartia* were succeeded by early Ilerdian (= SBZ6-SBZ8) large species of *Nummulites*, *Discocyclina*, *Alveolina* and *Assilina* (Weiss 1993; Akhtar & Butt 1999, 2000; Sameeni & Butt 2004). These marine faunal changes in the region during the late

Lithostratigraphical unit	Primary reference	GSP ( Shah 1977)	Geographical distribution
Sakesar Limestone	Fermor (1935)	Sakesar Formation	Salt Range and Surghar Range
Nammal Limestone and Shale	Fermor (1935)	Nammal Formation	
Nammal Marl	Danilchik & Shah (1987)		
Habib Rahi Member	Shah (1977)	Kohat Formation	Kohat area, northern Salt Range and Kala Chitta Range
Sadkal Member			
Kaladhand Member			
Kohat Formation			
Kohat Shales	Eames (1952)		
Sirki Shale			
Upper Chharat			
Nummulitic Shales			
Kohat Limestone	Davies (1927)		
Kohat Shales	Pinfold (1918)		
Nummulitic Shales			
Alveolina Beds		Wynne (1874)	
Kuldana Formation	Latif (1970)	Kuldana Formation	Southern Hazara Range, Kala Chitta Range, northern Salt Range and Kohat area
Mami Khel Clay	Meissner <i>et al.</i> (1968)		
Lower Chharat Series	Eames (1952)		
Variegated Shales	Pinfold (1918)		
Kuldana Series	Middlemiss (1896)		
Kuldana Beds	Wynne (1874)		
Lora Formation	Latif (1970)	Chorgali Formation	Eastern Salt Range, Kala Chitta Range and Hazara Range
Badhrar Beds	Davies & Pinfold (1937)		
Chorgali Beds	Pascoe (1920)		
Passage Beds	Pinfold (1918)		
Jatta Gypsum	Meissner <i>et al.</i> (1968)	Jatta Gypsum	Kohat area
Kohat Series	Gee (1945)	Margala Hill Formation	Kala Chitta Range, northern Salt Range, Hazara Range and eastern Kohat area
Margala Hill Limestone	Latif (1970)		
Nummulitic Series	Middlemiss (1896)		
Hill Limestone	Wynne (1873)		
Nummulitic Formation	Waagen & Wynne (1872)	Bahadur Salt	Kohat area
Bahadur Salt	Meissner <i>et al.</i> (1968)		
Kohat Saline Series	Gee (1945)	Shekhan Formation	
Gypsiferous beds	Eames (1952)		
Upper Shekhan Limestone			
Middle Shekhan Limestone			
Lower Shekhan Limestone			
Shekhan Limestone	Davies (1927)	Panoba Formation	
Panoba Shale	Eames (1952)		
Green Clay and Sandstone	Gee (1934)		
Part of Group z (e2 b)	Pascoe (1920)		
Part of Group (3) ezc			
Green Clay	Wynne (1874)	Patala Formation	
Kuzagali Shale	Latif (1970)		
Tarkhobi Shales	Eames (1952)		
Patala Shale	Davies & Pinfold (1937)		
Nummulitic Series	Middlemiss (1896)		
Hill Limestone	Wynne (1873)	Lockhart Formation	Salt Range, Surghar Range, Kohat area, Kala Chitta Range and Hazara Range
Nummulitic Formation	Waagen & Wynne (1872)		
Mari Limestone	Latif (1970)		
Tarkhobi Limestone	Eames (1952)		
Khairabad Limestone	Gee (1934)		
Hill Limestone	Cotter (1933)		
Lockhart Limestone	Davies (1930)		
Nummulitic Series	Middlemiss (1896)		
Hill Limestone	Wynne (1873)		
Nummulitic Formation	Waagen & Wynne (1872)		
Mari Limestone	Latif (1970)	Hangu Formation	
Dhak Pass Formation	Danilchik & Shah (1987)		
Langrial Iron Ore Horizon	Khan & Ahmad (1966)		
Dhak Pass Beds	Davies & Pinfold (1937)		
Hangu Sandstone	Davies (1930)		
Hangu Shale			
Nummulitic Series	Middlemiss (1896)		
Nummulitic Formation	Waagen & Wynne (1872)		

**Table 2.** Lithostratigraphical nomenclature for the Upper Indus Basin, Pakistan.

Thanetian-early Ypresian may have been associated with long term global warming events of the lower Cenozoic (Kelly *et al.* 1996; Zachos *et al.* 2001; Scheibner *et al.* 2005).

The Ypresian-early Lutetian (P7-P10) sediments show a shallowing upward sequence, associated with the Ypresian-Lutetian marine transgression-regression (Haq *et al.* 1987) (Figs 4, 6, 7). In the northeast (Kala Chitta, Hazara, Salt and Surghar ranges) these sediments comprise carbonate rich units (Margala Hill Formation/Nammal Formation; Shah 1977; Akhtar & Butt 1999; Afzal & Butt 2000) and in the northwest (Kohat area) a mudstone/shale rich unit (Panoba Formation; Köthe *et al.* 1988; Weiss 1993) and a carbonate-rich unit (Shekhan Formation; Köthe *et al.* 1988; Weiss 1993). The higher parts of the succession include evaporites (= the Bahadar Khel Salt-Jatta Gypsum; Shah 1977) and finally the continental red bed/sandstone mammal-bearing Kuldana Formation (Gingerich 2003) (Figs 4, 7). The mammals of the upper Subathu Formation or Kalakot Zone of India (stratigraphically coeval to the Kuldana Formation; Sahni & Jolly 1993) are comparable with the mammals of the Kuldana Formation (Sahni & Jolly 1993; Gingerich 2003). The marine regression is also recognizable in the south-southwestern parts of the basin (Lower Indus Basin), where the Ghazij Formation developed gypsum-rich, coal and mammal-bearing beds (Clyde *et al.* 2003) (Figs 6, 7). The mammal taxa from the Ghazij Formation indicate a pattern of decreasing endemism, increasing cosmopolitanism and increasing modernity through time (= P7-lower P9; Clyde *et al.* 2003). This suggests a bridging contact of the Indian plate with the Asian plate in parts of the northwestern Lower Indus Basin, which was broken up by marine deposition of limestone and shale of the upper Ghazij and lower Kirthar formations during early Lutetian time (Johnson *et al.* 1999). The shale and carbonates of

Chapter 2: Revised stratigraphy of the lower Cenozoic succession of the Greater Indus Basin

Lithostratigraphical unit	Primary reference	GSP (Shah 1977)	Present terminology		Geographical distribution	
Drazinda Member	Shah (1977)	Kirthar Formation	Kirthar Formation		Kirthar Range, Sulaiman Range and parts of Kohat area	
Pir Koh Limestone and Marl Member						
Sirki member						
Habib Rahi Limestone Member						
Drazinda Shale	Hemphill & Kidwai (1973)					
Upper Gorag Member	Hunting Survey Corporation (1961)					
Lower Kirthar Member						
Spintangi Limestone						
Brahui Limestone						
Pellatispira Beds	Eames (1952)					
Upper Chocolate Clays						
Lower Chocolate Clays						
White Marl Band						
Sirki Shale						
Spintangi Limestone	Oldham (1890)					
Sohnari Member	Shah (1977)	Laki Formation			Southern Kirthar Range and Sulaiman Range	
Meting Shales and Limestone Member						
Laki Group	Hunting Survey Corporation (1961)					
Sohnari Member						
Tiyon Formation						
Basal Laki Laterite	Nuttall (1926)					
Meting Shales and Limestone	Vredenburg (1906)					
Shaheed Garh Formation	Kazmi (1995)	Ghazij Formation	Ghazij Formation		Sulaiman Range and Kirthar Range	
Ghazij Formation	Cheema <i>et al.</i> (1977)					
Marap Conglomerate Member	Shah (1977)					
Baska Shale and Albaster Member						
Baska Shales	Hemphill & Kidwai (1973)					
Upper part of Gidar Dhor Group	Hunting Survey Corporation (1961)					
Tiyon Formation						
Ghazij Shales						
Marap Conglomerate	Ghazij Formation					
Chat beds						Nagappa (1959)
Ghazij Formation						Williams (1959)
Zinda Pir Limestone (upper part)						Eames (1952)
Upper Rakhi Gaj Shales						
Ghazij Shales						
Green and Nodular Shales						
Rubbly Limestone						
Shales with Albaster		Oldham (1890)				
Ghazij Group						
Dungan Formation	Kazmi (1995)	Dungan Formation	Upper		Sulaiman Range and northern Kirthar Range	
Karkh Group	Hunting Survey Corporation (1961)					
Dab Formation						
Dungan Group (excluding Moro Formation)						
Zinda Pir Limestone (lower part)	Eames (1952)					
Zinda Pir Shales						
Lower Rakhi Gaj Shales	Williams (1959)					
Dungan Formation						
Dungan Limestone						
Ranikot Group	Blandford (1878)					
Dungan Formation	Kazmi (1995)					
Upper Ranikot Formation and upper parts of the Bad Kachu, Rattaro and Thar formations and lower part of the Jakker Group(Limestone)	Hunting Survey Corporation (1961)	Lakhra Formation			Kirthar Range	
Upper Ranikot (Limestone)						
Ranikot Group	Blandford (1878)					
Dungan Formation	Kazmi (1995)	Bara Formation			Kirthar Range and northern Sulaiman	
Lower parts of the Jakker Group, Thar, Rattaro and Bad Kachu	Hunting Survey Corporation (1961)					
Ranikot Formation	Williams (1959)					
Gorge Beds	Eames (1952)					
Lower Ranikot (sandstone)	Vredenburg (1906)					
Ranikot Group	Blandford (1878)					
Dungan Formation	Kazmi (1995)	Khadro Formation	Lower		Kirthar Range and parts of the Sulaiman Range	
Khadro Formation	Williams (1959)					
Thar Formation	Hunting Survey Corporation (1961)					
Bad Kachu						
The basal parts of Karkh, Gidar Dhor and Jakker groups						
Venericardita Shales	Eames (1952)					
Ranikot Group	Blandford (1878)					
Cardita Beaumonti Beds						

**Table 3.** Lithostratigraphical nomenclature of the Lower Indus Basin, Pakistan.

the Sakesar Formation, a marine correlative of the Kuldana Formation in the western Salt Range and Surghar Range, is overlain by Miocene-Recent terrestrial sediments derived from the Himalaya (Shah 1977), marking the closure of Tethys in the south-eastern Upper Indus Basin (Figs 4, 7).

The late Lutetian-Priabonian regression (Haq *et al.* 1987) is represented by the upper Kirthar Formation in the south-southwest and the correlative uppermost Kohat Formation in the north-northwest. This followed closure of the Tethys in the north-northwestern parts of the basin (e.g. Kohat area, Kala Chitta and Hazara ranges) (Figs 4, 6, 7). The gradual retreat of the Tethys Sea continued south-southwest through late Lutetian to Bartonian time and it finally closed in the Priabonian (P15; Warraich *et al.* 2000; Wakefield & Monteil 2002). Oligocene marine sedimentation was restricted to the south of the Lower Indus Basin (Raza 2001a), while the rest of the Greater Indus Basin in Pakistan remained a non-depositional lowland until the formation of Neogene molasse (Shah 1977; Raza 2001a).

### **Conclusions**

The lower Cenozoic succession of the Greater Indus Basin in Pakistan preserves an excellent sedimentary and biotal record of the east Tethyan Sea. These provide significant stratigraphical evidence of locally and globally significant geologically important events.

The succession is dominated by shallow marine shelf sediments intermixed with deep marine sediments rich in stratigraphically important microbiota. Previously published stratigraphical data have been reinterpreted and many stratigraphical levels have been revised. In addition, biostratigraphically significant shallow benthonic foraminifera

from the Lockhart Formation are illustrated. Inter-basinal correlations between various units and with the global standard biostratigraphy and chronostratigraphy are presented. These have enabled recognition of unconformities associated with ongoing India-Asia tectonics and global sea level change about 55 million years ago. The closure of Tethys was initiated from the north and northwest during early Lutetian time and was completed by the Priabonian in the south and southwest. This also implies that the Indian Plate came in contact with the Asian Plate in the north first, and later in the southwest, which resulted in the closure of the Tethys Sea and cessation of sedimentation in the basin.

---

## **Chapter 3**

---

Paleocene-Early Eocene larger  
benthic foraminifera of the  
Indus Basin, Pakistan:  
systematic palaeontology

---

## **Chapter 3: Paleocene-Early Eocene larger benthic foraminifera of the Indus Basin, Pakistan: systematic palaeontology**

### **Introduction**

This study describes Paleocene-Early Eocene larger benthic foraminifera (LBFs) from newly collected sections and oil well cores in the Upper Indus Basin (Kotal Pass section and Shakardara Well-1) and Lower Indus Basin (Mughal Kot, Zranda, Muree Brewery and Hanna Lake sections) of Pakistan (see Fig. 1). The study involves: 1) a thorough appraisal of the systematic palaeontology of these foraminifera with, where possible, comparison with figured and type material; and 2) a revised assessment of their biostratigraphic ranges from a Palaeogene Tethyan context.

A total of 45 species of LBFs are described from the Indus Basin. The identification of LBFs is based mostly on random and oriented thin sections. This is because the highly indurated carbonate rocks prohibit extraction of individual specimens. Anatomical and morphological terms are those used by Hottinger (1960, 2006, 2009) and Sirel (1997a, 1997b). The foraminifer classification proposed by Loeblich & Tappan (1988) has been followed for the systematics of LBF species and genera with the style of the Palaeontographical Society of London for systematic description. The species synonymy lists given here are abridged, mentioning the original, figured and described references only. However, where a complete synonymy is considered vital to the discussion, then this has been included. Generic description/diagnosis is given where necessary for species determination. The International Code of Zoological Nomenclature is followed to designate types where needed.

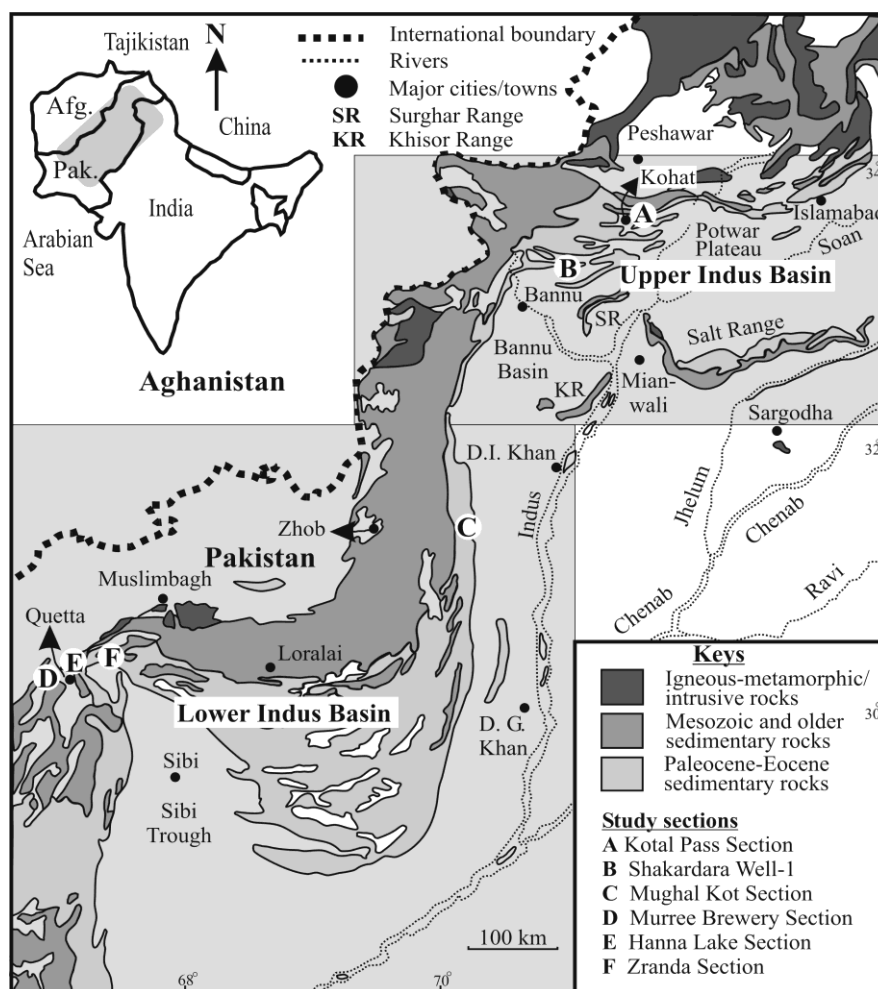


**Figure 1.** Map of the Upper and parts of the Lower Indus basins showing distribution of Paleocene-Eocene sedimentary rocks and position of studied sections (A-F) (modified after Eames 1952).

Identified LBFs were photographed in plane-polarized light with a digital camera on a Nikon petrographic microscope in the Department of Geology, University of Leicester. For biostratigraphic ranges, the shallow benthic biozonation (SBZ) scheme of Serra-Kiel *et al.* (1998), with amendments for the placement of the Paleocene-Eocene boundary at a level equivalent to the biostratigraphic boundary between biozones SBZ4 and SBZ5 (see Scheibner & Speijer 2009), has been adopted. Stratigraphic names used in this study are from Afzal *et al.* (2009) and biostratigraphic determination of LBFs follows Afzal *et al.* (in press). The dimensions given for individual specimens are minimum to maximum diameter (D) and thickness (T) for LBF tests with additional

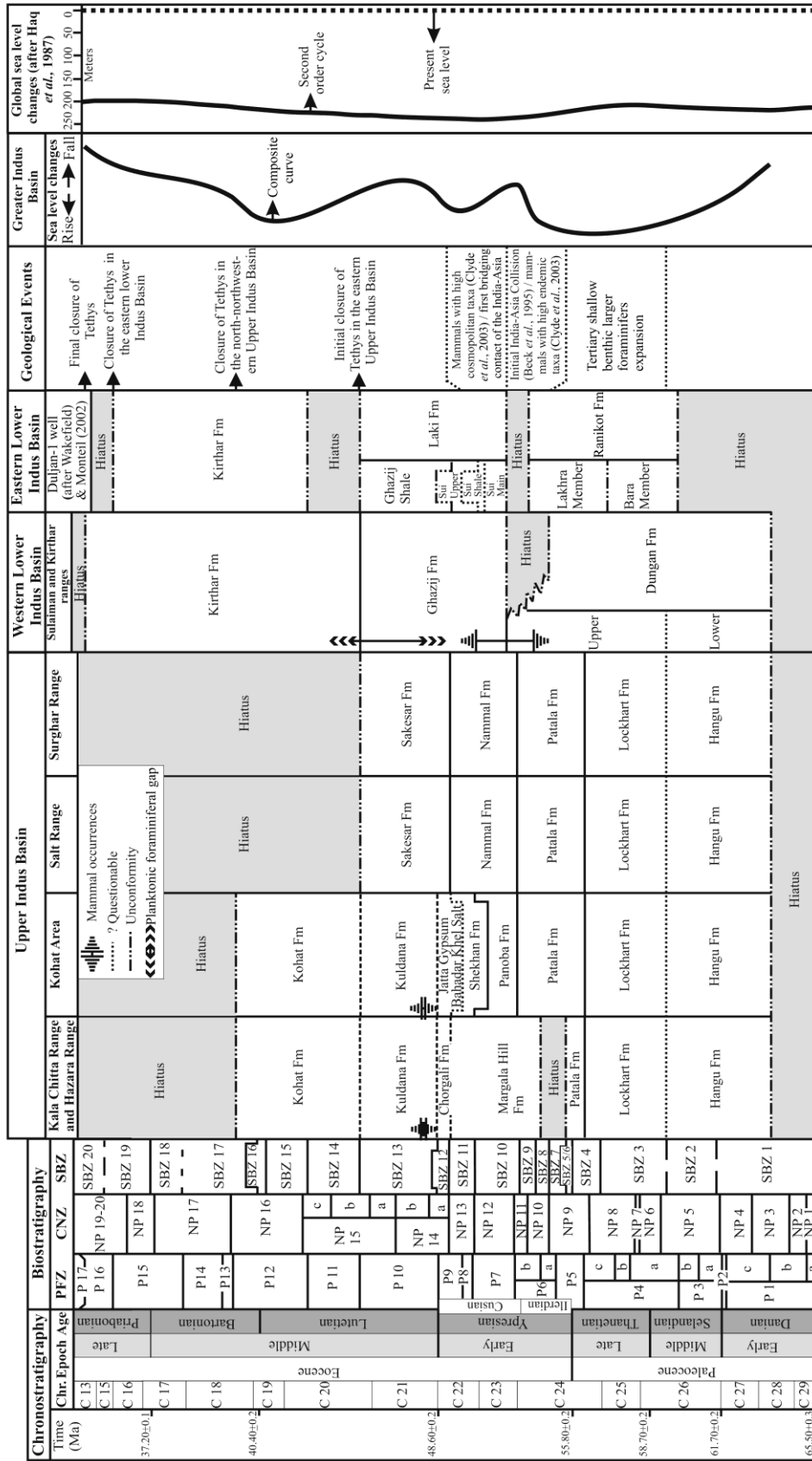


**Figure 2.** Regional stratigraphical correlation of the lower Cenozoic successions of the Greater Indus Basin, Pakistan, showing significant geological events and their correlation with basin stratigraphy and global sea level changes (after Afzal *et al.* 2009).

information on other key features (e.g. chambers, proloculus, embryonic apparatus), measured on multiple specimens. The stratigraphic distribution of these foraminifera is summarized in figures 3-7.

### **Stratigraphic setting**

The earliest Palaeogene transgression in the Greater Indus Basin deposited continental near-shore facies to shallow marine-deltaic facies of the Hangu Formation in the Upper Indus Basin and mixed carbonate siliciclastic to open-marine facies of the Dungan Formation in the Lower Indus Basin (Afzal *et al.* 2009, Fig. 2). Later, widespread carbonate platform deposition took place, represented by the Lockhart Formation in the Upper Indus Basin and the upper Dungan Formation in parts of the Lower Indus Basin (Afzal *et al.* 2009) (Figs 1, 2). Open marine sedimentation, as indicated by the planktonic foraminifer-bearing (= biozones P3-P6) shales of the Dungan Formation, formed deposits in the northwestern Sulaiman Range (e.g. Rakhi Nala and Zinda Pir areas) (Afzal *et al.* 2009). Continued transgression during the latest Paleocene-Early Eocene (= biozones P4c-P6) buried existing carbonate platforms and deposited both shallow and deep marine clastics of the Patala Formation in most of the Upper Indus Basin and shales of the Ghazij Formation (= biozones P7-P10) in parts of the Lower Indus Basin (Afzal *et al.* 2009) (Figs 1, 2). However, in some areas, for example the eastern Lower Indus Basin (e.g. Zranda, Muree Brewery and Hanna Lake sections of the present study), shallow marine carbonate deposition continued through the Late Paleocene to Early Eocene (i.e. Dungan Formation) (Afzal *et al.* 2009, in press; Kassi *et al.* 2009). The Ypresian-early Lutetian (biozones P7-P10) marked a shallowing upward

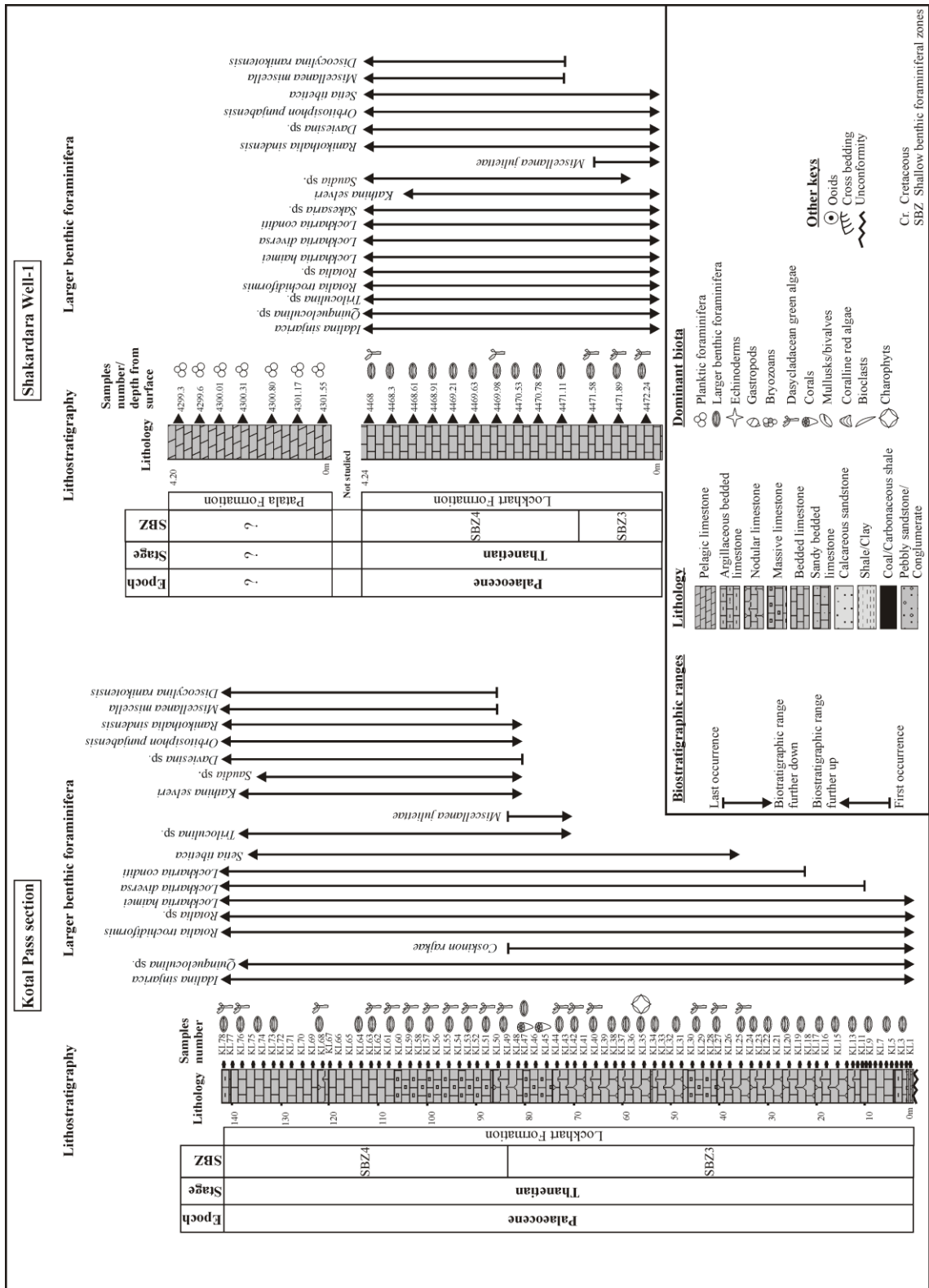
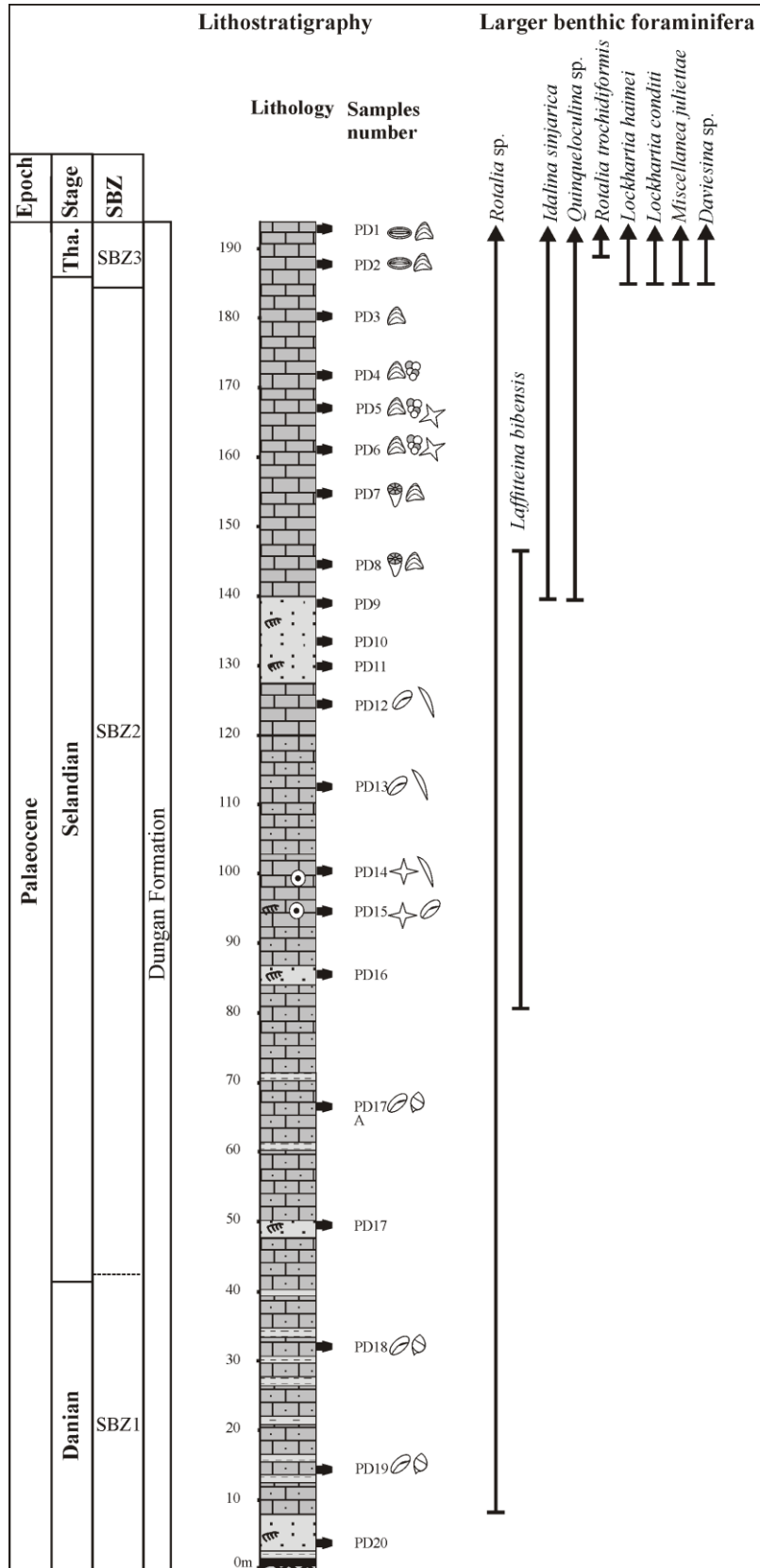


Figure 3. Stratigraphic distribution of larger benthic foraminifera of the Late Paleocene Lockhart Formation in the Upper Indus Basin (Kotal Pass section and Shakardara Well-1).

succession, depositing shallow marine carbonates of the Margala Hill, Nammal and Shekhan formations with the mudstone/shale-rich Panoba Formation in the Upper Indus Basin (Figs 1, 2). This was followed by a succession of evaporites (the Bahadar Khel Salt-Jatta Gypsum) and, finally, continental red bed/sandstone deposition of the mammal-bearing Kuldana Formation in the northern part and carbonates and shales of the Sakesar Formation in the southern part of the Upper Indus Basin (Afzal *et al.* 2009). Miocene-Recent terrestrial sediments derived from the Himalaya overlie the marine carbonates and shales of the Sakesar Formation in the Salt and Surghar ranges, marking the closure of the Tethys Ocean in the southeastern Upper Indus Basin (Afzal *et al.* 2009). However, late Lutetian-Priabonian marine deposition continued in some regions as represented by the upper Kirthar Formation in the Lower Indus Basin and the correlative uppermost Kohat Formation in the Upper Indus Basin. This followed closure of the Tethys Ocean in the north to northwestern parts of the Upper Indus Basin (e.g. Kohat area, Kala Chitta and Hazara ranges). The Tethys Ocean gradually retreated to the south-southwest of the Indus Basin through late Lutetian to Bartonian time and it finally closed in the Priabonian (Biozone P15; Afzal *et al.* 2009, Fig. 2). Oligocene marine sedimentation was restricted to the south of the Lower Indus Basin, while the rest of the Greater Indus Basin in Pakistan remained non-depositional lowland until the formation of Neogene molasse (Afzal *et al.* 2009).

### **Studied sections**

Two hundred surface rock samples from 5 outcrop sections and 20 core samples from a petroleum well core were collected. Detailed description of studied sections is given in Afzal *et al.* (in press) and a short summary is presented below.



**Figure 4.** Stratigraphic distribution of LBFs of the Paleocene Dungan Formation in the Mughal Kot section, Lower Indus Basin, Pakistan. Key as for Figure 3.

### **Upper Indus Basin**

1. *Kotal Pass section.* – The Kotal Pass section is situated in the northernmost part (33°38'01"N and 71°28'21"E) of the Upper Indus Basin in the Kohat Hill Range of northern Pakistan (Fig. 1). The exposed succession in Kotal pass consists of Jurassic to Paleocene marine carbonates and clastics. Seventyeight samples (KL1-78) at 1 to 2 m interval spacing from the Late Paleocene Lockhart Formation have been collected (Fig. 3). The Lockhart Formation is 144 m thick and is composed of limestone rich in dasycladaceans and LBFs (mainly smaller rotaliids, agglutinated forms, miliolids and rare miscellanids etc.) producing wackestone and packstone with rare grainstone and patch-reef boundstone textures (Fig. 3).

2. *Shakardara Well-1.* –The well is approximately 70 km south of Kohat (33°13'24"N and 71°29'39"E), Khyber Pakhtunkhwa Province, Pakistan, drilled by the Oil and Gas Development Company Limited, Pakistan (OGDCL) (Fig. 1). Two cores (Core-1 and Core-2) from the Late Paleocene-Early Eocene stratigraphic interval (= Lockhart and Patala formations) were recovered. There are no Paleocene-Eocene LBFs in Core-1, probably due to the deep pelagic environments as indicated by the abundance of planktonic foraminifera (Fig. 3). However, Core-2 consists of dasycladacean- and LBF-rich packstones and wackestones that have produced a number of LBF taxa.

### **Lower Indus Basin**

3. *Mughal Kot section:* – This section is located near the Mughal Kot Post (31°26'29"N and 70°05'07"E), 155 km west of Dera Ismail Khan city (Fig. 1). The exposed deposits range from marine Jurassic to continental Recent. A total of 21 surface rock samples at 5 m and 10 m intervals were collected from the Paleocene (Fig. 4). The Dungan Formation is 200 m thick, composed of a mixed carbonate- siliciclastic lower

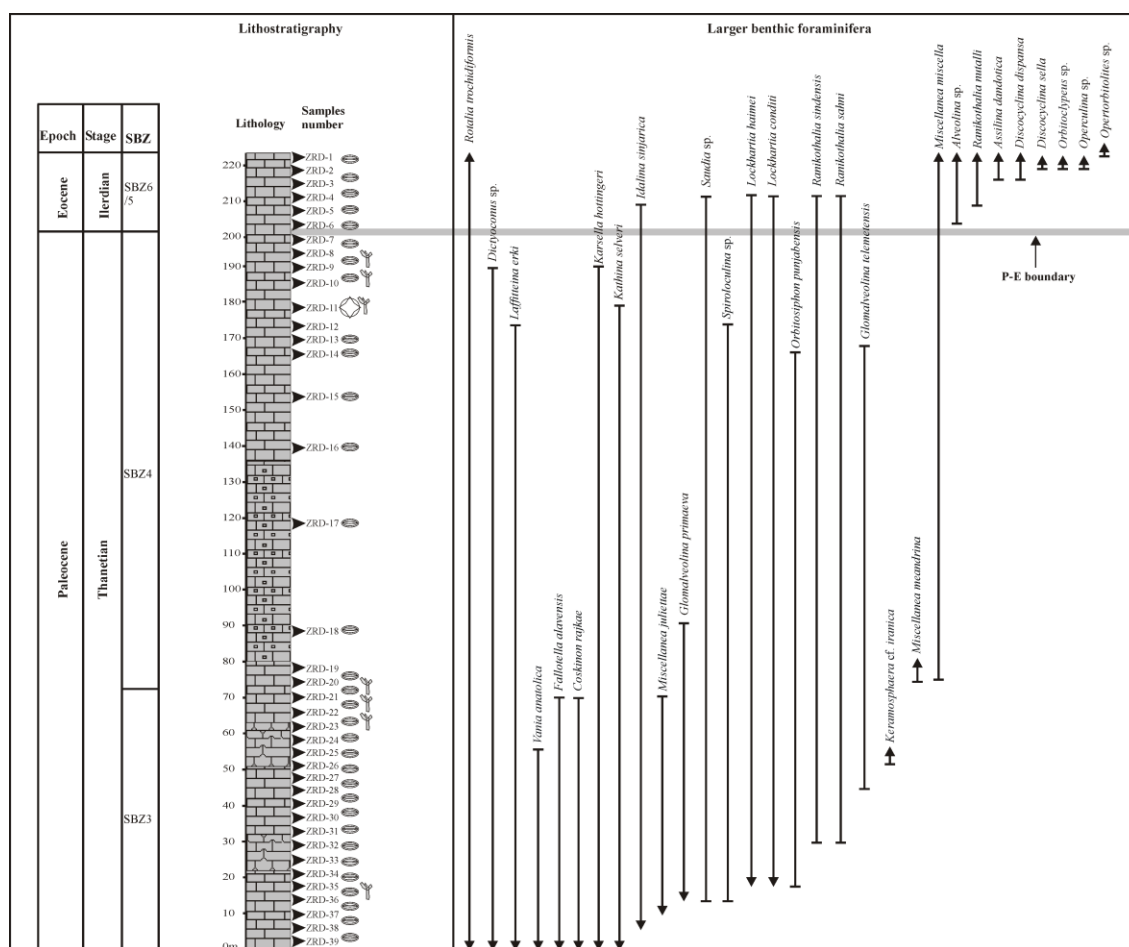


**Figure 5.** Stratigraphic distribution of LBFs of the Late Paleocene-Early Eocene Dungan Formation in the Zranda section, Lower Indus Basin, Pakistan. Key as for Figure 3.

unit succeeded by a LBF- to coral-algal rich rudstone, bindstone, grainstone and packstone upper unit (Fig. 4). The lower unit contains rare LBFs, represented by smaller rovaliids. However, the upper unit yields a number of LBFs.

4. *Zranda section.* – The Zranda section is located near Zranda village (30°28'27"N and 67°37'07"E), 25 km northeast of Kach, Balochistan (Fig. 1). The lithostratigraphic succession consists of the Late Cretaceous volcanoclastic-sedimentary Bibai Formation, Late Paleocene-earliest Eocene shallow marine carbonates of the Dungan Formation, and Early Eocene open marine clastics of the Ghazij Formation (Kassi *et al.* 2009). The Dungan Formation is 222 m thick, consisting of LBF-rich wackestone, packstone and

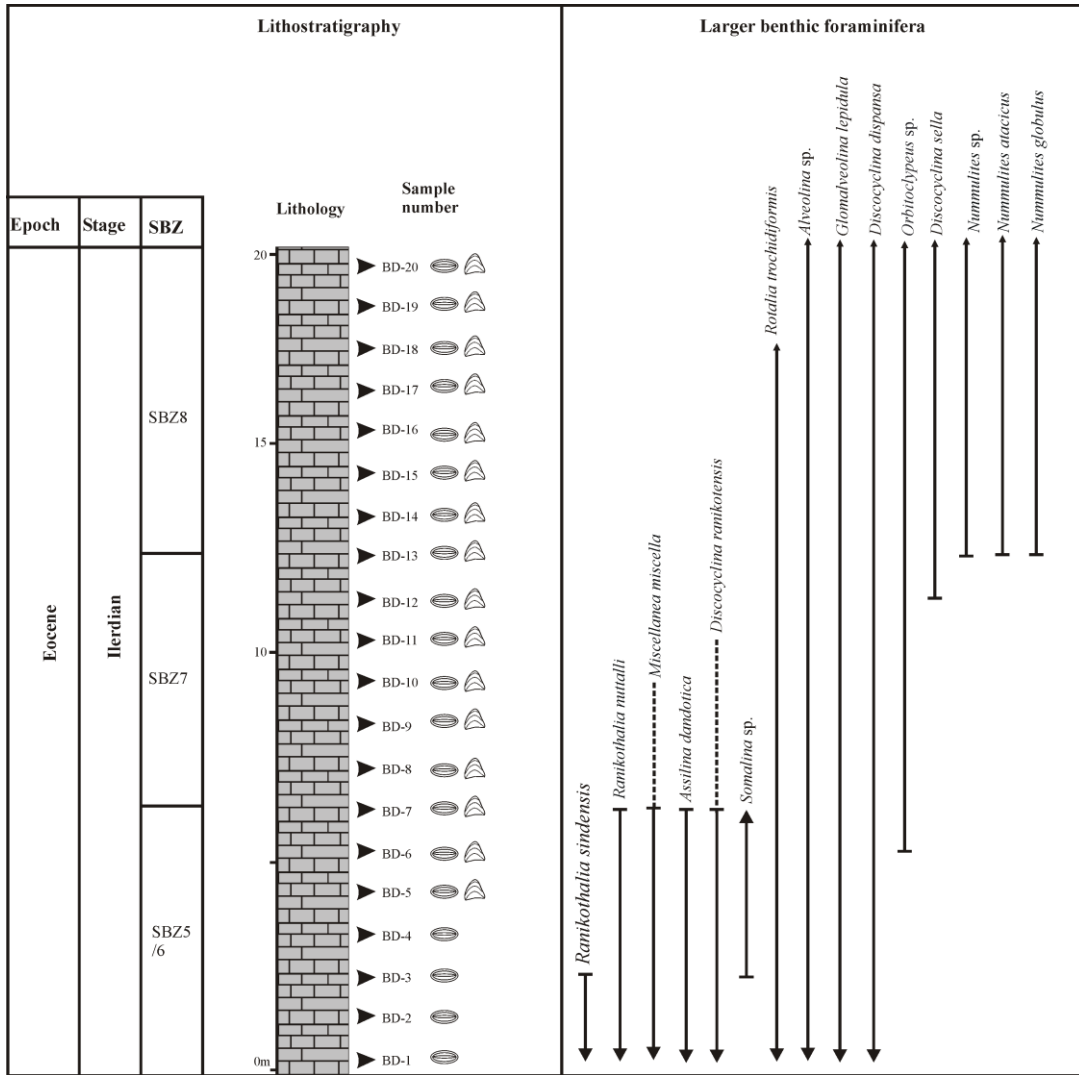


**Figure 6.** Stratigraphic distribution of LBFs of the Early Eocene Dungan Formation in the Muree Brewery section, Lower Indus Basin, Pakistan. Key as for Figure 3.

grainstone (Fig. 5). A total of 39 rock samples (ZRD1-39) at 2 to 3 m interval spacing were collected (Fig. 5).

5. *Muree Brewery section.* – The well exposed Muree Brewery section is situated 8 km west (30°11'22"N and 66°56'44"E) of Quetta city in Balochistan Province (Fig. 1). The section exposes a thick succession of Late Cretaceous (Parh, Hanna Lake Limestone and Fort Munro formations) to Early Eocene (Dungan and Ghazij formations) marine deposits (Kassi *et al.* 2009). In the Muree Brewery section, the Dungan Formation is 19.2 m thick, and is mainly composed of LBF-rich grainstone and packstone. A total of

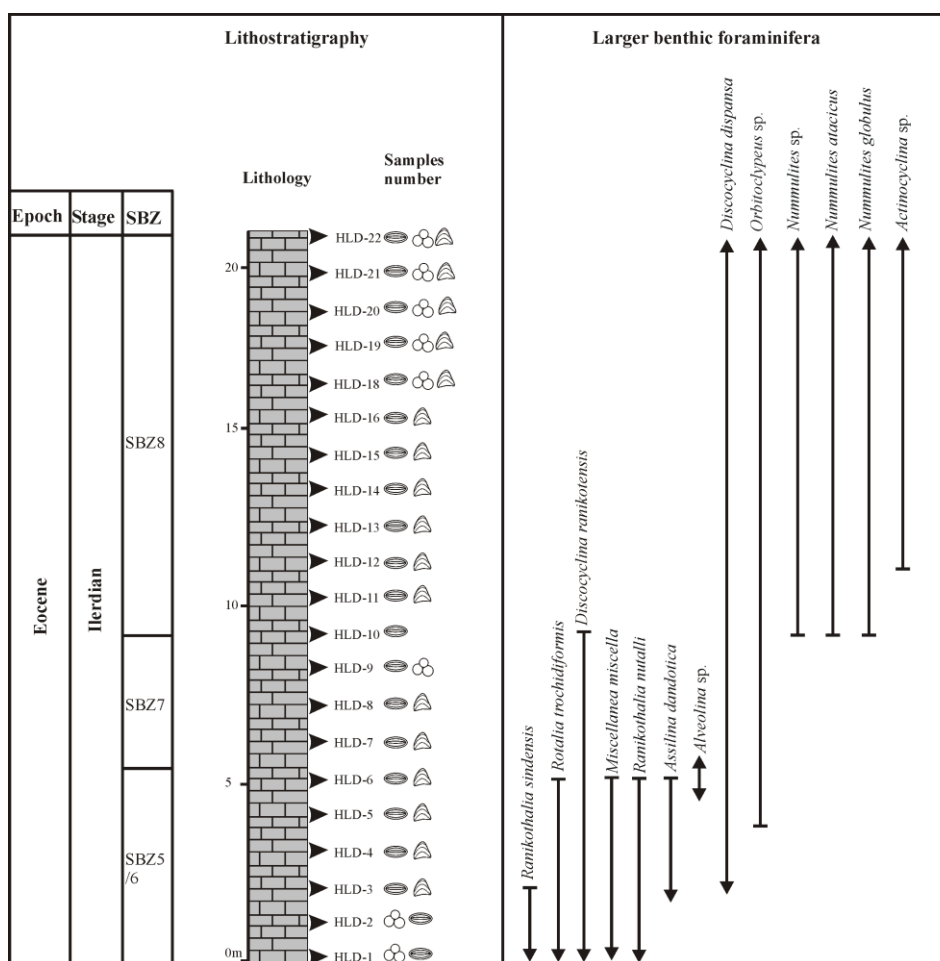


**Figure 7.** Stratigraphic distribution of LBFs of the Early Eocene Dungan Formation in the Hanna Lake section, Lower Indus Basin, Pakistan. Key as for Figure 3.

20 rock samples (BD1-20) at intervals of less than 1 m spacing have been collected (Fig. 6).

6. *Hanna Lake section.* – This section is located near Hanna Lake (30°15'17"N and 67°05'45"E), 10 km northeast of Quetta city, Balochistan (Fig. 1). The Hanna Lake section has a similar stratigraphic setting to the nearby Muree Brewery section. However, the thickness of the Dungan Formation here is 22 m and it is composed largely of LBF-rich packstone, wackestone and grainstone with varied amounts of coralline algae and planktonic foraminifera (Fig. 7). A total of 22 rock samples (HLD1-22) at intervals of 1 m spacing have been collected.

### **Systematic palaeontology**

In assessing the taxonomy of the LBFs from the Indus Basin I have consulted the extensive foraminifer collections of Smout (1954) and Davies (1952) that are housed in the Palaeontology Department of the Natural History Museum, London (NHM). Other collections consulted include the Davies (1927, 1930, 1937), Nuttall (1926) and Davies & Pinfold (1937) collections at the Calcutta Museum of the Geological Survey of India; the Sirel (1969, 1997a) collection at the General Directorate of Mineral Research and Exploration of Turkey, Ankara; the Hottinger (1960, 2009) and Leppig (1988) collections at the Naturhistorisches Museum, Basel (NMB); the Mangin (1954) collection at the National Museum of Natural History of the United State of America (NMNH); and the Sirel & Gündüz (1985) collection at the Museum d'Histoire Naturelle, Geneve. All specimens described and figured here are housed in the collections of the British Geological Survey (BGS), Keyworth, Nottingham, UK (see Appendix 9 for BGS repository numbers).

Suborder ROTALIINA Loeblich & Tappan, 1987

Superfamily ROTALIACEA Loeblich & Tappan, 1987

Family ROTALIIDAE Ehrenberg, 1839

Genus **LOCKHARTIA** Davies, 1932

*Type species. Dictyoconoides haimeii* Davies, 1927, from the Thal area of NW Pakistan.

**Lockhartia haimeii** (Davies, 1927) Plate 1, Figures 1-8

1927 *Dictyoconoides haimeii* sp. nov. Davies, p. 280-281, pl. XXI, figs 13-15; pl. XXII, fig. 6.

1932 *Lockhartia haimeii* (Davies); Davies, p. 407, pl. II, figs 4-6.

1937 *Lockhartia haimeii* (Davies); Davies & Pinfold, p. 45-46, pl. VII, figs 9-13, 15.

1954 *Lockhartia haimeii* (Davies, 1927); Smout, p. 49-50, pl. II, figs 1-14.

1991 *Lockhartia haimeii* (Davies); Butt, pl. 2, fig. h.

1999 *Lockhartia haimeii* (Davies); Akhtar & Butt, p. 131-132, pl. 2, figs. 3-5. (q.v. for full synonymy).

2008 *Lockhartia haimeii* (Davies); BouDagher-Fadel, p. 355, pl. 6.28, fig. 12.

2009 *Lockhartia haimeii* Davies, 1927; Afzal *et al.*, p. 17, pl. 1, figs 7, 9.

In press *Lockhartia haimeii* (Davies); Afzal *et al.*, Fig. 8F.

*Holotype.* Designated Davies (1927, pl. XXI, fig. 14) from the Late Paleocene Ranikot Formation, Thal area of Pakistan. This material was kept in a private collection of the author and the repository is presently unknown.

*Material.* Seventy-six axial sections from samples KL-1-7, 14-33, 41-53, 56-61, 70-73, 74-78 (Kotal Pass section); 32 axial sections from samples 4472.24, 4471.89, 4471.11, 4470.78, 4470.53, 4469.98, 4469.63, 4468.91, 4468.61, 4468.3 (Shakardara Well-1); 24 axial sections from samples ZRD4-6, 9-10, 15-16, 23-24, 28-29, 32-33, 35, 37-39 (Zranda section).

*Dimensions.* T. 602 $\mu$ m–1775 $\mu$ m (50 specimens); D. 995 $\mu$ m–3350 $\mu$ m (50 specimens).

*Diagnosis.* Pillars and plates distinct, peripheral smooth band at margin of base, perforation coarse, chambers wedge-shaped, ornament of coarse bars and pustules (amended from Smout 1954).

*Description.* Test conical dorsally with convex basal margin. Spire comprises three to four whorls. Chambers are punctate, lack a marginal band and have indented sutures. Base has a smooth peripheral band with a zone of small sub-equal coarse pustules and

bars. Umbilical area is large with crowded long pillars and plates. In axial section, the chambers are evolute with thickened, coarsely perforated outer walls.

*Discussion.* *L. haimeii* is distinguishable from *L. prehaimeii* Smout, 1954 by its coarse pustules and bars and from *L. diversa* Smout, 1954 by its crowded pillars and plates. *L. tipperi* (Davies, 1937) differs from *L. haimeii* by its fine perforation of the outer wall. *L. conditi* (Nuttall, 1926) is distinguished by its huge pillars, indented marginal sutures and fine perforations in the outer wall.

*Distribution.* *L. haimeii* is a common species of the Lockhart Formation in the Kotal Pass section and Shakardara Well-1, and of the Dungan Formation in the Zranda section. In this study, the species is associated with LBFs typical of the Late Paleocene-earliest Eocene SBZ3-SBZ6 biozones interval including *Miscellanea juliettae*, *M. miscella*, *Ranikothalia sindensis*, *R. nuttalli* and *Alveolina*. In Tethyan carbonate successions (from Europe to India), *L. haimeii* is widely reported from the Late Paleocene-Early Eocene interval (e.g. Butterlin & Fourcade 1989; Racey 1995; Serra-Kiel *et al.* 1998; Jauhri & Agarwal 2001; Mathur *et al.* 2009; Afzal *et al.* in press and references therein).

**Lockhartia conditi** (Nuttall, 1926) Plate 1, Figures 9-16

1926 *Dictyoconoides conditi* sp. nov. Nuttall, p. 119, pl. XI, figs 7-8.

1927 *Dictyoconoides conditi* Nuttall; Davies, p. 279, pl. XXI, figs 10-12.

1930 *Dictyoconoides conditi* Nuttall; Davies, p. 76-77, pl. X, figs. 9.

1937 *Lockhartia conditi* (Nuttall); Davies & Pinfold, p. 47-48, pl. V, fig. 24.

1954 *Lockhartia conditi* (Nuttall, 1926); Smout, p. 55-56, pl. V, figs 16-19.

1999 *Lockhartia conditi* (Nuttall); Akhtar & Butt, p. 132, pl. 3, figs 1-2. (q.v. for full synonymy).

2008 *Lockhartia conditi* (Nuttall); BouDagher-Fadel, p. 355, pl. 6.28, figs 14-15.

2009 *Lockhartia conditi* Nuttall, 1926; Afzal *et al.*, p. 17, pl. 1, figs 2,4.

In press *Lockhartia conditi* (Nuttall); Afzal *et al.*, fig. 8D.

*Holotype.* Designated Nuttall (1926, pl. XI, fig. 7) from the Late Paleocene Ranikot Formation of Meting area, Sind, Pakistan. This material was kept in a private collection of the author and the repository is presently unknown.

*Material.* For this study 12 axial sections from samples 4472.24, 4471.89, 4471.11, 4470.78, 4470.53, 4469.98, 4469.63 (Shakardara Well-1); 61 axial sections from samples KL3-35, 38-45, 48-53, 56-58, 61-64, 68-78 (Kotal Pass section); 34 samples ZRD4-9, 13-22, 25-31, 33-36 (Zranda section).

*Dimensions.* T. 803 $\mu$ m-1190 $\mu$ m (35 specimens); D. 1300 $\mu$ m-2225 $\mu$ m (34 specimens).

*Diagnosis.* High trochospiral, conical test with few huge pillars in umbilical region, marginal sutures are indented, fine perforation (amended from Smout 1954).

*Description.* Test high trochospiral, conical dorsally with sub-acute margin and slightly convex base. Chambers finely perforate. Larger, but fewer pillars in umbilical region. In axial section, umbilical cavities are constricted with small portions of the horizontal plates between few large thick pillars. Large specimens have an increase in length of the gerontic chambers of the last whorl.

*Discussion.* *L. conditi* is distinguished from *L. haimei* (Davies, 1927), *L. hunti* Ovey, 1947, and *L. tipperi* (Davies, 1926) by its high trochospiral, conical shell with few thick pillars in the umbilical region (see Pl. 1, Figs 9-12, 14-16). Small portions of the horizontal plates between the pillars may be distinguished in specimens from Qatar (Smout 1954) and also in the figure of the holotype given by Nuttall (1926, pl. 11, fig. 7).

*Distribution.* *L. conditi* is common in the Lockhart Formation of the Kotal Pass section and Shakardara Well-1, and in the Dungan Formation of the Zranda section where it commonly occurs with *Alveolina*, *Assilina dandotica*, *Discocyclusa dispansa*, *Ranikothalia sindensis* and *R. nuttalli*, suggesting a biostratigraphical range of SBZ3-SBZ5/6 biozones. In Tethys, *L. conditi* is commonly reported from the Late Paleocene to Early-Middle Eocene (Butterlin & Fourcade 1989).

**Lockhartia conica** Smout, 1954 Plate 1, Figures 17-18

1954 *Lockhartia conica* sp. nov. Smout, p. 35-54, pl. IV, figs 1-3.

2005 *Lockhartia conica* Smout; Afzal *et al.*, pl. 1, fig. 5.

In press *Lockhartia conica* Smout; Afzal *et al.*, fig. 8E.

*Holotype.* Designated Smout (1954, pl. IV, fig. 1), NHM No. P. 40065, from the Paleocene of Qatar; paratypes, NHM No. P. 40195-6, figured by Smout (1954, pl. IV, figs 2-3).

*Material.* Two axial sections from sample 4472.24 (Shakardara Well-1).

*Dimensions.* T. 1120µm-1400µm (2 specimens); D. 800µm-1020µm (2 specimens).

*Diagnosis.* High conical test with weak pillars and plates, smooth peripheral band, high wedge-shaped chambers.

*Description.* Test highly conical with chamber nearly twice as high as long. Chambers wedge-shaped. Margin is acute and ventral surface plane. Peripheral band is smooth on which the radial sutures of the last whorl are hardly visible. Umbilical area is occupied by feebly developed pillars and plates.

*Discussion.* *L. conica* is distinguished from other species of *Lockhartia* by its high conical test with smooth peripheral band, weak pillars and high chambers.

*Distribution.* *L. conica* occurs in the lower part of Core-2 in Shakardara Well-1 (samples 4472.24-4471.11), associated with *Miscellanea juliettae* and *M. miscella*, indicating a biostratigraphic range of SBZ3-SBZ4 biozones. Various studies in the wider Tethys (including Pakistan) report *L. conica* from the Paleocene-Early Eocene (e.g. Butterlin & Fourcade 1989; Weiss 1993; Akhtar & Butt 1999).

**Lockhartia diversa** Smout, 1954 Plate 1, Figures 19-21.

1954 *Lockhartia diversa* sp. nov. Smout, p. 52-53, pl. III, figs 1-20.

2008 *Lockhartia diversa* Smout, 1954; Ismail & Boukhary, p. 93, pl. 2, fig. 6.

*Holotype.* Designated Smout (1954, pl. III, fig. 1), NHM No. P. 40060, from the Paleocene of Qatar; paratypes, NHM No. P. 40061-4, 40187-94, figured by Smout (1954, pl. III, figs 2-9).

*Material.* Eleven axial sections from samples 4472.24, 4471.89, 4471.11, 4468.61 (Shakardara Well-1); 10 axial sections from samples KL18-30, 51-59, 75-78 (Kotal Pass section).

*Dimensions.* T. 816µm-2080µm (13 specimens); D. 1240µm-2980µm (13 specimens).

*Diagnosis.* Test oblately spheroidal with irregular shaped short pillars; elongated, high, chambers.

*Description.* Test rounded with an oblate spheroid dorsal surface and slightly convex base. Chambers are high, elongated in outline, punctate with ornament on sutures. Septa straight, strongly inclined. Smooth peripheral band with very irregular shaped, short pillars; often shows several bars radiating from the last chamber.

*Discussion.* The irregular shaped short pillars and elongated chambers of *L. diversa* are distinct from the plates and pillars of *L. haimei* (Davies, 1927), *L. tipperi* (Davies, 1937) and *L. prehaimei* Smout, 1954.

*Distribution.* *L. diversa* is recorded in the Lockhart Formation in the Kotal pass section and Core-2 of the Shakardara Well-1. It is associated with *Ranikothalia sindensis*, *Miscellanea miscella* and *Discocyclina ranikotensis* indicating a Late Paleocene (SBZ3-SBZ4 biozones) age. *L. diversa* has been reported from the Paleocene of Qatar and Iraq (Smout 1954), Oman (Racey 1995), Turkey (Sirel 1998) and Iran (Rahaghi 1983).

Genus **SAKESARIA** Davies, 1937

*Type species.* *Sakesaria cotteri* Davies in Davies & Pinfold, 1937, from the Nammal and Sakesar formations, Salt Range, Pakistan.

**Sakesaria sp.** Plate 1, Figures 22-24

*Material.* Four axial sections from samples 4468, 4470.78, 4471.58 (Shakardara Well-1).

*Dimensions.* T. 1150µm-1800µm (4 specimens); D. 1000µm-1430µm (4 specimens).

*Description.* Elongate conical to sub-cylindrical test, very high acute trochospiral coiling, elongated chambers, bulged base, more conical apex. Chambers are finely punctuate with pustules at the junction of septal and spiral sutures.

*Discussion.* The acute spire, more bulging base and conical test indicate assignment of this material to *Sakesaria*. However, there is insufficient material to identify the species.

*Distribution.* This taxon is recorded in the Core-2 of Shakardara Well-1, normally associated with *Miscellanea juliettae*, *Ranikothalia sindensis*, *Lockhartia haimei* and

*Miscellanea miscella*, indicating an SBZ3-SBZ4 biozonal range. Elsewhere, species of *Sakesaria* are reported from the Paleocene-Early Eocene of Qatar (Smout 1954), Yemen (Ismail & Boukhary 2008) and Oman (Racey 1995).

Genus **LAFFITTEINA** Marie, 1946

*Type species. Laffitteina bibensis* Marie, 1946, from the Paleocene of Montian, France.

**Laffitteina bibensis** Marie, 1946 Plate 2, Figures 1-3

1923 *Nummulites mengaudi* nov. sp. Astre, p. 360, pl. 12.

1946 *Laffitteina bibensis* nov. sp. Marie, p. 431-432, text-figs 14-16, pl. 5, figs 1-6.

1996 *Laffitteina mengaudi* (Astre); Sirel, pl. I, figs. 1-22.

1998 *Laffitteina mengaudi* (Astre); Sirel, p. 88, pl. 46, figs. 1-23, pl. 47, figs. 1-22.

2005 *Laffitteina bibensis* Marie (1946); Inan *et al.*, p. 376, figs 4(E), 5(B), 7(D).

(q.v. for full synonymy).

In press *Laffitteina bibensis* Marie; Afzal *et al.*, fig. 8A-C.

*Holotype.* Designated Marie (1945, pl. 5, figs 3-4) as collection No. 4410, from the early Paleocene limestone of the Montian, France. The number may refer to a private collection (of the author?) and the repository for this material is presently unknown.

*Material.* Three axial and 2 equatorial sections from samples PD8, 12, 14, 16, 12 (Mughal Kot section).

*Dimensions.* T. 300µm-700µm (3 specimens); D. 600µm-1500µm (5 specimens).

*Diagnosis.* Test planispirally coiled, planoconvex to slightly biconvex; septa double, with ramifying interseptal canals; strong umbilical plug.

*Description.* Test planispiral, planoconvex or slightly biconvex with umbilical thickening on both sides, elongated chambers, double septa that tilt backwards with ramifying interseptal canals. Finely perforated outer wall. Well-defined plug in the umbilical region.

*Discussion.* *L. bibensis* differs from other species of *Laffitteina* by having a nearly planoconvex or slightly biconvex test with a more prominent plug in the umbilical region.

*Distribution.* *L. bibensis* is recorded in the middle part of the Dungan Formation in the Mughal Kot section, associated with *Rotalia* sp. and *Idalina sinjarica* and the coralline alga *Distichoplax biserialis*, which indicate a SBZ1-SBZ2 biozonal range. *L. bibensis* has been reported from the Paleocene of Iran (Bignot & Neumann 1991) and the Danian to Thanetian of NE Turkey (Sirel 1998; Inan *et al.* 2005).

**Laffitteina erki** (Sirel, 1969) Plate 2, Figures 4-9

1969 *Orduina erki* Sirel, p. 145, pl. 1, figs 1A-D; pl. 2, figs 1-5; pl. 3, fig. 3.

1988 *Kathina erki* (Sirel); Loeblich & Tappan, p. 661, pl. 760, figs 6-10.

1994 *Laffitteina erki* (Sirel); Sirel, p. 47, pl. I, pl. II.

1998 *Laffitteina erki* (Sirel); Sirel, p. 91, pl. 51, figs. 1-8.

2005 *Laffitteina erki* (Sirel), 1969; Inan *et al.*, p. 376, figs 4(E), 7(E). (q.v. for full synonymy).

in press *Laffitteina erki* (Sirel); Afzal *et al.*, fig. 8H.

*Holotype.* Designated Sirel (1969, pl. 2, fig. 1; pl. 3, fig. 1), General Directorate of Mineral Research and Exploration of Turkey, Ankara, collection No. SE1, from the Paleocene of the Gököy area, Turkey.

*Material.* Thirteen axial and 6 equatorial sections from samples ZRD12-15, 21-30, 34-39 (Zranda section).

*Dimensions.* T. 700µm-2020µm (26 specimens); D. 900µm-3050µm (21 specimens).

*Diagnosis.* Strongly trochospiral test with convex ventral side, flat to concave dorsal side; double septa; numerous pillars in umbilical region with coarsely perforated outer wall.

*Description.* Test high trochospiral with convex ventral side and flat to concave dorsal side. Umbilical area filled by numerous pillars. Thin vertical canals between the umbilical pillars; septa double, with ramifying interseptal canals that open as two alternating rows of pores along the sutures on the dorsal side. Coarsely perforate outer wall.

*Discussion.* *L. erki* is distinguished from all other species of *Laffitteina* such as *L. bibensis* Marie, 1946 and *L. koyulhisarensis* (Sirel, 1996) by its large size and highly trochospiral test.

*Distribution.* *L. erki* is recorded in the Dungan Formation of the Zranda section, associated with *Glomalveolina primaeva*, *Miscellanea juliettae*, *M. miscella*, *Miscellanites meandrina*, *Fallotella alavensis* and *Coskinon rajkae*, indicating a SBZ3-SBZ4 biostratigraphic range. *L. erki* has been reported from other parts of Tethys (e.g. Slovenia, Özgen & Akyazi 2001; Turkey, Özgen-Erdem *et al.* 2005; Inan *et al.* 2005), where a range of biozones SBZ3-SBZ4 is indicated.

### Genus **ROTALIA** Lamarck, 1804

*Type species.* *Rotalia trochidiformis* Lamarck, 1804, from the Eocene of the Paris Basin, France,

**Rotalia trochidiformis** Lamarck, 1804      Plate 2, Figures 20-21

1804 *Rotalites trochidiformis* Lamarck, p. 183-185, pl. 62, figs b-c.

1932 *Rotalia trochidiformis* (Lamarck); Davies, p. 408, pl. 2, figs, 8,10-15; pl. 3, figs. 1-13; pl. 4, figs. 3-6, 9-11 ,

1954 *Rotalia trochidiformis* (Lamarck, 1804); Smout, p. 43-45, pl. I, figs 1-6.

1974 *Rotalia trochidiformis* (Lamarck); Murray & Wright, p. 20-23, pl. 11, figs 4, 5.

1990 *Rotalia trochidiformis* (Lamarck) emend.; Haynes & Whittaker, p. 97-99, pl. 1-3, text-figs 1-3. (q.v. for full synonymy).

1999 *Rotalia trochidiformis* Lamarck; Akhtar & Butt, p. 132, pl. III, fig. 3.

2008 *Rotalia trochidiformis* Lamarck; BouDagher-Fadel, p. 347, pl. 6.25, fig. 5.

2009 *Rotalia trochidiformis* Lamarck, 1804; Afzal *et al.* p. 17, pl. 1, fig. 12.

*Type material.* Lamarck (1804, pl. 62, figs b-c) did not assign types to his original material from the Eocene of Grignon, Paris Basin, France. Subsequently, Davies (1932, pl. 3, figs. 4,5,7) selected a lectotype from the original type series, deposited within the Defrance Collection in the Museum d'Histoire Naturelle, Caen, France which was destroyed by a bomb attack on Caen during World War II (Haynes & Whittaker 1990, p. 96). The sole remaining primary type specimen of Lamarck is housed in the Muséum d'Histoire Naturelle, Geneva, Switzerland, designated as paralectotype by Davies (1932, pl. 2, fig. 8).

*Material.* Ten equatorial and 21 axial sections from samples KL1-78 (Kotal Pass section); 20 axial sections from samples 4472.24-4468 (Shakardara Well-1); 10 axial sections from samples PD1-2 (Mughal Kot section); 52 axial sections from samples ZRD1-39 (Zranda section).

*Dimensions.* T. 600µm-1700µm (70 specimens); D. 900µm-2400µm (70 specimens).

*Diagnosis.* Test trochoid, biconvex with evolute dorsal side slightly higher than the involute ventral side; periphery acute, keeled, entire. Chambers are trapezium in shape, increase in size as added with backward curved sutures and an umbilical aperture in the form of openings. Sutures backward curving; well-developed vertical pillars and fissures in umbilical region (amended from Haynes & Whittaker 1990).

*Description.* Test trochospiral with convex and smooth dorsal side and convex to plane ventral side; periphery acute, keeled in its entirety. Dorsal septal sutures are straight and reclined. Ornament on base of test comprises a number of granules separated by deep fissures, which run zigzag along the sutures. Trapezium-shaped chambers with backward curved sutures and umbilical aperture in the form of openings; chambers increase in size as added. Earlier chambers show strong development of vertical pillars and secondary and tertiary fissures cutting back into the walls.

*Discussion.* *R. trochidiformis* is distinguished from *R. hensoni* Smout, 1954 and other species of *Rotalia* by its trochospiral and biconvex test and its discontinuous umbilical pillars.

*Distribution.* *R. trochidiformis* is present throughout the Lockhart Formation of the Kotal Pass section and Shakardara Well-1 and in the Dungan Formation in the Zranda section. In the Muree Brewery section, it occurs in the lower to upper parts of the Dungan Formation. These occurrences indicate a SBZ3-SBZ8/9? biostratigraphic range for *R. trochidiformis*. *R. trochidiformis* is common in Tethys and ranges from the Paleocene to the Early Eocene (biozones SBZ3-SBZ8, and possibly into SBZ9) (e.g. Qatar, Smout 1954; Pakistan, Weiss 1993, Akhtar & Butt 1999; NE Turkey, Inan *et al.* 2005; N Turkey, Özgen-Erdem 2005; Northern India, Mathur *et al.* 2009; Oman, White 1994).

**Rotalia sp.** Plate 2, Figures 16-19

*Material.* Twenty-three axial sections from samples KL11-41 (Kotal Pass section); 31 axial sections from samples ZRD1-3, 11-18, 36-39 (Zranda section).

*Dimensions.* T. 300µm-1150µm (31 specimens); D. 650µm-1970µm (31 specimens).

*Description.* Test biconvex, trochospiral with thick lamellar pillars filling umbilical area. Septal flap attaches to the peripheral margin of septum which doubles septal wall. Wall calcareous, perforated except in imperforate peripheral margin. Strong spiral canal below cortical chamber layer. Pustules and granules in the umbilical area are simple, extending toward margin. Umbilical fissures are well-defined.

*Discussion.* *Rotalia* sp. has a relatively small test compared to *R. trochidiformis* Lamarck, 1804.

*Distribution.* This species is present in all studied sections. *Rotalia* is cosmopolitan and has been widely reported from Tethys (Loeblich & Tappan 1988).

Genus **KATHINA** Smout, 1954

*Type species.* *Kathina delseota* Smout, 1954, from the Paleocene of Qatar.

**Kathina selveri** Smout, 1954 Plate 2, Figures 10-15

1954 *Kathina selveri* sp. nov. Smout, p. 62-63, pl. VI, figs 11-13.

2009 *Kathina selveri* Smout, 1954; Afzal *et al.*, p. 17, pl. 1, fig. 8.

In press *Kathina selveri* Smout; Afzal *et al.*, fig. 8G.

*Holotype.* Designated Smout (1954, pl. VI, fig. 11), NHM No. P. 40095, from the Paleocene of Qatar.

*Material.* Ten axial sections from samples KL48-59, 71-74 (Kotal pass section); 15 axial sections from samples ZRD10, 15-16, 19-20, 26-30, 34-39 (Zranda section); 9 from samples 4471.89-4468.61 (Shakardara well-1).

*Dimensions.* T. 600 $\mu$ m -1500 $\mu$ m (35 specimens); D. 850 $\mu$ m- 2400 $\mu$ m (30 specimens).

*Diagnosis.* Unequally biconical test with solid axial plug; smooth dorsal and peripheral grooves on ventral side (amended from Smout 1954).

*Description.* Test unequally biconical, finely perforate, smooth dorsal surface and radial grooves on ventral side; septa double, straight and radial. Radial rows of vertical canals to pores present on the base of the chamber; those of the inner whorl are scattered round the plug. In axial section, chambers are nearly evolute dorsally, and taper ventrally towards the umbilicus. Laminae can be seen around the test, thick at the dorsal pole, thicker in the ventral plug, and thinning out towards the margin.

*Discussion.* *K. selveri* is distinguished from *K. major* Smout, 1954 by its solid axial plug and smaller test size. *K. nammalensis* Haque, 1956 is distinguished from *K. selveri* by its crowded septa and a smooth test on both sides.

*Distribution.* *K. selveri* is recorded in the Lockhart Formation in the Kotal Pass section and Core-2 of the Shakardara Well-1 and Dungan Formation in the Zranda section. This species occurs in association with LBFs typical of the SBZ3-SBZ4 biozones. It has been reported from the late Paleocene of northern Turkey (Özgen-Erdem 2005), Italy (Özgen 2001), Slovenia (Özgen & Akyazi 2001), Qatar (Smout 1954) and Oman (White 1994).

Superfamily ORBITOIDOIDEA Schwager, 1876

Family LEPIDORBITOIDIDAE Vaughan, 1933

Genus **SETIA** Ferrandez-Canadell, 2002

*Type species.* *Lepidorbitoides tibetica* Douvillé, 1916, by subsequent designation of Ferrandez-Canadell (2002, p. 9-10, pl. 2, figs 1-29; pl. 3, figs 1-11); from the Paleocene of Tibet.

*Diagnosis.* Bilamellar-perforate test of discoidal, more or less pronounced concavo-convex shape, and circular to somewhat oval outline with lobate margin; with a main equatorial layer of arcuate to sub-rectangular chamberlets arranged in concentric annuli. Dorsal and ventral differentiated sides, with lateral chamberlets on the dorsal side and a central canal system forming a three-dimensional network, sometimes with enlarged, vacuolar cavities in the ventral side. Piles in both ventral and dorsal sides, which produce granules in the lateral surfaces, arranged in a concentric ring. Megalospheric forms with bilocular embryo followed either by a first single auxiliary chamber or by a chamber constituted by two auxiliary chamberlets depending on the species, and orbitoidal growth changing progressively into annular-cyclic growth, with annular chambers subdivided into rectangular chamberlets. Microspheric forms with an initial spiral stage. Equatorial chamberlets are connected by three different types of communications: those of adjacent annuli by stolons; those of the same annulus, by a distal annular passage; and those of alternate (not adjacent) annuli by radial passages of the central system (after Ferrandez-Canadell 2002, p. 9).

**Setia tibetica** (Douvillé, 1916)      Plate 3, Figures 1-6

1916 *Lepidorbitoides tibetica* Douvillé, p. 34, pl. XIV, figs 1-6.

1940 *Orbitosiphon punjabensis* (Douvillé); Rao, p. 414-415, fig. 1.

1944 *Orbitosiphon tibetica* (Douvillé, 1916); Rao, p. 95-99, pl. 1, figs 2-3.

1956 *Actinosiphon tibetica* (Douville); Smout & Haque, p. 52, pl. 11, fig. 6.

1999 *Actinosiphon tibetica* (Douville); Akhtar & Butt, p. 140-142, pl. 4, fig. 2.

2002 *Setia tibetica* (Douville) 1916 emend.; Ferrandez-Canadell, p. 9-11, pl. 2, figs 1-7, 10-29; pl. 3, figs 1-11; text figs 3-4. (q.v. for full synonymy).

*Lectotype.* Douville (1916) did not assign types to his original material from the Paleocene of Tibet. Douville's original suite of specimens is deposited in the Calcutta Museum of the Geological Survey of India, collection No. 12817, 12819. Subsequently, Ferrandez-Canadell (2002) designated specimen No.12819 as the lectotype and the specimens figured by Douville (1916) as paralectotypes.

*Material.* Nine equatorial and 13 axial sections from samples 4470.78, 4470.53, 4469.98, 4468.91, 4468.61 (Shakardara Well-1); 13 axial sections from samples KL63, 70, 72, 74 (Kotal Pass section).

*Dimensions.* T. 800 $\mu$ m-2000 $\mu$ m (21 specimens); D. 2100 $\mu$ m-4600 $\mu$ m (11 specimens).

*Diagnosis.* Test rounded-lenticular, large bilocular embryo with spherical-sub spherical protoconch and rounded deuterconch of same size; embryo has two equatorial auxiliary chamberlets; lateral chamberlets on one side with piles and network of canal systems on other side.

*Description.* All specimens described here are megalospheric. Test discoidal, round-lenticular, concavo-convex shape with layers of equatorial chambers. Initial equatorial chamberlets are arc-shaped, becoming gradually rectangular toward margin of the test. Embryo is bilocular with spherical to subspherical protoconch followed by a rounded deuterconch of same size. First chamber after the embryo has two equatorial auxiliary chamberlets, one on each side of the embryo in symmetrical arrangement, later with numerous chambers arranged in cycles. Lateral chamberlets well-developed on one side

of median layer, while other side possesses a network of canals. Five to eight layers of well-developed lateral chambers near the centre of the test, decreasing to one or two layers towards the periphery.

*Discussion.* *S. tibetica* is distinguishable from species of the closely related genus *Orbitosiphon* by possessing lateral chamberlets on both sides of the median layer and two auxiliary chamberlets. It is differentiated from *S. primitiva* Ferrandez-Canadell, 2002 by its large embryo size followed by a first chamber consisting of two auxiliary chamberlets.

*Distribution.* *S. tibetica* is recorded in the upper Lockhart Formation in the Kotal pass section and Core-2 of Shakardara Well-1. It is associated with *Ranikothalia sindensis*, *Miscellanea juliettae*, *M. miscella* and *Discocyclina ranikotensis* indicating a SBZ3-SBZ4 biozonal range. This species is endemic to the south-central Asian region (India, Pakistan and Tibet) and has been reported from the Late Paleocene (Davies & Pinfold 1937; Adams 1987; Ferrandez-Canadell 2002; Afzal *et al.* in press).

#### Genus **ORBITOSIPHON** Rao, 1940

*Types species.* *Lepidocyclina (Polylepidina) punjabensis* Davies in Davies & Pinfold 1937, from the Paleocene Lockhart Formation, Salt Range, Pakistan.

*Diagnosis.* Bilamellar-perforate orbitoidiform test of discoidal, concavo-convex shape, with a single layer of equatorial arcuate chamberlets arranged in concentric annuli, and lateral chamberlets with piles on both sides. Bilocular megalospheric embryo, followed by a single auxiliary chamber. Equatorial chamberlets connected by crosswise-oblique stolons. Annular stolons are present in distal chamberlets. Microspheric form up to 1.4 time larger than megalospheric form. Microspheric nepiont not known (after Ferrandez-Canadell 2002, p. 5).

**Orbitosiphon punjabensis** (Davies, 1937) Plate 3, Figures 7-10

1937 *Lepidocyclina (Polylepidina) punjabensis* Davies, p. 53, pl. VII, figs 1-8, 14, 16.

1944 *Orbitosiphon tibetica* (Douville, 1916); Rao, p. 95-99, fig. 3.

2002 *Orbitosiphon punjabensis* (Davies) 1937 emend.; Ferrandez-Canadell, p. 5-6, pl. 1, figs 1-26. (q.v. for full synonymy).

*Holotype*. Designated Davies in Davies & Pinfold (1937, pl. VII, figs 1-2), Calcutta Museum of the Geological Survey of India collection No. 15887, from the Late Paleocene Lockhart Formation, Salt Range, Pakistan.

*Material*. Four equatorial and 8 axial sections from samples 4470.78, 4470.53, 4469.98, 4468.91, 4468.61, 4468 (Shakardara Well-1).

*Dimensions*. T. 750 $\mu$ m-2100 $\mu$ m (5 specimens); D. 1900 $\mu$ m-4000 $\mu$ m (8 specimens).

*Diagnosis*. Discoidal, concave-convex test, bilocular embryo consisting of subspherical protoconch and rounded deuterococonch of slightly larger size, followed by single auxiliary chamber; ogival shaped equatorial chamberlets; lateral chamberlets on both side.

*Description*. All specimens are megalospheric. Test discoidal, concave-convex shaped test. Embryo bilocular with a subspherical protoconch and rounded deuterococonch. Protoconch slightly larger than deuterococonch, followed by single auxiliary chamber on one side of the embryo. Later chambers show orbitoidal type growth, forming annulus. Equatorial chamberlets are of ogival shape and show spiral arrangement, connected by crosswise-tilted stolons. Lateral chamberlets with piles are well-developed on both sides of meridian layer.

*Discussion.* *O. punjabensis* is distinguished from species of the morphologically similar genus *Actinosiphon* Vaghan, 1929 by its ogival shaped equatorial chamberlets, embryonic apparatus and annular stolon system. It is differentiated from the species of *Setia* by possessing an embryo with a single auxiliary chamber.

*Distribution.* *Orbitosiphon punjabensis* co-occurs with *Setia tibetica* in the Lockhart Formation of the Kotal pass section and Core-2 of Shakardara Well-1, indicating a SBZ3-SBZ4 biostratigraphic range. This species has been reported from the Late Paleocene of India, Tibet, Pakistan and Iran (Davies & Pinfold 1937; Ferrandez-Canadell 2002; Afzal *et al.* in press).

#### Genus **DAVIESINA** Smout, 1954

*Type species.* *Daviesina khatiyahi* Smout, 1954, from the Paleocene of Qatar.

**Daviesina sp.** Plate 3, Figures 11-12

*Material.* Five axial sections from samples 4472.24m, 4471.89m, 4471.11m, 4470.78 (Shakardara Well-1); 4 axial sections from samples KL48-49 (Kotal Pass section); 1 axial section from sample PD1 (Mughal Kot section).

*Dimensions.* T. 500µm-1230µm (3 specimens); D. 900µm-2650µm (4 sections)

*Description.* Test flattened with unequal alar prolongations, rapidly opening spire, doubled asymmetric umbilical plates. Test wall thick, perforated and ornamented with thick pillars. Secondarily doubled septa with no marginal cord, but with slightly coarser granules. Margin sharp, whorls finely granular. Chambers are partly involute and the alar prolongations are strong and long. Well-defined fissures and pillars in unmbilical region with complex unequally distributed intrasepta canals.

*Discussion.* Based on morphological features in axial sections, *Daviesina* sp. can be differentiated from *Daviesina khatiyahi* Smout, 1954 by its strong, long alar prolongations. *Daviesina* sp. is distinguished from species of the closely similar genus *Miscellanea* Pfender, 1935, by its asymmetrical doubling of the margin and doubled umbilical plates. However, due to insufficient material and lack of equatorial sections, comparison with other species of *Daviesina* is difficult.

*Distribution.* *Daviesina* sp. is recorded in the upper part of Lockhart Formation in the Kotal Pass section and Core-2 of Shakardara Well-1 and uppermost Dungan Formation in Mughal Kot section. It is associated with LBF typical of SBZ3-SBZ4 biozones. Species of *Daviesina* are commonly reported from the Paleocene-Eocene of Tethys (Serra-Kiel *et al.* 1998; Wan *et. al.* 2002; BouDagher-Fadel 2008).

Superfamily NUMMULITOIDEA de Blainville, 1827

Family PELLATISPIRIDAE Hanzawa, 1937

Genus MISCELLANEA Pfender, 1935

*Type species.* *Nummulites miscella* d'Archiac & Haime, 1853, from the Paleocene of Sind, Pakistan.

**Miscellanea miscella** (d'Archiac & Haime, 1853) Plate 4, Figures 1-5

1853 *Nummulites miscella*; d'Archiac & Haime, p. 345, pl. 35, figs 4a-c.

1937 *Miscellanea miscella* (d'Archiac & Haime) *pars.*; Davies & Pinfold, p. 43, pl. VI, figs 2-3, ?5, 7-8.

1991 *Miscellanea miscella* (d'Archiac & Haime); Butt, pl. 1, figs A-B.

1998 *Miscellanea miscella* (d'Archiac & Haime); Sirel, p. 94, pl. 57, figs 1-10.

2008 *Miscellanea miscella* (d'Archiac & Haime); Boudagher-Fadel, p. 328, pl. 6/15, figs 3-5.

2009 *Miscellanea miscella* (d'Archiac & Haime); Hottinger, p. 4-5, pl. 1, figs 14-20; pl. 2, figs 1-7; pl. 3, figs 1-15; pl. 4, figs 1-11; pl. 5, figs 1-11; pl. 6, figs 8-9. (q.v. for full synonymy).

2009 *Miscellanea miscella* d'Archiac & Haime, 1853; Afzal *et al.*, p. 17, pl. 1, fig. 1, 3, 5.

In press *Miscellanea miscella* (d'Archiac & Haime); Afzal *et al.*, fig. 8M-N.

*Type material.* The original type material from Sind, Pakistan, described by d'Archiac & Haime (1853) is lost and the exact location of the original discovery is not known (see Hottinger 2009). According to Hottinger (2009, p. 5), a specimen collected from Sind by Peter Marks (1959) housed in the Naturhistorisches Museum, Basel (NMB), Switzerland, No. Pr 3315 is closest morphologically to the original described types. This specimen is illustrated in Leppig (1988, p. 703, pl. 1, fig. 1; pl. 2, fig. 1; pl. 3, fig. 1). My taxonomic understanding of this species therefore follows the material of Leppig (1988).

*Material.* Thirty-four axial and 4 equatorial sections from samples KL49-59, 72-78 (Kotal pass); 54 axial and equatorial sections from samples ZRD1-20 (Zranda section); 2 axial sections from sample HLD3 (Hanna Lake); 4 axial and 3 equatorial sections from samples BD3-6 (Muree Brewery); 40 axial and 10 equatorial sections from samples 4470.78, 4470.53, 4469.98, 4469.63, 4468.91 (Shakardara Well-1).

*Dimensions.* Megalospheric forms, T. 720µm-1600µm (40 specimens), D. 1300µm-3380µm (43 specimens); microspheric forms, T. 800µm-1900µm (35 specimens), D. 2110µm-4377µm (39 specimens).

*Diagnosis.* Test large, lenticular, biconical to flattened; chambers planispiral-involute with backwardly inclined and curved septa, interseptal canals.

*Description.* Megalospheric form: test lenticular in shape, biconical and not keeled, with sub acute periphery. Chambers are planispiral-involute and equitant with backwardly-inclined septa. In peripheral region of equatorial section, septa between successive alar prolongations are radial. Interseptal canals are present. Megalosphere spherical, with diameter of 200µm-400µm. Deuteroconch has semilunar shape in equatorial section and surrounds proloculus in axial section. No marginal cord. Top of the chambers appear rounded in equatorial sections, extending backwards over the top of the previous chamber.

Microspheric form: This differs from the megalospheric form in having a larger test of flattened lenticular shape with rounded periphery and more evenly granular ornament. Margin is broadened and thickened. Higher chambers with backwardly-inclined and curved septa. Spacing and curve of septa in the outer whorl are often irregular.

*Discussion.* *M. miscella* is differentiated from *Miscellanites meandrinus* (Carter, 1861) by possessing planispiral-involute and equitant chambers. *M. juliettae* Leppig, 1988 and *M. yvettae* Leppig, 1988 are distinguished from *M. miscella* by their significantly smaller test sizes.

*Distribution.* *M. miscella* is one of the commonly occurring LBFs in studied sections. It has been recorded in the upper Lockhart Formation in the Kotal Pass section, in Core-2 of the Shakardara Well-1, in upper parts of the Dungan Formation in the Zranda section and in lower parts of the Dungan Formation in the Hanna Lake and Muree Brewery sections. In these sections, *M. miscella* co-occurs with *Ranikothalia sindensis*, *R. nuttalli*, *Assilina dandotica* and *Alveolina* sp., which indicates a biostratigraphic range of SBZ4-SBZ6 biozones. *M. miscella* has been widely reported from the late Paleocene in Tethyan carbonate platform successions (e.g. Egypt, NE India, southern Tibet, Oman, Spain, northern Turkey, see Afzal *et al.* in press). However, in other parts of Tethys, *M.*

*miscella* has been reported from horizons equivalent to the SBZ5 Biozone (e.g. Afghanistan, north-eastern Turkey, Iran, India, SW Slovenia, in Afzal *et al.* in press and references therein) and even the SBZ6 Biozone (e.g. India, Mathur *et al.* 2009; Tewari *et al.* 2010).

**Miscellanea juliettae** Leppig, 1988 Plate 4, Figures 6-10

1988 *Miscellanea juliettae pfenderae* Leppig, p. 700-702, pl. 1, fig. 4; pl. 2, fig. 4; pl. 3, figs 4/1, 4/2; pl. 4, figs 1-8.

1999 *Miscellanea miscella* (d' Archiac & Haime); Akhtar & Butt, p. 138, figs 1-4.

2009 *Miscellanea juliettae* Leppig, 1988; Hottinger, p. 6, pl. 1, figs 21-27; pl. 10, figs 1-20; pl. 11, figs 1-11. (q.v. for full synonymy).

In press *Miscellanea juliettae* Leppig; Afzal *et al.*, fig. 8I-J.

*Holotype*. Designated Leppig (1988, pl. 1, fig. 4; pl. 4, fig. 1.), NMB No. C 36625, from the Paleocene of Sierra de Canatabria, Motes Oberenes, Spain.

*Material*. Eight axial and 9 equatorial sections from samples KL41-42, 48 (Kotal Pass section); 4 axial sections from samples PD1-2 (Mughal Kot section); 34 axial and 43 equatorial sections from samples ZRD21-24, 27-30, 32, 34-37 (Zranda section); 11 axial section from samples 4472.24, 4471.58 (Shakardara Well-1).

*Dimensions*. T. 450µm-1100µm (30 specimens); D. 950µm-2200µm (35 specimens).

*Diagnosis*. Test small, planispiral, lenticular, strongly biconvex with bilocular embryo; pillars are smaller, restricted to the umbilical area.

*Description*. All specimens are megalospheric. Shell small, planispiral, lenticular, strongly biconvex with equatorial spiral not expanding to outer whorl. Megalosphere with bilocular embryo, having diameter of 300µm-450µm in axial section and 150µm-

400µm in equatorial section. Rounded holes are present in umbilical plates. In equatorial section, chambers form a pointed arch shape. Septa are straight to slightly inclined. Pillars in umbilical area are delicate and smaller, restricted to umbilical region.

*Discussion.* *M. juliettae* is distinguished from *M. miscella* and *Miscellanites meandrinus* (Carter, 1861) by its smaller test size, small pillars and bilocular embryo.

*Distribution.* *M. juliettae* is recorded in the lower Lockhart Formation in the Kotal Pass section, Core-2 of Shakardara Well-1, the lower Dungan Formation in the Zranda section and the uppermost Dungan Formation in the Mughal Kot section. In these sections, it is associated with *Lockhartia haimei*, *Fallotella alavensis*, *Coskinon rajkae* and *Glomalveolina primaeva*, indicating the SBZ3 Biozone. This species has been recorded in the Late Paleocene (SBZ3 Biozone) successions of Tethys (Leppig 1988; Serra-Kiel *et al.* 1998; Hottinger 2009).

#### Genus **MISCELLANITES** Hottinger, 2009

*Type species.* *Miscellanea iranica* Rahaghi, 1983, from the Paleocene of Iran.

*Diagnosis.* Globular or subglobular test formed by a planispiral-involute chamber arrangement. The globular shape of the test is linked with a single row of multiple interiomarginal foramina that tend to facilitate the formation of low but elongate chambers reaching from pole to pole, as in the alveolinids. The free, outer surface of the chamber walls are covered by a simple and shallow enveloping canal system that may develop a single generation of slender pustules between the orifices of the enveloping canals. The megalosphere is more or less spherical followed by a deuteroconch of similar size and shape. The bottom of the chamber is covered by a paries proximus that extends from the septal flap into the alar prolongation (amended from Hottinger 2009).

**Miscellanites meandrinus** (Carter, 1861) Plate 4, Figures 11-12

1861 *Alveolina meandrina* Carter, p. 251, pl. 17, figs 4a-f.

1954 *Miscellanea meandrina* (Carter, 1861); Smout, p. 74-75, pl. X, figs 1-14.

1998 *Miscellanea ? meandrina* (Carter); Sirel, p. 99, pl. 59, figs 1-6; pl. 60, figs 1-10.

2008 *Miscellanea meandrina* (Carter); BouDagher-Fadel, p. 328, pl. 6/15, figs 6-8.

2009 *Miscellanites meandrinus* (Carter, 1861); Hottinger, p. 7-8, pl. 14, figs 1-14; pl. 15, figs 1-14. (q.v. for full synonymy).

In press *Miscellanea meandrina* (Carter); Afzal *et al.*, fig. 8K-L.

*Lectotype.* Carter (1861) did not designate types from his original material from the Paleocene Dungan Formation in Kelat area of Baluchistan, Pakistan. Later, Smout (1954, p. 75) studied Carter collection at the NHM and designated specimen No. P. 30046 as lectotype.

*Material.* Two equatorial sections from sample ZRD20 (Zranda section).

*Dimensions.* Megalospheric form, D. 1700µm-2500µm (1 specimen); microspheric form, D. 3000µm-5000µm (1 specimen).

*Diagnosis.* Large test, ovoid with rounded periphery; numerous, low, short chevron-shaped chambers, arranged in linear pattern in megalospheric form and meandrine in microspheric form.

*Description.* Megalospheric form: test large, ovoid with rounded periphery and planispiral-involute arrangement of numerous, low and short chevron-shaped chambers (especially in outer whorls), arranged in linear pattern. Outer whorls are tighter. Septa are curved and regular, running from the margin to pole. Megalosphere large (200µm-350µm in diameter). Thicker outer wall with high chambers, cut into pillars.

Microspheric form: shell similar in shape and characters to megalospheric form but larger in size with extended pole to pole chambers in last whorl, replacing linear shape with a meandrine pattern.

*Discussion.* *M. meandrinus* is differentiated from *M. primitivus* (Rahaghi, 1983) by its rounded periphery and tighter outer whorl.

*Distribution.* *M. meandrinus* is recorded in the middle part of the Dungan Formation in the Zranda section, associated with *Miscellanea miscella*, indicating a SBZ4 biozonal age. *M. meandrinus* occurs in France, Egypt and in Turkey, where it is associated with fauna of similar age (SBZ4 Biozone, Hottinger 2009).

Family: NUMMULITIDAE de Blainville, 1827

Genus: **RANIKOTHALIA** Caudri, 1944

*Type species.* *Nummulites nuttalli* Davies, 1927, from the Thal area of NW Pakistan.

**Ranikothalia sindensis** (Davies, 1927) Plate 5, Figures 1-8

1927 *Operculina sindensis* sp. nov. Davies, p. 274, pl. 19, figs 10-13.

1937 *Nummulites sindensis* (Davies); Davies & Pinfold, p. 20-21, pl. 4, fig. 21.

1991 *Ranikothalia sindensis* (Davies); Butt, p. 77-80, pl. 1, figs 1-h; pl.2, figs 1, c, d-g; pl.3, figs a-f; pl.4, fig. a.

1999 *Ranikothalia sindensis* (Davies); Akhtar & Butt, p. 134, pl. 3, fig. 4. (q.v. for full synonymy).

2009 *Ranikothalia sindensis* Davies, 1927; Afzal *et al.*, p. 17, pl. 1, figs 10-11.

In press *Ranikothalia sindensis* (Davies); Afzal *et al.*, fig. 8Q.

*Holotype.* Designated Davies (1927, pl. XIX, fig. 10-12), Calcutta Museum of the Geological Survey of India collection No. K. 6/987, from the Paleocene of the Thal area, NW Pakistan.

*Material.* Ten axial sections from samples 4472.24, 4471.89, 4471.11, 4470.78, 4470.53, 4469.98 (Shakardara Well-1); 2 axial sections from samples KL74-75 (Kotal Pass section); 13 axial sections from samples ZRD4-5, 7, 16, 20, 27-28 (Zranda section).

*Dimensions.* Megalospheric form, T. 600 $\mu$ m-800 $\mu$ m (15 specimens), D. 2000 $\mu$ m-3200 $\mu$ m (30 specimens); Microspheric form, T. 900 $\mu$ m-1200 $\mu$ m (20 specimens), D. 3000 $\mu$ m-5000 $\mu$ m (35 specimens).

*Diagnosis.* Discoidal test, lenticular to inflated with subevolute rapidly opening spire; marginal cord strong on all whorls; long alar prolongation; lacks septal filaments.

*Description.* Megalospheric form: test discoidal, lenticular, or inflated with rapidly opening spire. Megalosphere small, sub-globular in shape and has 200 $\mu$ m-300 $\mu$ m axial diameter. Marginal cord thick and usually strong on all whorls. In axial section, it has very long alar prolongations.

Microspheric form: Not much different from megalospheric form but possesses large, slightly less inflated test.

*Discussion.* *R. sindensis* is differentiated from *R. nuttalli* (Davies, 1927), *R. sahani* Davies, 1952 and *R. bermudezi* (Palmer, 1934) by lack of septal filaments, rapidly opening spire and strong marginal cord on all whorls.

*Distribution.* *R. sindensis* is recorded in the Lockhart Formation in the Kotal Pass and Core-2 of the Shakardara Well-1 and the Dungan Formation in the Zranda, Muree Brewery and Hanna Lake sections. It is associated with *Miscellanea juliettae*, *M. miscella*, *Glomalveolina primaeva*, *R. nuttalli*, *Alveolina* sp. and *Assilina dandotica*,

indicating an SBZ3-SBZ5/6 biozonal range. *R. sindensis* has been widely reported from the Late Paleocene-earliest Eocene of Tethys (Serra-Kiel *et al.* 1998; Afzal *et al.* in press).

**Ranikothalia nuttalli** (Davies, 1927) Plate 5, Figures 9-14

1927 *Nummulites nuttalli* sp. nov. Davies, p. 266-269, pl. XVIII, figs 3-4; pl. XIX, figs 7-9.

1937 *Nummulites nuttalli* Davies; Davies & Pinfold, p. 18-19, pl. III, figs, 1-2, 9; pl. VI, figs 19-20.

1970 *Ranikothalia nuttalli* (Davies); Kaefer, p. 10, figs 4-6.

1988 *Ranikothalia nuttalli* (Davies); Haynes, p. 126, pl. 1, figs 6-10.

1991 *Ranikothalia nuttalli* (Davies); Butt, p. 77-78, pl. 1, fig. A.

1995 *Ranikothalia nuttalli* (Davies) 1927; Racey, p. 77-78, pl. 7, figs 6-12, 15-18, 21. (q.v. for full synonymy).

1999 *Ranikothalia nuttalli* (Davies); Akhtar & Butt, p. 134-136, pl. III, fig. 5.

2008 *Ranikothalia nuttalli*; Scheibner & Speijer, p. 94, pl. 1, fig. C.

2009 *Ranikothalia nuttalli*; Scheibner & Speijer, p. 208, fig. 10A.

In press *Ranikothalia nuttalli* (Davies); Afzal *et al.* fig. 9B.

*Holotype.* Designated Davies (1927, pl. XVIII, fig. 3), Calcutta Museum of the Geological Survey of India collection No. K. 6/977, from the Jhirak area, Sind, Pakistan.

*Material.* Ten axial sections from samples ZRD1-5 (Zranda section); 8 axial sections from samples BD3-7 (Muree Brewery section); 4 axial sections from samples HLD3-6 (Hanna Lake section).

*Dimensions.* T. 800µm-1850µm (15 specimens); D. 2500µm-3900µm (15 specimens).

*Diagnosis.* Involute, lenticular to inflated lenticular test; regular, gradually opening spire; septal filaments present; marginal cord thicker in the last whorl.

*Description.* All the specimens described here are megalospheric. Test involute, lenticular to inflated lenticular with regular, gradually opening spire. Septal filaments are present. Test has rounded periphery. Marginal cord is thicker in the last whorl. In axial section, coarser granules at poles are present with occasional finer granules. All whorls show alar prolongations.

*Discussion.* *R. nuttalli* is distinguished from *R. sahnii* (Davies, 1952) and *R. sindensis* (Davies, 1927) by its more gradually opening spire, possession of septal filaments and a thickened marginal cord on the last whorl. *R. nuttalli* is distinguishable by its thick marginal cord and involute complanate test, which is not developed in genera such as *Operculina* d'Orbigny, 1926, *Assilina* d'Orbigny, 1839 and *Nummulites* Lamarck, 1801.

*Distribution.* *R. nuttalli* is recorded in the uppermost Dungan Formation in the Zranda section and the lower Dungan Formation in the Hanna Lake and Muree Brewery sections. In these sections it co-occurs with *Assilina dandotica*, *Discocyclina dispansa*, *Alveolina* sp. and *Glomalveolina lepidula*, indicating an SBZ5/6 biozonal range. *R. nuttalli* is recorded in the Late Paleocene (SBZ4 Biozone) sediments of Egypt (Scheibner & Speijer 2009). In other Tethyan carbonate platform successions, *R. nuttalli* has been reported from the SBZ5-SBZ6 and possibly SBZ7 biozones (e.g. Europe-northern Africa and India, Afzal *et al.* in press and references therein).

**Ranikothalia sahnii** Davies, 1952 Plate 5, Figures 15-16

1952 *Ranikothalia sahnii* Davies, p. 156, pl. 1, figs 1, 4-5, 7-8.

1988 *Ranikothalia savitriae* Davies; Haynes, p. 233, pl. 1, figs 1-4, 6-8.

1995 *Ranikothalia sahani* Davies; Racey, p. 78-79, pl. 7, figs 13-14, 19-20, 22. (q.v. for full synonymy).

In press *Ranikothalia sahani* Davies; Afzal *et al.*, fig. 8P.

*Holotype.* Designated Davies (1952, pl. 1, fig.1), NHM No. P40347, from the Late Paleocene of Togoland, West Africa.

*Material.* Four axial sections from samples ZRD27-28, 32 (Zranda section).

*Dimensions.* T. 900 $\mu$ m -1300 $\mu$ m (4 specimens); D. 2900 $\mu$ m-3650 $\mu$ m (4 specimens).

*Diagnosis.* Test lenticular; spire initially thick involute and later complanate; relatively thick marginal cord.

*Description.* All specimens are megalospheric. Test of lenticular outline with initial thick involute and final complanate spire. Rounded periphery and crowded granules on poles; strong septal filaments. Megalosphere spherical-subglobular of 200 $\mu$ m-300 $\mu$ m axial diameter. Marginal cord relatively thick with coarse canals.

*Discussion.* Morphologically, *R. sahani* is intermediate between *R. nuttalli* (Davies, 1927) and *R. sindensis* (Davies, 1927). *R. sahani* is differentiated from *R. sindensis* by its relatively less thick marginal cord and less rapidly opening spire, and from *R. nuttalli* by its relatively more rapid opening spire and thinner test.

*Distribution.* It co-occurs with *R. sindensis* in the Dungan Formation of the Zranda section, which indicates an SBZ3-SBZ5/6 biozonal range. *R. sahani* is reported from the Late Paleocene of France and West Africa and from the Late Paleocene-earliest Eocene of Oman (Davies 1952; Racey 1995; Afzal *et al.* in press).

### Genus **OPERCULINA** d'Orbigny, 1826

*Type species.* *Lenticulites complanatus* DeFrance, 1822.

**Operculina sp.** Plate 5, Figures 17-19

*Material.* Twelve axial sections from samples ZRD1-2 (Zranda section); 6 axial sections from samples HLD11, 14, 17 (Hanna Lake section).

*Dimensions.* T. 1100 $\mu$ m-2100 $\mu$ m (15 specimens); D. 3300 $\mu$ m-5000 $\mu$ m (15 specimens).

*Description.* All specimens described here are microspheric. Test planispiral, evolute lenticular to compressed and loosely coiled with rapidly expanding spire/whorls and alar prolongation. Marginal cord is well-developed with numerous fine canals. Finely perforate outer wall.

*Discussion.* Lack of equatorial sections makes it difficult to compare *Operculina sp.* with other species of *Operculina*. However, *Operculina sp.* is distinguishable from species of the closely similar genus *Ranikothalia* by its relatively weak marginal cord and involute spire in *Ranikothalia* and from *Nummulites* Lamarck, 1801 by its loose coiling.

*Distribution.* *Operculina sp.* is recorded in the uppermost Dungan Formation in the Zranda section and is present throughout the Dungan Formation in the Hanna Lake section, normally associated with *Assilina dandotica*, *Nummulites globulus*, *Discocyclina dispansa*, *D. sella* and rarely with *Alveolina sp.* These occurrences indicate a biozonal range of SBZ5-SBZ8 for *Operculina sp.* in the sections studied. *Operculina* is a cosmopolitan genus with species ranging from the Late Paleocene to Recent (BouDagher-Fadel 2008).

Genus **ASSILINA** d'Orbigny, 1839

*Type species.* *Assilina depressa* d'Orbigny, 1826 [= *Nummulites spira* de Roissy, 1805], from the Middle Eocene of the Island of Rab, Yugoslavia.

***Assilina dandotica*** Davies, 1937 Plate 6, Figures 1-8

1937 *Assilina dandotica* sp. nov. Davies in Davies & Pinfold, p. 28, pl. 4, figs 1-3, 6-8.

1981 *Assilina dandotica* L.M. Davies, 1937; Schaub, p. 206, pl. 84, figs 1-6.

1995 *Assilina dandotica* Davies 1937; Racey, p. 70, pl. 9, figs 1-5.

In press *Assilina dandotica* Davies; Afzal *et al.*, fig. 9C-D.

*Holotype.* Designated Davies & Pinfold (1937, 1937, pl. IV, fig. 1), Calcutta Museum of the Geological Survey of India collection No. 15811, from the Patala Formation, Salt Range, Pakistan.

*Material.* Two nearly equatorial and 5 axial sections from samples ZRD1-3 (Zranda section); 3 axial sections from samples HLD3-5 (Hanna Lake section); 2 axial sections from sample BD3 (Muree Brewery section).

*Dimensions.* T. 700µm-1100µm (6 specimens); D. 2000µm-2800µm (5 specimens).

*Diagnosis.* Test small, thick, lenticular-inflated with rounded periphery; tight, regular spire; rectangular chambers with dense septa in early whorls and curved to inclined in adult whorls.

*Description.* All specimens are megalospheric. Test small, convex lenticular to inflated with round periphery and tight spire. Ornament on surface consists of granules, extending from the centre of the shell to the periphery. In equatorial section, spiral growth is regular, tight, slowly opening. Chambers rectangular in shape, higher than

long with dense septa in initial whorls, become curved to inclined in outer whorls. In axial section, test is thick, lenticular inflated. Proloculus 90µm-165µm in diameter.

*Discussion.* *A. dandotica* is differentiated from *A. ranikoti* Nuttall, 1926 by its thick test and tight spire and from *A. pustulosa* Doncieux, 1926 by its smaller test size and quasi-evolute test.

*Distribution.* *A. dandotica* is recorded in the Dungan Formation in the Zranda, Hanna Lake and Muree Brewery sections, associated with *Ranikothalia nuttalli*, *Alveolina* sp., *Miscellanea miscella* and *Discocyclina dispansa*, indicating a SBZ5-SBZ6 biozonal range. *A. dandotica* has been reported from the earliest Eocene of Tethys (Europe to India, Schaub 1981; Racey 1995; Serra-Kiel *et al.* 1998; Afzal *et al.* in press).

#### Genus NUMMULITES Lamarck, 1801

*Type species.* *Camerina laevigata* Bruguière, 1789 from the Middle Eocene of the Paris Basin, France.

#### **Nummulites atacicus** Leymerie, 1846      Plate 7, Figures 1-5

1846 *Nummulites atacicus* Leymerie, p. 358, pl. 13, figs 13a-e.

1981 *Nummulites atacicus* Leymerie, 1846; Schaub, p. 119, pl. 25, figs 1-51.

1995 *Nummulites atacicus* Leymerie 1846; Racey, p. 32, pl. 2, figs 18-20.

In press *Nummulites atacicus* Leymerie; Afzal *et al.*, fig. 9Q-R.

*Lectotype.* Leymerie (1846) did not designate types from his original material from the Early Eocene of Mont Cayla, commune d'Agel, Hérault, southern France. Later, Schaub (1981) studied Leymerie's collection at the Museum of Toulouse, France and

designated the specimen in figure 13 of plate 13 in Leymerie (1846) as the lectotype, specimen number unknown.

*Material.* Twenty-four axial and 2 equatorial sections from samples BD13-15, 17 (Muree Brewery section); 10 axial sections from sample HLD17-19 (Hanna Lake section).

*Dimensions.* Microspheric form, T. 1100 $\mu$ m-1800 $\mu$ m (14 specimens), D. 2600 $\mu$ m-3500 $\mu$ m (14 specimens); megalospheric form, T. 900 $\mu$ m-1200 $\mu$ m (12 specimens), D. 1600 $\mu$ m-2200 $\mu$ m (12 specimens).

*Diagnosis.* Small, lenticular-biconical test, sharp margins with thick, regular and tight spire; chambers isometric subquadrate to subrhomboidal shape with regular, slightly inclined septa; marginal cord uniform; large proloculus.

*Description.* Megalospheric form: test small, lenticular to biconical with sharp edges. In equatorial section, spire is thick in all whorls and has regular growth. Septa slightly inclined and arched, regularly distributed. Chambers are isometric and of subquadrate to subrhomboidal shape. In axial section, thin pillars radiate from the umbilical region toward test periphery. Marginal cord moderately uniform. Proloculus has diameter of 300 $\mu$ m-400 $\mu$ m.

Microspheric form: test large, convex with semi sharp edges. Spire thick, regular and tight. Marginal cord uniformly thin.

*Discussion.* *N. atacicus* is distinguished from *N. praecursor* De La Harpe, 1883 by its regular septa and isometric and subquadrate- to subrhomboidal-shaped chambers, and from *N. globulus* Leymerie, 1846 by possessing relatively straight septa, a more rapidly opening spire and larger proloculus. It is differentiated from *N. discorbinus* (Schlotheim, 1820) by possessing fewer chambers per whorl, curved septa and slightly less tightly coiled spire.

*Distribution.* *N. atacicus* occurs in the upper Dungan Formation in the Hanna Lake and Muree Brewery sections, associated with *N. globulus*, *Discocyclina dispansa*, *Actinocyclina* sp. and *Alveolina* sp., indicating the SBZ8 biozone. It is widely reported from the Early Eocene successions of Tethys (e.g. Europe, northern Africa, India, Schaub 1981; Racey 1995; Serra-Kiel *et al.* 1998; Afzal *et al.* in press).

**Nummulites globulus** Leymerie, 1846      Plate 7, Figures 6-13

1846 *Nummulites globulus* Leymerie, p. 359, pl. 13, figs 14a-d.

1981 *Nummulites globulus* Leymerie, 1846; Schaub, p. 137, pl. 40, figs 1-80.

1995 *Nummulites globulus* Leymerie 1846; Racey, p. 48-49, pl. 5, figs 18, 22-23.

(q.v. for full synonymy).

In press *Nummulites globulus* Leymerie; Afzal *et al.*, fig. 9S-T.

*Lectotype.* Leymerie (1846) did not designate types for his original material from the Early Eocene of Mont Cayla, commune d'Agel, Hérault, southern France. Subsequently, Schaub (1981) studied Leymerie's syntype material at the Museum of Toulouse, France and designated a lectotype (Schaub 1981, p.137, pl. 40, fig. 1a-c, specimen number unknown).

*Material.* One off-centred equatorial and 10 axial sections from samples BD13-17, 19 (Muree Brewery section); 8 axial sections from samples HLD10-14, 20 (Hanna Lake section).

*Dimensions.* Megalospheric form, T. 850µm-1100µm (18 specimens), D. 2000µm-2950µm (18 specimens); microspheric form, T. 1100µm-2000µm (10 specimens); D. 1800µm-3500µm (10 specimens).

*Diagnosis.* Small, thick, biconical, inflated-globular test with thick polar pillars; compact, regular spire; small proloculus.

*Description.* Megalospheric form: test small, thick, lenticular, inflated to globular with sharp periphery and thick polar pillars. Spire compact, regular. Proloculus small, about 50µm-140µm in diameter, subspherical in shape. The wall of the last whorl is thinner than in earlier whorls.

Microspheric form: test thick, biconical to lenticular with sharp or rounded edges. Polar pillars are thick and large extending from the centre of the test towards the periphery. Spire regular.

*Discussion.* *N. globulus* resembles *N. discorbinus* (Schlotheim, 1820) but differs in having a relatively loose spire. It is distinguishable from *N. atacicus* by its smaller proloculus size and thick polar pillars.

*Distribution.* *N. globulus* occurs in association with *N. atacicus*, *Discocyclusina dispansa*, *Actinocyclusina* sp. and *Alveolina* sp. in the upper Dungan Formation in the Muree Brewery and Hanna Lake sections, indicating a SBZ8 biozonal age. It is widely reported from the Early Eocene (mid Ilerdian - early Cuisian) of Tethys carbonate platform successions (Europe, Africa and India, Schaub 1981; Racey 1995; Serra-Kiel *et al.* 1998; Afzal *et al.* in press).

#### Family DISCOCYCLINIDAE Galloway, 1928

#### Genus **DISCOCYCLINA** Gümbel, 1870

*Type species.* *Orbitolites prattii* Michelin, 1846, from the Late Eocene of Biarritz, France.

***Discocyclusina ranikotensis*** Davies, 1927      Plate 8, Figures 1-6

1927 *Discocyclina ranikotensis* sp. nov. Davies, p. 281-282, pl. XXII, figs 10-12.

1937 *Discocyclina ranikotensis* Davies; Davies & Pinfold, p. 55, pl. III, fig. 22.

1959 *Discocyclina ranikotensis* (Davies); Nagappa, p. 180, pl. 8, figs 2-3.

1991 *Discocyclina ranikotensis* Davies; Butt, p. 82, pl. 3, fig. g.

1999 *Discocyclina ranikotensis* Davies; Akhtar & Butt, p. 140, pl.2, figs 1-2.

In press *Discocyclina ranikotensis* Davies; Afzal *et al.*, fig. 9I.

*Holotype.* Designated Davies (1927, pl. XXII, fig. 11), from the Late Paleocene Lockhart Formation, Thal area, Pakistan. The Davies collection is located in the Grant Institute of Geology, University of Edinburgh, UK (specimen number unknown).

*Material.* Five axial sections from sample ZRD2 (Zranda section); 10 axial and 2 equatorial sections from samples HLD3-5 (Hanna Lake section).

*Diagnosis.* Small, unribbed, flattened test with low umbo; crowded pillars.

*Description.* All specimens are microspheric. Test thin, unribbed, strongly compressed to flattened, with crowded pillars and low umbo. In axial section, lateral chamberlets are rectangular in shape or faintly hexagonal to elongate, 20µm-30µm in length and 10µm-15µm in height. Equatorial layer is thinner in the centre of the test (thickness of 10µm-20µm), becomes thicker (30µm-50µm) towards margin. In equatorial section, chamberlets are thin, rectangular and are 40µm-50µm high and 30µm-40µm long.

*Discussion.* *D. ranikotensis* is distinguishable from other unribbed Late Paleocene-Early Eocene forms such as *D. dispansa* (Sowerby, 1840) and *D. seunesi* Douville, 1922 by its small flattened test with very low umbo. It is different from *D. pratti* (Michelin, 1846) by possessing more crowded pillars.

*Distribution.* *D. ranikotensis* occurs in the upper Lockhart Formation of the Kotal pass section and Core-2 of the Shakardara Well-1, associated with *Ranikothalia sindensis*

and *Miscellanea miscella*. In the Muree Brewery and Hanna Lake sections, it is recorded in the lower part of the Dungan Formation, associated with *Assilina dandotica*, *R. nuttalli* and *Nummulites atacicus*. These occurrences in the Indus Basin indicate a biostratigraphical range of SBZ4-SBZ8 biozones for *D. ranikotensis*. It has also been reported from the Late Paleocene to Early Eocene of Pakistan and India (e.g. Nagappa 1959; Samanta 1969; Afzal *et al.* in press). *D. ranikotensis* appears to be endemic to the Indian region (east Tethys) as it has not been reported from west Tethys carbonate platforms, where different lineages of discocyclinids developed during the Late Paleocene-Early Eocene (e.g. Samanta 1969; Adams 1970; Serra-Kiel *et al.* 1998; Less *et al.* 2007).

**Discocyclina dispansa** (Sowerby, 1840) Plate 8, Figures 7-17

1840 *Lycophris dispansa* Sowerby, p. 327, pl. 24, figs 16a-b.

1963 *Discocyclina (Discocyclina) dispansa* (Sowerby); Gupta, p. 39-40, pl. 1, figs 1-9; pl. 2, figs 1, 3-9.

1965 *Discocyclina dispansa* (Sowerby); Samanta, p. 422, pl. 1, figs 1-3, 5.

1985 *Discocyclina dispansa* (Sowerby); Samanta & Lahiri, p. 254, pl. 3, figs 1-5; pl. 8, figs 1-2; pl. 11, figs 1-12. (q.v. for full synonymy).

In press *Discocyclina dispansa* (Sowerby); Afzal *et al.*, fig. 9F-G.

*Type material.* Sowerby (1840, pl. 24, figs 16a-b) did not designate types from his original material from the Middle Eocene of Kutch area, India. The repository of Sowerby's (1840) original material is unknown (Nuttall 1926, present study). Gupta (1963, pl. 1, figs 1-9; pl. 2, figs 1, 3-9) recollected specimens of *Discocyclina dispansa*

from the type locality and designated neotype, now housed in the Indian Institute of Technology (Kharagpur), India (specimen number unknown).

*Material.* Two equatorial sections of megalospheric form and 1 equatorial and 2 axial sections of microspheric form from samples HLD3, 14, 16 (Hanna Lake section); 4 axial sections of megalospheric form from samples ZRD2-3 (Zranda section); 5 axial section of megalospheric form from samples BD13, 15 (Muree Brewery section).

*Dimensions.* Megalospheric form, T. 1300 $\mu$ m-2700 $\mu$ m (7 specimens), D. 2700 $\mu$ m-4000 $\mu$ m (8 specimens); microspheric form, T. 1600 $\mu$ m-3000 $\mu$ m (8 specimens), D. 3000 $\mu$ m-7000 $\mu$ m (8 specimens).

*Diagnosis.* Evenly lenticular test with archiaci-type adauxiliary chamberlets; embryo semi-nephro- to trybiololepidine, subspherical protoconch, spherical deuterococonch; equatorial chamberlets small, elongated in shape; thick pillars; moderate size embryonic chambers.

*Description.* Megalospheric form: Test small-medium size, evenly lenticular with a marked umbo in some specimens. Embryo semi-nephro- to trybiololepidine and archiaci type adauxiliary chamberlets. Protoconch subspherical in shape and has outer diameter of 100 $\mu$ m-135 $\mu$ m. Deuterococonch is spherical and has outer diameter of 180 $\mu$ m-240 $\mu$ m. Equatorial chamberlets are elongate and are 20 $\mu$ m-30 $\mu$ m in width and 50 $\mu$ m-80 $\mu$ m in height. Annular chamber walls of equatorial chamberlets often show regular concentric arrangement, but in some specimens irregular circular patterns are observed. Lateral chamberlets are 120 $\mu$ m-250 $\mu$ m in width and 40 $\mu$ m-80 $\mu$ m in height, moderately layered, rarely show overlapping. Equatorial layer is 10 $\mu$ m-20 $\mu$ m thick. Strong thick pillars are present.

Microspheric form: Test large, lenticular in shape. The lateral chamberlets are more or less regularly layered. Pillars are thicker than megalospheric forms. Equatorial layer has

thickness of 20µm-35µm. Equatorial chamberlets are 80µm-150µm high and 30µm-50µm wide. Lateral chamberlets are 120µm-155µm wide and 30µm-45µm high.

*Discussion.* *D. dispansa* differs from *D. sowerbyi* (Sowerby, 1840) in having moderate sized embryonic chambers and smaller dimensions of equatorial chamberlets. It is distinguishable from *D. seunesi* Douville, 1922 by having semi-nephro- to trybiololepidine embryo and archiaci type adauxiliary chamberlets and from *D. ranikotensis* Davies, 1927 by its larger lenticular test and greater number of thicker pillars.

*Distribution.* It is recorded in the Dungan Formation in the Zranda, Muree Brewery and Hanna Lake sections, and co-occurs with *Ranikothalia nuttalli*, *Miscellanea miscella* and *Assilina dandotica* and later with *Actinocyclus* sp., *Nummulites globulus* and *N. ataticus*. These faunal associations indicate an SBZ5-SBZ8 biozonal range. *D. dispansa* is the most widespread species of *Discocyclus* in Tethys, reported to range from the Ypresian to Priabonian (Less *et al.* 2007; Afzal *et al.* in press).

**Discocyclus sella** (d' Archiac, 1850)      Plate 9, Figures 1-3

1850 *Orbitolites sella* d' Archiac, p. 405, pl. 8, figs 16-16a.

1965 *Discocyclus sella* (d' Archiac); Samanta, p. 426, pl. 2, figs 1-7; pl. 4. Fig. 11.

1989 *Discocyclus sella* (d' Archiac); Matsumaru & Kimora, p. 264, figs 4-5. (q.v. for full synonymy).

In press *Discocyclus sella* (d' Archiac); Afzal *et al.*, fig. 9H.

*Lectotype.* d' Archiac (1850, pl. 16-16a) did not designate types from his original material from the Eocene of Biarritz (SW Aquitaine), France. d' Archiac's (1850)

original material is housed in the École des Mines de Paris, France (specimen number unknown). d' Archiac (1850) pI. 8, fig. 16 is designated here as a lectotype.

*Material.* One axial section of microspheric form from sample HLD4 (Hanna Lake section); 2 axial sections of micro- and 2 of megalospheric forms from samples BD11, 19 (Muree Brewery section).

*Dimensions.* Microspheric form, T. 800µm-1100µm (2 specimens), D. 3600µm-8000µm (2 specimens); megalospheric form, T. 600µm-850µm (2 specimens), D. 3200µm-4500µm (2 specimens).

*Diagnosis.* Test large, compressed lenticular-flattened; elongated rectangular lateral, low chambers; pillars are strong and thick in peripheral region.

*Description.* Megalospheric form: only axial sections are described here. Test medium size, strongly compressed lenticular to flattened with thin sharp edges. Lateral chamberlets are elongated rectangular in shape and 10µm-15µm wide and 20µm-30µm high. In axial section, protoconch has outer diameter of 80µm-95µm and deuterococonch of 150µm-210µm. Equatorial layer thickness varies between 10µm and 35µm. Pillars are strong and thick in peripheral region, become thinner toward the centre of the test.

Microspheric form: test has similar features but larger dimensions. Pillars are thicker than in megalospheric forms. Equatorial layer has thickness of 15µm-40µm. In axial section, lateral chambers are 15µm-25µm high and 25µm-40µm wide.

*Discussion.* *D. sella* is differentiated from *D. ranikotensis* Davies, 1927 by its larger test and its low lateral chamberlets, and from *D. dispansa* (Sowerby, 1840) and *D. seunesi* Douville, 1922 by its compressed lenticular to flattened test.

*Distribution.* *D. sella* is recorded in the upper Dungan Formation in the Zranda and Muree Brewery sections, usually associated with *Assilina dandotica*, *Ranikothalia nuttalli*, *D. dispansa*, *Nummulites atacicus* and *N. globulus*. These occurrences indicate

an SBZ5/6-SBZ8 biozonal range for *D. sella* in the Indus Basin. *D. sella* has also been reported from the Eocene of France, Spain, India, Italy and Japan (Samanta 1969; Matsumaru & Kimora 1989; Afzal *et al.* in press).

Genus **ACTINOCYCLINA** Gümbel, 1870

*Type species.* *Orbitolites radians* d'Archiac, 1850, from the Eocene of Biarritz, France.

**Actinocyclus sp.** Plate 9, Figures 4-5

*Material.* Eight axial sections of microspheric and 4 axial sections of megalospheric forms from samples HLD12-14, 18, 20-21 (Hanna Lake section).

*Dimensions.* Microspheric form, T. 600µm-1000µm (8 specimens), D. 4300µm-8000µm (8 specimens); megalospheric form, T. 500µm-1200µm (4 specimens), D. 3500µm-6000µm (4 specimens).

*Description.* Megalospheric form: Test thin, lenticular to stellate. It has structures similar to *Discocyclus* but differs in having distinct rays or ridges formed by a proliferation of broad and low lateral chambers, extending slightly beyond the periphery. In axial section, protoconch is subspherical with a diameter of approximately 80µm-130µm. Deuteroconch has not entirely encircled the protoconch and has a diameter of 150µm-300µm. Pillars are thick and run along the rays. Wall of lateral chambers thin, surface with numerous granules between and upon the elevated ribs, those toward the periphery appearing in concentric circles. Lateral chamberlets are rectangular in shape, 10µm-20µm high and 40µm-100µm wide.

Microspheric form: has similar features to the megalospheric form, but has larger test size. Lateral chamberlets are elongated rectangular in shape, 20µm-30µm high and 60µm-130µm wide.

*Discussion.* Lack of equatorial sections makes it difficult to identify the species (Gümbel, 1870). However, *Actinocyclus* sp. is distinguished from the closely similar genera *Discocyclus* and *Orbitoclypeus* by its distinct rays and stellate test.

*Distribution.* *Actinocyclus* sp. is recorded in the upper Dungan Formation in the Hanna Lake section, associated with LBFs typical of the SBZ8 Biozone such as *Nummulites ataticus* and *N. globulus*. It is a cosmopolitan taxon and has been widely reported from the Eocene succession of Tethys (BouDagher-Fadel 2008).

Family ORBITOCLYPEIDAE Brönnimann 1945

Genus **ORBITOCLYPEUS** Silvestri, 1907

*Type species.* *Orbitoclypeus himerensis* Silvestri, 1907, from the Eocene of Palermo, Southern Italy.

**Orbitoclypeus** sp. Plate 9, Figures 6-12

*Material.* Tens of axial sections of microspheric form and 15 axial and 7 equatorial sections of megalospheric form from samples HLD10-21 (Hanna Lake section); 2 equatorial sections of megalospheric form from sample BD17 (Muree Brewery section).

*Dimensions.* Microspheric form, T. 1000µm-2000µm (20 specimens), D. 5000µm-9000µm (20 specimens); megalospheric form, T. 800µm-1400µm (20 specimens), D. 3200µm-5000µm (20 specimens).

*Description.* Megalospheric form: test medium size, lenticular with excentric to eulepidine-embryon, archiaci type adauxiliary chamberlets. Equatorial chamberlets are square to hexagonal in shape and arranged into undulated annuli with various type growth. Equatorial chamberlets are 20µm-50µm wide and 30µm-60µm high. Internal

diameter of protoconch ranges from 140µm-160µm; protoconch completely surrounded by deutoconch. Deutoconch has internal diameter of 220µm-280µm. In axial section, thick pillars are visible, extending from the central part of test toward periphery. Lateral chamberlets are 20µm-50µm wide and 10µm-20µm high.

Microspheric form: shows similar structures to megalospheric form, but possesses larger dimensions.

*Discussion.* *Orbitoclypeus* sp. is differentiated from *O. schopeni* (Checchia-Rispoli, 1909), *O. munieri* (Schlumberger, 1904) and *O. douvillei* (Schlumberger, 1903) by possessing excentri- to eulepidine-embryon and archiaci type adauxiliary chamberlets.

*Distribution.* *Orbitoclypeus* sp. is one of the commonest LBFs of the Dungan Formation in the Zranda, Muree Brewery and Hanna Lake sections. In these sections, it is associated with *Assilina dandotica*, *Discocyclina dispansa*, *Miscellanea miscella*, *Ranikothalia nuttalli*, *Alveolina* sp., *Nummulites atacicus* and *N. globulus*, indicating an SBZ5-SBZ8 biozonal range.

Suborder MILIOLINA Delage & Herouard, 1896

Superfamily MILIOLACEA Ehrenberg, 1839

Family SPIROLOCULINIDAE Wiesner, 1920

Genus **SPIROLOCULINA** d'Orbigny, 1826

*Type species.* *Spiroloculina depressa* d'Orbigny, 1826, from the Holocene of North Pacific Ocean (Mariana Islands?).

**Spiroloculina** sp. Plate 10, Figures 1-3

*Material.* Six axial sections from samples ZRD12, 23, 32, 35-36 (Zranda section).

*Dimensions.* T. 1800µm-2300µm (6 specimens); D. 2200µm-2800µm (specimens).

*Description.* All specimens are megalospheric. Test planispiral, ovate to fusiform in shape with more rounded periphery. Walls imperforate, porcelaneous. Proloculus small, subspherical in outline, having diameter of 200µm-350µm, followed by 4 to 6 whorls. Each whorl possesses two chambers, each one half coil in length.

*Discussion.* Lack of equatorial sections and extracted free specimens make it difficult to identify species. However, it is distinguishable from species of closely similar genera such as *Triloculina*, *Quinqueloculina* and *Idalina* by its planispiral, ovate test and one half coil chambers.

*Distribution.* *Spiroloculina* sp. is recorded in the Dungan Formation in the Zranda section where it co-occurs with *Glomalveolina primaeva*, *Lockhartia haimei*, *Miscellanea juliettae*, *M. miscella* and *Ranikothalia sindensis*. These indicate an SBZ3-SBZ4 biozonal age.

Family HAUERINIDAE Schwager, 1876

Genus **QUINQUELOCULINA** d'Orbigny, 1826

*Type species.* *Serpula seminulum* Linné, 1758, from the Holocene of Canada.

**Quinqueloculina** sp. Plate 10, Figures 4-7

*Material.* Ten equatorial sections from samples ZRD21, 27, 34-38 (Zranda section).

*Dimensions.* D. 800µm-1500µm (10 specimens).

*Description.* All specimens described here are megalospheric. Test oval to subtriangular in cross section. Early chambers are strongly quinqueloculine, overlapping each other, later quinqueloculine throughout. 4 to 5 chambers in each whorl, gradually increasing in

size as added; peripheral chambers nearly cylindrical. Chamber periphery in early whorls is sharp and angular, gradually become rounded in later whorls. Wall porcelaneous, imperforate. Proloculus small, spherical in shape with diameter of 80µm-130µm.

*Discussion.* Lack of axial sections and extracted free specimens make it difficult to identify to species level. However, it is distinguished from species of the closely similar genus *Triloculina* by its distinctive quinqueloculine chambers throughout, and test outline.

*Distribution.* *Quinqueloculina* sp. is one of the commonly occurring LBF in the Lockhart Formation of Shakardara Well-1 and the Kotal Pass section, and the Dungan Formation in the Zranda and Mughal Kot sections. *Quinqueloculina* sp. is associated with *Idalina sinjarica*, *Glomalveolina primaeva*, *Lockhartia haimei*, *Miscellanea juliettae* and *Coskinon rajkae*, which indicate a biostratigraphic range of SBZ3-SBZ4 biozones.

#### Genus **TRILOCULINA** d'Orbigny, 1826

*Type species.* *Miliolites trigonula* Lamarck, 1804, from the Eocene of Paris Basin, France.

**Triloculina** sp.      Plate 10, Figures 8-9

*Material.* Two equatorial sections from sample 4468 (Shakardara Well-1); 5 equatorial sections from sample ZRD24 (Zranda section).

*Dimensions.* 400µm-800µm (7 specimens).

*Description.* Test triangular to subtriangular in shape. Chambers are elongated with rounded periphery, arranged initially as in *Quinqueloculina*, then triloculine with three planes of coiling. There are three large, elongated chambers making a triangular pattern in the final whorl. Wall imperforate, porcelaneous.

*Discussion.* Lack of axial sections and extracted free specimens make it difficult to identify to species level. However, it is differentiated from species of the closely similar genus *Quinqueloculina* by its later triloculine coiling and triangular-subtriangular test shape.

*Distribution.* *Triloculina* sp. is recorded in the Lockhart Formation of the Shakardara Well-1 and the Kotal Pass section, and in the Dungan Formation in the Zranda section, associated with *Coskinon rajkae*, *Lockhartia haimei*, *Idalina sinjarica*, *Glomalveolina primaeva* and *Ranikothalia sindensis*. These associations indicate an SBZ3-SBZ4 biozonal range.

Genus **IDALINA** Schlumberger & Munier-Chalmas, 1884

*Type species.* *Idalina antiqua* Schlumberger & Munier-Chalmas, 1884, from the Cretaceous of France.

***Idalina sinjarica*** Grimsdale, 1952      Plate 10, Figures 10-14

1952      *Idalina sinjarica* Grimsdale, p. 230, pl. 20, figs 11-14.

In press      *Idalina sinjarica* Grimsdale; Afzal *et al.*, fig. 8S.

*Lectotype.* Grimsdale (1952) did not assign a type from his original material from the Paleocene-Early Eocene Sinjar Limestone of Jebel Sinjar, NW Iraq. Grimsdale's original suite of specimens is deposited in the NHM, collection No. P. 40672, 40706-

40708. The specimen NHM No. P. 40672 (well-preserved transverse section) is here designated as a lectotype (Grimsdale 1952, pl. 20, fig. 14) and specimens NHM No. P. 40706-40708 as paralectotypes (Grimsdale 1952, pl. 20, figs 11-13).

*Material.* Twenty-one axial sections from samples ZRD5, 8-9, 12-16, 21-26, 30-38 (Zranda section); 5 axial sections from samples 4471.89, 4468 (Shakardara Well-1).

*Dimensions.* T. 300 $\mu$ m-1400 $\mu$ m (10s of specimens); D. 1000 $\mu$ m-2300 $\mu$ m (10s of specimens).

*Diagnosis.* Large, subspherical to oval-fusiform test with small globular proloculus; initial coiling quinqueloculine with small angular, overlapping chambers, followed by triloculine-biloculine coiling with large rounded-margin chambers.

*Description.* Test subspherical, oval to fusiform. Proloculus small globular in shape, having 50 $\mu$ m-80 $\mu$ m diameter, followed by chambers one half coil in length. Initial coiling is quinqueloculine, later becoming biloculine. Chambers in initial whorls are angular, small and strongly overlapping, becoming larger with rounded peripheries in the later whorls. Chambers possess thick inner wall. Test wall porcelaneous and imperforate.

*Discussion.* *I. sinjarica* is distinguished from the Cretaceous species of *Idalina* by its larger test size and strong quinqueloculine initial and biloculine adult coiling. *I. sinjarica* differs from *I. berthelini* Schlumberger, 1905 by lacking striate ornament, and from *I. antiqua* Schlumberger & Munier-Chalmas, 1884 by possessing chambers with a thick inner wall.

*Distribution.* *I. sinjarica* is present in the Lockhart Formation of the Kotal pass section and the Shakardara Well-1, and in the Dungan Formation in the Mughal Kot and Zranda sections. In these sections, *I. sinjarica* is associated with *Laffitteina bibensis*, *L. erki*, *Miscellanea juliettae*, *M. miscella*, *Glomalveolina primaeva*, *Alveolina* sp. and

*Fallotella alavensis*, which suggest a biostratigraphic range within the SBZ2-SBZ6 biozones. *I. sinjarica* has been reported from the Late Paleocene-earliest Eocene of Tethys elsewhere (Serra-Kiel *et al.* 1998; Drobne *et al.* 2002; Afzal *et al.* in press).

Superfamily ALVEOLINOIDEA Ehrenberg, 1839

Family ALVEOLINIDAE Ehrenberg, 1839

Genus **GLOMALVEOLINA** Hottinger, 1962

Type species. *Alveolina dachelensis* Schwager, 1883, from the Paleocene of Egypt.

**Glomalveolina primaeva** Reichel, 1937      Plate 11 Figures 1-6

1936 *Alveolina (Glomalveolina) primaeva* Reichel, p. 88, test-fig. 29 (12-14), pl. 1, figs 3-7.

1960 *Alveolina (Glomalveolina) primaeva* Reichel; Hottinger, p. 31-32, pl. 1, figs 3-7.

2008 *Glomalveolina primaeva*; Scheibner & Speijer, p. 24, pl. 1, fig. E.

2009 *Glomalveolina primaeva*; Scheibner & Speijer, p. 210, fig. 11A.

In press *Glomalveolina primaeva* Reichel; Afzal *et al.*, fig. 8O.

*Holotype*. Designated Reichel (1937, pl. 1, figs 3-4), NMB No. Ms/C 12781, from the Paleocene of Marsoulas (Pyrenees), Spain.

*Material*. Five axial sections of megalospheric form and 7 axial sections of microspheric form from samples ZRD18, 23-25, 34-36 (Zranda section).

*Dimensions*. Megalospheric form, D. 700µm-1300µm (5 specimens); Microspheric form, D. 1400µm-1800µm (6 specimens).

*Diagnosis.* Small globular test, small spherical proloculus; initial 2 to 3 tight milioline-spined whorls, followed by 4 to 6 planispiral and loose whorls; thick chamber walls and septula.

*Description.* Test small, globular in shape with relatively loose opening spire. In axial section, proloculus small, spherical in shape, 70µm-100µm in diameter, followed by 2 to 3 tight milioline-spined whorls; these are followed by 4 to 6 planispiral and loose whorls. Chamberlets are smaller subspherical in the early whorls and become relatively larger and of rectangular to elongated shape in later whorls. Chamber walls and septula are thick. Thickness of the basal layer is about the height of whorl.

*Discussion.* *G. primaeva* is differentiated from *G. lepidula* (Schwager, 1883) by its relatively loose spire and from *Gl. telemetensis* Hottinger, 1960 and *G. levis* Hottinger, 1960 by its small test size.

*Distribution.* *G. primaeva* is recorded in the lower Dungan Formation in the Zranda section, associated with *Miscellanea juliettae*, *Coskinon rajkae* and *Fallotella alavensis* and later with *M. miscella*, indicating a SBZ3-SBZ4 biozonal range. *G. primaeva* is widely reported from the early-late Thanetian (SBZ3-SBZ4 biozones) of Tethyan carbonate successions (e.g. Hottinger 1960; White 1992; Serra-Kiel *et al.* 1998; Jauhri & Agarwal 2001; Pignatti *et al.* 2008; Scheibner & Speijer 2009; Afzal *et al.* in press).

**Glomalveolina telemetensis** Hottinger, 1960      Plate 11, Figures 7-10

1960 *Alveolina* (*Glomalveolina*) *telemetensis* n. sp. Hottinger, p. 35, pl. 1, figs 15-18.

2009 *Glomalveolina telemetensis*; Scheibner & Speijer, p. 210, fig. 11D.

In press *Glomalveolina telemetensis* Hottinger; Afzal *et al.*, fig. 8T.

*Holotype.* Designated Hottinger (1960, pl. 1, fig. 15), NMB No. Ua 7/C 14410, from the Paleocene of Gebel Telemet, Egypt.

*Material.* Four axial sections of megalospheric form and 3 axial sections of microspheric form from samples ZRD9, 19, 21, 25 (Zranda section).

*Dimensions.* Megalospheric form, D. 1600 $\mu$ m-2200 $\mu$ m (4 specimens); microspheric form, D. 1900 $\mu$ m-2700 $\mu$ m (3 specimens).

*Diagnosis.* Spherical to subspherical test, moderately open coiling; 2 to 4 initial whorls are tight, followed by 6 to 8 moderately open.

*Description.* Test spherical to subspherical with moderately open coiling. Proloculus spherical in shape, having diameter of 80 $\mu$ m-120 $\mu$ m, followed by 2 to 4 tight whorls and by 6 to 8 moderately open adult whorls. Chambers are spherical to subspherical in early whorls and slightly elongated in later whorls. Thickness of the basal layer is about half the height of whorl.

*Discussion.* *G. telemetensis* is distinguished from *G. primaeva* and *G. lepidula* (Schwager, 1883) by its large test and moderately opening coiling, and from *G. levis* Hottinger, 1960 by possessing spherical to subspherical test shape.

*Distribution.* *G. telemetensis* is recorded in the Dungan Formation in the Zranda section, associated with *G. primaeva*, *Fallotella alavensis*, *Coskinon rajkae* and *Miscellanea miscella*, indicating an SBZ3-SBZ4 biostratigraphic range. It has been reported from the Thanetian (SBZ3-SBZ4 biozones) of Egypt (Scheibner & Speijer 2009).

**Glomalveolina lepidula** (Schwager, 1883) Plate 11, Figures 11-13

1883 *Alveolina ellipsoidalis* Schwager var. *lepidula* Schwager, p. 98, pl. 25, figs 3a-g.

1960 *Alveolina (Glomalveolina) lepidula* (Schwager); Hottinger, p. 57, pl. 1, figs 25-29; pl. 2, Figs 9, 25.

2007 *Glomalveolina lepidula* (Schwager), 1883; Özgen-Erdem *et al.*, p. 913, fig. 5a. (q.v. for full synonymy).

2009 *Glomalveolina lepidula*; Scheibner & Speijer, p. 210, fig. 11F.

In press *Glomalveolina lepidula* (Schwager); Afzal *et al.*, fig. 9O.

*Neotype.* Original syntype material of Schwager (1883) is lost. Consequently, Hottinger (1960, pl. 1, fig. 27) designated specimen NMB No. Ua 8a/C 13113 from the Ilerdian of Gebel Telemet, Egypt as a neotype.

*Material.* Two equatorial and 2 axial sections from sample BD5 (Muree Brewery section).

*Dimensions.* Megalospheric form, D. 700µm-950µm (2 specimens); microspheric form, D. 900µm-1350µm (2 specimens).

*Diagnosis.* Small oval-shaped test, tight coiling; initial 1-2 whorls are streptospiral with milioline-type chambers, followed by 6-9 planispiral whorls; thin basal layer.

*Description.* Test is small, oval with tight coiling. Proloculus spherical with a diameter of 70µm-80µm, followed by 1 to 2 whorls with milioline-chambers. These are followed by 6 to 9 whorls of adult chambers. Small microsphere is followed by early streptospiral coiled chambers of two cycles. Later chambers are planispirally coiled. Basal layer is thin. In some axial sections, axial thickening of the basal layer is observed. Chamberlets are spherical in shape in the inner whorls and ovoid or rectangular in the outer whorls.

*Discussion.* The small oval test and tight coiling differentiate this species from *G. primaeva* Reichel, 1937, *G. telemetensis* Hottinger, 1960 and *G. levis* Hottinger, 1960.

*Distribution.* It is recorded in the Dungan Formation in the Muree Brewery section, associated with *Miscellanea miscella*, *Ranikothalia nuttalli* and *Assilina dandotica* and later with *Nummulites atacicus* and *N. globulus*. These occurrences indicate a range of SBZ5-SBZ8 biozones for *G. lepidula*. *G. lepidula* is one of the commonly occurring *Glomalveolina* in the Early Eocene (SBZ5-SBZ9 biozones) of Tethys (Hottinger 1960; Serra-Kiel 1998; Scheibner & Speijer 2009; Afzal *et al.* in press).

Genus **ALVEOLINA** d'Orbigny, 1826

*Type species.* *Oryzaria boscii* DeFrance, 1826, from the Eocene of Pontoise, France.

**Alveolina sp.** Plate 12, Figures 1-11

*Material.* Seventeen random sections from samples BD3-8, 13-18 (Muree Brewery); 13 random sections from samples HLD6-7 (Hanna Lake).

*Dimensions.* D. 2500µm-3700µm (20 specimens).

*Description.* Test nearly spherical to oval with flosculinized circular whorls. Whorls are 7 to 9 in number, showing loose to tight flosculinized coiling. Chamberlets are ovoid or rectangular in shape, small, dense in the juvenile stage, slightly depressed in the adult stage. Basal layer is thin to thick.

*Discussion.* Due to random and non-oriented sections, species determination is difficult. However, *Alveolina* sp. is distinguished from species of the closely similar genus *Glomalveolina* by possessing a large test, distinct basal layer and strong flosculinization.

*Distribution.* *Alveolina* sp. is present throughout the Dungan Formation in the Muree Brewery section, associated with *Miscellanea miscella*, *Assilina dandotica*,

*Ranikothalia nuttalli* and *Nummulites atacicus*. In the Zranda section, it is recorded in the uppermost Dungan Formation, associated with *M. miscella*, *R. nuttalli* and *Ass. dandotica*. In the Hanna Lake section, *Alveolina* sp. is recorded in the lower Dungan Formation, associated with *M. miscella*, *R. nuttalli* and *Ass. dandotica*. Based on these occurrences, a SBZ5-SBZ8 biozonal range is indicated for *Alveolina* sp. *Alveolina* is one of the important biozonal LBFs, widely recorded in the Eocene of Tethys (e.g. Hottinger 1960; Serra-Kiel *et al.* 1998; Afzal *et al.* in press).

Superfamily SORITOIDEA Ehrenberg, 1839

Family SORITIDAE, Ehrenberg, 1839

Genus **SOMALINA** Silvestri, 1939

*Type species. Somalina stefaninii* Silvestri, 1939, from the Lower Eocene of Somalia.

**Somalina** sp. Plate 13, Figure 1-4

*Material.* Three axial sections of microspheric form and 2 axial sections of megalospheric form from samples BD3-5 (Murree Brewery section).

*Dimensions.* Megalospheric form, D. 2700µm-3400µm (2 specimens), T. 600µm-800µm (2 specimens); microspheric form, T. 800µm-1500µm (3 specimens); D. 4000µm-6000µm (5 specimens).

*Description.* Megalospheric test medium, lenticular, occasionally slightly to strongly undulate. In axial section, embryonic apparatus comprising a small proloculus and a flexostyle. Protoconch rounded, rectangular to subrectangular, 50µm-100µm in diameter, showing simple loop-type shape. Post embryonic chambers arcuate, not

increasing in height significantly from the centre to the periphery of the test. Microspheric test medium to large size with partially vacuolated lateral walls.

*Discussion.* *Somalina* sp. axial sections have morphological similarities with those of *S. hottingeri* White, 1997; however, *Somalina* sp. has a smaller protoconch. It is differentiated from *S. stefaninii* Silvestri, 1939 by possessing a simple loop-type protoconch. However, lack of equatorial sections makes detailed comparison of *Somalina* sp. with other species of *Somalina* difficult.

*Distribution.* It is recorded in the lower Dungan Formation in the Murree Brewery section, associated with *Ranikothalia nuttalli*, *Assilina dandotica*, *Miscellanea miscella* and *Discocyclina dispansa*, indicating an SBZ5-SBZ6 biozonal range. *Somalina* has been reported from the Early to Middle Eocene of UEA, Iran, Afghanistan, Egypt and Oman (e.g. White 1997; Boukhary *et al.* 2006; Afzal *et al.* in press).

#### Genus **OPERTORBITOLITES** Nuttall, 1925

*Type species.* *Opertorbitolites douvillei* Nuttall, 1925, from the Bolan Pass area, Balochistan, Pakistan.

#### **Opertorbitolites** sp. Plate 13, Figure 5

*Material.* One axial section from sample ZRD1 (Zranda section).

*Dimensions.* D. 5430 $\mu$ m (1 specimen); T. 1240 $\mu$ m (1 specimen).

*Description.* Test lenticular with cyclic chambers subdivided into numerous small chamberlets. Test consists of a median chamber layer, covered with successive laminae on the sides above and below. Median chambers are elongate-cylindrical in shape, extending across the whole test length. Median layer is thicker in the peripheral region

and thinner in the central part of the test. Protoconch large, spherical in shape, having diameter of 540 $\mu$ m, resulting in umbilical thickening.

*Discussion.* This is clearly a species of *Opertorbitolites* and is distinguishable from *Orbitolites* species by its lenticular test shape and laminae on both sides of median chambers layers. It is different from species of *Somalina* in lacking vacuolate lateral lamellar structures. However, due to insufficient material and lack of equatorial sections, a species identification is not possible.

*Distribution.* *Opertorbitolites* sp. is present in the uppermost Dungan Formation in the Zranda section, associated with *Ranikothalia nuttalli*, *Miscellanea miscella* and *Assilina dandotica*, indicating an SBZ5/6 biozonal age. It has been widely reported from the Early Eocene of Middle East, Turkey, Mediterranean, Indian continent and West Africa (BouDagher-Fadel 2008; Afzal *et al.* in press).

Family KERAMOSPHAERIDAE Brady, 1884

Genus **KERAMOSPHAERA** Brady, 1882

*Type species.* *Keramosphaera murrayi* Brady 1882, from the Holocene of Antarctica.

**Keramosphaera cf. iranica** Rahaghi, 1983 Plate 10, Figure 14

? 1983 *Keramosphaera iranica* n. sp. Rahaghi, p. 47, pl. 19, figs 1-9; pl. 20, figs 1-11.

In press *Keramosphaera cf. iranica* Rahaghi; Afzal *et al.*, fig. 8 X.

*Material.* One equatorial section from sample ZRD26 (Zranda section).

*Dimension.* D. 1750 $\mu$ m.

*Description.* Test spherical in shape with spherical concentric series of chambers. Chambers are irregularly shaped in outline, ranging from ellipsoidal to subquadrangular, arranged in irregular concentric layers. Chambers are smaller in size in early layers, gradually increasing in size as added, with chamber wall thickness varying between 20µm and 35µm.

*Discussion.* Spherical test with irregular concentric layers of ellipsoidal-subquadrangular shape chambers of *K. cf. iranica* are very similar with those of *Keramosphaera iranica* Rahaghi, 1983. *K. cf. iranica* is distinguished from *K. murrayi* Brady, 1882 by its smaller test and from *K. allobrogensis* (Steinhauser, 1969) by possessing a larger test.

*Distribution.* It is recorded in the lower Dungan Formation in the Zranda section, associated with *Glomalveolina primaeva*, suggesting an SBZ3 biozonal age. *K. iranica* has been reported from the Late Paleocene of Iran (Rahaghi 1983).

Suborder TEXTULARIINA Delage & Herouard, 1896

Superfamily LITUOLOIDEA de Blainville, 1825

Family SPIROCYCLINIDAE Munier-Chalmas, 1887

Genus **SAUDIA** Henson, 1948

*Type species.* *Saudia discoidea* Henson, 1948, from the Early Eocene of Saudi Arabia.

**Saudia sp.** Plate 13, Figures 7-10

*Material.* Five axial sections from samples ZRD23, 29, 36 (Zranda section).

*Dimensions.* D. 4500µm-5500µm (5 specimens); T. 500µm-950µm (5 specimens).

*Description.* All specimens are microspheric. Test large, discoidal to reniform in shape with gently rounded margins. In axial section, chambers are small in size, cylindrical to irregular in shape, arranged as lateral zone, forming a thin network of beam and rafter like structures. In median region, interseptal pillars are present, and these appear to connect chambers. In adult chambers, additional pillars are added.

*Discussion.* *Saudia* sp. is distinguished from *S. discoidea* Henson, 1948 and *S. labyrinthica* Grimsdale, 1952 by its small chambers and thin relatively simple network of pillars and rafters and from. It is differentiated from the closely related genus *Thomasella* (Sirel, 1998) by its relatively simple pillar system and from *Vania* (Sirel & Gündüz, 1985) species by possessing pillars.

*Distribution.* *Saudia* sp. is recorded in the upper Lockhart Formation of the Kotal pass section, Core-2 of Shakardara Well-1 and Dungan Formation in the Zranda section. In these sections, it is associated with *Glomalveolina primaeva*, *G. telemetensis*, *Coskinon rajkae*, *Miscellanea miscella*, *Lockhartia haimei*, *Idalina sinjarica* and *Ranikothalia nuttalli*, indicating an SBZ3-SBZ5/6 biozonal range. *Saudia* is reported from the Paleocene to Middle Eocene of the Mediterranean, Turkey, Middle East and West Africa (BouDagher-Fadel 2008).

Superfamily ORBITOLINOIDEA Martin, 1890

Family ORBITOLINIDAE Martin, 1890

Genus **FALLOTELLA** Mangin, 1954

*Type species.* *Fallotella alavensis* Mangin, 1954, from the Paleocene of Vitoria, Alava, Spain.

**Fallotella alavensis** Mangin, 1954      Plate 14, Figures 1-4

1954 *Fallotella alavensis* Mangin, p. 209-217, pl. 3, figs 1-6.

1960 *Fallotella alavensis* Mangin; Douglass, pl. 6, figs 14-19.

1980 *Fallotella (Fallotella) alavensis* Mangin 1954; Hottinger & Drobne, p. 236-237, pl. 2, figs 1, 3; pl. 14, figs 1-27). (q.v. for full synonymy).

1988 *Fallotella alavensis* Mangin, 1954; Loeblich & Tappan, p. 159, pl. 173, figs 1-7.

In press *Fallotella alavensis* Mangin; Afzal *et al.*, fig. 8W.

*Type material.* Mangin (1954, pl. 3, figs 1-6) did not assign types within his original material from the Paleocene of Vitoria, Alava, Spain. The repository for Mangin's original suite of specimens is not known. Subsequently, Douglass (1960, pl. 6, figs 14-19) designated specimens NMNH No. MO. 626535-626537 as neotypes.

*Material.* Nine axial sections from samples ZRD36, 38-39 (Zranda section).

*Dimensions.* D. 1100 $\mu$ m-1450 $\mu$ m (9 specimens); T. 1200 $\mu$ m-1950 $\mu$ m (9 axial sections).

*Diagnosis.* Test small, high conical with subcylindrical adult growth, simple to moderately complex exoskeleton (beams) and endoskeleton (pillars); horizontal partitions (rafters) are absent.

*Description.* Small, high conical test, simple to moderately complex exoskeleton (beams) with several radial beams perpendicular to the septa, new beams intercalated in the larger chambers, making space between chambers nearly constant. Vertical partitions solid, short, restricted to the lower part of chamber. Horizontal partitions (rafters) are absent. Endoskeleton shows pillars with smoothed horizontal connection in proximal chamber part; irregular-shaped connection in distal chamber part. Chambers are elongated rectangular in shape.

*Discussion.* *F. alavensis* is distinguished from *Fallotella kochanskae* Hottinger & Drobne, 1980 by its lack of horizontal partitions and from other conical forms by its simple to moderately complex exoskeletal and endoskeletal structures.

*Distribution.* *F. alavensis* occurs in the lower part of the Dungan Formation in the Zranda Section. It is associated with *Coskinon rajkae*, *Vania anatolica*, *Idalina sinjarica*, *Karsella hottingeri* and *Miscellanea juliettae*, indicating the SBZ3 Biozone. It has been reported from similar age successions in Tethys (e.g. Egypt, Iran, Slovenia, Turkey, Spain, Hottinger & Drobne 1980; Serra-Kiel *et al.* 1998; Zamagni *et al.* 2008; Scheibner & Speijer 2009).

Genus **KARSELLA** Sirel, 1997a

*Type species.* *Karsella hottingeri* Sirel, 1997a, from the Paleocene of Van, East Turkey.

*Diagnosis.* Shell large, high conical with convex base, up to 4.7 mm in height and 3.3 mm in breath, apically located subspherical megalosphere followed by large hemispherical chambers of early stage. Periembrionic chambers are arranged in a trochoid spire of one half whorls, microspheric embryo unknown; adult chambers rectilinear and discoidal (cup-shaped) that enlarge rapidly in diameter as added in both generations. Exoskeleton consists of thick agglutinated wall, numerous elongate vertical partitions (beams) subdividing the chamber interior, there may be more generations of beams intercalated between adjacent major ones in the marginal zone and the longer primary beams that thicken rapidly, becoming irregular undulating and that continue into the central zone of cone, several generations of beams and rafters forming numerous chamberlets in the central zone and alveolar compartments in the marginal zone of the cone, the chamberlets alternating in position from chamber to chamber; endoskeletal thick pillars are subcircular in section; aperture in the early coil a single

opening per chamber, in the rectilinear portions a circle of irregularly spaced pores occur on the central zone of discoidal chamber floor, marginal foramina present, dimorphism distinct (after Sirel 1997a, p. 208).

**Karsella hottingeri** Sirel, 1997a Plate 14, Figures 5-10

1997a *Karsella hottingeri* n. sp. Sirel, p. 210, pl. 1, figs 1-10; pl. 2, figs 1-4.

*Holotype*. Designated Sirel (1997a, pl. 1, fig. 2), General Directorate of Mineral Research and Exploration, Ankara, Turkey collection No. 104/3, from the Thanetian of East Turkey.

*Material*. Thirteen axial and 8 basal sections from samples ZRD24-26, 34-36, 39 (Zranda section).

*Dimensions*. D. 2600 $\mu$ m-3300 $\mu$ m (21 specimens); T. 2400 $\mu$ m-3850 $\mu$ m (13 specimens).

*Diagnosis*. Large, high conical test with complex exoskeletal and endoskeletal partitions; exoskeleton consists of 3 to 4 or more generations of undulated beams; endoskeleton consists of thick circular pillars; chambers are rectangular to discoidal in shape.

*Description*. All specimens are microspheric. Test complex, large, high conical with convex base. In basal section, exoskeleton (peripheral zone) consists of undulated 3 to 4 or more generations of beams, subdividing chamber interior, beams become thicker, longer and irregularly undulated toward central region. In central region, several generations of beams and rafters forming numerous chamberlets and in peripheral zone alveolar partitions. Endoskeleton consists of thick circular pillars with irregularly spaced pores in the central region and foramina in peripheral zone. In axial section, chambers are rectangular to discoidal in shape, increasing in diameter as added.

Megalospheric embryo at apex of test, large, subspherical in shape and of 190µm-300µm in diameter, followed by periembryonic chambers.

*Discussion.* *K. hottingeri* is differentiated from morphologically similar forms such as *Dictyoconus* and *Falotella alavensis* Mangin, 1954 in possessing large-test dimensions (i.e. D. 2600µm-3300µm; T. 2400µm-3850µm), and more complex exoskeletal and endoskeletal partitions.

*Distribution.* *K. hottingeri* occurs in the Dungan Formation in the Zranda section, associated with *Glomalveolina primaeva*, *Falotella alavensis*, *Miscellanea juliettae* *Vania anatolica*, indicating an SBZ3-SBZ4 biozonal range. *K. hottingeri* is reported from the Thanetian of Turkey (Sirel 1997a) and Iran (Hottinger & Drobne 1980).

#### Genus **DICTYOCONUS** Blanckenhorn, 1900

*Type species.* *Patellina egyptiensis* Chapman, 1900, from the Middle Eocene of Egypt.

**Dictyoconus sp.** Plate 13, Figures 11-15

In press *Dictyoconus* sp.; Afzal *et al.*, fig. 8U.

*Material.* Eight axial and 2 basal sections from samples ZRD9, 13, 19, 39 (Zranda section).

*Dimensions.* D. 1800µm-2980µm (10 specimens); T. 1900µm-3000µm (8 specimens).

*Description.* Test conical, megalospheric embryo with spherical-sub spherical eccentric proloculus of 330µm-550µm diameter and hemispherical deuteroconch located below the apex, followed by almost planispiral chambers and then by more numerous rectangular chambers. Microspheric generation with numerous spiraling chambers; wall with thin marginal epidermis covering the long widely spaced primary exoskeletal beams,

two orders of intercalated shorter beams, and two orders of horizontal partitions or rafters in each chamber resulting in a complex reticular subepidermal network; numerous endoskeletal pillars are visible in basal section with a series of pores over the base of the cone.

*Discussion.* *Dictyoconus* sp. is distinguished from *D. egyptiensis* (Chapman, 1900) by its small spherical-sub spherical eccentric proloculus. *D. turriculus* Hottinger & Drobne, 1980 differs from *Dictyoconus* sp. in having an extremely high-conical test.

*Distribution.* *Dictyoconus* is one of the common LBFs in the Dungan Formation in the Zranda section. It is associated with *Coskinon rajkae*, *Fallotella alavensis*, *Vania anatolica* and *Glomalveolina primaeva* and later with *Miscellanea miscella* and *Ranikothalia sindensis*, indicating an SBZ3-SBZ4 biozonal range. It has been reported from the Cretaceous to Eocene of Tethys (BouDagher-Fadel 2008).

Superfamily COSKINOLINOIDEA Moullade, 1965

Family COSKINOLINIDAE, Moullade, 1965

Genus **COSKINON** Hottinger & Drobne, 1980

*Type species.* *Coskinon rajkae* Hottinger & Drobne, 1980, from the Paleocene of Golöz (North of Slavnic Mountain), Slovenia.

**Coskinon rajkae** Hottinger & Drobne, 1980      Plate 15, Figures 1-5

1980 *Coskinon* (*Coskinon*) *rajkae* n. sp. Hottinger & Drobne, p. 231-232, pl. 2, figs 2-4; pl. 12, figs 1-28. (q.v. for full synonymy).

In press *Coskinon rajkae* Hottinger & Drobne; Afzal *et al.*, fig. 8V.

*Holotype.* Designated Hottinger & Drobne (1980, pl. 12, fig. 1), collection No. Go 8/4, from the Paleocene of Golž (North of Slavnic mountain), Slovenia, housed in the Institute of Paleontology of the Slovenian Academy of Sciences and Arts, Ljubljana, Slovenia.

*Material.* Ten axial and 2 basal sections from samples ZRD32, 36, 39 (Zranda section).

*Dimensions.* D. 1000µm-1850µm (12 specimens); T. 1100µm-1800µm (10 specimens).

*Diagnosis.* Small, high conical test with trochospiral coiling; proloculus apical; lacks any exoskeleton in the marginal zone; longer juvenile stage.

*Description.* Test conical, with low trochospiral coiling, proloculus apical, followed by reduced early coiled stage, later uniserial, lacks any exoskeleton in the marginal zone. Longer juvenile stage. Scattered endoskeletal pillars present in the uniserial stage; chambers elongated with sharp margins, slightly larger than high.

*Discussion.* *C. rajkae* is distinguished from *C. floridana* (Cole, 1941) by its smaller test size and longer juvenile stage. It is differentiated from the species of the morphologically similar genus *Coskinolina* by lacking any exoskeleton in the marginal zone.

*Distribution.* *C. rajkae* is recorded in the lower Dungan Formation in the Zranda section and the lower Lockhart Formation in the Kotal Pass section, associated with *Fallotella alavensis*, *Vania anatolica*, *Lockhartia haimei*, *Miscellanea juliettae* and *Glomalveolina primaeva*, indicating a SBZ3 biozonal age. It has been reported from a similar biostratigraphic interval in the Tethys (Hottinger & Drobne 1980; Loeblich & Tappan 1988; Serra-Kiel *et al.* 1998; Zamagni *et al.* 2008; Afzal *et al.* in press).

Superfamily ATAXOPHRAGMIOIDEA Schwager, 1877

Family DICYCLINIDAE Hellen & Tappan, 1964

Genus **VANIA** Sirel & Gündüz, 1985

*Type species.* *Vania anatolica* Sirel & Gündüz, 1985 from the Thanetian of Van, East Turkey.

**Vania anatolica** Sirel & Gündüz, 1985      Plate 15, Figures 6-12

1985 *Vania anatolica* n. sp. Sirel & Gündüz, p. 22-23, pl. I, figs 1-3; pl. II, figs 1-6; pl. III, figs 1-8. (q.v. for full synonymy).

*Holotypes.* Designated Sirel & Gündüz (1985, pl.1, figs I, 2), Museum d'Histoire Naturelle, Geneve collection No. 85-01, from the Thanetian of Van, East Turkey.

*Material.* Eight axial sections from samples ZRD34, 36, 38 (Zranda section).

*Dimensions.* D. 2200µm-4100µm (8 specimens); T. 100µm-500µm (8 specimens).

*Diagnosis.* Test discoidal to slightly biconcave, fairly rounded margins; reniform to flabelliform chambers; wall finely perforated with two rows of pores on margin.

*Description.* Test imperforate discoidal to slightly biconcave with somewhat rounded margins. Chambers are reniform to flabelliform in outline. Lateral walls with a network consisting of radially main beams, shorter beams and beamlets parallel to the septa. Interior subdivided by radially arranged beams and intercalated secondary beams, those of successive chambers aligned, with short rafters parallel to the septa forming a sub-epidermal network. Wall finely agglutinated imperforate with two alternating rows of pores on the periphery.

*Discussion.* *V. anatolica* is different from the morphologically similar species of the genus *Pseudobroeckinella* Deloffre & Hamaoui, 1969 in possessing flabelliform and reniform chambers. Species of *Qataria* Henson, 1948 and *Dohaia* Henson, 1948 are

distinguishable from *V. anatolica* by their numerous apertures appearing as small perforations on the peripheral wall of the test.

*Distribution.* *V. anatolica* co-occurs with *Coskinon rajkae*, *Fallotella alavensis* and *Glomalveolina primaeva* in the lower Dungan Formation in the Zranda section, which indicates a SBZ3 biozonal age. It has been reported from the early Thanetian successions of Turkey (e.g. Sirel & Gündüz 1985).

## **Larger foraminifera plates**

---

Chapter 3: Paleocene-Early Eocene larger benthic foraminifera of the Indus Basin, Pakistan: systematic palaeontology

**Plate 1** *Lockhartia*, *Sakesaria*

*Lockhartia haimeii* (Davies, 1927)

- 1: axial section, sample ZRD7, specimen a.
- 2: axial section, sample KL25, specimen a.
- 3: nearly equatorial section, sample 4471.11, specimen a.
- 4: axial section, sample KL71, specimen a.
- 5: axial section, sample ZRD35, specimen a.
- 6: nearly axial section, sample 4468, specimen a.
- 7-8: axial section, sample ZRD33, specimen a.

*Lockhartia conditi* (Nuttall, 1926)

- 9: axial section, sample KL27, specimen a.
- 10: axial section, sample KL53, specimen a.
- 11: axial section, sample 4471.89, specimen a.
- 12: axial section, sample 4468.91, specimen a.
- 13: off-centred axial section, sample KL58, specimen a.
- 14: axial section, sample KL40, specimen a.
- 15: axial section, sample KL27, specimen b.
- 16: axial section, sample KL74, specimen a.

*Lockhartia conica* Smout, 1954

- 17-18: axial section, sample 4472.24, specimen a.

*Lockhartia diversa* Smout, 1954

- 19: axial section, sample 4472.24, specimen b.
- 20: nearly axial section, sample KL33, specimen a.
- 21: axial section, sample KL35, specimen b.

*Sakesaria* sp.

- 22: nearly axial section, sample 4468, specimen b.
- 23: axial section, sample 4470.78, specimen b.
- 24: axial section, sample 4471.58, specimen b.



**Plate 2** *Laffitteina*, *Kathina*, *Rotalia*

*Laffitteina bibensis* Marie, 1946

- 1: axial section, sample PD16, specimen a.
- 2: nearly axial section, sample PD8, specimen a.
- 3: equatorial section, sample PD8, specimen b.

*Laffitteina erki* (Sirel, 1969)

- 4: axial section, sample ZRD39, specimen a.
- 5: axial section, sample ZRD29, specimen a.
- 6: nearly axial section, sample ZRD21, specimen a.
- 7: off-centred axial section, sample ZRD12, specimen a.
- 8: off-centred axial section, sample ZRD20, specimen a.
- 9: equatorial section, sample ZRD24, specimen a.

*Kathina selveri* Smout, 1954

- 10: axial section, sample ZRD32, specimen a.
- 11: axial section, sample 4468.61, specimen a.
- 12: axial section, sample ZRD36, specimen a.
- 13: axial section, sample ZRD28, specimen a.
- 14: axial section, sample ZRD39, specimen b.
- 15: axial section, sample ZRD33, specimen b.

*Rotalia* sp.

- 16-17: axial section, sample 4468.91, specimen b.
- 18-19: axial section, sample KL41, specimen a.

*Rotalia trochidiformis* Lamarck, 1804

- 20: axial section, sample KL42, specimen a.
- 21: equatorial section, sample KL39, specimen a.



**Plate 3** *Setia*, *Orbitosiphon*, *Daviesina*

*Setia tibetica* (Douvillé, 1916)

1-2: equatorial sections, showing embryo and initial chambers, sample 4468.61, specimen b.

3: axial section, showing lateral chamberlets, sample 4468, specimen c.

4: axial section, showing lateral chamberlets on both sides of equatorial plane, sample 4471.11, specimen b.

5-6: axial sections, showing embryonic chambers, sample 4471.11, specimen, c.

*Orbitosiphon punjabensis* (Davies, 1937)

7: equatorial sections, showing embryonic chambers, sample 4468.91, specimen c.

8-9: axial section, showing lateral chamberlets on both sides of equatorial plane, sample 4468.3, specimen a.

10: axial section, showing lateral chamberlets, sample 4468, specimen d.

*Daviesina* sp.

11: off-centred axial section, microspheric form, sample 4468.3, specimen, b.

12: axial section, microspheric form, sample 4471.11, specimen d.

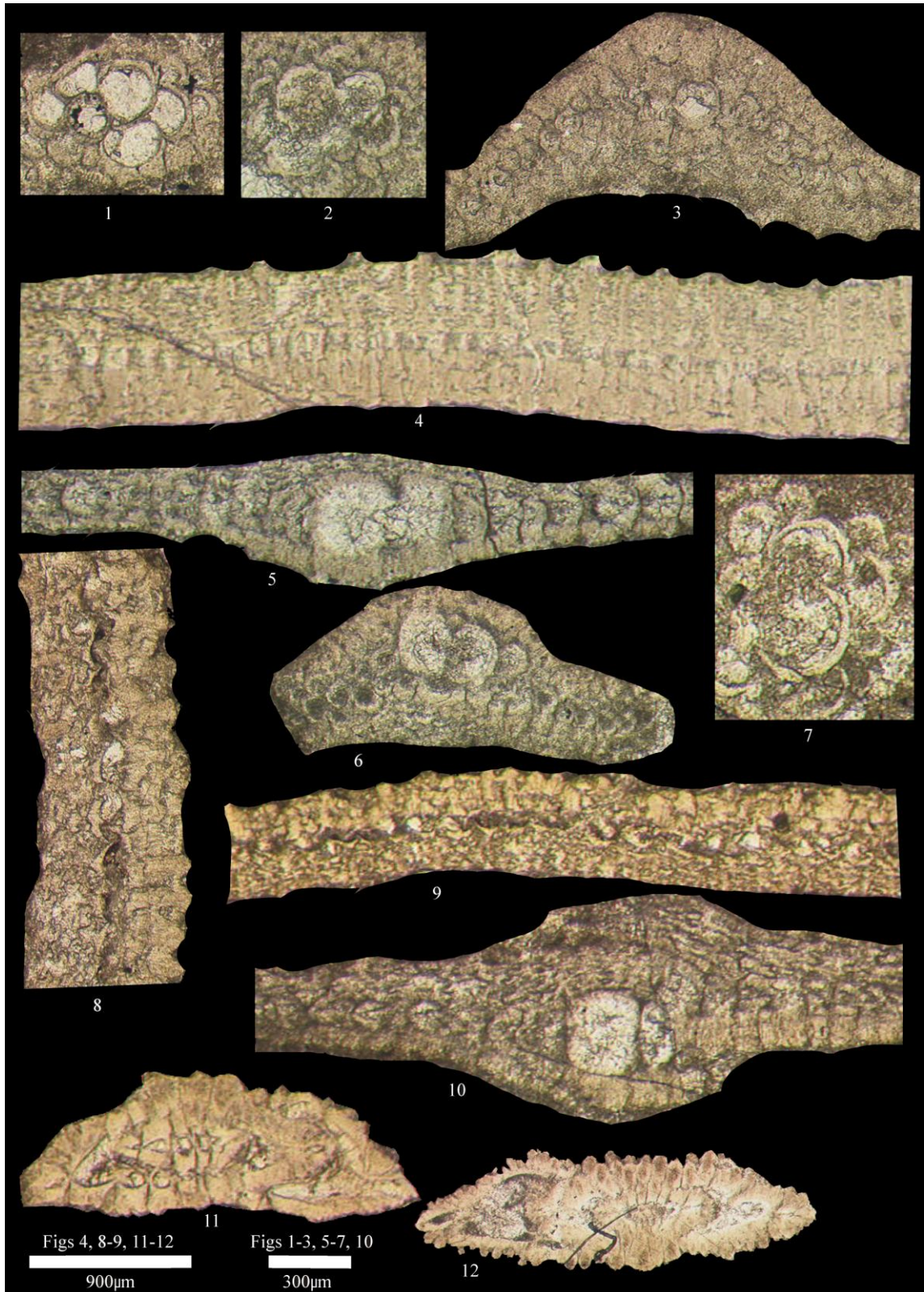


**Plate 4** *Miscellanea*

*Miscellanea miscella* (D'Archiac & Haime, 1853)

- 1: axial section, megalospheric form, sample ZRD3, specimen a.
- 2: axial section, megalospheric form, sample 4468.61, specimen c.
- 3: equatorial section, Megalospheric form, sample ZRD13, specimen d.
- 4: axial section, microspheric form, sample ZRD16, specimen a.
- 5: equatorial section, microspheric form, sample 4468.61, specimen d.

*Miscellanea juliettae* Leppig, 1988

- 6: axial section, megalospheric form, sample ZRD28, specimen b.
- 7: axial section, megalospheric form, sample ZRD29, specimen b.
- 8: nearly equatorial section, megalospheric form, sample ZRD27, specimen a.
- 9: axial section, megalospheric form, sample 4472.24, specimen c.
- 10: equatorial section, megalospheric form, sample ZRD28, specimen c.

*Miscellanites meandrinus* (Carter, 1861)

- 11: equatorial section, microspheric form, sample ZRD20, specimen b.
- 12: Equatorial section, megalospheric form, sample ZRD20, specimen c.



**Plate 5** *Ranikothalia*, *Operculina*

*Ranikothalia sindensis* (Davies, 1927)

- 1: axial section, microspheric form, sample 4471.89, specimen b.
- 2: off-centred axial section, microspheric form, sample ZRD32, specimen b.
- 3-4: axial section, microspheric form, sample ZRD29, 3, specimen c; 4, specimen d.
- 5: off-centred axial section, megalospheric form, sample ZRD28, specimen d.
- 6: axial section, megalospheric form, sample ZRD29, specimen e.
- 7-8: axial section, marginal cord, sample ZRD4, specimen a.

*Ranikothalia nuttalli* (Davies, 1927)

- 9: axial section, megalospheric form, sample ZRD1, specimen a.
- 10-11: axial section, megalospheric form, sample ZRD5, 10, specimen a; 11, specimen b.
- 12: nearly axial section, megalospheric form, sample HLD3, specimen a.
- 13: off-centred axial section, megalospheric form, sample HLD4, specimen a.
- 14: axial section, marginal cord, sample HLD3, specimen b.

*Ranikothalia sahani* Davies, 1952

- 15: axial section, megalosphere, sample ZRD5, specimen c.
- 16: axial section, megalosphere, sample ZRD28, specimen e.

*Operculina* sp.

- 17: axial section, sample HLD15, specimen a.
- 18: off-centred axial section, sample BD14, specimen a.
- 19: axial section, sample BD18, specimen a.



**Plate 6** *Assilina*

*Assilina dandotica* Davies, 1937

- 1: nearly equatorial section, megalospheric form, sample HLD3, specimen c.
- 2: axial section, megalospheric form, sample, ZRD2, specimen a.
- 3: axial section, megalospheric form, sample, ZRD3, specimen b.
- 4: axial section, megalospheric form, sample, HLD4, specimen b.
- 5: axial section, megalospheric form, sample, HLD5, specimen a.
- 6: nearly equatorial section, megalospheric form showing surface expression of septa, sample ZRD1, specimen b.
- 7: axial section, megalospheric form, sample BD3, specimen a.
- 8: axial section, megalospheric form, sample BD4, specimen a.

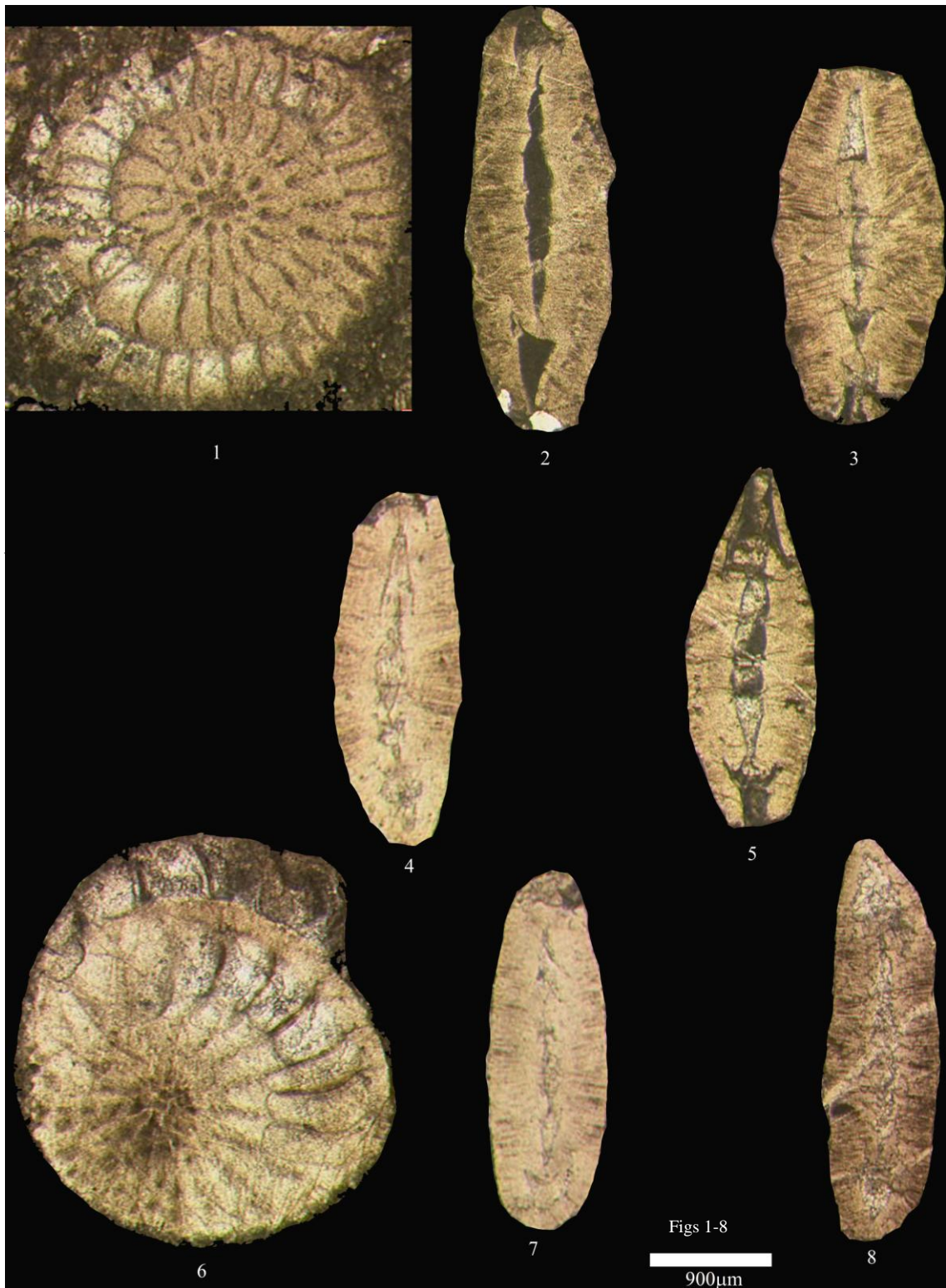


**Plate 7** *Nummulites*

*Nummulites atacicus* Leymerie, 1846

- 1: axial section, microspheric form, sample BD13, specimen a.
- 2: nearly axial section, microspheric form, sample BD13, specimen b.
- 3: nearly axial section, microspheric form, sample BD15, specimen a.
- 4: nearly equatorial section, megalospheric form, sample HLD 11, specimen a.
- 5: axial section, microspheric form, sample BD14, specimen b.

*Nummulites globulus* Leymerie, 1846

- 6: axial section, microspheric form, sample BD16, specimen a.
- 7: axial section, microspheric sample BD13, specimen c.
- 8: axial section, microspheric form, sample HLD13, specimen c.
- 9: nearly axial section, megalospheric form, sample HLD12, specimen a.
- 10: axial section, megalospheric form, sample BD14, specimen c.
- 11: off-centred equatorial section, megalospheric form, sample BD16, specimen b.
- 12-13: axial section, megalospheric form, sample HLD18, 12, specimen a; 13, specimen b.



**Plate 8** *Discocyclusina*

*Discocyclusina ranikotensis* Davies, 1927

- 1: axial section, microspheric form, sample ZRD2, specimen b.
- 2-3: axial sections, microspheric form, sample HLD10, specimen a.
- 4-5: axial sections, microspheric form, sample HLD9, 4, specimen a; 5, specimen b.
- 6: equatorial section, microspheric form sample BD11, specimen b.

*Discocyclusina dispansa* (Sowerby, 1840)

- 7-8: axial section, microspheric form, sample HLD3, 7, specimen d; 8, specimen e.
- 9: axial section, microspheric form, sample HLD4, specimen c.
- 10-11: axial section, megalospheric form, sample ZRD3, specimen c.
- 12: axial section, megalospheric form, sample BD13, specimen d.
- 13: equatorial section, megalospheric form, sample equatorial chamberlets, sample HLD14, specimen d.
- 14: equatorial section, microspheric form, showing arrangement of equatorial chamberlets, sample HLD14, specimen e.
- 15: equatorial section, megalospheric form, sample HLD14, specimen d.
- 16: equatorial section, megalospheric form, showing embryonic apparatus, sample HLD16, specimen a.
- 17: equatorial section, megalospheric form, showing embryonic apparatus, sample BD15, specimen b.

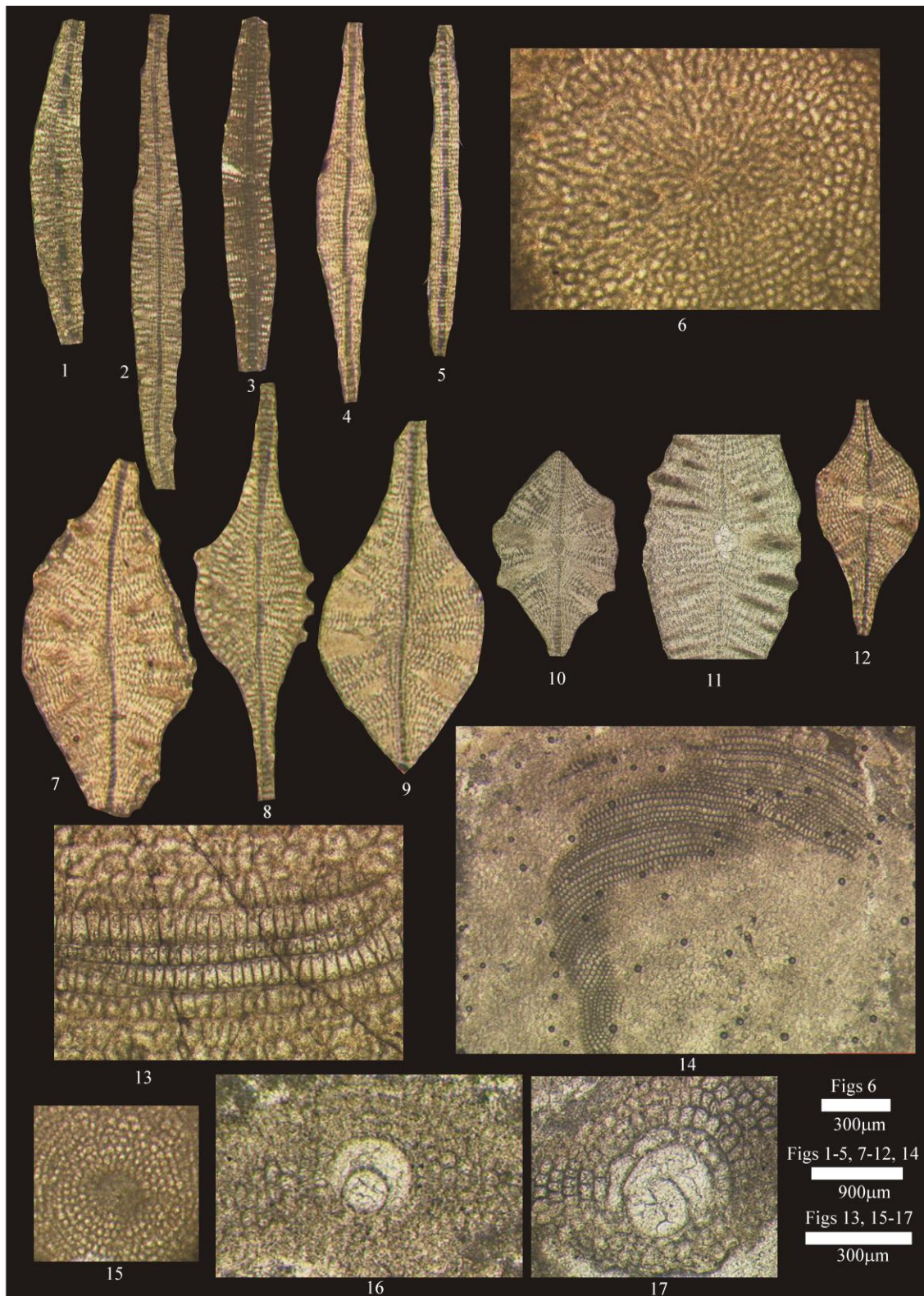


**Plate 9** *Discocyclina*, *Orbitoclypeus*, *Actinocyclina*

*Discocyclina sella* (d, Archiac, 1850)

- 1: axial section, microspheric form, sample HLD4, specimen d.
- 2: axial section, microspheric form, sample BD19, specimen a.
- 3: axial section, megalospheric form, sample BD11, specimen c.

*Actinocyclina* sp.

- 4: axial section, megalospheric form, sample HLD18, specimen c.
- 5: axial section, microspheric form, sample HLD21, specimen a.

*Orbitoclypeus* sp.

- 6: axial section, microspheric form, sample HLD12, specimen b.
- 7: axial section, microspheric form, sample HLD13, specimen b.
- 8: axial section, megalospheric form, sample HLD16, specimen b.
- 9: axial section, megalospheric form, sample HLD17, specimen a.
- 10: axial section, megalospheric form, showing embryonic chambers, samples HLD14, specimen d.
- 11: equatorial section, megalospheric form, showing embryonic chambers, samples BD17, specimen a.
- 12: equatorial section, megalospheric form, sample HLD18, specimen d.

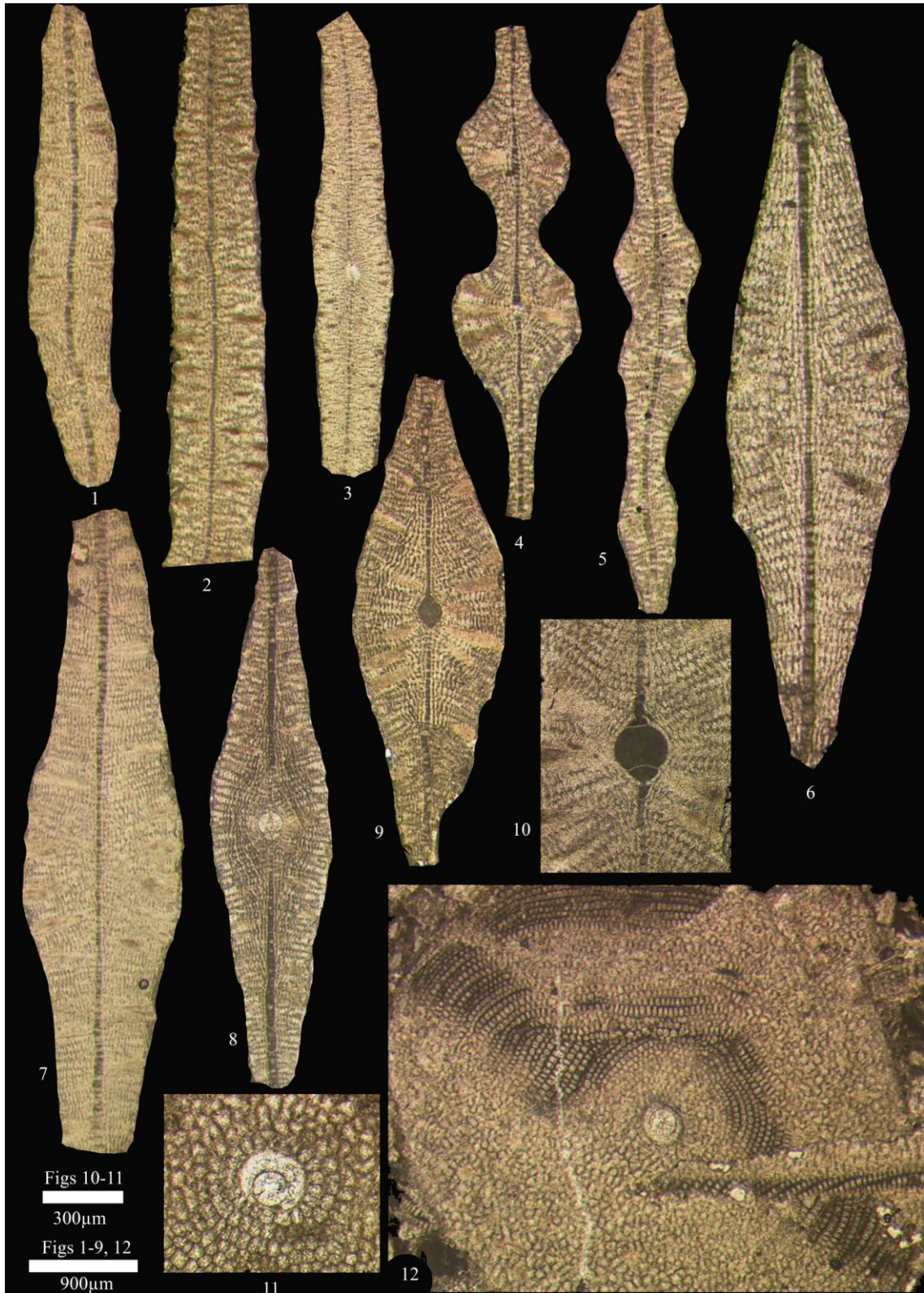


**Plate 10** *Spiroloculina*, *Quinqueloculina*, *Triloculina*, *Idalina*

*Spiroloculina* sp.

- 1: axial section, megalospheric form, sample ZRD12, specimen b.
- 2: axial section of deformed specimen of megalospheric form, sample ZRD23, specimen a.
- 3: off-centered axial section, megalospheric form, sample ZRD36, specimen b.

*Quinqueloculina* sp.

- 4: equatorial section, megalospheric form, sample ZRD35, specimen b.
- 5: equatorial section, megalospheric form, sample ZRD27, specimen b.
- 6: off-centred equatorial section, sample KL40, specimen b.
- 7: equatorial section, megalospheric form, sample KL52, specimen a.

*Triloculina* sp.

- 8: equatorial section, sample 4468, specimen e.
- 9: Equatorial section, sample ZRD24, specimen b.

*Idalina sinjarica* Grimsdale, 1952

- 10: axial section, sample 4471.89, specimen c.
- 11-12: axial sections, sample ZRD36, specimen c.
- 13: off-centred axial section, sample ZRD32, specimen c.
- 14: off-centred axial section, sample ZRD39, specimen c.



**Plate 11** *Glomalveolina*

*Glomalveolina primaeva* Reichel, 1937

- 1: off-centred axial section, microspheric form, sample ZRD36, specimen d.
- 2: axial section, microspheric form, sample ZRD25, specimen a.
- 3: axial section, megalospheric form, sample ZRD18, specimen a.
- 4: equatorial section, megalospheric form, sample ZRD18, specimen b.
- 5: off-centred axial section, microspheric form?, sample ZRD24, specimen c.
- 6: off-centred axial sections, microspheric form, sample ZRD23, specimen b.

*Glomalveolina telemetensis* Hottinger, 1960

- 7: axial section, microspheric form, sample ZRD25, specimen b.
- 8: axial section, microspheric form, sample ZRD19, specimen a.
- 9: axial section, megalospheric form, sample ZRD21, specimen b.
- 10: axial section, megalospheric form, sample ZRD9, specimen a.

*Glomalveolina lepidula* (Schwager, 1883)

- 11: off-centred equatorial section, megalospheric form, sample BD5, specimen a.
- 12: equatorial section, megalospheric form, sample BD5, specimen b.
- 13: axial section, microspheric form, sample BD5, specimen c.

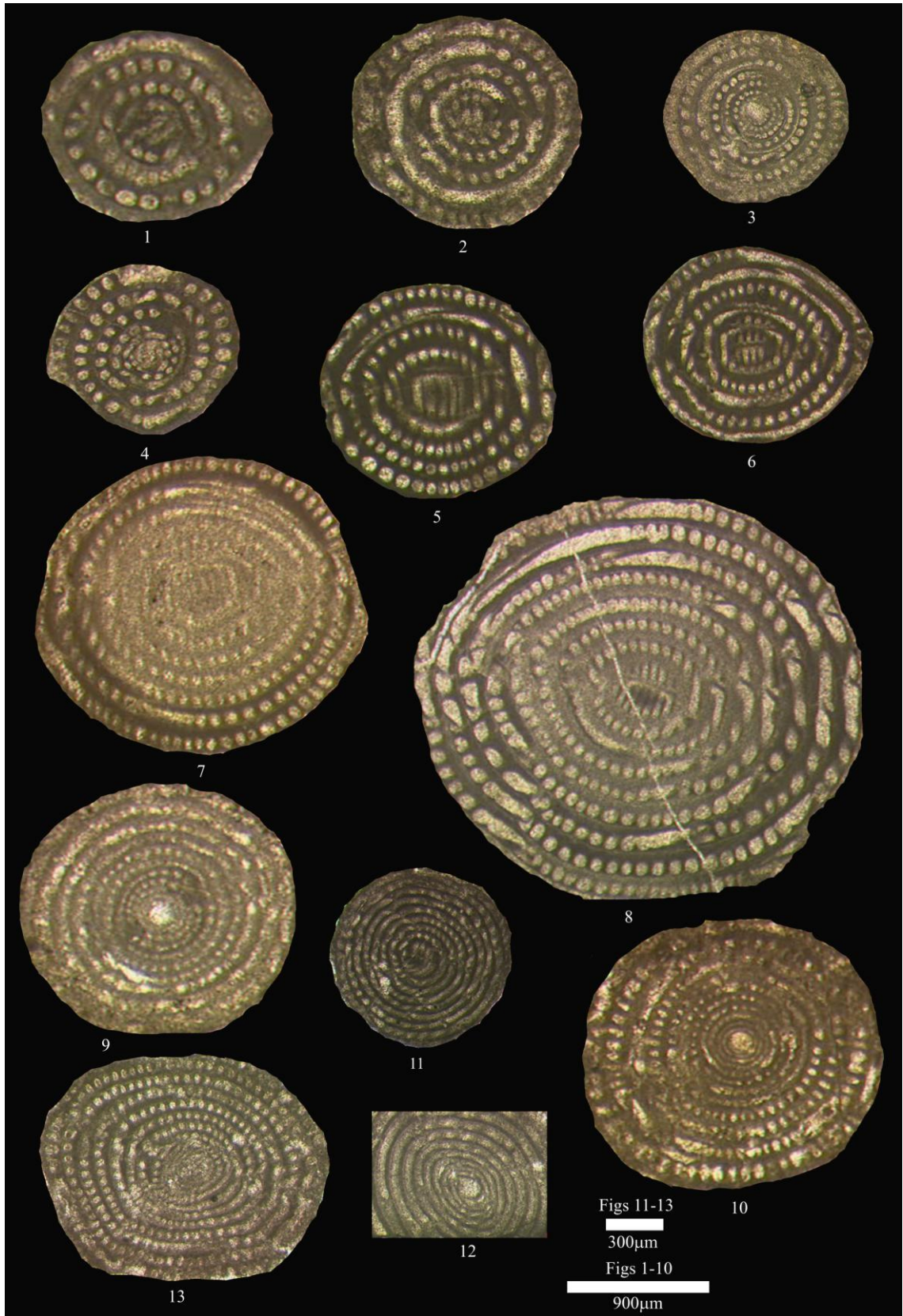


**Plate 12** *Alveolina*

*Alveolina* sp.

- 1: subaxial section, sample ZRD6, specimen a.
- 2-3: off-centred axial section, sample ZRD2, specimen c.
- 4-5: off-centred axial section, sample ZRD1, specimen c.
- 6: subaxial section, sample BD17, specimen b.
- 7: off-centred axial section, sample HLD6, specimen a.
- 8: off-centred axial section, sample BD5, specimen d.
- 9-10: subaxial section, sample BD17, specimen c.
- 11: off-centred axial section, sample BD19, specimen b.

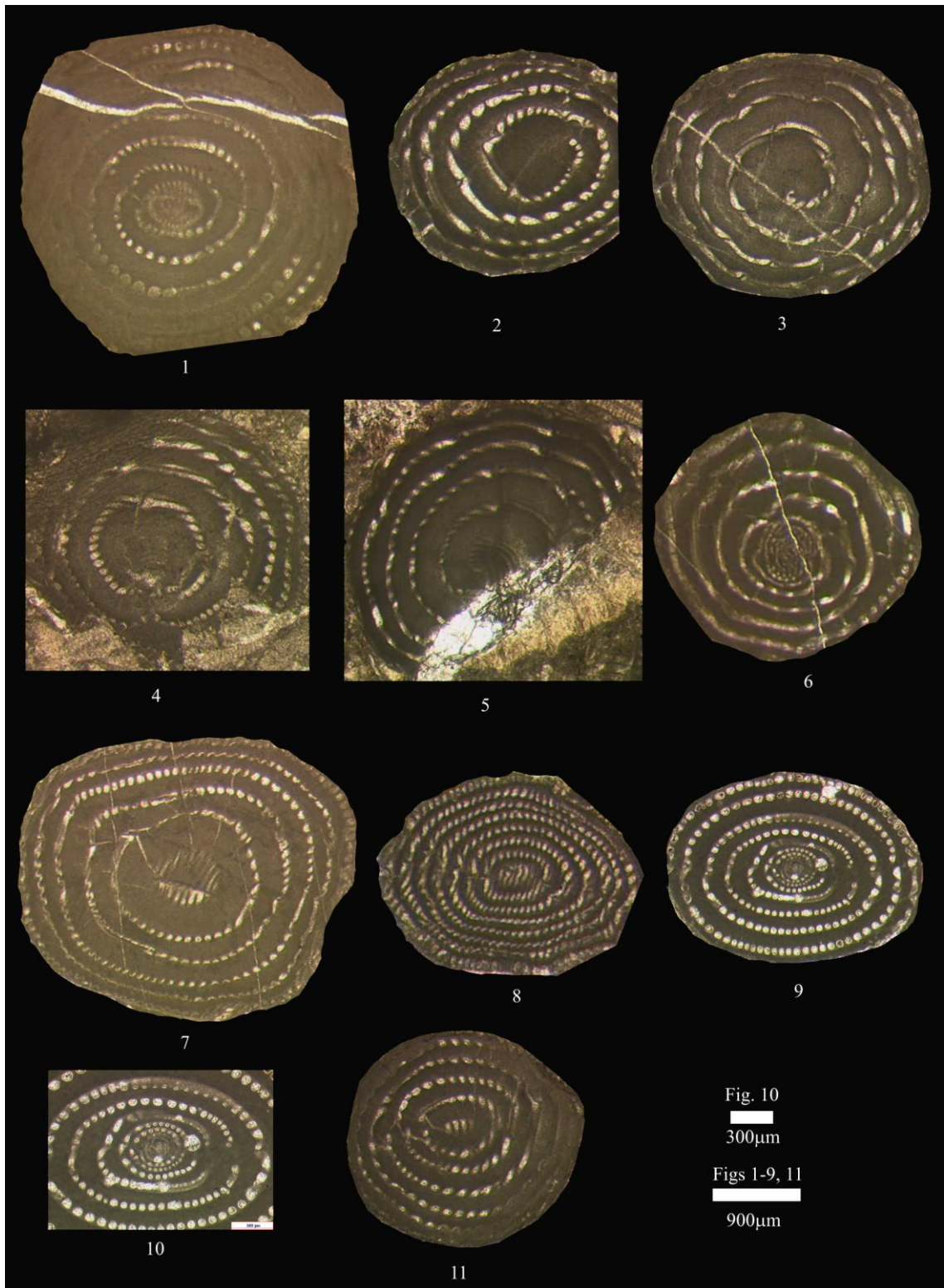


**Plate 13** *Somalina*, *Opertorbitolites*, *Saudia*, *Keramosphaera*

*Somalina* sp.

- 1: axial section, microspheric form, sample BD3, specimen b.
- 2: axial section, microspheric form, sample BD4, specimen b.
- 3: axial section, microspheric form, sample BD4, specimen c.
- 4: axial section, megalospheric form, sample BD5, specimen e.

*Opertorbitolites* sp.

- 5: axial section, megalospheric form, sample ZRD1, specimen d.

*Keramosphaera* cf. *iranica* Rahaghi, 1983

- 6: equatorial section, sample ZRD24, specimen d.

*Saudia* sp.

- 7-8: axial section, sample ZRD36, specimen e.
- 9: axial section, sample ZRD29, specimen f.
- 10: axial section, sample ZRD23, specimen c.

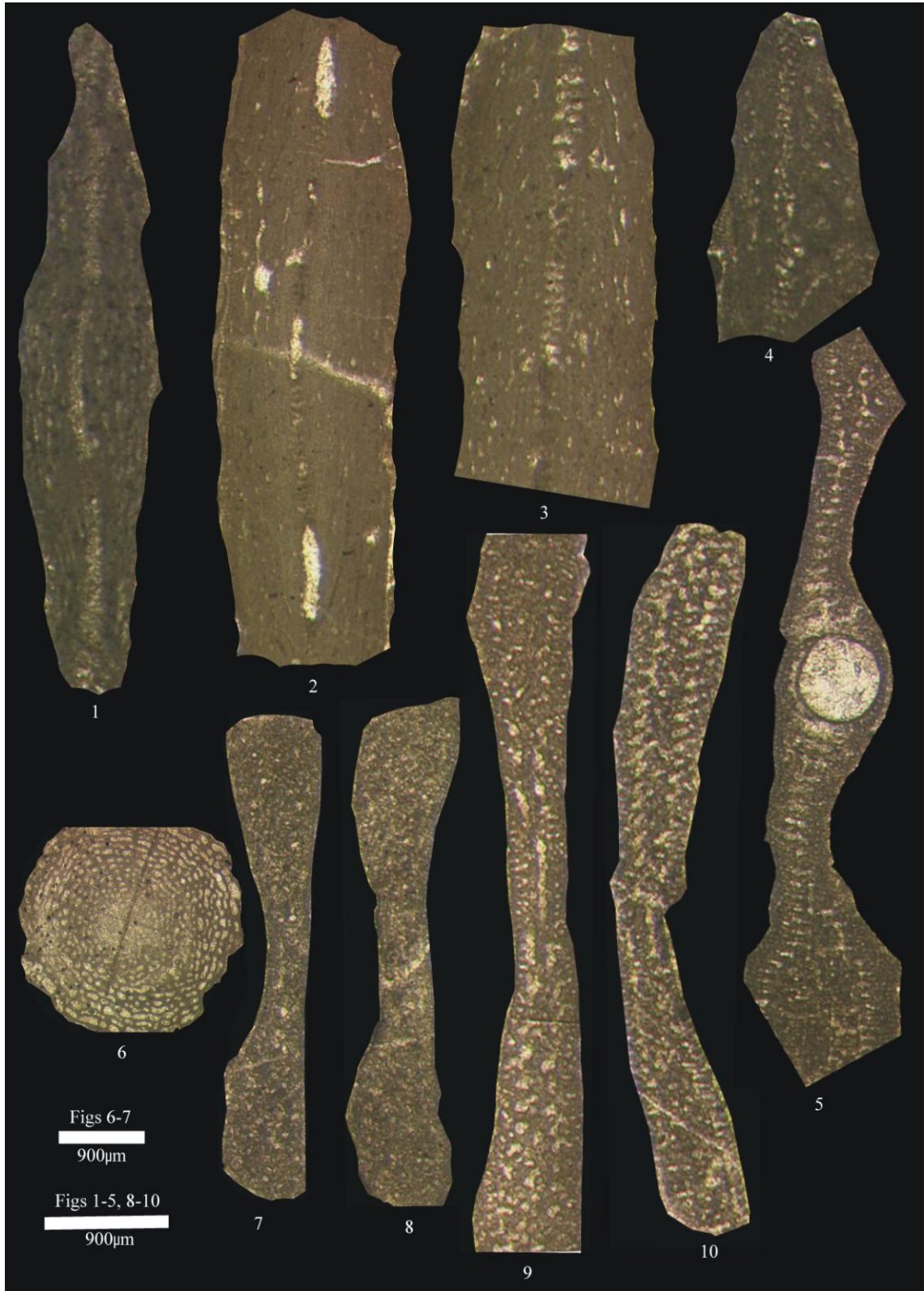


**Plate 14** *Fallotella*, *Karsella*, *Dictyoconus*

*Fallotella alavensis* Mangin, 1954

1-4: axial section, sample ZRD39, 1, specimen d; 2, specimen e; 3, specimen f; 4, specimen g.

*Karsella hottingeri* Sirel, 1997

5: basal section, showing exoskeleton (beams and rafters) and endoskeleton (pillars and foramina) structures, sample ZRD27, specimen c.

6: basal section, showing 3 to 4 generation of beams in peripheral zone and pillars and basal foramina in the central part, sample ZRD17, specimen a.

7: axial section, showing complex arrangement of numerous chamberlets, sample ZRD34, specimen a.

8: subaxial section, showing chamberlets and network of beams and rafters, sample ZRD33, specimen c.

9: axial section, showing arrangement of numerous chamberlets, sample ZRD34, specimen b.

10: axial section, megalospheric form, showing large megalosphere followed by periembryonic chamber, sample ZRD32, specimen d.

*Dictyoconus* sp.

11: axial section, sample ZRD19, specimen b.

12: axial section, sample ZRD13, specimen b.

13: axial section, sample ZRD9, specimen b.

14: axial section, showing megalospheric embryo, sample ZRD19, specimen c.

15: basal section, sample ZRD39, specimen h.

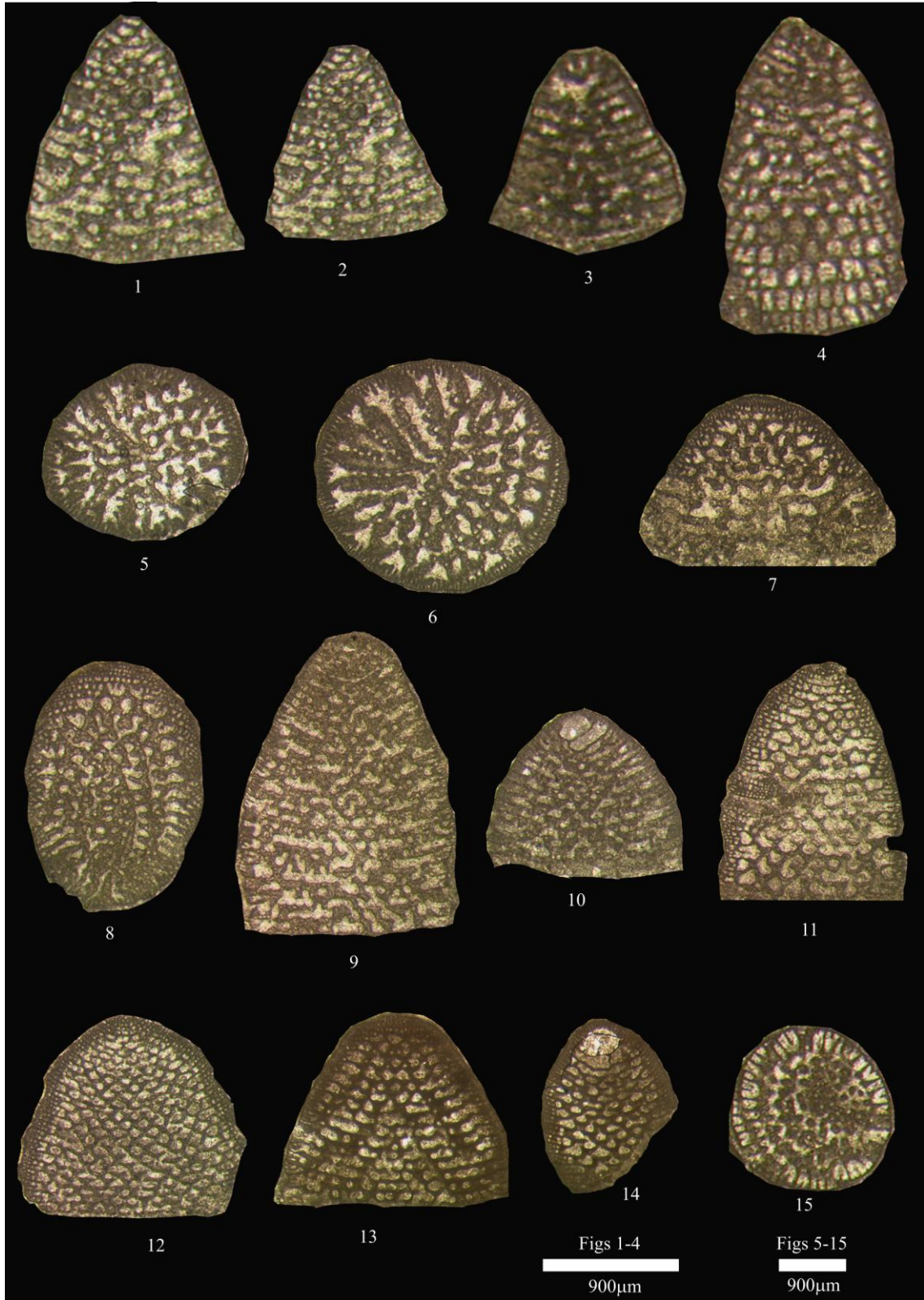


**Plate 15** *Coskinon*, *Vania*

*Coskinon rajkae* Hottinger & Drobne, 1980

1: axial section, sample ZRD39, specimen i.

2-4: axial section, sample ZRD38, 2, specimen a; 3, specimen b; 4, specimen c.

5: basal section, sample ZRD39, specimen j.

*Vania anatolica* Sirel & Gündüz, 1985

6: subaxial section, showing two rows of apertures and sub-epidermal partitions, sample ZRD28, specimen f.

7: axial section, showing raniform chambers, sample ZRD36, specimen f.

8-10: axial section, showing successive aligned chambers, sample ZRD38, 8, specimen d; 9-10, specimen e.

11-12: axial section, showing successive aligned chambers, sample ZRD34, 11, specimen c; 12, specimen d.



---

## Chapter 4

---

Evolution of Paleocene to Early Eocene larger benthic foraminifer assemblages of the Indus Basin, Pakistan

---

## **Chapter 4: Evolution of Paleocene to Early Eocene larger benthic foraminifer assemblages of the Indus Basin, Pakistan**

### **Abstract**

The Paleocene-Early Eocene carbonate successions of the Indus Basin in Pakistan formed on the north-western continental shelf margin of the Indian Plate in the east Tethys Ocean. Based on larger benthic foraminifera (LBF) eight Tethyan foraminiferal biozones (SBZ1-SBZ8) spanning the Paleocene to Early Eocene are identified. The base of the Eocene is identified by the first appearance of *Alveolina* sp. Other stratigraphically important LBFs that are characteristic of the earliest Eocene are *Ranikothalia nuttalli*, *Discocyclina dispansa* and *Assilina dandotica*. Stable isotope analysis through the Paleocene-Eocene (P-E) boundary identifies more positive  $\delta^{13}\text{C}$  values for the Late Paleocene (+3.4‰ to +3.0‰) and lower values (+2.7‰ to +1.6‰) for the earliest Eocene. However, there is insufficient sampling resolution to identify the maximum negative  $\delta^{13}\text{C}$  excursion of the Paleocene-Eocene Thermal Maximum. During Late Paleocene times LBF assemblages in the Indus Basin were taxonomically close to those of west Tethys, facilitating biostratigraphic correlation. However, this faunal continuity is lost at the P-E boundary and the earliest Eocene succession lacks typical west Tethys *Nummulites*, whilst *Alveolina* are rare: LBFs such as *Miscellanea* and *Ranikothalia* continue to dominate in the Indus Basin. The absence of *Nummulites* from the earliest Eocene of Pakistan and rarity of *Alveolina*, elsewhere used as the prime marker for the base of the Eocene, may imply biogeographical barriers between east and west Tethys, perhaps caused by the initial stages of India-Asia collision. Later, at the level of the Eocene SBZ8 biozone, faunal links were re-established and many

foraminifera with west Tethys affinities appeared in east Tethys, suggesting the barriers to migration ceased.

## **Introduction**

The Paleocene-Early Eocene shallow marine carbonates of the Lockhart and Dungan formations in the Indus Basin of Pakistan contain stratigraphically important larger benthic foraminifera (LBF), which have been used for local (Indian subcontinent) and regional (especially Tethyan) biostratigraphy (e.g. Hottinger 1960, 1971; Adams 1970; Kureshy 1978; Schaub 1981; Serra-Kiel *et al.* 1998; Jauhri & Agarwal 2001; Green *et al.* 2008; Afzal *et al.* 2009 and references therein). The most recently established Paleocene-Early Eocene LBF biostratigraphic schemes for the Indus Basin in Pakistan include the Tertiary “Letter Stage” biozones (Adams 1970), the Tertiary LBF biozones (e.g. Kureshy 1978; Butt 1991), the Early Eocene alveolinid biozones of the Salt Range (e.g. Sameeni & Butt 2004), and the LBF assemblages of Weiss (1993). Most of these schemes are fragmentary and difficult to correlate with standard biostratigraphic schemes. Other LBF studies are of mostly coarse-resolution or deal only with phylogenetic lineages or taxonomies (see Afzal *et al.* 2009 for a summary of problems). The precise biostratigraphic position of the Paleocene-Eocene boundary (P-E) in the shallow marine successions of this region was, prior to the present study, was ambiguous.

The Tethyan shallow marine benthic foraminifera biozonation (SBZ) scheme of Serra-Kiel *et al.* (1998) provides a basis for correlation of carbonate platforms and pelagic successions of the Paleocene to Eocene by establishing twenty LBF biozones (SBZ1-SBZ20), correlated with the planktonic foraminifera P1-P18 biozones of Berggren *et al.* (1995) and nannofossil biozones (e.g. the NP1-NZ21 biozones of

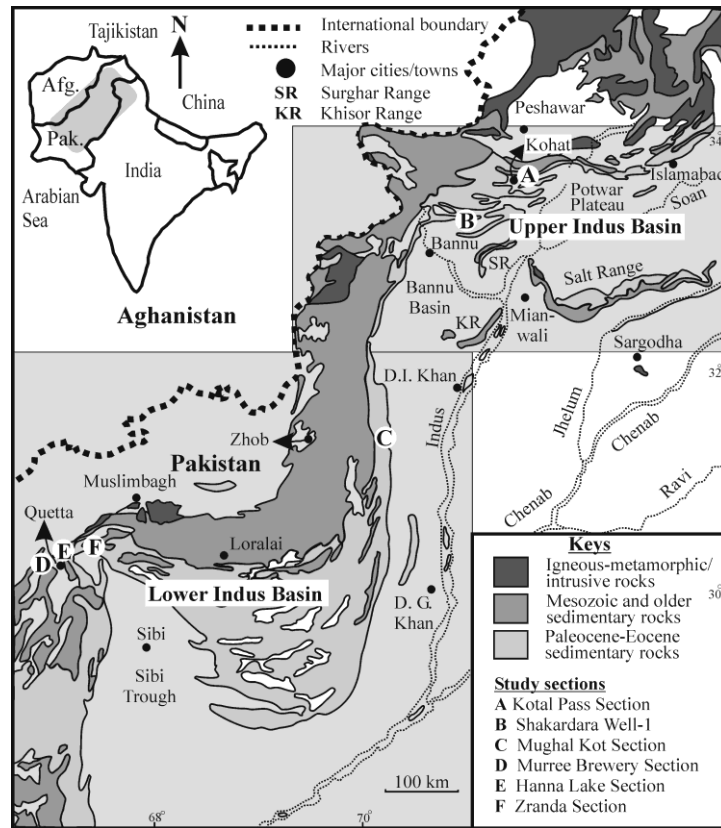


**Figure 1.** Map of the Upper Indus Basin and parts of the Lower Indus Basin showing distribution of Paleocene-Eocene sedimentary rocks and key stratigraphical sections (modified after Eames 1952). The Lower and Upper Indus Basins collectively form the Greater Indus Basin.

Martini 1971). This SBZ scheme is based on the earlier LBF biostratigraphic studies of Hottinger (1960), Hottinger *et al.* (1964), Schaub (1981) and Hottinger & Drobne (1988), and is applicable to the Tethyan shallow marine realm as far south as Somalia and southeast to the Indian subcontinent (Hottinger 1971; Pignatti 1994; Jauhri 1998; Scheibner & Speijer 2008a). In northern India and Pakistan (east Tethys), the LBFs of the Late Paleocene-earliest Eocene show unusual faunal associations, where the typical latest Paleocene *Miscellanea* and *Ranikothalia* co-occur with typical earliest Eocene *Alveolina*, whilst *Nummulites*, a marker of the earliest Eocene in west Tethys, occurs only later (Hottinger 1971; Jauhri 1998; Akhtar & Butt 2000; Jauhri *et al.* 2006; Afzal *et al.* 2009; Tewari *et al.* 2010). Earlier studies on LBFs in Pakistan either did not recognize these faunal differences between east and west Tethys at the P-E boundary or

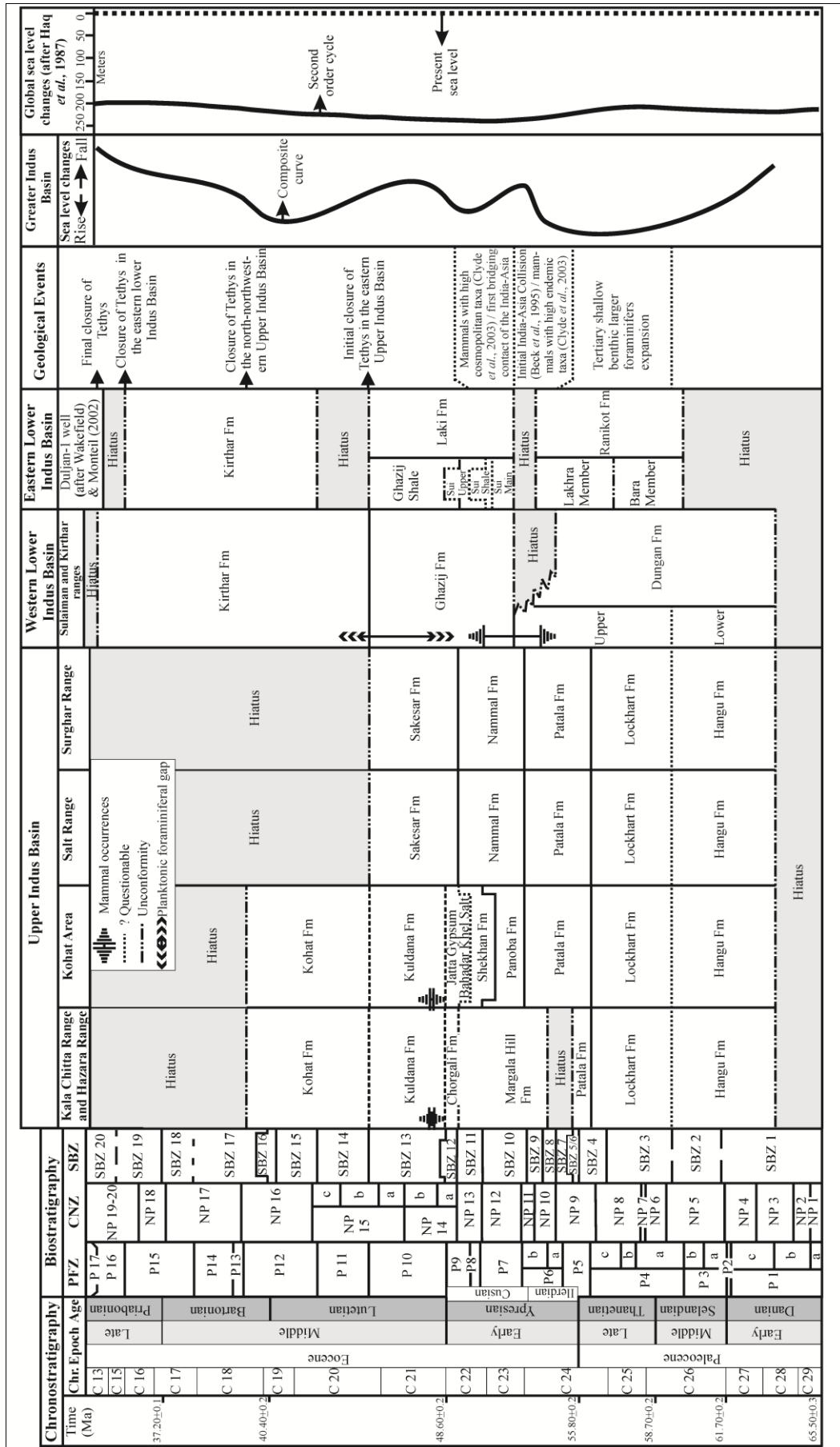


**Figure 2.** Regional stratigraphical correlation of the lower Cenozoic succession of the Greater Indus Basin, Pakistan, showing significant geological events and their correlation with basin stratigraphy and global sea level changes (after Afzal *et al.* 2009).

paid little attention to this interval. Therefore, clarification of the formal successions through the P-E boundary in this region is vital for regional and international correlation of important geological events (e.g. Paleocene-Eocene Thermal Maximum [PETM] and India-Asia collision tectonics). It is now apparent that, despite some faunal differences (e.g. in Hottinger 1971; Scheibner & Speijer 2008a; present study), the LBFs of the Indus Basin in Pakistan contain many Tethyan elements (e.g. Hottinger 1960; Hottinger & Drobne 1988; Serra-Kiel *et al.* 1998; Scheibner *et al.* 2005; Scheibner & Speijer 2008a, 2009). Consequently, they can be used to establish a refined biostratigraphic biozonation correlated to the standard Tethyan SBZ scheme (e.g. Serra-Kiel *et al.* 1998; Scheibner *et al.* 2005; Scheibner & Speijer 2009). Here I aim to: 1) establish a LBF biostratigraphic scheme for the Paleocene-Early Eocene carbonate platform succession in the Indus Basin of Pakistan; 2) precisely resolve the Paleocene/Eocene boundary in these successions; 3) discuss the biostratigraphic significance of LBFs that show variable stratigraphic ranges across the Paleocene-Eocene boundary in this region including species of *Miscellanea*, *Ranikothalia* and *Nummulites*; and 4) discuss LBF faunal differences in the Tethyan provinces (east and west) and the roles of India-Asia collision and the PETM in generating these differences.

### **Geological setting**

The geological setting of the Greater Indus Basin of Pakistan is discussed in Afzal *et al.* (2009; herein see Fig 1). The tectonic history and stratigraphical framework of the region are strongly influenced by the collision of the Indo-Pakistan and Asian plates, and estimates of the timing of the initial collision vary from 65 Ma to 45 Ma (Beck *et*

*al.* 1995; Rowley 1996; Hodges 2000; Afzal *et al.* 2009). A hiatus equivalent to planktonic foraminiferal biozones upper P5 to P7 in the Indus Basin has been related to the early collision of India with Asia (see Afzal *et al.* 2009) (Fig. 2). Carbonate platform deposition was interrupted by this tectonic event, for example the termination of platform sedimentation in the Upper Indus Basin during the latest Paleocene (see Afzal *et al.* 2009 for summary). However, in parts of the Lower Indus Basin, platform sedimentation continued through the Paleocene-Early Eocene, represented for example in the Muree Brewery, Hanna Lake and Zranda sections of the present study (Fig. 1).

### **Stratigraphy**

The earliest marine Cenozoic sedimentation in the basin seems to have commenced with the Palaeogene transgression depositing continental near-shore facies to shallow marine-deltaic facies of the Hangu Formation in the Upper Indus Basin and mixed carbonate siliciclastic to open-marine facies of the Dungan Formation in the Lower Indus Basin (Afzal *et al.* 2009 and references therein). This marine flooding was succeeded by widespread carbonate platform deposition represented by the Lockhart Formation in the Upper Indus Basin and the upper Dungan Formation in parts of the Lower Indus Basin (Afzal *et al.* 2009) (Fig. 2). By contrast, the planktonic foraminifer-bearing (= biozones P3-P6) shales of the Dungan Formation in the northwestern Sulaiman Range (e.g. Rakhi Nala and Zinda Pir areas) were deposited in an open marine environment (Afzal *et al.* 2009). The carbonate platform was buried by deep and shallow marine clastics of the Patala Formation (= biozones P4c-P6) in most of the Upper Indus Basin and by shales of the Ghazij Formation (= biozones P7-P10) in parts of the Lower Indus Basin (Afzal *et al.* 2009) (Fig. 2). However, carbonate continued through the Late Paleocene to Early Eocene (i.e. Dungan Formation) (Afzal *et al.* 2009;

Kassi *et al.* 2009). During the Ypresian-early Lutetian (biozones P7-P10) in the Upper Indus Basin, shallow marine carbonates of the Margala Hill, Nammal and Shekhan formations with the mudstone/shale-rich Panoba Formation were deposited (Fig. 2). The higher parts of the succession include evaporites (the Bahadar Khel Salt-Jatta Gypsum) and, finally, the continental red bed/sandstone mammal-bearing Kuldana Formation in the northern part and carbonates and shales of the Sakesar Formation in the southern part of the Upper Indus Basin (Afzal *et al.* 2009). The Sakesar Formation in the Salt and Surghar ranges is overlain by Miocene-Recent terrestrial sediments derived from the Himalaya, marking the closure of the Tethys Ocean in the southeastern Upper Indus Basin (Afzal *et al.* 2009). The late Lutetian-Priabonian is represented by the upper Kirthar Formation in the Lower Indus Basin and by the correlative uppermost Kohat Formation in the Upper Indus Basin. This followed closure of the Tethys Ocean in the north to northwestern parts of the Upper Indus Basin (e.g. Kohat area, Kala Chitta and Hazara ranges). The gradual retreat of the Tethys Ocean continued south-southwest through late Lutetian to Bartonian time and it finally closed in the Priabonian (Biozone P15; Afzal *et al.* 2009). Oligocene marine sedimentation was restricted to the south of the Lower Indus Basin, while the rest of the Greater Indus Basin in Pakistan remained non-depositional lowland until the formation of Neogene molasse (Afzal *et al.* 2009).

## **Materials, methods and studied sections**

### *Materials and methods*

I use the terminology of Afzal *et al.* (2009) for the Paleocene-Eocene lithostratigraphy and that of Shah (1977) for the Palaeozoic and Mesozoic. I have collected and logged the Late Paleocene Lockhart Formation in one outcrop section and one petroleum well core in the Upper Indus Basin (Fig. 1), and the Paleocene-Early Eocene Dungan

Formation in four outcrop sections of the Lower Indus Basin (Fig. 1). Some 200 limestone samples were collected including 180 from six outcrop sections. I have prepared standard limestone thin sections of 2.5cm × 5cm and 2.5 × 7cm dimensions for petrographic microscopy. The identification of LBFs in these thin sections is based on foraminifera that have not been re-worked (based on preservation and palaeoecological context) and using well-oriented sections (of LBFs) only, complemented by study of limestone slabs. The LBFs were photographed in plane-polarized light with a digital camera on a Nikon petrographic microscope in the Department of Geology, University of Leicester. Discrete specimens of LBFs could not be collected as the sediments are indurated. For biostratigraphic determination, the SBZ scheme of Serra-Kiel *et al.* (1998), with amendments for the placement of the P-E boundary at the boundary between biozones SBZ4 and SBZ5 (see Scheibner & Speijer 2009), has been adopted. The boundary between biozones SBZ4 and SBZ5 coincides with the base of the Ilerdian Stage (Pujalte *et al.* 2009a). To allow precise correlation and avoid confusion, I have adopted the standard SBZ scheme names (e.g. SBZ1-SBZ8). The biozonal marker species of both local and Tethyan realms have been used to identify these biozones.

For stable isotopes ( $\delta^{13}\text{C}$ ), bulk carbonates from three sections (Zranda, Muree Brewery and Hanna Lake) were selected. Some 58 samples were analyzed covering the Late Paleocene-Early Eocene. I used only well-preserved limestone for stable isotope analysis that appeared not to be re-worked or diagenetically altered (based on the type, preservation, fragmentation and ecological mode of contained biota). The sample material was ground in agate and the equivalent of 10 mg of carbonate was reacted with anhydrous phosphoric acid *in vacuo* overnight at a constant 25°C. The CO<sub>2</sub> liberated was separated from water vapour under vacuum and collected for analysis. Measurements were made on a VG Optima mass spectrometer at the NERC Isotope

Geosciences Laboratory, Keyworth, Nottingham, UK. Overall analytical reproducibility for these samples is normally better than 0.2‰ for  $\delta^{13}\text{C}$ . Isotope values ( $\delta^{13}\text{C}$ ) are reported as per mil (‰) deviations of the isotopic ratios ( $^{13}\text{C}/^{12}\text{C}$ ) calculated to the VPDB scale using a within-run laboratory standard calibrated against NBS standards.

*Studied sections in the Upper Indus Basin*

*1. Kotal Pass section.* – The Kotal Pass section is situated in the northernmost part (33°38'01"N and 71°28'21"E) of the Upper Indus Basin in the Kohat Hill Range of northern Pakistan (Fig. 1). The section exposes a thick succession of Jurassic to Paleocene rocks, which constitutes the hanging wall sequence of the Main Boundary Thrust (MBT) along which Jurassic rocks are thrust southward over the Eocene-Miocene succession of the Kohat Foreland Basin (Khan *et al.* 1990). In the Kotal Pass section, 78 samples at 1 to 2 m spacing from the Late Paleocene Lockhart Formation have been collected (Fig. 3). The Lockhart Formation is 144 m thick and is composed of limestone rich in dasycladaceans and LBFs (mainly smaller rotaliids, agglutinated forms, miliolids and rare miscellanids etc.) producing wackestone and packstone with rare grainstone and patch-reef boundstone textures (Fig. 3).

*2. Shakardara Well-1.* – The Shakardara Well-1 was drilled in the Shakardara-Nandrakki Exploration lease of the Oil and Gas Development Company Limited, Pakistan (OGDCL). The well is approximately 70 km south of Kohat (33°13'24"N and 71°29'39"E), Khyber Pakhtunkhwa Province, Pakistan (Fig. 1). The well was drilled to 4548 m depth, with Cretaceous to Pliocene sediments recorded. Two cores (Core-1 and Core-2) from the Late Paleocene-Early Eocene stratigraphic age (= Lockhart and Patala formations) were recovered. Core-1 from interval 4299.3 m – 4303.5 m, is dominantly composed of dark grey pelagic limestone rich in planktonic foraminifera. There are no

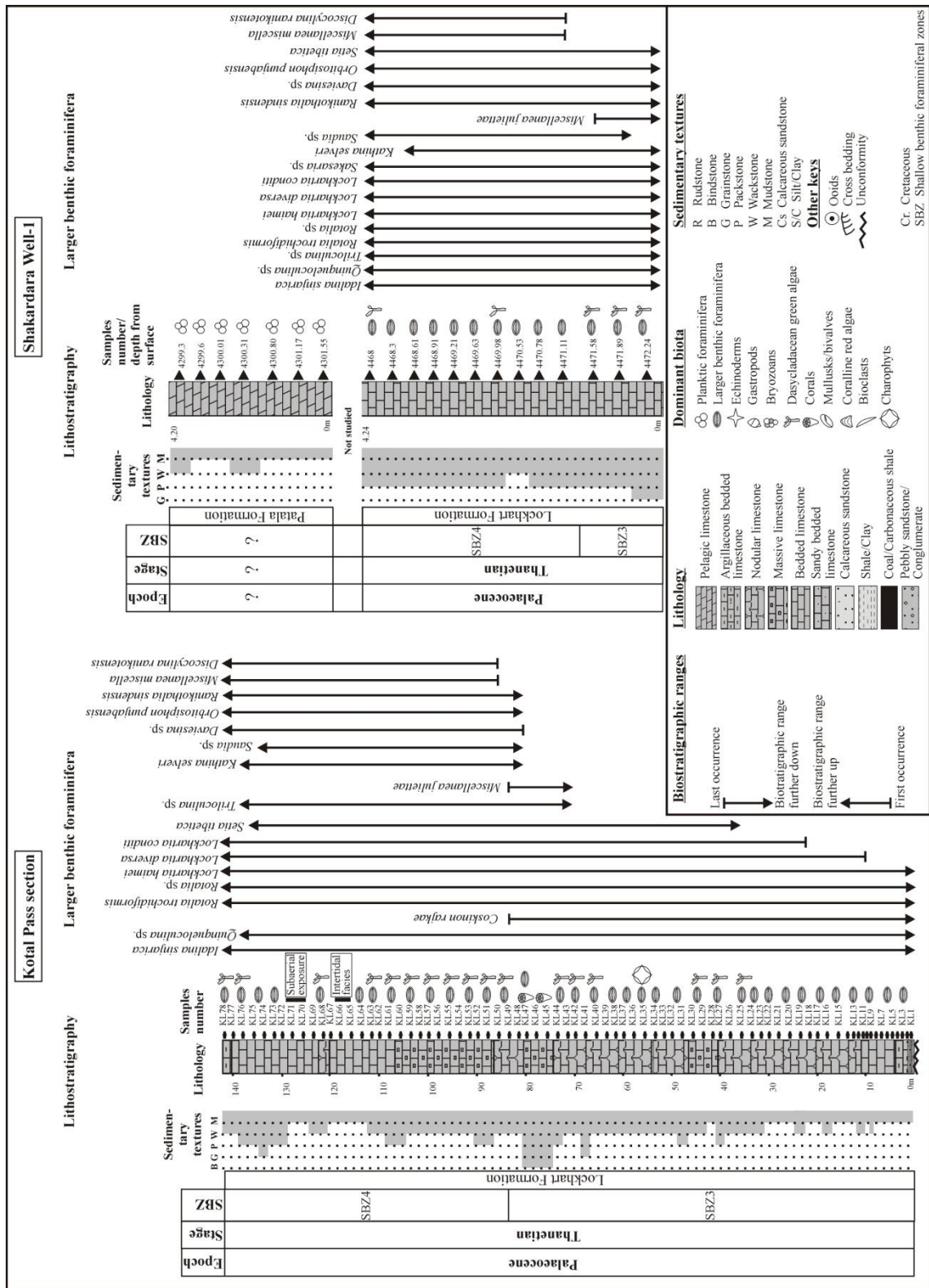


**Figure 3.** Lithostratigraphy and biostratigraphic ranges of larger benthic foraminifera of the Late Paleocene Lockhart Formation, Upper Indus Basin, Pakistan.

Paleocene-Eocene LBFs in Core-1, probably due to the deep pelagic environments it

represents (Fig. 3). However, interval 4468 m – 4474 m of Core-2 consists of dasycladacean- and LBF-rich packstones and wackestones that have produced a number of age diagnostic LBF taxa. Thirteen core samples (polished thin sections) have been studied, which yielded a number of marker species of the SBZ3-SBZ4 biozones (Fig. 3).

#### *Studied sections in the Lower Indus Basin*

3. *Mughal Kot section:* – This section is located near the Mughal Kot Post (31°26'29"N and 70°05'07"E), 155 km west of Dera Ismail Khan city (Fig. 1). The Mughal Kot section represents the north-eastern Sulaiman Range in the Lower Indus Basin (Fig 1). The exposed deposits range from marine Jurassic to continental Recent. The Paleocene Dungan Formation is 200 m thick, composed of a mixed carbonate-siliciclastic lower unit succeeded by a LBF- to coral-algal rich rudstone, bindstone, grainstone and packstone upper unit (Fig. 4). A total of 21 surface rock samples at 5 m and 10 m intervals were collected (Fig. 4). The lower unit contains rare LBFs. When present, foraminifera of this lower unit are characterized by smaller rotaliids of the SBZ1 biozone. However, the upper unit yields a number of age-diagnostic LBFs and coralline algae of the SBZ2-SBZ3 biozones (Fig. 4).

4. *Zranda section.* – The Zranda section is located near Zranda village (30°28'27"N and 67°37'07"E), 25 km northeast of Kach, Balochistan (Fig. 1). The lithostratigraphic succession is similar to that of the Kach–Ziarat valley, comprising the Late Cretaceous volcanoclastic-sedimentary Bibai Formation, Late Paleocene-earliest Eocene shallow marine carbonates of the Dungan Formation and Early Eocene open marine clastics of the Ghazij Formation (Kassi *et al.* 2009). In the Zranda section, the Dungan Formation is 222 m thick, consisting of LBF-rich wackestone, packstone and grainstone containing

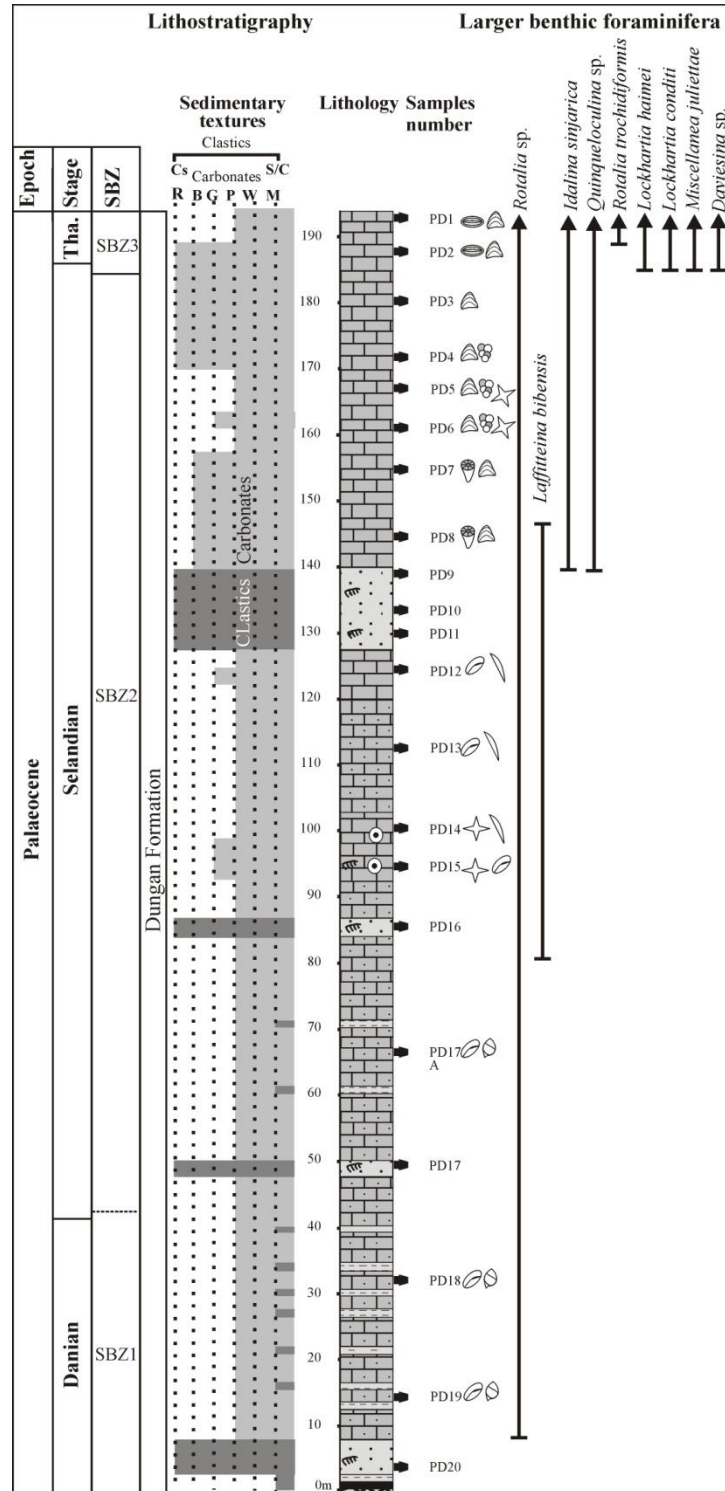


**Figure 4.** Lithostratigraphy and biostratigraphic ranges of larger benthic foraminifera of the Paleocene Dungan Formation in the Mughal Kot section, Lower Indus Basin, Pakistan. Key as for Figure 3.

abundant age diagnostic taxa of the SBZ3-SBZ6 biozones (Fig. 5). A total of 39 rock samples at 2 to 3 m spacing were collected (Fig. 5).

5. *Muree Brewery section.* – The well exposed Muree Brewery section is situated 8 km west (30°11'22"N and 66°56'44"E) of Quetta city in Balochistan Province (Fig. 1). The section represents the western Sulaiman Range of the Lower Indus Basin and exposes a thick succession of Late Cretaceous (Parh, Hanna Lake Limestone and Fort Munro formations) to Early Eocene (Dungan and Ghazij formations) marine deposits (Kassi *et al.* 2009). In the Muree Brewery section, the Dungan Formation is 19.2 m thick, and is mainly composed of LBF-rich grainstone and packstone containing stratigraphically significant markers of the Early Eocene (= biozones SBZ5-SBZ8) (Fig. 6). A total of 20 rock samples at intervals of less than 1 m spacing have been collected (Fig. 6). Because of its easy accessibility and rich occurrences of LBFs, this section has been visited by various workers (see Afzal *et al.* 2009; Kassi *et al.* 2009 for summary) but here I present the first high resolution stratigraphical study.

6. *Hanna Lake section.* – This section is located near Hanna Lake (30°15'17"N and 67°05'45"E), 10 km northeast of Quetta city, Balochistan (Fig. 1). The Hanna Lake section has a similar stratigraphic setting to the nearby Muree Brewery section (see Kassi *et al.* 2009). However, the thickness of the Dungan Formation here is 22 m and it is composed largely of LBF-rich packstone, wackestone and grainstone with varied amounts of coralline algae and planktonic foraminifera (Fig. 7). A total of 22 rock samples at 1 m spacing have been collected. A number of LBF marker species of the SBZ5-SBZ8 biozones are represented.

### **Stable isotope stratigraphy**

The prominent geochemical feature in the lower Palaeogene stratigraphic record is a negative (of –2.5 to –4‰) carbon isotope ( $\delta^{13}\text{C}$ ) excursion (CIE) (Zachos *et al.* 2001). This excursion reflects a major perturbation of the global carbon cycle resulting from a

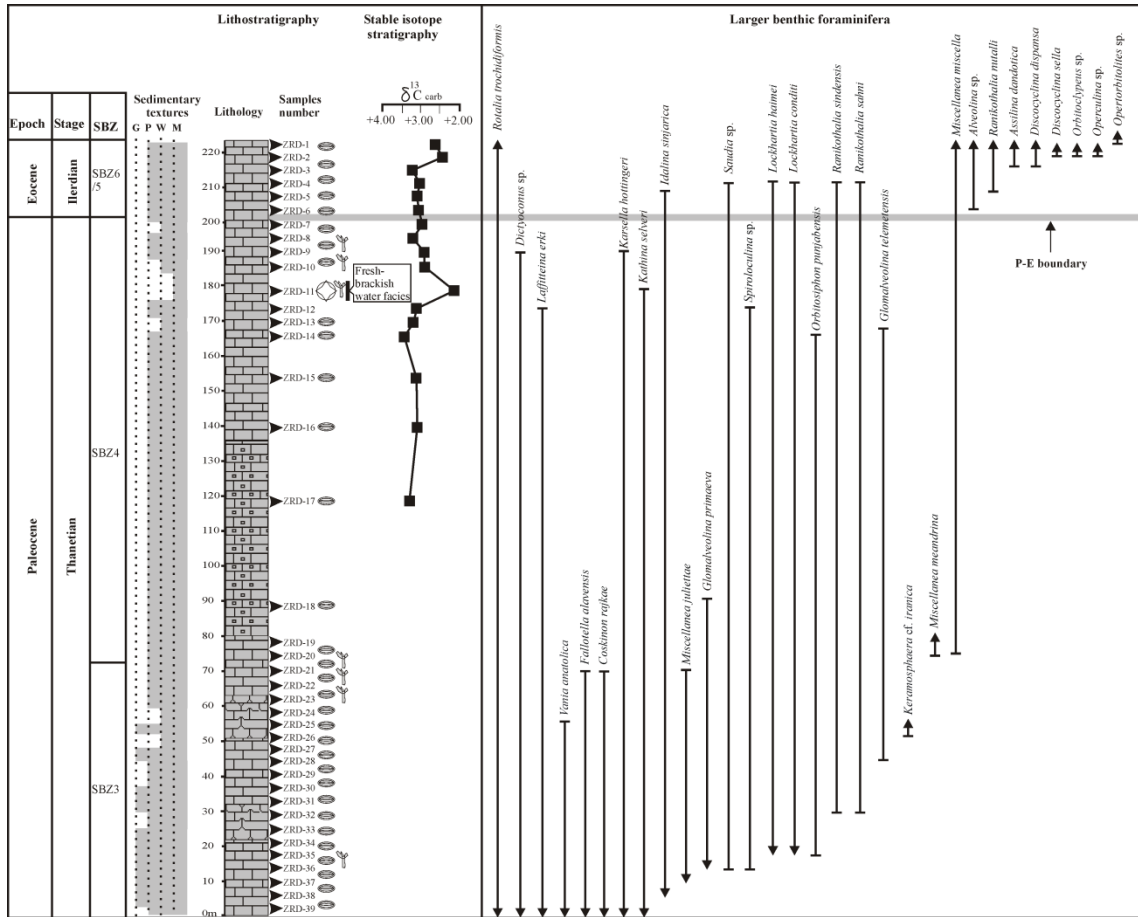


**Figure 5.** Lithostratigraphy, stable isotopes and biostratigraphic ranges of larger benthic foraminifera of the Late Paleocene-Early Eocene Dungan Formation in the Zranda section, Lower Indus Basin, Pakistan. Key as for Figure 3.

dramatic global warming event, the Paleocene-Eocene Thermal Maximum (e.g. Zachos *et al.* 2001). The PETM CIE has been accepted as the marker criterion for the Global Stratotype Section and Point (GSSP) for the Paleocene-Eocene (P-E) boundary in Egypt (Aubry & Ouda 2003; Aubry *et al.* 2007). The CIE is detectible in marine and terrestrial records world-wide (e.g. Zachos *et al.* 2001; Bowen *et al.* 2001; Magioncalda *et al.* 2004; Thiry *et al.* 2006). In the GSSP section of Dababiya, Egypt, a sharp decrease in  $\delta^{13}\text{C}$  from  $-24\text{‰}$  to  $-26.5\text{‰}$  marks the onset of the CIE which is followed by a gradual decrease until it reaches its lowest values (i.e.  $-27.5\text{‰}$ ) (Dupuis *et al.* 2003; Aubry *et al.* 2007). The  $\delta^{13}\text{C}_{\text{org}}$  values then increase progressively until pre-excursion values are reached (Dupuis *et al.* 2003). Carbon isotope records derived from carbonates ( $\delta^{13}\text{C}_{\text{carb}}$ )

in the Dababiya section and in nearby sections are of similar amplitude (e.g. Aubry *et al.* 1999; Dupuis *et al.* 2003).

Here I describe for the first time, a detailed  $\delta^{13}\text{C}_{\text{carb}}$  stratigraphy for the early Palaeogene of the Indus Basin. In the Zranda section, Late Paleocene  $\delta^{13}\text{C}_{\text{carb}}$  values vary between +3.0‰ to +3.4‰ (Fig. 5). The CIE peak in our sections has not been detected, probably because of the spacing of samples (ca 2 m to 3 m apart). A  $\delta^{13}\text{C}$  spike in one sample (ZRD-11) just below the P-E boundary in the Zranda section appears to be associated with fresh and brackish water facies (Fig. 5). A decrease in  $\delta^{13}\text{C}_{\text{carb}}$  values to between +2.4‰ to +3.1‰ in the Zranda section and less positive values of +1.8‰ to +2.6‰ in the Muree Brewery section and +1.6‰ to +2.7‰ in the Hanna Lake section indicates a marked change in the earliest Eocene (post PETM CIE maximum) (Figs 5-7). In the succeeding Early Eocene succession,  $\delta^{13}\text{C}_{\text{carb}}$  values fluctuate between +2.1‰ and +1.2‰ in the Muree Brewery and Hanna Lake sections (Figs 6-7).

The Late Paleocene  $\delta^{13}\text{C}_{\text{carb}}$  values of the Indus Basin are comparable with those recorded in coeval platform carbonate sections (i.e. around +3.0‰) in Egypt by Scheibner *et al.* (2005) and Scheibner & Speijer (2009). The lower  $\delta^{13}\text{C}_{\text{carb}}$  values from the Eocene in the Indus Basin succession may reflect the later stages of the global decrease of  $\delta^{13}\text{C}$  during the earliest Eocene (Dupuis *et al.* 2003). The  $\delta^{13}\text{C}_{\text{carb}}$  values of the earliest Eocene as recorded in Egypt are around +1.0‰ (e.g. Scheibner *et al.* 2005; Scheibner & Speijer 2009), which are lower than Indus Basin  $\delta^{13}\text{C}_{\text{carb}}$  values (between +1.6‰ to +3.1‰). However,  $\delta^{13}\text{C}_{\text{carb}}$  values of the Late Paleocene-Early Eocene limestones of the Indus Basin are similar to values measured on well-preserved marine planktonic and deep-benthic foraminiferal tests and bulk carbonate elsewhere in Tethys, probably because these limestones were indurated during early diagenesis and became

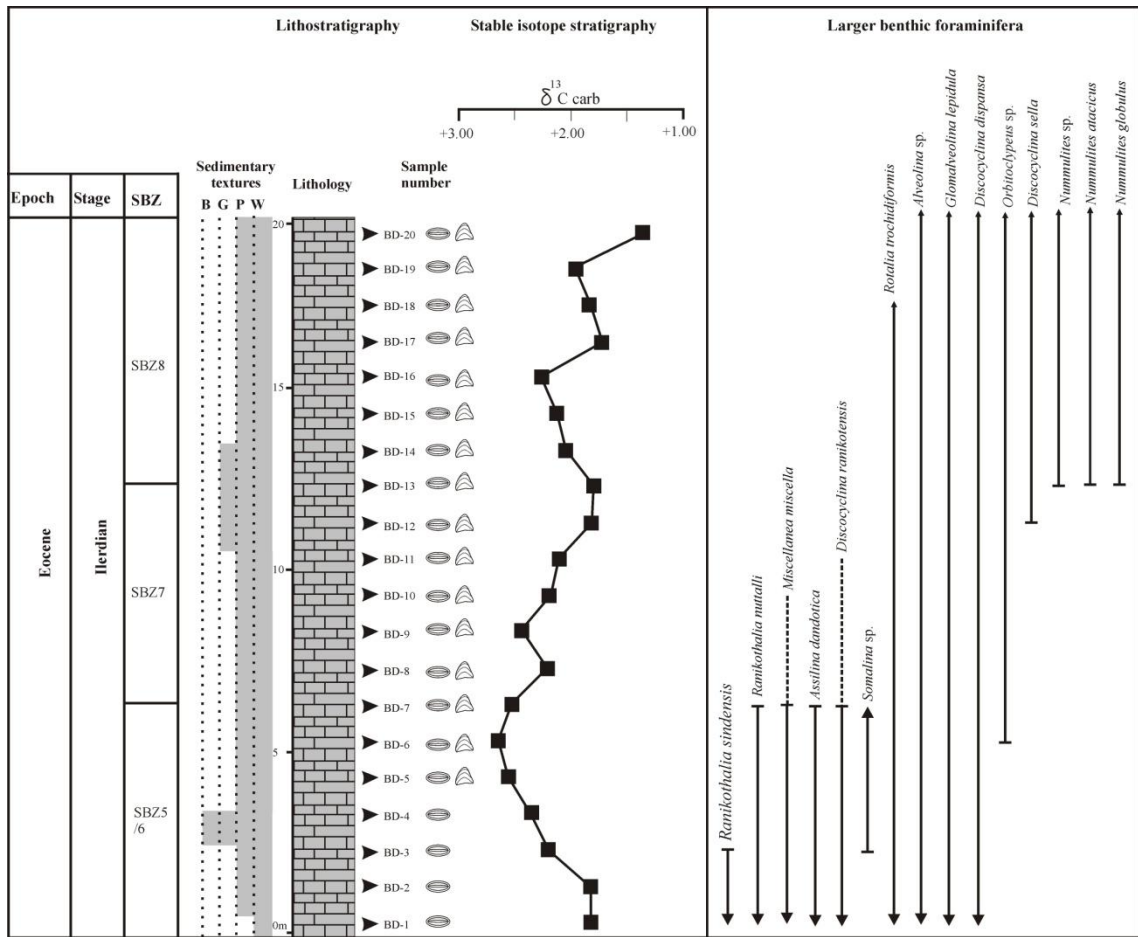


**Figure 6.** Lithostratigraphy, stable isotopes and biostratigraphic ranges of larger benthic foraminifera of the Early Eocene Dungan Formation in the Muree Brewery section, Lower Indus Basin, Pakistan. Key as for Figure 3.

closed systems with respect to carbon exchange (Schmitz *et al.* 1997, 2001).

### LBF biostratigraphy

Here I have recognized Paleocene-Early Eocene LBF biozones SBZ1-SBZ8. These biozones are identified on the basis of one or more key markers and their first and last occurrences (Figs 8-9). A short summary of key LBFs that delineate these biozones in our sections is given below and detailed species occurrences are shown in figures 3-7.

The first occurrence of *Laffitteina bibensis* marks the SBZ1 Biozone. The boundary between the SBZ1 and SBZ2 biozones is not straightforward, owing to a lack of marker LBFs and the variable stratigraphic range of *Lf. bibensis* in the Indus Basin

succession (Fig. 4). However, the first occurrence of *Idalina sinjarica* together with the coralline alga *Distichoplax biserialis* suggests the SBZ2 Biozone (Fig. 4). The SBZ3 Biozone is clearly recognized by the biostratigraphic ranges of *Coskinon rajkae*, *Fallotella alavensis*, *Vania anatolica* and *Miscellanea juliettae* (Figs 3-5). Other key LBFs first appearing within Biozone SBZ3 include *Ranikothalia sindensis*, *R. sahani*, *Lockhartia haimei*, *L. conditi*, *Lf. erki*, *Kathina selveri*, *Setia tibetica* and *Orbitosiphon punjabensis*. The boundary between biozones SBZ3 and SBZ4 is marked by the appearance of *M. meandrina*, *M. miscella* and *Discocyclina ranikotensis* (Figs 3, 5). The appearance of *Alveolina* is taken as the base of the earliest Eocene (biozones SBZ5/6, Hottinger 1960; Serra-Kiel *et al.* 1998; Scheibner & Speijer 2009, Fig. 5). In addition to *Alveolina*, the appearance of other marker species including *Assilina dandotica*, *D. dispansa* and *R. nuttalli* marks the earliest Eocene (Fig. 5). The last occurrences of *R. sindensis* and *R. sahani* were recorded within biozones SBZ5/6 (Figs 5-7). *Opertorbitolites*, *Orbitoclypeus sp.*, *D. sella* and *Somalina* first appear within the SBZ5/6 biozones (Figs 5-7). Identification of Biozone SBZ7 has proved difficult due to the stratigraphically late appearance of *Nummulites* in the Indus Basin, the low diversity of the fauna through this interval, and the generally poorly oriented sections of alveolinids and assilidids making taxonomic determination difficult. Nevertheless, the presence of a continuous carbonate succession through the SBZ6 to SBZ8 biozones in the Muree Brewery and Hanna Lake sections indicates that the SBZ7 Biozone is an interregnum, demarcated by diagnostic LBFs from the underlying and succeeding strata (Figs 6-7). Thus, the base of Biozone SBZ7 in our sections is taken immediately above the last occurrences of *R. nuttalli* and *A. dandotica* (Figs 6-7). The last occurrence of *M. miscella* is recorded within Biozone SBZ7. The first *Nummulites* in our sections are *N. atacicus* and *N. globulus* which are typical of Biozone SBZ8 elsewhere in Tethys

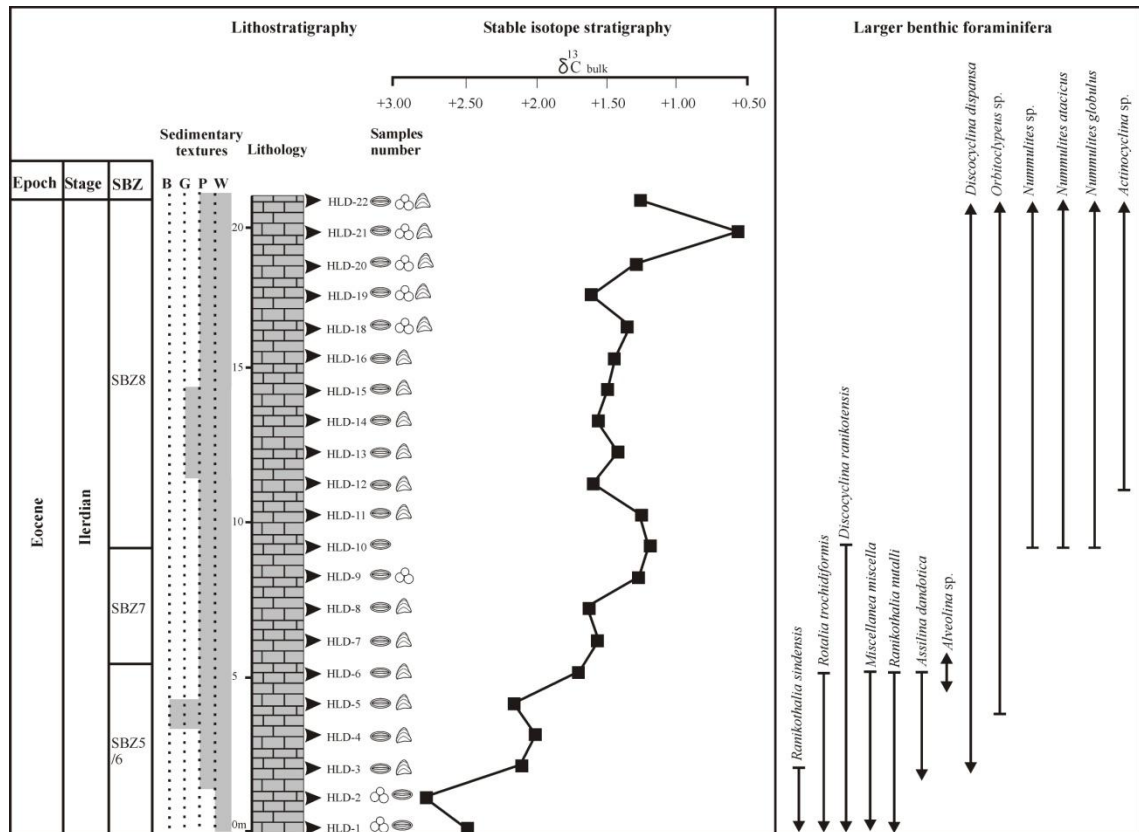


**Figure 7.** Lithostratigraphy, stable isotopes and biostratigraphic ranges of larger benthic foraminifera of the Early Eocene Dungan Formation in the Hanna Lake section, Lower Indus Basin, Pakistan. Key as for Figure 3.

platform carbonate successions (e.g. Serra-Kiel *et al.* 1998) (Figs 6-7). The top of Biozone SBZ8 cannot be identified due to succeeding open-marine clastic sediments (inhospitable lithofacies for LBFs) of the Ghazij Formation in our sections.

### Comparison of LBF ranges with those in other regions of Tethys

LBF marker species used in this study are index taxa described for the SBZ1-SBZ8 biozones by Serra-Kiel *et al.* (1998). LBFs which show ranges different from those described by Serra-Kiel *et al.* (1998) are evaluated based on their faunal associates in the Indus Basin (Figs 3-7) and on their occurrences elsewhere. Key LBFs which were not described by Serra-Kiel *et al.* (1998), but which are critical for biostratigraphic

analysis in the Indus Basin, have been compared here with data from other Tethyan carbonate platform successions.

#### *Paleocene LBFs*

According to Serra-Kiel *et al.* (1998), *Laffitteina bibensis* is restricted to the basal Paleocene SBZ1 Biozone. However, in the Mughal Kot section, its association with *Idalina sinjarica* and Selandian coralline algae *Distichoplax biserialis* (Aguirre *et al.* 2007) suggests it also occurs within the SBZ2 Biozone. Longer biostratigraphic ranges for *Lf. bibensis* have also been reported from the Paleocene of Iran (Bignot & Neumann 1991) and the Danian to Thanetian successions of NE Turkey (Sirel 1998; Inan *et al.* 2005).

Serra-Kiel *et al.* (1998) described *Idalina sinjarica* as ranging from biozones SBZ3 to SBZ6. However, its first appearance together with the coralline alga *Distichoplax biserialis* which is typical from the Selandian onward (Aguirre *et al.* 2007), and lack of biozonal markers for the SBZ3 Biozone in the Mughal Kot section supports an early appearance of *I. sinjarica* in the SBZ2 Biozone (Fig. 4). Drobne *et al.* (2002) also reported the first appearance of *I. sinjarica* within the SBZ2 Biozone from the Indo-Pacific, Tethyan and Caribbean regions.

According to Hottinger (1960), Serra-Kiel *et al.* (1998), Pignatti *et al.* (2008) and Scheibner & Speijer (2009), *Glomalveolina primaeva* is restricted to Biozone SBZ3. However, in the Zranda section, the association of *G. primaeva* with *Miscellanea juliettae*, *Coskinon rajkae* and *Fallotella alavensis* and later with *M. miscella* suggests it also ranges into Biozone SBZ4 (Fig. 5). Similarly, Jauhri & Agarwal (2001) reported *G. primaeva* in association with *G. levis* (= Biozone SBZ4) in NE India and White (1992) recorded a SBZ3-SBZ6 range for *G. primaeva* in Oman.

In Tethyan platform successions (including Pakistan and India), a

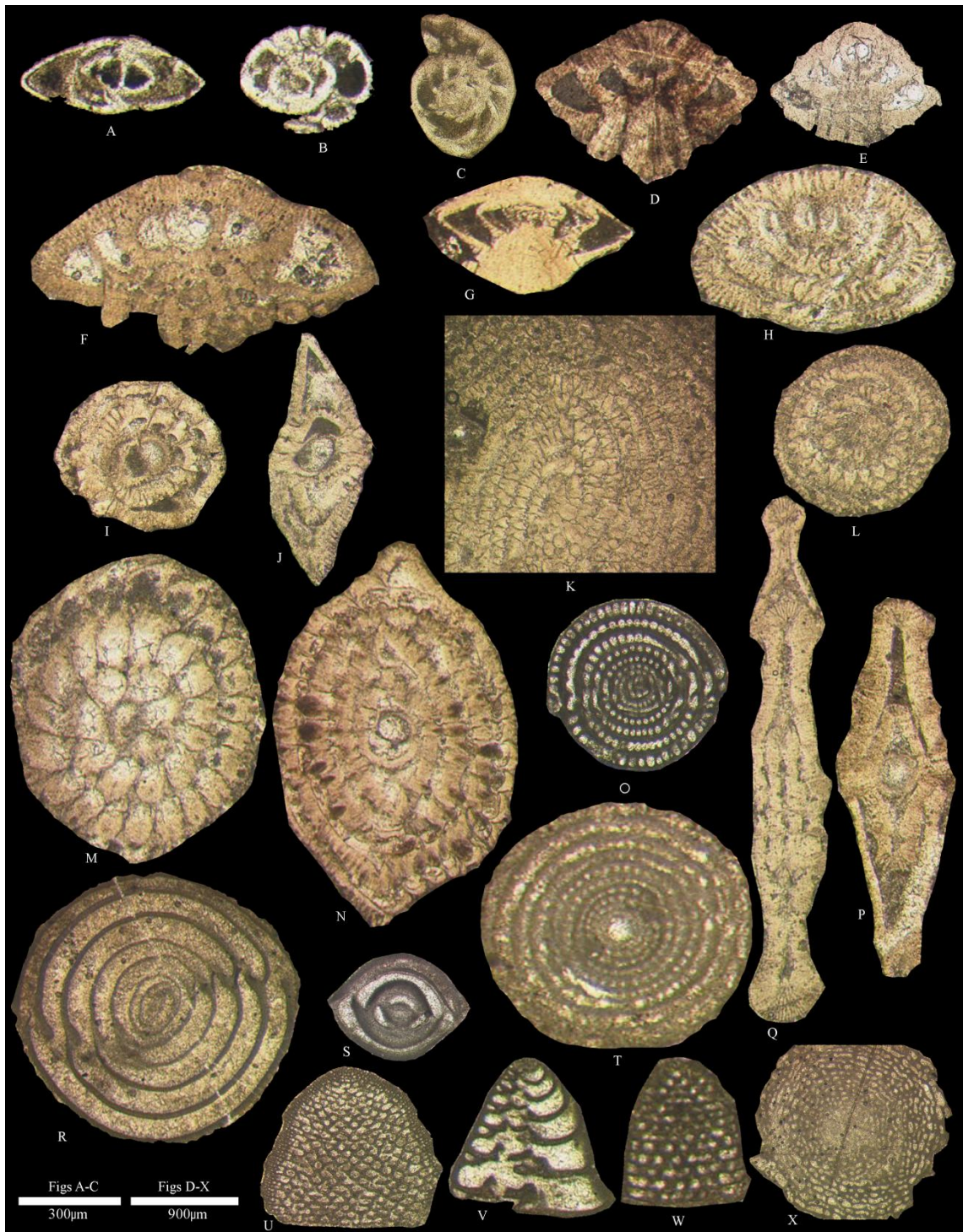


**Figure 8.** Biostratigraphically important larger benthic foraminifera from the Paleocene-Early Eocene (SBZ1-SBZ5/6), Indus Basin, Pakistan. All microphotographs are plane-polarized light. A-C, *Laffitteina bibensis* Marie, SBZ1-SBZ2; A, axial section, s. no. PD-16; B, off-centre axial section, s. no. PD-8; C, equatorial section, s. no. PD-8. D, *Lockhartia conditi* (Nuttall), SBZ3-SBZ5/6, axial section, s. no. KL53. E, *Lockhartia conica* Smout, SBZ3-SBZ4, axial section, s. no. 4472.24. F, *Lockhartia haimeii* (Davies), SBZ3-SBZ5/6, axial section, s. no. ZRD-33. G, *Kathina selveri* Smout, SBZ3-SBZ4, axial section, s. no. 4468.61. H, *Laffitteina erki* (Sirel), SBZ3-SBZ4, near axial section, s. no. ZRD-21. I-J, *Miscellanea juliettae* Leppig, SBZ3, megalospheric form; I, equatorial section, s. no. PD-1; J, axial section, s. no. ZRD-28. K-L, *Miscellanea*

*meandrina* (Carter), SBZ4; K, microspheric form, equatorial section, s. no. ZRD-20; L, megalospheric form, equatorial section, s. no. ZRD-20. M-N, *Miscellanea miscella* (D'Archaic & Haime), SBZ4, megalospheric form; M, equatorial section, s. no. ZRD-13; N, near axial section, s. no. ZRD-8. O, *Glomalveolina primaeva* Reichel, SBZ3-SBZ4, non-centered axial section, s. no. ZRD-36. P, *Ranikothalia sahani* Davies, SBZ3-SBZ5/6 megalospheric form, axial section, s. no. ZRD-4. Q, *Ranikothalia sindensis* (Davies), SBZ3-SBZ5/6, microspheric form, axial section, s. no. ZRD-4. R, *Spiroloculina* sp., axial section, s. no. ZRD-12. S, *Idalina sinjarica* Grimsdale, SBZ2-SBZ5/6, axial section, s. no. 4471.89. T, *Glomalveolina telemetensis* Hottinger, SBZ3-SBZ4, axial section, s. no. ZRD-9. U, *Dictyoconus* sp., SBZ3-SBZ5/6, axial section, s. no. ZRD-34. V, *Coskinon rajkae* Hottinger & Drobne, SBZ3, axial section, s. no. ZRD39. W, *Fallotella alavensis* Mangin, SBZ3, s. no. ZRD-39. X, *Keramosphaera* cf. *iranica* Rahaghi, SBZ3-SBZ4? near equatorial section, s. no. ZRD-26. SBZ-shallow benthic biozones. Sample numbers (s. no.) with ZRD are from Zranda section (Fig. 5); KL from Kotal Pass section (Fig. 3); PD from Mughal Kot section (Fig. 4); 4472.24 from Shakardara Well-1 (Fig. 3).

biostratigraphic range of biozones SBZ3 to SBZ4 has been recorded for *Lockhartia haimei* (e.g. Butt 1991; Weiss 1993; Serra-Kiel *et al.* 1998; Akhtar & Butt 1999; Jauhri & Agarwal 2001; Mathur *et al.* 2009). However, in the Zranda section, *L. haimei* together with *L. conditi* are associated with *Alveolina*, *Assilina dandotica*, *Discocyclina dispansa*, *Ranikothalia sindensis* and *R. nuttalli* which suggest a stratigraphically higher occurrence within the SBZ5/6 biozones (Fig. 5). Similarly, Butterlin & Fourcade (1989) reported longer biostratigraphic ranges for *L. haimei* and *L. conditi*, showing their highest occurrences in the Early-Middle Eocene. I have not recorded *L. conica* and *L. diversa* in the Eocene of the Indus Basin, but they frequently occur in the Late Paleocene (in biozones SBZ3 and SBZ4) (Fig. 3-7). Similar biostratigraphical ranges for *L. conica* and *L. diversa* have been shown in Qatar (Smout 1954), and for *L. diversa* in western Tethys (Butterlin & Fourcade 1989) and in Turkey (Sirel 1998). However, various studies in the wider Tethyan region (including Pakistan) indicate that *L. conica* is not restricted to the Paleocene and that this taxon extends into the Early Eocene (e.g. Butterlin & Fourcade 1989; Weiss 1993; Akhtar & Butt 1999).

*Rotalia trochidiformis* is a commonly occurring LBF in Tethys and ranges from

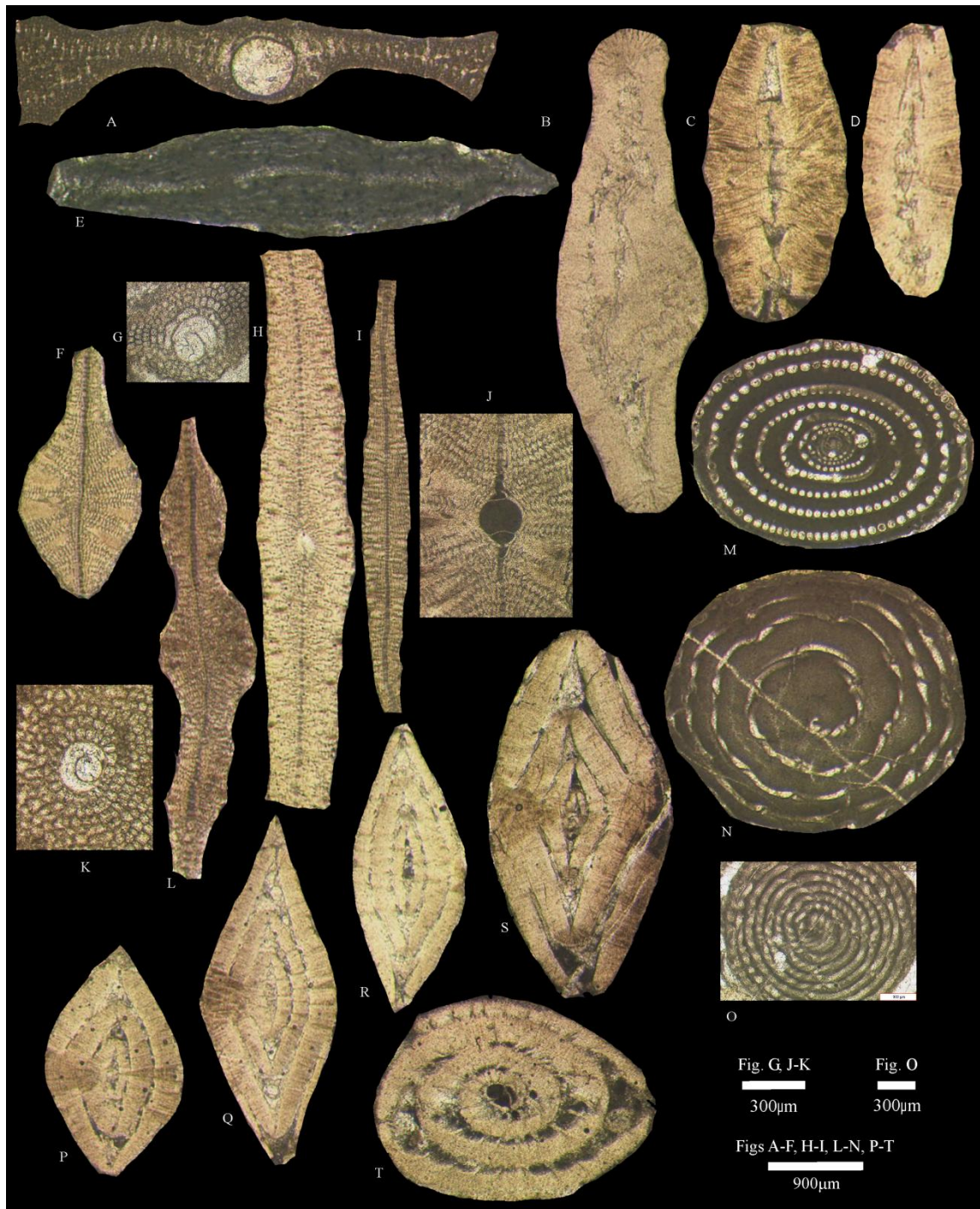


**Figure 9.** Biostratigraphically significant larger benthic foraminifera from the Early Eocene (SBZ5-SBZ8 biozones), Indus Basin, Pakistan. All microphotographs are plane-polarized light. A, *Opertorbitolites* sp., SBZ5/6, axial section, s. no. ZRD-1. B, *Ranikothalia nuttalli* (Davies), SBZ5/6, axial section, s. no. HLD-3. C-D, *Assilina dandotica* Davies, SBZ5/6; C, near axial section; s. no. HLD-3; D, axial section, s. no. HLD-6. E, *Somalina* sp., SBZ5/6, axial section, s. no. BD-3. F-G, *Discocyclina dispansa* (Sowerby), SBZ5/6-SBZ8; F, microspheric form, axial section, s. no. BD-15; G, embryo of megalospheric form, equatorial section, s. no. HLD-14. H, *Discocyclina sella* (d'Archiac), SBZ5/6-SBZ8, microspheric form, axial section, s. no. BD-11. I, *Discocyclina ranikotensis* Davies, SBZ4-SBZ7, microspheric form, axial section, s. no. ZRD- 2. J, *Orbitoclypeus* sp., SBZ5/6-SBZ8, embryo of megalospheric form, axial section, s. no. HLD-14. K-L, *Discocyclina ranikotensis* Davies, SBZ4-SBZ7, microspheric form, axial section, s. no. ZRD- 2. M, *Somalina* sp., SBZ5/6, axial section, s. no. BD-3. N, *Somalina* sp., SBZ5/6, axial section, s. no. BD-3. O, *Somalina* sp., SBZ5/6, axial section, s. no. BD-3. P-Q, *Somalina* sp., SBZ5/6, axial section, s. no. BD-3. R, *Somalina* sp., SBZ5/6, axial section, s. no. BD-3. S, *Somalina* sp., SBZ5/6, axial section, s. no. BD-3. T, *Somalina* sp., SBZ5/6, axial section, s. no. BD-3. Scale bars: 300µm for Figs. G, J-K and Fig. O; 900µm for Figs. A-F, H-I, L-N, P-T.

section, s. no. HLD-13. K, *Orbitoclypeus* sp., SBZ5/6-SBZ8, embryo of megalospheric form, equatorial section, s. no. HLD-13. L, *Actinocyclus* sp., SBZ8, axial section, s. no. HLD-14. M, *Alveolina* sp., SBZ5/6-SBZ8, off-centered axial section, s. no. BD-15. N, *Alveolina* sp., SBZ5/6-SBZ8, off-centered equatorial section, s. no. ZRD-2. O, *Glomalveolina lepidula* (Schwager), SBZ5/6-SBZ8, off-centered axial section, s. no. BD-5. P, *Nummulites* sp., SBZ8, axial section, s. no. BD-14. Q-R, *Nummulites atacicus* Leymerie, SBZ8, megalospheric form, axial section, s. no. BD-13. S-T, *Nummulites globulus* Leymerie, SBZ8, megalospheric form, s. no. HLD-19; S, axial section; T, off-centered equatorial section. SBZ-shallow benthic biozones. Sample numbers (s. no.) with ZRD are from Zranda section (Fig. 5); BD from Muree Brewery section (Fig. 6); HLD from Hanna Lake section (Fig. 7).

the Paleocene to the Early Eocene (biozones SBZ3-SBZ8, and possibly into SBZ9) (e.g. Qatar, Smout 1954; Pakistan, Weiss 1993, Akhtar & Butt 1999; NE Turkey, Inan *et al.* 2005; N Turkey, Özgen-Erdem 2005; Northern India, Mathur *et al.* 2009). In the Zranda section, the biostratigraphic ranges of *Laffitteina erki* and *Kathina selveri* are shown as biozones SBZ3-SBZ4 based on their faunal association (Fig. 5). This is in accordance with occurrences in Slovenia (Özgen & Akyazi 2001) and Turkey (Özgen-Erdem *et al.* 2005; Inan *et al.* 2005), where a range of biozones SBZ3-SBZ4 for *Lf. erki* and *K. selveri* is indicated.

According to Serra-Kiel *et al.* (1998), *Ranikothalia sindensis* first appeared at the base of Biozone SBZ4 in Tethys. However, in the Zranda and Kotal Pass sections and Shakardara Well-1, the occurrence of *R. sindensis* together with *R. sahani* in association with *Miscellanea juliettae*, *Lockhartia haimei*, *Coskinon rajkae* and *Fallotella alavensis* suggests an earlier first appearance within the SBZ3 Biozone (Figs 3, 5). Tosquella *et al.* (1998) found *R. sindensis* restricted to the SBZ3 Biozone in the Pyrenean Basin, France. In Oman, India and Pakistan, *R. sindensis* has been reported from the Late Paleocene to earliest Eocene (Nagappa 1959a; Butt 1991; Racey 1995).

Ferrandez-Canadell (2002) described *Setia tibetica* and *Orbitosiphon punjabensis* as endemic to the south-central Asian region. In studied sections, I have recorded these genera associated with LBFs characteristic of the SBZ3 and SBZ4

biozones, for example in the Shakardara Well-1, Kotal Pass and Zranda sections (Figs 3, 5). This is in agreement with the findings of Ferrandez-Canadell (2002), who reported these LBFs from the uppermost Hangu, Lockhart and lower Patala formations in the Salt Range area of the Upper Indus Basin, which according to Afzal *et al.* (2009) can be regarded as assignable to biozones SBZ3 and SBZ4.

*Discocyclina ranikotensis* first appears within the SBZ4 Biozone in our successions (Fig. 3). In Pakistan and India, other studies have also indicated that *D. ranikotensis* ranges from the Late Paleocene to Early Eocene (e.g. Nagappa 1959b; Samanta 1969; Butt 1991; Weiss 1993; Akhtar & Butt 1999, 2000). The species appears to be endemic to the Indian region (east Tethys) as it has not been reported from west Tethys carbonate platforms, where different lineages of discocyclinids developed during the Late Paleocene (e.g. Samanta 1969; Adams 1970; Sera-Kiel *et al.* 1998; Less *et al.* 2007).

#### *Early Eocene LBFs*

The placement of the P-E boundary based on LBFs has been intensively debated (see Scheibner & Speijer 2009; Pujalte *et al.* 2009a for summary). However, it has now been agreed that the well-known larger foraminifer-turnover (LFT, appearance of larger *Orbitolites*, *Alveolina*, and *Nummulites*, Orue-Etxebarria *et al.* 2001) coincides with the onset of the PETM CIE (Scheibner & Speijer 2009; Pujalte *et al.* 2009a). In pelagic successions, the PETM CIE has been correlated with the boundary between planktonic foraminiferal biozones P5 and E1 and nannofossil biozones NP9a and NP9b (Aubry 1995; Berggren & Pearson 2005) (Fig. 10). In shallow marine successions, the boundary between biozones SBZ4 and SBZ5 of Serra-Kiel *et al.* (1998) is coeval with the onset of the CIE and thus the P-E boundary (Orue-Etxebarria *et al.* 2001; Pujalte *et al.* 2003; Pujalte *et al.* 2009a; Scheibner & Speijer 2009) (Fig. 10).

According to Serra-Kiel *et al.* (1998), *Assilina dandotica* is restricted to the SBZ5 Biozone in the Tethyan realm. However, Tosquella *et al.* (1998) demonstrated that *A. dandotica* extends to the SBZ6 Biozone. *Ranikothalia nuttalli* ranges from the SBZ5 to SBZ6 biozones in Tethyan platform successions (e.g. Serra-Kiel *et al.* 1998). Scheibner & Speijer (2009) recorded *R. nuttalli* within the SBZ4 Biozone in Egypt. In our sections, I have not found *R. nuttalli* in the Paleocene (Figs 3, 5-10), which is in agreement with previous LBF studies in Pakistan and India (e.g. Jauhri 1998; Jauhri *et al.* 2006; Jauhri & Agarwal 2001; Afzal *et al.* 2009). However, *R. nuttalli* ranges from the SBZ5 to SBZ6 biozones in India, for example in the Ladakh (Mathur *et al.* 2009) and Assam-Shillong areas (Jauhri 1998; Jauhri & Agarwal 2001; Jauhri *et al.* 2006; Tewari *et al.* 2010). Therefore, the last occurrence of *A. dandotica* together with *R. nuttalli* in Indus Basin successions is correlated to the upper boundary of the SBZ5/6 biozones (Figs 5-7, 10).

*Miscellanea miscella* has been reported from Afghanistan (Kaeffer 1970), north-eastern Turkey (Sirel 1997b), Iran (Rahaghi 1983) and India (e.g. Jauhri 1998; Jauhri & Agarwal 2001; Jauhri *et al.* 2006) from horizons equivalent to the SBZ5 Biozone. In parts of the Lower Indus Basin of Pakistan (e.g. in the Sind and Balochistan provinces), *M. miscella* occurs in association with LBFs characteristic of the SBZ5 Biozone (e.g. Hottinger 1971; Hottinger *et al.* 1998; Akhtar & Butt, 2000). However, in India, *M. miscella* has been reported to range up to the SBZ6 Biozone (e.g. Mathur *et al.* 2009; Tewari *et al.* 2010). In the Hanna Lake and Zranda sections the disappearance of *M. miscella* together with *Assilina dandotica* and *Ranikothalia nuttalli* suggest its upper biostratigraphic limit is within the SBZ6 Biozone (Figs 6-7). In the Muree Brewery section, the occurrence of *M. miscella* in the interregnum interval between the last occurrences of LBFs typical of the SBZ5/6 biozones (e.g. *A. dandotica*, *R. nuttalli* etc.)

and first appearance of *Nummulites atacicus* and *N. globulus* (= SBZ8 Biozone) suggests that its biostratigraphic range may extend into Biozone SBZ7 (Fig. 6).

Serra-Kiel *et al.* (1998) showed that *Ranikothalia sindensis* ranges up to the SBZ5 Biozone in Tethyan successions. Racey (1995) reported *R. sahni* associated with *Assilina dandotica* (= Biozone SBZ5) in Oman. In the Zranda section, the last occurrences of *R. sindensis* and *R. sahni* were recorded within the SBZ5/6 Biozones (Fig. 5).

In our sections and based on previous studies of LBFs in the Indus Basin, *Discocyclina dispansa* is associated with LBFs of the earliest Eocene (e.g. Butt 1991; Akhtar & Butt 1999, 2000) (Figs 5-7). However, LBF studies in west Tethys indicate that *D. dispansa* ranges from biozones SBZ7 to SBZ20 (e.g. Serra-Kiel *et al.* 1998; Less *et al.* 2007; Less & Kovács 2009).

### **Evolution of Early Palaeogene LBFs in the east Tethys Ocean**

The evolution of LBFs during the Early Palaeogene was characterized primarily by a long-term reorganization of faunal communities following the K-T crisis (which caused extinction of 83% of LBFs, BouDagher-Fadel 2008). Here, based on biostratigraphic analysis, I investigate LBF long-term evolutionary patterns in east Tethys.

Biozones SBZ1-SBZ2 are represented by the few surviving LBF lineages from the K-T crisis and dominated by taxa with a small test and no dimorphism (Hottinger 1998, 2001) (Fig. 10). This phase is represented in the Indus Basin by only a few genera of smaller rotaliids (*Rotalia* and *Laffitteina*) and miliolids (*Idalina*) (Fig. 4). *Lockhartia*, *Bangiana*, *Miscellanea* and *Ornatononion* are absent in SBZ1-SBZ2 biozones in east Tethys (India and Pakistan) (e.g. Adams 1970; Kureshy 1978; Jauhri 1998; Jauhri & Agarwal 2001; Jauhri *et al.* 2006; Green *et al.* 2008; Mathur *et al.* 2009; Afzal *et al.*

SBZ	West Tethys LBF assemblages	East Tethys LBF assemblages	
	Europe-Africa	India-Tibet	This study (Indus Basin, Pakistan)
SBZ7- SBZ8	Alveolinids (A) Orthopragminids (A) Assilinids (A) Operculinids (A) <i>Nummulites</i> (A)	Alveolinids (C) Orthopragminids (A) Assilinids (C) Operculinids (C) <i>Nummulites</i> (C)	Alveolinids (C) Orthopragminids (A) Assilinids (C) Operculinids (C) <i>Nummulites</i> (C)
SBZ5/6	Alveolinids (A) Orthopragminids (C) Orbitolitids (A) Assilinids (A) Operculinids (A) <i>Nummulites</i> (A) Glomalveolinids (C)	India: Miscellanids (A) Ranikothalids (A) Rotaliids (C) Alveolinids (R) Orthopragminids (C) Assilinids (R) Glomalveolinids (R) Orbitolitids (R)  Tibet: <i>Nummulites</i> (A) Alveolinids (A) Orthopragminids (C) Orbitolitids (A)	Miscellanids (A) Ranikothalids (A) Rotaliids (A) Alveolinids (R) Orthopragminids (C) Assilinids (R) Glomalveolinids (R) Orbitolitids (R)
SBZ4	Rotaliids (C) Miliolids (R) Miscellanids (A) Glomalveolinids (C) Ranikothalids (A) Orthopragminids (A) Assilinids (R)	Rotaliids (A) Miliolids (R) Miscellanids (A) Glomalveolinids (R) Ranikothalids (C) Orthopragminids (R) Orbitoidal form (R)	Rotaliids (A) Miliolids (R) Miscellanids (A) Glomalveolinids (R) Ranikothalids (C) Orthopragminids (R) Orbitoidal form (C)
SBZ3	Rotaliids (C) Miliolids (C) Miscellanids (C) Glomalveolinids (A) Conical agglutinated forms (C) Ranikothalids (R) Orthopragminids (C)	Rotaliids (A) Miliolids (A) Miscellanids (C) Glomalveolinids (C) Ranikothalids (R) Orbitoidal forms (C)	Rotaliids (A) Miliolids (A) Miscellanids (R-C) Glomalveolinids (C) Conical agglutinated forms (C) Ranikothalids (R) Orbitoidal forms (C)
SBZ1- SBZ2	Rotaliids (C) Miscellanids (C) <i>Bangiana</i> (R)	Rotaliids (R)	Rotaliids (R) Miliolids (R)

**Table 1.** Comparison of the key Paleocene-Early Eocene LBF assemblages of the east and west Tethys. Shallow benthic biozones (SBZ) after Serra-Kiel *et al.* (1998) and Scheibner & Speijer (2009). A, abundant; C, common; R, rare.

2009; Tewari *et al.* 2010), though they are commonly reported from this interval in west Tethys (e.g. Serra-Kiel *et al.* 1998) (Table 1). Potential explanations for this difference could either be inhospitable environments in the east Tethys region as deposition of pure carbonate did not commence fully till the SBZ3 Biozone (e.g. Jauhri 1998; Jauhri

& Agarwal 2001; Jauhri *et al.* 2006; Green *et al.* 2008; Mathur *et al.* 2009; Afzal *et al.* 2009; Tewari *et al.* 2010), or an inability to reach the area from the region of origin of the taxa.

The SBZ3-SBZ4 biozones are characterized by increasing generic diversity and reflect a time when LBFs began experimenting with new morphologies (Hottinger 2001; Scheibner & Speijer 2008a) (Fig. 10). This interval in the Indus Basin commenced with the appearance of many new taxonomic lineages including genera of rotaliids (*Lockhartia* and *Kathina*), miliolids (*Triloculina* and *Quinqueloculina*), pellatispirids (*Miscellanea*), alveolinids (*Glomalveolina*), coskinolinids (*Coskinon*), spirocyclinids (*Saudia*), dictyoconids (*Dictyoconus* and *Fallotella*), nummulitids (*Ranikothalia*, *Assilina* and *Operculina*), discocyclinids (*Discocyclina*) and lepidorbitoids (*Daviesina*, *Orbitosiphon* and *Setia*) (Figs 3-5, Table 1). This faunal pattern is consistent with other parts of Tethys (Hottinger 1997, 1998; Jauhri 1998; Serra-Kiel *et al.* 1998; Jauhri & Agarwal 2001; Jauhri *et al.* 2006; Green *et al.* 2008; Scheibner & Speijer 2008a, 2009; Zamagni *et al.* 2008; Mathur *et al.* 2009; Tewari *et al.* 2010) (Table 1).

In biozones SBZ5-SBZ6, a general reorganization in LBF communities is recorded with a diversification of species, marking the recovery of LBF k-strategists (characterized by long life and low reproductive potential) (Hottinger 1997, 2001, Fig. 10). The latest Paleocene (Biozone SBZ4) miscellanids and ranikothalids are replaced by Early Eocene alveolinids and nummulitids, which come to dominate LBF assemblages in the western Tethyan realm at the P-E boundary (e.g. Scheibner *et al.* 2005; Scheibner & Speijer 2008a), the so-called larger foraminifer-turnover (LFT, Orue-Etxebarria *et al.* 2001).

However, in the Indus Basin, LBF assemblages of the lowest Eocene (biozones



**Figure 10.** Tethyan Paleocene to Early Eocene biostratigraphy, and comparison of trends in evolution and distribution of larger benthic foraminifera (in the Indus Basin),  $\delta^{18}\text{O}$  isotopes, coral reef abundance, and trophic resource continuum (TRC: level of nutrients in ocean water). Events associated with the Paleocene-Eocene boundary: CIE-carbon isotope excursion; BEE-benthic extinction event; LFT-larger foraminifer-turnover; PETM-Paleocene-Eocene Thermal Maximum (modified from Scheibner & Speijer 2008a).

SBZ5/6) are still dominated by *Ranikothalia* and *Miscellanea*, while new LBFs that first emerged within this time interval elsewhere (e.g. *Assilina*, *Alveolina* and *Discocyclina*) are less important and *Nummulites* are absent (Figs 5-7, 10, Table 1). Later, in the Early Eocene there was a gradual diversification of *Discocyclina*, *Operculina* and *Assilina* species and an appearance of new forms including large *Orbitoclypeus*, *Opertorbitolites* and *Somalina*, while *Ranikothalia* disappeared and *Miscellanea* became less important by the end of the SBZ5/6 biozones. Similar LBF assemblages have been recorded in other parts of east Tethys (especially India and Pakistan) (e.g. Nagappa 1959b; Hottinger 1971; Jauhri 1998; Akhtar & Butt 2000; Jauhri & Agarwal 2001; Jauhri *et al.* 2006; Scheibner & Speijer 2008a; Tewari *et al.* 2010) (Table 1). Such LBF assemblages in east Tethys thus differ profoundly from west Tethys (see Table 1).

The SBZ7-SBZ8 biozonal interval is characterized by foraminiferal size-increase and further diversification of successful LBF lineages in Tethys (Hottinger 2001) (Fig. 10). In the Indus Basin, *Miscellanea* disappear in the SBZ7 Biozone while *Assilina*, *Discocyclina*, *Operculina* and *Alveolina* start to diversify and show a clear gradual size increase and dimorphism. The first *Nummulites* appear in the SBZ8 Biozone and rapidly become an important component, while *Alveolina*, *Discocyclina*, *Assilina* and *Operculina* continue to show diversification with the evolution of new lineages, for example *Actinocyclina* (Figs 6-7, 10). These foraminiferan assemblages are comparable to those of west Tethys and they occur in carbonate platform-building quantity (Table 1).

### **LBFs and India-Asia Collision at the P-E boundary**

The leading edge of the Indo-Pakistan plate underwent subduction and orogenic processes at about 55 Ma (the Paleocene-Eocene boundary, Khan & Srivastava 2006; Najman 2006; Copley *et al.* 2010) (Fig. 11). Significant stratigraphic changes in parts of the basin have been recorded at the P-E boundary producing unconformities, intermittent shallow- and deep-marine sediments and in some places a dramatic shift from marine to continental deposits, the latter containing endemic land mammals in parts of the Indus Basin (see Afzal *et al.* 2009 and references therein) (Fig. 2). This may have been caused by compression, uplift and erosion associated with India-Asia collision (Afzal *et al.* 2009) (Fig. 2).

Plate tectonic movements control the spatial distribution and variability of suitable shallow marine habitats for benthic foraminifera (Renema *et al.* 2008). Subject to global climatic constraints, tectonic events will modulate ocean circulation, resulting in changes in surface water characteristics as well as altering connectivity between populations (Renema *et al.* 2008). The early collision of India with Asia may have generated biogeographic barriers between east (India and Pakistan) and west (Europe, North Africa) Tethys, preventing migration of certain LBFs (e.g. species of *Nummulites* and *Alveolina*) between these two provinces (Fig. 11). The biogeographic patterns of modern LBFs can be interrogated using molecular techniques, but in fossil populations morphological characteristics are used to detect biogeographic barriers such as intervening eutrophic waters or land masses (e.g. Langer & Hottinger, 2000; Renema *et al.* 2008). Within the tropical/subtropical belt, present-day LBFs can migrate relatively easily along marine shelves and even between islands separated by deep water provided that these are not far apart (Adams 1989). The terminal Paleocene-earliest Eocene palaeogeographic reconstruction by Smith *et al.* (1994) shows northern India at low

northerly latitudes, with a jettisoned ‘Seychelles block’ then sitting midway between the Indian sub-continent and Madagascar (e.g. Todal & Edholm 1998) (Fig. 11A). Ali & Aitchison (2008) suggested that India may have possessed both southerly and northerly connections with other continents (Africa in the south and Asia in the north) possibly forming a route for terrestrial and freshwater faunal migration (Fig. 11A). The biological record also indicates that Asian land mammals were present on the Indian sub-continent in the Early Eocene (e.g., Clyde *et al.* 2003; Rose *et al.* 2006; Sahni 2006), as were certain freshwater gastropods (Köhler & Glaubrecht 2007). This suggests that India-Asia collision at the P-E boundary had probably created land bridges with other continents which could have acted as barriers for the migration of shallow marine biota (including LBFs) occupying marine platforms surrounding the Indian continent (Fig. 11A).

However, although India-Pakistan may have had connections with southerly and northerly landmasses, there is no evidence for a westerly placed landmass that may have restricted LBF migration from west Tethys (see Ali & Aitchison 2008 and references therein for palaeogeography). Thus, in the absence of a land barrier, LBF migration may have been restricted by an oceanographic barrier, though the nature of this is uncertain (Fig. 11A). Similar oceanographic barriers separate elements of the modern Mediterranean biota (e.g. some barnacles and near-shore fish) from those of the Atlantic (Springer 1982; Pannacciulli *et al.* 1997). Biogeographical isolation may also have led to lower diversity in east Tethys, promoting lower competition for the same habitat space and enhancing the survival of existing lineages (e.g. *Miscellanea* and *Ranikothalia*) (Leppig 1988) during the earliest Eocene (biozones SBZ5/6). The persistence of *Miscellanea* and *Ranikothalia* during the earliest Eocene in east Tethys

indicates that inhospitable lithofacies types are not the reason for the absence of *Nummulites* as both groups of LBFs occupy the same types of habitat (Hottinger 1997).

The different LBF assemblages of east and west Tethys during the earliest Eocene are succeeded by a cosmopolitan fauna in the SBZ8 Biozone, suggesting that the continued northward drift of the Indian plate (e.g. Copley *et al.* 2010) may have collapsed biogeographic barriers between the two Tethyan regions.

### **Response of LBF assemblages to the PETM in east Tethys**

As well as the long-term evolutionary changes to the Palaeogene foraminiferal assemblages (Hottinger 1997, 2001, 2006), a short-term climatic perturbation (PETM CIE) at the P-E boundary (Zachos *et al.* 2003) had a major impact on shallow marine biota (LBFs and coral-reefs) (Scheibner *et al.* 2005; Scheibner & Speijer 2008a, 2008b) (Fig. 10). This climate perturbation caused the extinction of 25% of LBFs (BouDagher-Fadel 2008).

During the PETM, sea surface temperatures rose by 5°C in low latitudes and 8°C in mid to high latitudes (Zachos *et al.* 2003; Tripathi & Elderfield 2004), and humidity and increased rainfall resulted in increased terrestrial runoff from areas bordering Tethys (Bolle & Adatte 2001). There was also enhanced upwelling of deep water onto the shelf (Speijer & Wagner 2002). This led to a transient expansion of the trophic resource continuum (i.e. the quantity of nutrients in sea water) resulting in eutrophic conditions on the continental shelves bordering the Tethys Ocean (Speijer *et al.* 1997). Black shale deposition in Tethys (Speijer & Wagner 2002; Gavrilov *et al.* 2003), the collapse of the oligotrophic *Gavelinella beccariiiformis* benthic foraminifera (Speijer *et al.* 1997), and widespread *Apectodinium* blooms (Crouch *et al.* 2003; Crouch & Brinkhuis 2005) have been linked with increased productivity related to the PETM.

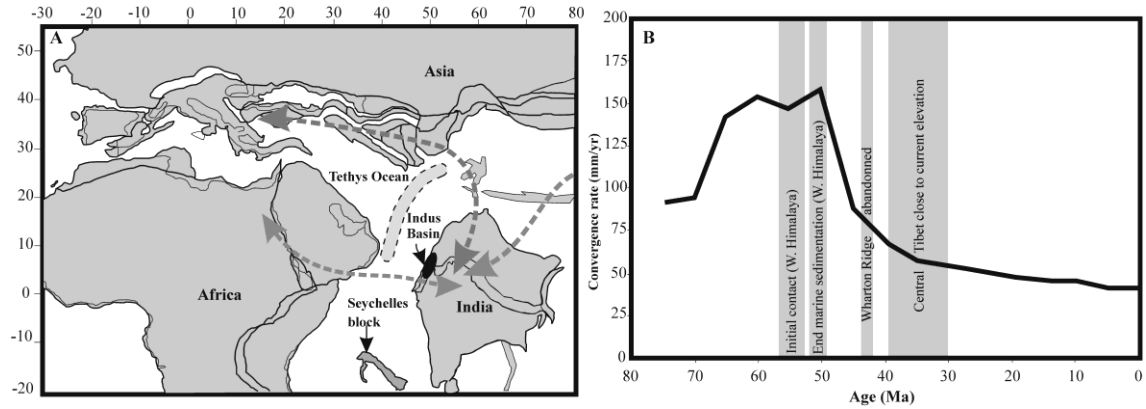


**Figure 11.** Palaeogeography and collision history of the Indian sub-continent. A, Earliest Eocene (SBZ5/6 biozones) reconstruction (based on Smith *et al.* 1994 with data from Gaetani & Garzanti 1991; Gingerich *et al.* 1997). Dark grey dashed line with arrow heads show possible routes (through land masses) for rodent mammal migration between India and other continents. These land masses likely acted as geographic barriers for LBFs to reach shallow marine habitats of the Indian subcontinent. A postulated oceanographic barrier (possibly larger distances and/or eutrophic waters) is shown as a grey band between east and west Tethys, which may also have prevented LBFs migrating from west to east. B, Depicts the rate of convergence (black line) between India and Asia from 75 Ma (after Copley *et al.* 2010). The grey bands show the timings of notable events in the history of collision. The collision is thought to have begun at the western edge of the plate boundary during P-E boundary times (Rowley 1996; Copley *et al.* 2010).

LBFs are considered k-strategists (Hottinger 1983, 1998) and are, therefore, the first to disappear during a breakdown or interruption of stable oligotrophic conditions (Hottinger 1983). According to Scheibner *et al.* (2005) and Scheibner & Speijer (2008a), the PETM represents such an interruption causing the disappearance of typical latest Paleocene k-strategist LBFs (e.g. *Miscellanea*, *Ranikothalia*) from carbonate platforms in west Tethys, while more moderate k-strategists like glomalveolinids thrived without apparent disruption through the P-E boundary. Later, oligotrophic conditions were re-established in the basins and on the platforms during the earliest Eocene and LBFs recovered, with the radiation of *Alveolina* and *Nummulites* (LFT of Orue-Etxebarria *et al.* 2001).

However, in east Tethys, LBFs such as *Miscellanea* and *Ranikothalia* dominated the earliest Eocene carbonate platforms while *Alveolina* was less important and

*Nummulites* absent (e.g. Nagappa 1959b; Hottinger 1971; Jauhri 1998; Akhtar & Butt 2000; Jauhri & Agarwal 2001; Jauhri *et al.* 2006; Scheibner & Speijer 2008a). Other parts of Tethys also show the persistence of *Miscellanea* and *Ranikothalia* beyond the P-E boundary, but as a minor component in association with *Alveolina* and *Nummulites*-dominated assemblages. For example, *Miscellanea* has been reported together with *Alveolina vredenburgi* (= Biozone SBZ5) in Turkey (Hottinger 1960; Sirel 1997b), Afghanistan (Kaeffer 1970), Iran (Rahaghi 1983) and Iraq (Hottinger 1960), and *Ranikothalia* together with *Discoyclina* in the early Ilerdian of the Northern Calcareous Alps (Moussavian 1984). Recently in SW Slovenia, Zamagni (PhD thesis 2009) reported *Ranikothalia* and *Miscellanea* in the SBZ5 Biozone and *Ranikothalia* up to Biozone SBZ7? together with small-sized *Alveolina* and *Nummulites*.

These data from Tethys suggest that LBFs like *Miscellanea* and *Ranikothalia* were not significantly affected by the PETM and that they rapidly adapted to new climatic and environmental regimes, being most successful in east Tethys. Direct ecological comparison of these LBFs with modern forms is not possible as they became extinct during the Early Eocene. However, palaeoecological studies based on carbonate microfacies types and palaeoecological investigations of other fauna associated with *Miscellanea* and *Ranikothalia* show that they were k-strategists and, as most k-strategists carry symbionts, lived within the upper photic zone in carbonate shelf environments (Pignatti 1994; Hottinger 1997). Recent studies of living LBFs have demonstrated that taxa with symbionts show a taxon-specific response to environmental changes including nutrient and turbidity stress (Langer & Hottinger 2000; Hallock *et al.* 2003; Renema 2008). Hallock (1987, 1988) described the community structure of symbiont-bearing benthic foraminifera as a function of nutrient flux, directly influencing euphotic zone depth. These studies predict that species that are highly

specialised to particular levels of light availability can respond to some loss of water transparency (a function of plankton densities and fluvial influx of dissolved organic matter and suspended sediments) by partially compressing their depth ranges. However, if water transparency is reduced too much, most will probably disappear, especially if less specialised species are present (Hallock 1987). Furthermore, Renema & Troelstra (2001) studied LBFs in the tropical Spermonde Shelf (SW Sulawesi, Indonesia) and demonstrated that species show a greater flexibility in their habitat preferences; not all taxa react in the same way to the described environmental parameters. Environmental factors, and possibly also interaction with other species, affect the distribution of LBFs (Hohenegger 2004) and thereby, local survivorship or recruitment (Newberry *et al.* 1996, Nekola & White 1999). The persistence of *Miscellanea* and *Ranikothalia* in east Tethys during the earliest Eocene (biozones SBZ5/6) may suggest their flexibility in palaeoecological adaptation under stressful conditions, controlled by local palaeoecological conditions and eco-space competition with other species. The lack of *Nummulites* and scarcity of *Alveolina* during the earliest Eocene may have facilitated the survival of these LBFs in east Tethys. In other parts of Tethys, where typical Paleocene LBFs were completely replaced in the Eocene by *Nummulites*, *Assilina* and *Alveolina* (e.g. Orue-Etxebarria *et al.* 2001; Pujalte *et al.* 2009b; Scheibner *et al.* 2005; Scheibner & Speijer 2008a, 2009), k-strategists appear to have been supplanted (Leppig 1988) during a rapid adaptive radiation of these genera.

Based on the discussion presented here, I postulate that the LFT was not an instantaneous and synchronous event across the whole of the Tethyan region caused only by the PETM (as suggested by Orue-Etxebarria *et al.* 2001; Scheibner *et al.* 2005; Scheibner & Speijer 2008a, 2009; Pujalte *et al.* 2009b) but was a gradual process primarily driven by long-term evolutionary patterns of LBFs (Hottinger 2001). Other

factors, like local palaeoecological conditions, eco-space competition between taxa, and local tectonics may have played an important role in the timing and extent of the LFT in Tethyan carbonate platforms.

## Conclusions

- (1) The LBFs of the Indus Basin provide a biostratigraphy through the Paleocene to Early Eocene (SBZ1-SBZ8 biozones). The first appearance of *Alveolina*, together with *Assilina dandotica*, *Ranikothalia nuttalli* and *Discocyclina dispansa*, marks the earliest Eocene.
- (2) Stable isotope data for  $\delta^{13}\text{C}_{\text{carb}}$  show more positive values for the Late Paleocene (+3.4‰ to +3.0‰) and lower values (+2.7‰ to +1.6‰) for the earliest Eocene.
- (3) The absence of *Nummulites* and scarcity of *Alveolina* in east Tethys during the earliest Eocene may have been caused by the early collision of India with Asia, creating biogeographic barriers between west and east Tethys. This may have lowered LBF diversity in east Tethys and enhanced the chance of survival of typical Late Paleocene *Miscellanea* and *Ranikothalia* into the Eocene.
- (4) The PETM event did not affect LBFs such as *Miscellanea* and *Ranikothalia* severely and uniformly, and thus the long-term evolutionary patterns together with local palaeoecological conditions, eco-space competition between taxa, and local tectonics have played an important role in the timing and extent of the larger foraminifer-turnover.

---

## **Chapter 5**

---

Palaeoenvironmental evolution  
of East Tethys shallow marine  
benthic communities during  
the Late Paleocene - Early  
Eocene climate and  
oceanographic change

---

## **Chapter 5: Palaeoenvironmental evolution of East Tethys shallow marine benthic communities during Late Paleocene - Early Eocene climate and oceanographic change**

### **Abstract**

Investigation of the Indus Basin carbonate ramp biota of the late Paleocene - Early Eocene provides, for the first time, a detailed evaluation of the evolution of east Tethyan shallow marine biota during an interval of marked climate change and regional tectonic reconfiguration. It also allows assessment of pan-Tethyan shallow shelf ecosystem evolution through an important interval of global change. Microfacies analysis of the Thanetian succession of the Indus Basin demonstrates a transgressive sequence from tidal to open inner ramp settings. Foraminiferal shoals and small patch-reefs developed in the inner ramp setting during the early Thanetian; these likely controlled local hydrodynamic conditions, affecting salinities, temperatures and nutrient levels in proximal marine environments and promoting meso-oligotrophic communities (larger benthic foraminifera [LBFs] and dasycladacean algae). By comparing the early Thanetian ramp biota of the Indus Basin with that of west Tethys (coralgal-dominated communities), a latitudinal gradient in sea surface temperatures is identified. During late Thanetian times, microfacies were characterized by oligotrophic LBFs (miscellanids, rotaliids and ranikothalids) comparable to west Tethys, suggesting a pan-Tethyan biotic response to the long-term warming of the early Paleogene. A shift in microfacies from open inner ramp to tidal/supratidal settings during the late Thanetian suggests the influence of latest Paleocene eustatic change. Major environmental perturbation of the Paleocene Eocene Thermal Maximum (PETM) and regional India-Asia collision during

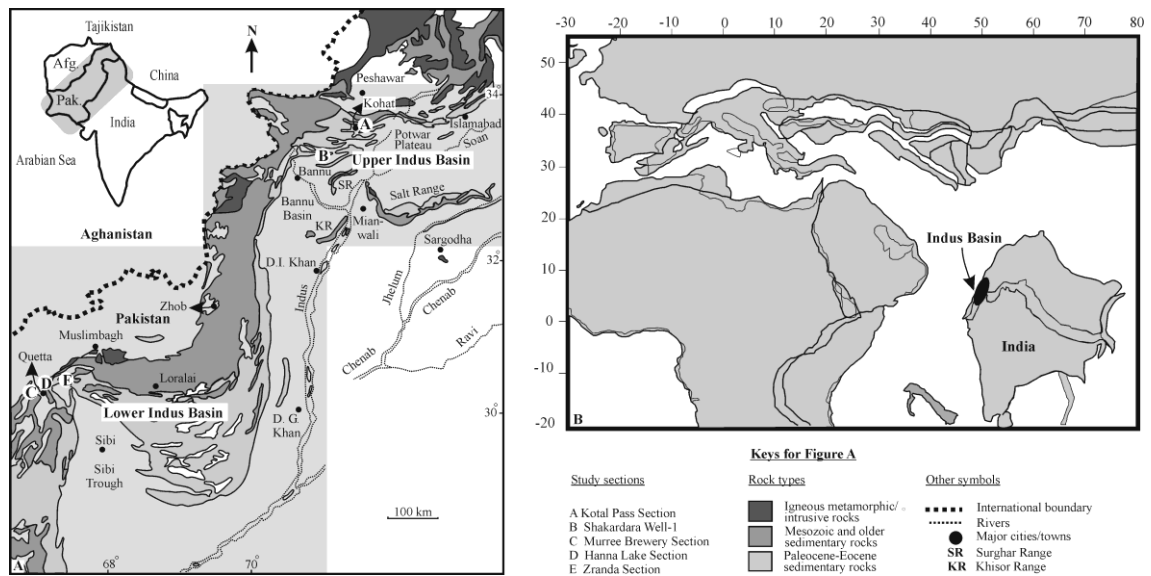


**Figure 1.** A, Map of the Upper Indus Basin and parts of the Lower Indus Basin showing distribution of Paleocene-Eocene sedimentary rocks and key stratigraphical sections (modified after Eames 1952). B, Palaeogeographic position of the Indus Basin, Pakistan during the Late Paleocene- Early Eocene (based on Hay *et al.* 1999).

the earliest Eocene produced a different response of the biota in east Tethys to that seen in the west. Microfacies in the early Ilerdian show low-diversity LBF assemblages (miscellanid-rotaliids with subordinate ranikothalids) in inner ramp settings, and encrusting foraminifera in the mid ramp, while *Nummulites* – characteristic of west Tethys at this time, are absent, and *Alveolina* and orbitolitids are rare. Later, during the uppermost early-mid Ilerdian, environmental conditions became more stable and highly oligotrophic/stable biota similar to that of west Tethys (mainly orthopragminid and nummulitid LBFs) appeared in ramp environments.

## Introduction

The climate history of the early Palaeogene is marked by long-term global warming, beginning in the Late Paleocene (Selandian, ~59 Ma) and terminating in the Early Eocene (Ypresian, ~51 Ma) (Zachos *et al.* 2001). In addition to this long-term warming

trend, a short-term (ca 200 kyr) hypothermal event at the Paleocene-Eocene boundary (P-E) known as the Paleocene-Eocene Thermal Maximum (PETM) had a significant impact on marine and terrestrial biota (Zachos *et al.* 2001). The PETM was characterized by a 5-8°C increase in mean global surface temperature and its signature in marine carbonates is marked by a negative carbon isotope excursion of ca -2.5 to -4‰ (CIE; Zachos *et al.* 2001, 2007). Various studies have documented changes in deep-sea and pelagic biota in response to this climatic perturbation (e.g. approximately 40% extinction of smaller benthic foraminifera, Pak & Miller 1992; Thomas 2007; rapid diversification of planktonic foraminifera and calcareous nannofossils, Gibbs *et al.* 2006; Petrizzo 2007). On land, major changes in floral communities have been recorded in response to increased temperature and atmospheric CO<sub>2</sub> levels (Harrington & Jaramillo 2007). The impact of the PETM on shallow marine carbonate biota (such as larger benthic foraminifera (LBF) and corals) has recently been documented (e.g. Orue-Etxebarria *et al.* 2001; Scheibner *et al.* 2005; Scheibner & Speijer 2008a, 2008b). The well-known larger foraminiferal turnover (LFT, marked by the appearance of adult dimorphism and large shell size) and decline of coral-reef communities in low-mid latitudes has been related to rising sea surface temperatures and changes in the trophic resource regime (quantity of nutrients in water) caused by the PETM (Scheibner *et al.* 2005; Scheibner & Speijer 2008a, 2008b; Pujalte *et al.* 2009).

Palaeontological data on the Late Paleocene-Early Eocene carbonate succession are scant from east Tethyan deposits, in marked contrast to the extensive data from west Tethyan carbonate successions. Previous studies in the Indus Basin of Pakistan provided a litho-biostratigraphical context for the interpretation of early Paleogene marine successions, but problems like poor or invalid stratigraphic determinations made it difficult to document and correlate geologically significant events (such as the PETM)

in the stratigraphical record of the basin (see Afzal *et al.* 2009 for summary of problems). Moreover, other studies dealing with sedimentological aspects of early Palaeogene successions (e.g. Meissner *et al.* 1974; Meissner *et al.* 1975; Butt 1987; Gibson 1990; Warwick & Shakoor 1993; Kassi *et al.* 1999; Ahmad & Dudson 2000; Ahmad & Ahmad 2001; Yaseen *et al.* 2007) paid little attention to the regional and global significance of carbonate successions and associated biota. Consequently, the precise temporal and genetic relationships among lithological and palaeontological observations for east Tethyan carbonate successions remain unresolved.

However, recent stratigraphic revision of the Paleocene-Eocene succession of Pakistan (Afzal *et al.* 2009) and the establishment of Tethyan LBF biostratigraphic biozones (e.g. Afzal *et al.* in press) for the carbonate succession in the Indus Basin provide an excellent opportunity to systematically analyse the evolution of shallow marine carbonate environments and associated biota through the Paleocene-Eocene (P-E) boundary in this region. These studies in the Indus Basin (Afzal *et al.* 2009 and in press) and examination of west Tethyan carbonate successions (see Scheibner & Speijer 2008 for summary) have shown profound biotic differences between east and west Tethys. During the earliest Eocene, east Tethyan carbonate successions (India and Pakistan) lack typical west Tethys *Nummulites*, whilst *Alveolina* is rare: LBFs typical for the Late Paleocene Tethys such as *Miscellanea* and *Ranikothalia* continue to dominate. In this study I present new data on carbonate microfacies (MFTs) and palaeontology (particularly LBFs, corals and algae) from five Late Paleocene-Early Eocene sections in the Indus Basin. The aims are to: 1) establish carbonate microfacies and describe the significance of associated palaeoecological assemblages (LBFs, algae and other biocomponents) through the P-E boundary; 2) constrain mechanisms of palaeoenvironmental evolution of the shallow marine carbonate biota; 3) examine the

effects of long-term early Paleogene and short-term P-E boundary (PETM) warming and of India-Asia collision on shallow marine ecosystems and biota; and 4) appraise the palaeoenvironmental implications of biotic differences between west (Europe-Africa) and east (India-Pakistan) Tethyan carbonate successions during the P-E boundary time.

### **Geological and stratigraphical setting**

A detailed geological and stratigraphical framework for the Indus Basin was discussed by Afzal *et al.* (2009, and in press). The Paleocene-Early Eocene sedimentary succession displays marked variations in lithostratigraphy, geological history and depositional environments, greatly influenced by India-Asia collisional tectonics (Afzal *et al.* 2009). Despite complications caused by complex tectonics, parts of the Indus Basin expose well-preserved Paleocene-Early Eocene shallow-marine carbonate units (e.g. Lockhart and Dungan formations). Four outcrop sections, the Kotal Pass, Muree Brewery, Hanna Lake and Zranda, and one petroleum-well, Shakardara Well-1, have been studied (Fig. 1).

### **Materials and Methods**

Some 179 samples were collected, including 78 from the Late Paleocene Lockhart Formation in the Kotal Pass section and 20 from the Shakardara Well-1 in the Upper Indus Basin (Fig. 1). In the Lower Indus Basin 39 samples from the Late Paleocene-Early Eocene Dungan Formation in the Zranda section, 20 in Muree Brewery and 22 from the Hanna Lake section were collected. The geological details of these sections have been described by Afzal *et al.* (in press). For carbonate microfacies (MFTs) analysis, I have prepared standard limestone thin sections (2.5cm × 5cm and 2.5 × 7cm) for petrographic analysis, complemented by limestone slab and field data (sedimentary

structures, fossils and stratigraphic relationships). Determination of MFT types is based on visual examination and quantitative-semi-quantitative (see appendices 1-5) analysis of lithology, grain types (biogenic or abiogenic), textures, fossil assemblages and bioclasts in thin section (Wilson 1975; Flügel 1982, 2004). The palaeoenvironmental and depositional conditions were reconstructed by combining sedimentological and palaeontological data. Furthermore, palaeoecological assemblages (with emphasis on LBFs and calcareous algae) are compared with modern counterparts and known facies models (e.g. Hottinger 1983; Reiss & Hottinger 1984; Hallock & Glenn 1986; Hottinger 1997; Langer & Hottinger 2000; Hohenegger & Yordanova 2001).

### **Microfacies and depositional environments**

A total of 24 microfacies types (MFT 1-MFT 24) have been distinguished, demonstrating a diverse array of depositional and palaeoenvironmental conditions. As there is no evidence of any major framework-building biota (e.g. barrier coral-reef) apart from small patch-reefs, the general depositional setting is interpreted as a carbonate ramp. The ramp is subdivided into inner ramp, mid ramp and outer ramp, using the terminology of Burchette & Wright (1992), comparable to the Early Eocene ramp in Metlaoui Group of Tunisia (Loucks *et al.* 1996). The term inner ramp in this study refers to depositional environments between upper shoreface (beach or lagoonal shorelines) and fair-weather wave base (FWWB), mid ramp between FWWB and storm-wave base (SWB) and outer ramp below SWB (Burchette & Wright 1992; Flügel 2004). The division of photic zones with respect to water depths is based on the criteria of Hottinger (1997), and includes an upper photic zone with two subzones, approximately from 0 to 40 m and from 40 to 80 m, and a lower photic zone, from 80 to 120/140 m. The stratigraphical distribution of MFTs is given in Figures 2-6,

representative photomicrographs in Plates 1-3 and the depositional models in Figure 7. A detailed description of MFTs is given in Appendix 6 and a short summary in the following section.

### **Late Paleocene microfacies**

Fifteen Late Paleocene MFTs were identified, belonging to six major inner ramp facies belts: supratidal, intertidal, subtidal, lagoonal shoal and restricted and open lagoon. These MFTs are developed in a succession of SBZ3 and SBZ4 biostratigraphic age (Figs 2-4).

*1. Supratidal-intertidal facies belt:* The MFTs of this facies belt are bioclastic wackestones (MFT1, Kotal Pass and Zranda sections, Figs 2, 4, 7, Pl. 1) and fenestrate mudstone-wackestones (MFT2, Kotal Pass section, Figs 2, 7, Pl. 1), that contain a very low-diversity biota (i.e. a few smaller benthic foraminifera, charophyta, and ostracods), and show typical intertidal-supratidal sedimentary features such as anhydrite rosettes, desiccation cracks, plant debris, terrestrial-sourced quartz grains, porostromate cyanobacteria fabrics and fenestrate structures (Wilson 1975; Shinn 1983; Flügel 2004). Deposition in these environments was influenced by impermanent submergence, and was regularly affected by tides or storms. Environmental stress, particularly deviations from normal marine salinity and the effects of persistent mechanical reworking are also reflected in these MFTs.

*2. Subtidal facies belt:* Dasycladacean algal wackestones-packstones (MFT3, Kotal Pass section, Figs 2, 7, Pl. 1) and smaller benthic foraminifer-rich wackestones (MFT4, Kotal Pass and Zranda sections, Figs 2, 4, 7, Pl. 1) were deposited in subtidal environments. In



*Valvulina*, cibicidids and discorbids) respectively, and subordinate smaller rotaliid and miliolid foraminifera. Other biota such as ostracods, molluscs and echinoderms are also present. Infrequent, reworked rotaliid LBFs, plant debris, terrestrial-sourced quartz grains and micritic pellets are present in parts. Restricted, shallow, well lit conditions, with low to moderate-energy water, are indicated based on biotic and sedimentary features (Wilson 1975; Flügel 2004).

3. *Restricted lagoon facies belt*: A restricted lagoon with freshwater influence and low- to moderate-energy water is reflected by the occurrences of smaller rotaliid foraminifer- and charophyta-dominated wackestones (MFT5, Kotal Pass section, Figs 2, 7, Pl. 1) (Murray 1991; Hottinger 1997; Geel 2000; Flügel 2004). These environments were occupied by a low diversity fauna, dominated by smaller robust rotaliid foraminifera (*Rotalia* and *Lockhartia*) and charophyta with subordinate smaller benthic (*Valvulina* and discorbids), agglutinated (*Textularia* and *Nodosaria*) and miliolid foraminifera. The shallowest, restricted parts of the lagoon were dominated by conical agglutinated foraminifer packstones (MFT6, Zranda section, Figs 4, 7, Pl. 1) (Hottinger & Drobne 1980; Hottinger 1983; Vecchio & Hottinger 2007), where hyaline LBFs such as smaller rotaliids, miliolids and orbitoidal foraminifera were infrequent. Smaller benthic and miliolid foraminifera-dominated packstones-grainstones (e.g. MFT7, Zranda section, Figs 4, 7, Pl. 1) were deposited in shallow restricted lagoonal settings in moderate-energy water (Hottinger & Drobne 1980; Hottinger 1997; Geel 2000; Hohenegger 2000; Romero *et al.* 2002; Scheibner *et al.* 2007). In general, these environments were characterized by a low-diversity fauna, low-moderate water energies and high salinities, with infrequent reworking of bioclasts from shallower and deeper environments by currents.

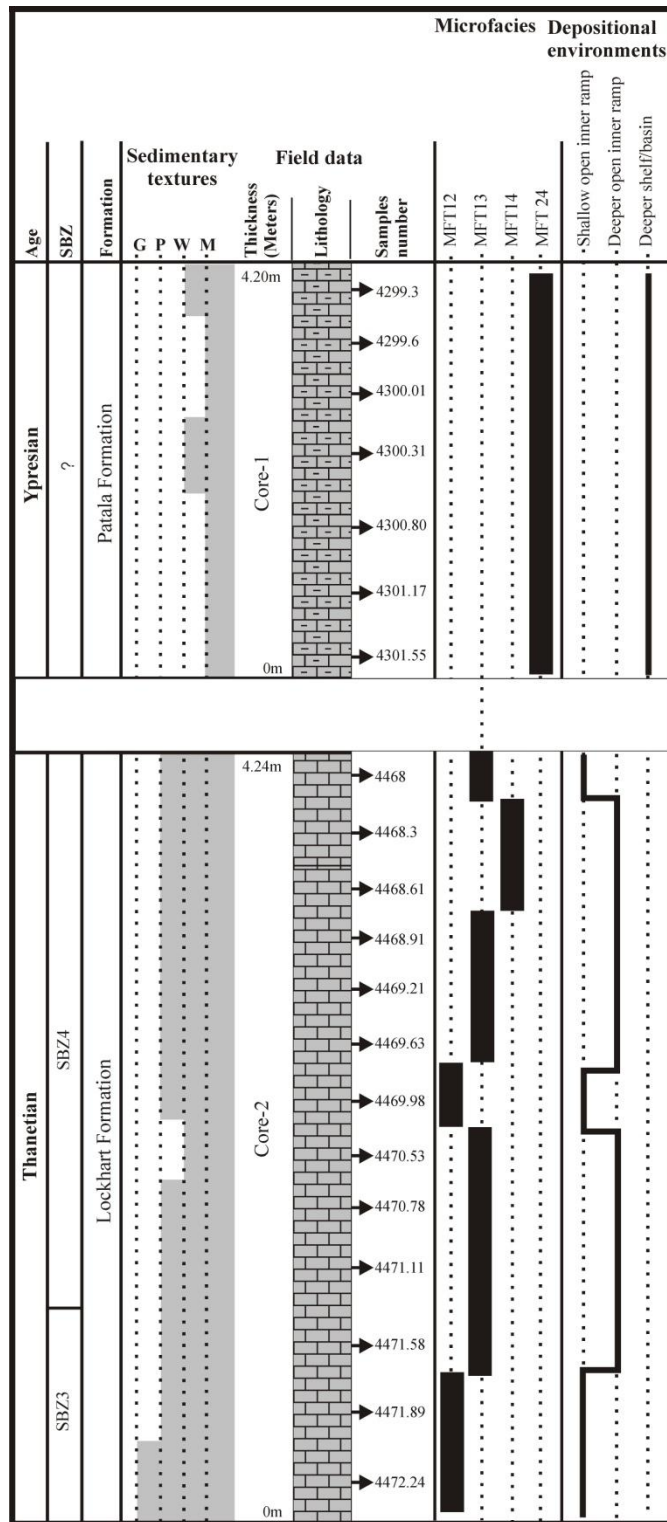


**Figure 3.** Lithological log of the Lockhart and Patala formations in the Shakardara Well-1 showing distribution of microfacies and depositional environments. LBF biozones (SBZ) after Afzal *et al.* (in press).

4. *Protected lagoon facies belt*: Low-energy water, shallow protected lagoonal environments within the upper photic zone were typified by porcelaneous miliolid (*Idalina*, *Quinqueloculina* and *Triloculina*) and glomalveolinid (*Glomalveolina*) foraminifer-dominated packstone-grainstones (MFT8, Zranda section, Figs 4, 7, Pl. 1) and smaller miliolid and rotaliid foraminifer-dominated wackestones-packstones (MFT9, Zranda section, Figs 4, 7, Pl. 2), rich in muddy-silty micritic matrix (Hottinger 1983, 1997; Reiss & Hottinger 1984; Geel 2000). These lagoonal environments were dominated by LBFs, and other biota, for example ostracods, molluscs, coral debris, dasycladacean algae and echinoderms, were insignificant. Other common LBFs are conical agglutinated *Dictyoconus* and *Fallotella*, whereas normal marine LBFs such as smaller *Miscellanea*, *Discocyclina* and orbitoidal forms are rare.

5. *Lagoon shoal facies belt*: In moderate to high-energy lagoonal settings, a benthic foraminiferal shoal formed which dominantly consists of robust forms of *Rotalia* and *Lockhartia* and other smaller benthic foraminifera (mainly *Textularia*, *Valvulina*, *Nodosaria* and various discorbids) (i.e. MFT10, Kotal Pass section, Figs 2, 7, Pl. 2). The biotic (co-occurrences of restricted and open lagoonal foraminifera such as miliolids, rotaliids, *Miscellanea* and *Ranikothalia*) and sedimentary features (high fragmentation, packstone-grainstone textures) suggest a hydrodynamically active setting with persistent reworking by currents/storms (Wilson 1975; Geel 2000; Flügel 2004).

6. *Open lagoon/inner ramp facies belt*: In the shallow, clear-water open lagoon environments, small patch reefs (e.g. MFT11, Kotal Pass section, Figs 2, 7, Pl. 2) developed, consisting of framework laminar-tabular corals and bioclasts (dasycladacean

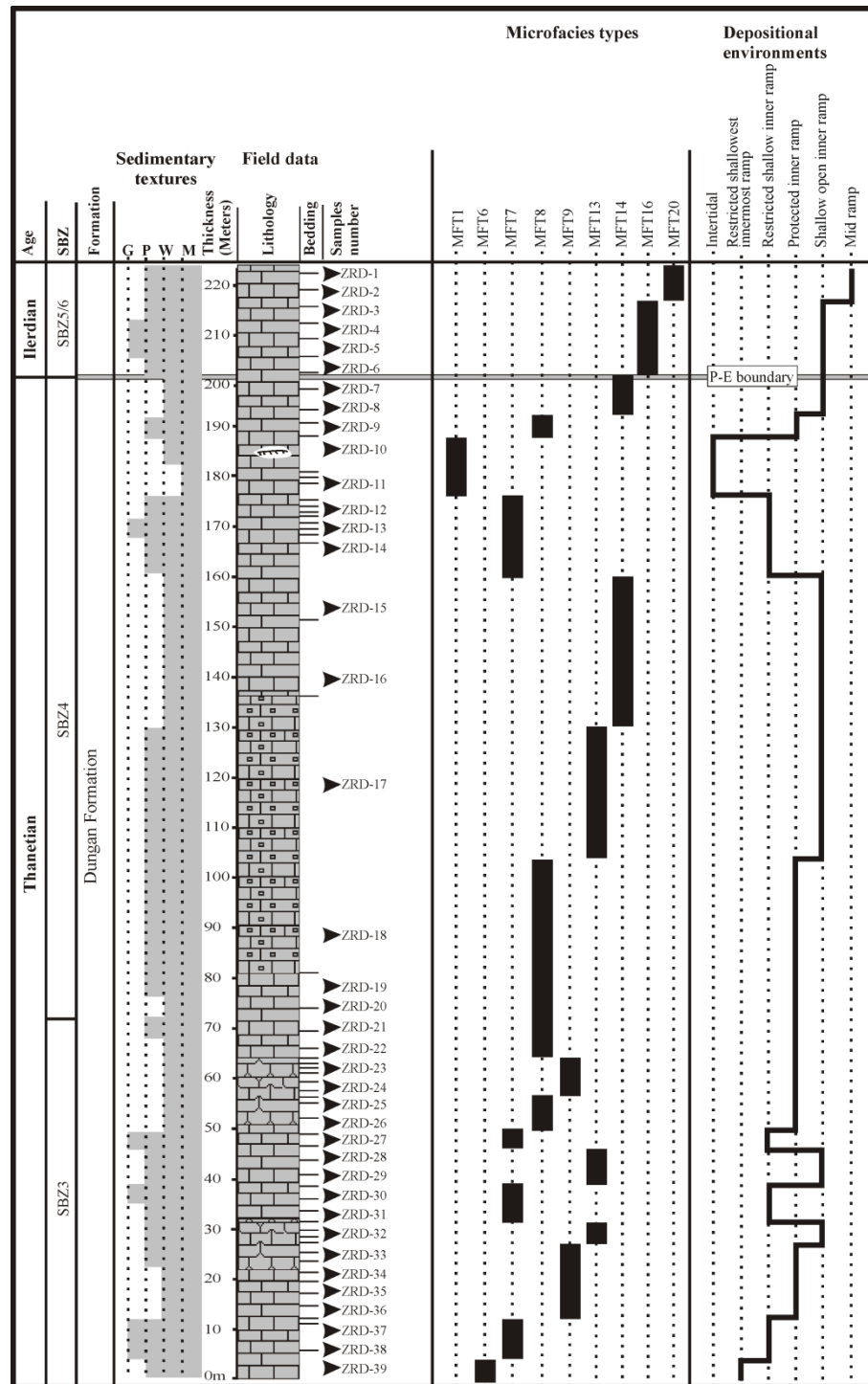


**Figure 4.** Lithological log of the Late Paleocene-earliest Eocene Dungan Formation in the Zranda section showing field data, distribution of microfacies and depositional environments. LBF biozones (SBZ) after Afzal *et al.* (in press).

algae, *Distichoplax biserialis*, bivalves, echinoderms, ostracods, gastropods and few *Rotalia* foraminifera) forming micritic-rich boundstone textures (Fagerstrom 1987;

Baceta *et al.* 2005). An algal or seagrass cover in a low to moderate-energy, well-lit and oxygenated shallow open lagoon can be deduced from the various abundant dasycladacean algae with diverse LBFs (miliolids and smaller rotaliids, orbitoidal forms, *Operculina*, *Assilina*, and *Miscellanea* and *Ranikothalia*) and other biota of ostracods, bivalves and echinoderms (MFT12, Kotal Pass section, Figs 2, 7, Pl. 2) (Wray 1977; Zamagni, *et al.* 2008). In relatively deeper, moderate-energy, low-light open lagoonal/inner ramp environments, a diverse array of LBF-dominated facies were deposited. A depth gradient along inner ramp environments can be identified from the paleoecological assemblages of LBFs: for example, relatively shallower parts were characterized by smaller miscellanid and rotaliid foraminifer-dominated packstones (MFT13, Kotal Pass section and Shakardara Well-1, Figs 3, 7, Pl. 2) (Pignatti 1994; Hottinger 1997; Özgen-Erdem *et al.* 2005); intermediate ramp areas by large miscellanid and rotaliid foraminifer-dominated wackestones (MFT14, Kotal Pass section and Shakardara Well-1, Figs 3, 7, Pl. 2) (Hottinger 1997; Geel 2000; Flügel 2004); and deeper inner ramp settings by larger miscellanid and smaller discocyclinid foraminifer-dominated packstones (MFT15, Shakardara Well-1, Figs 3, 7, Pl. 2) (Pignatti 1994; Hottinger 1997; Geel 2000).

### **Early Eocene microfacies**

The Early Eocene is represented by the Dungan Formation in three outcrop sections (Zranda, Muree Brewery and Hanna Lake; Figs 4-6). Detailed microfacies analysis enables sub-division of this formation into nine different MFTs, indicating four major facies belts (inner, mid and outer ramp, and outer ramp-upper slope). These MFTs are in a succession whose biostratigraphic age is of SBZ5 to SBZ8 biozones (Figs 4-6).

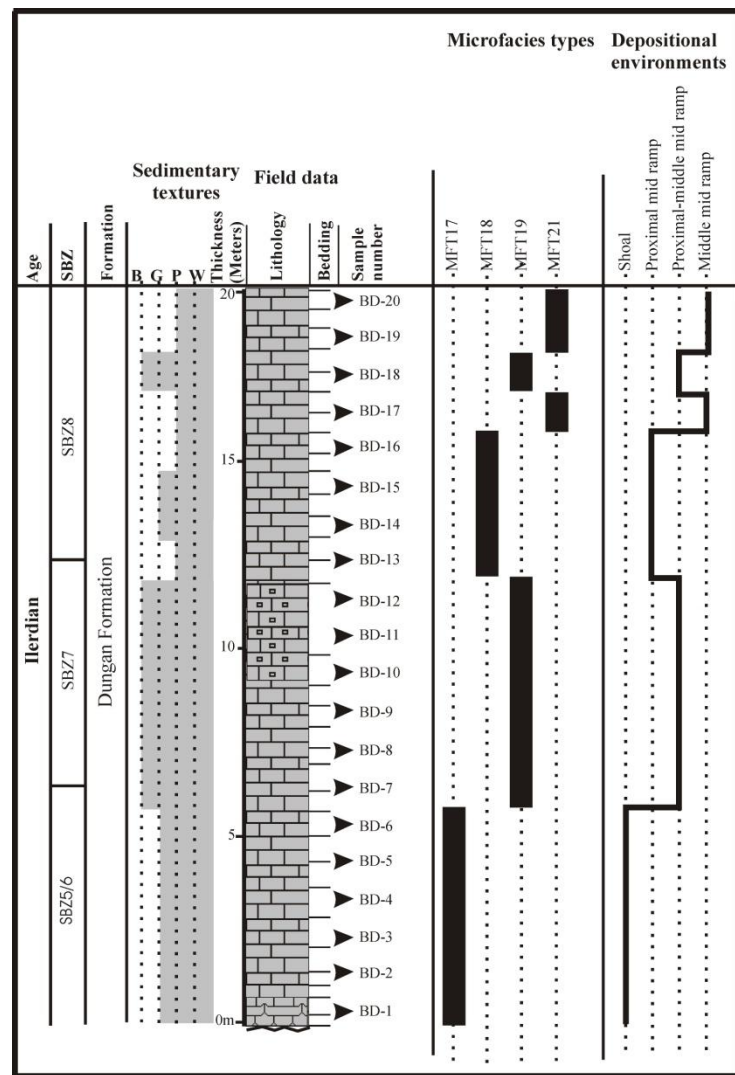


**Figure 5.** Lithological log of the Early Eocene Dungan Formation in the Muree Brewery section showing field data, distribution of microfacies and depositional environments. LBF biozones (SBZ) after Afzal *et al.* (in press).

*1. Inner ramp facies belt:* In general, the earliest Eocene (SBZ5/6 biozones) inner ramp environments were characterized by low-diversity LBF-dominated packstones-grainstones (MFT16, Zranda section, Figs 4, 7, Pl. 2). The dominant LBFs were large megalospheric *Miscellanea* with sub-ordinate large rotaliids (mainly *Lockhartia* and *Rotalia*), whereas other infrequent LBFs are smaller *Alveolina* and megalospheric *Ranikothalia*, *Assilina* and *Discocyclusina*. Fragmented and neomorphosed LBFs (mainly porcelaneous, agglutinated forms and smaller rotaliids) and macrofauna such as

echinoderms and molluscs form additional bioclasts in silty micritic-rich to microsparitic ground matrix. The faunal assemblages, together with sedimentary textures, suggest moderate-energy environments above FWFB (Hottinger 1997; Geel 2000; Flügel 2004). The high-energy setting above FWFB was likely between inner and mid ramp, and was identified from the grainstones (MFT17, Muree Brewery, Figs 5, 7, Pl. 3) rich in fauna of mixed inner (*Miscellanea*, small *Alveolina*, *Glomalveolina*, smaller miliolids and rovaliids) and mid (*Assilina*, *Discocyclusina* and encrusting foraminifera, branched coralline red algae) ramp environments. Diverse faunal assemblages of varied palaeoecological modes together with a high degree of fragmentation, abrasion and reworking likely resulted from constant current actions, mixing fauna of varied environments into a shoal (Hottinger 1997; Geel 2000; Flügel 2004).

2. *Proximal-middle mid ramp facies belt*: The proximal mid ramp was characterized by moderately-sorted, coarse-grained packstones-grainstones (MFT18, Muree Brewery section, Figs 5, 7, Pl. 3) that consist largely of discoidal to lenticular *Discocyclusina* and *Orbitoclypeus* and thick-walled small *Nummulites* with subordinate coralline algae (unattached and fragmented forms) (Loucks *et al.* 1998; Bassi 2005; Beavington-Penney *et al.* 2005; Barattolo *et al.* 2007). Laterally, in the proximal-middle part of the mid ramp, encrusting foraminifer-dominated boundstones with bioclastic wackestones (MFT19, Muree Brewery and Hanna Lake sections, Figs 5-7, Pl. 3) and large thick flattened *Operculina* and *Discocyclusina* foraminifer-dominated packstones (MFT20, Zranda section, Figs 4, 7, Pl. 3) were deposited (Loucks *et al.* 1998; Geel 2000; Langer & Hottinger 2000; Renema & Troelstra 2001; Ćosović *et al.* 2004; Zamagni *et al.* 2008. Orthopragminid (mainly *Discocyclusina* and *Orbitoclypeus*) and coralline red algal-

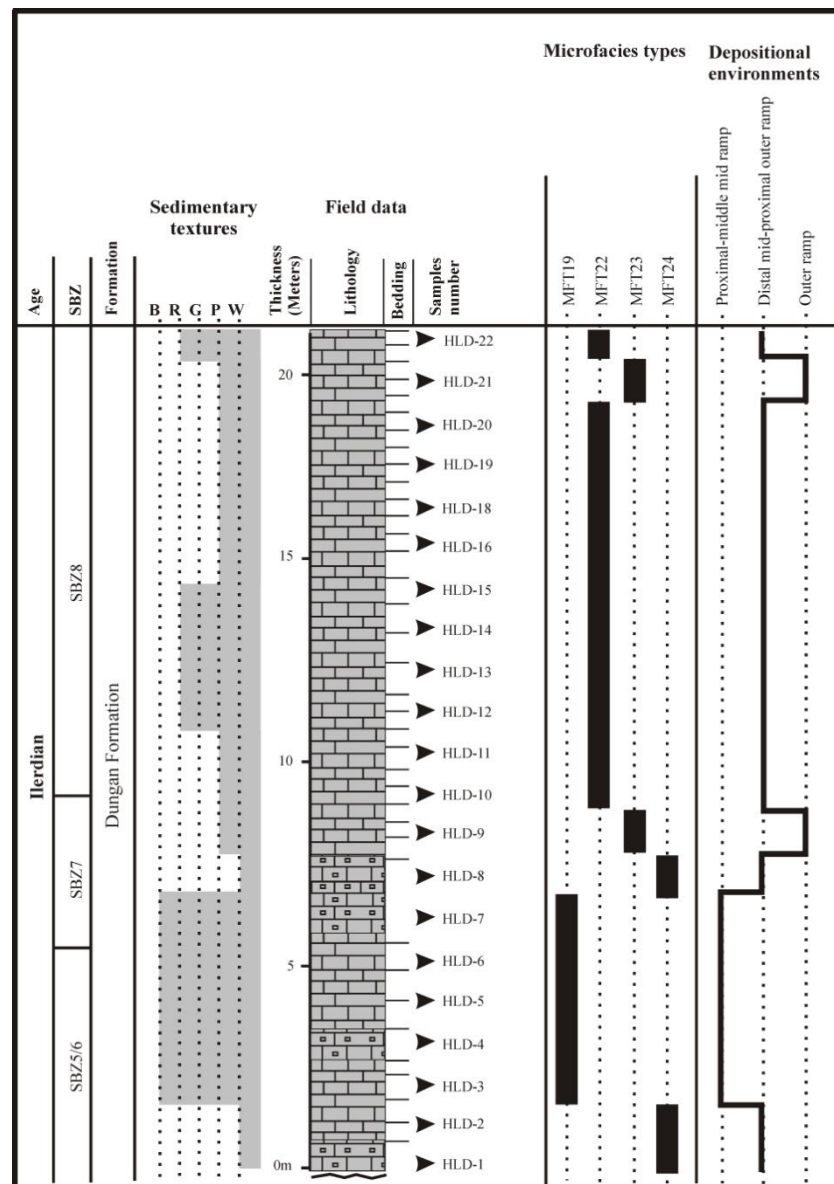


**Figure 6.** Lithological log of the Early Eocene Dungan Formation in the Hanna Lake section showing field data, distribution of microfacies and depositional environments. LBF biozones (SBZ) after Afzal *et al.* (in press).

dominated packstones (MFT21, Hanna Lake section, Figs 6-7, Pl. 3) were characteristic of the deeper, low-energy and low-light environments of the mid ramp (Hottinger 1997; Geel 2000; Nebelsick *et al.* 2001; Rasser & Nebelsick 2003; Beavington-Penney & Racey 2004). Other important biotas of these environments were coralline algae, echinoderms, bryozoans and the LBFs *Assilina* and *Actinocyclus*. The common occurrence of broken, poorly-preserved and abraded LBFs typical of a shallow inner

ramp (e.g. rotaliids, *Miscellanea*, *Ranikothalia*, small *Discocyclina*, Hottinger 1997; Geel 2000) indicates re-deposition in deeper waters by storm/current actions.

3. *Distal mid-outer ramp facies belt*: Orthopragminid (well-preserved large flattened *Discocyclina*, *Orbitoclypeus* and *Actinocyclina*) rudstones and packstones (MFT22, Hanna Lake section, Figs 6-7, Pl. 3) indicate lower photic zone conditions with low-energy water suggesting distal mid, to outer ramp settings (Yordanova & Hohenegger 2002; Beavington-Penney & Racey 2004; Ćosović *et al.* 2004; Bassi 2005). Below SWB, the outer ramp environment was characterized by orthopragminids (large flattened and thin-walled *Discocyclina*, *Actinocyclina* and *Orbitoclypeus*) and planktonic foraminifer-dominated packstones (MFT23, Hanna Lake section, Figs 6-7, Pl. 3), rich in fine micritic matrix with bioclastic debris (mainly fragmented LBFs, echinoderms, coralline algae and bryozoans) (Reiss & Hottinger 1984; Hohenegger & Yordanova 2001; Ćosović *et al.* 2004). Smaller benthic foraminifera (discorbids, cibicidids etc.) are common forms in these settings.

4. *Outer ramp to basin facies belt*: In the Hanna Lake section, planktonic foraminifer-dominated wackestone (MFT24, Figs 6-7) with common fragments of coralline red algae, echinoderms, rare bivalves and bryozoans and a few re-sedimented *Miscellanea* and *Discocyclina* suggest distal outer ramp environments (Geel 2000; Flügel 2004). However, in the Shakardara Well-1, wackestones (MFT24, Fig 3, 7, Pl. 3) are characterized by abundant planktonic foraminifera (mainly *Acarinina*, *Morozovella* and *Globigerina*) together with common occurrences of glauconite grains and bioclasts of thin-walled bivalves, indicating deeper depositional environments, likely deep outer ramp to upper slope (Geel 2000; Flügel 2004).

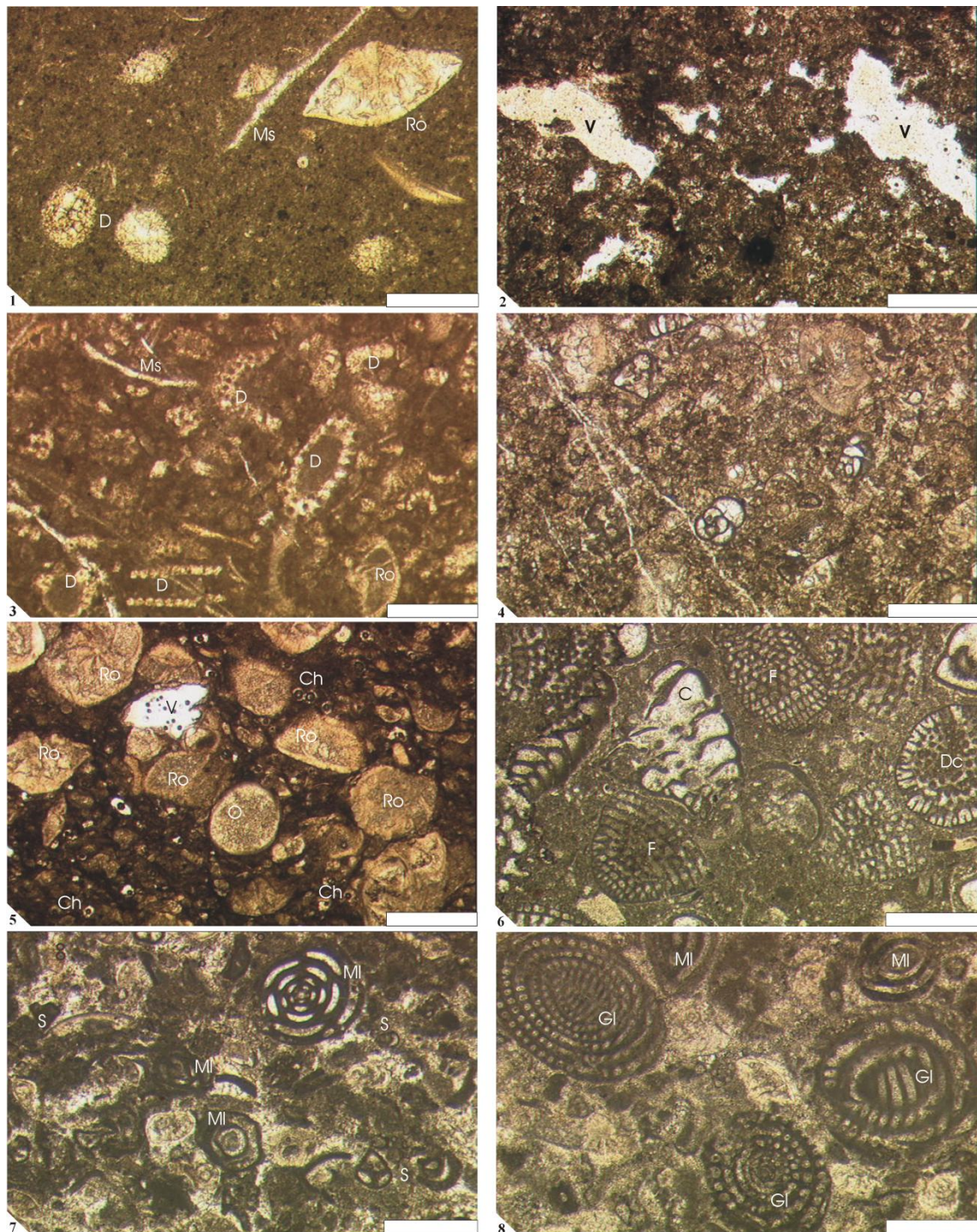


**Plate 1.** Late Paleocene microfacies and palaeoecological assemblages. 1. Bioclastic wackestone (MFT1), showing reworked *Rotalia* (Ro) LBFs, re-crystallized molluscs (Ms) and dasycladacean algal (D) fragments, sample ZRD11. 2. Fenestrate mudstone-wackestone (MFT 2), common vug features (V) surrounded by fine micritic matrix, sample KL13. 3. Dasycladacean algae wackstone-packstone (MFT3), defined by abundant dasycladacean algae (D), common mollusc fragments (Ms) and few *Rotalia* (Ro) foraminifera, sample KL39. 4. Smaller benthic foraminifer wackestone (MFT4), note different types of smaller benthic foraminifera, sample KL41. 5. Smaller rotaliid foraminifer and charophyta wackestone (MFT5), common *Rotalia* (Ro) LBFs associated with charophyta (Ch), note fenestrate vug (V), sample KL35. 6. Conical agglutinated

foraminifer packstone (MFT6), characterized by the abundance of *Coskinolina* (C), *Dictyoconus* (Dc) and *Fallotella* (F) LBFs, sample ZRD39. 7. Smaller benthic and miliolid foraminifer packstone-grainstone (MFT7), showing association of miliolid (MI) and smaller benthic (S) foraminifera, sample ZRD27. 8. Miliolid (MI) and glomalveolinid (GI) wackestone-packstone (MFT8), sample ZRD18. Scale for all images is 900µm.

### **Facies changes, biotic changes and palaeoenvironmental evolution**

The lateral and vertical distribution of facies and associated biota in the Late Paleocene-Early Eocene shallow-water carbonates of the Indus Basin can be explained by a combination of depth and nutrient gradients with varying controlling factors (local and regional). In the following section the palaeoecological and palaeoenvironmental significance of biotic assemblages in the reconstruction of carbonate ramp environments through the Late Paleocene-Early Eocene is assessed.

### **Late Paleocene**

The stratigraphically lower part of the Late Paleocene (lower SBZ3 Biozone) is characterized by shallow intertidal, subtidal and inner lagoonal restricted environments. Intertidal (MFT2) to restricted subtidal (MFT3, MFT4) environments are recorded in the Kotal Pass section, and show a very low-diversity biota (infrequent smaller benthic foraminifera, dasycladacean algae, molluscs and ostracods) on a muddy/micritic substrate, indicating low energy (Figs 2, 7). Environmental conditions included deviations from normal marine salinity, high-light, and constant reworking by storms (i.e. input from the nearby terrestrial environment and open subtidal/lagoonal environments) as reflected by low-diversity fauna, peloids, terrestrial-sourced quartz grains, plant debris and fenestrate and cyanobacteria fabrics (He *et al.* 2002; Flügel 2004). The restricted shallow inner carbonate ramp environments (MFT6, MFT7) as represented in the Zranda section were dominated by meso-oligotrophic LBF

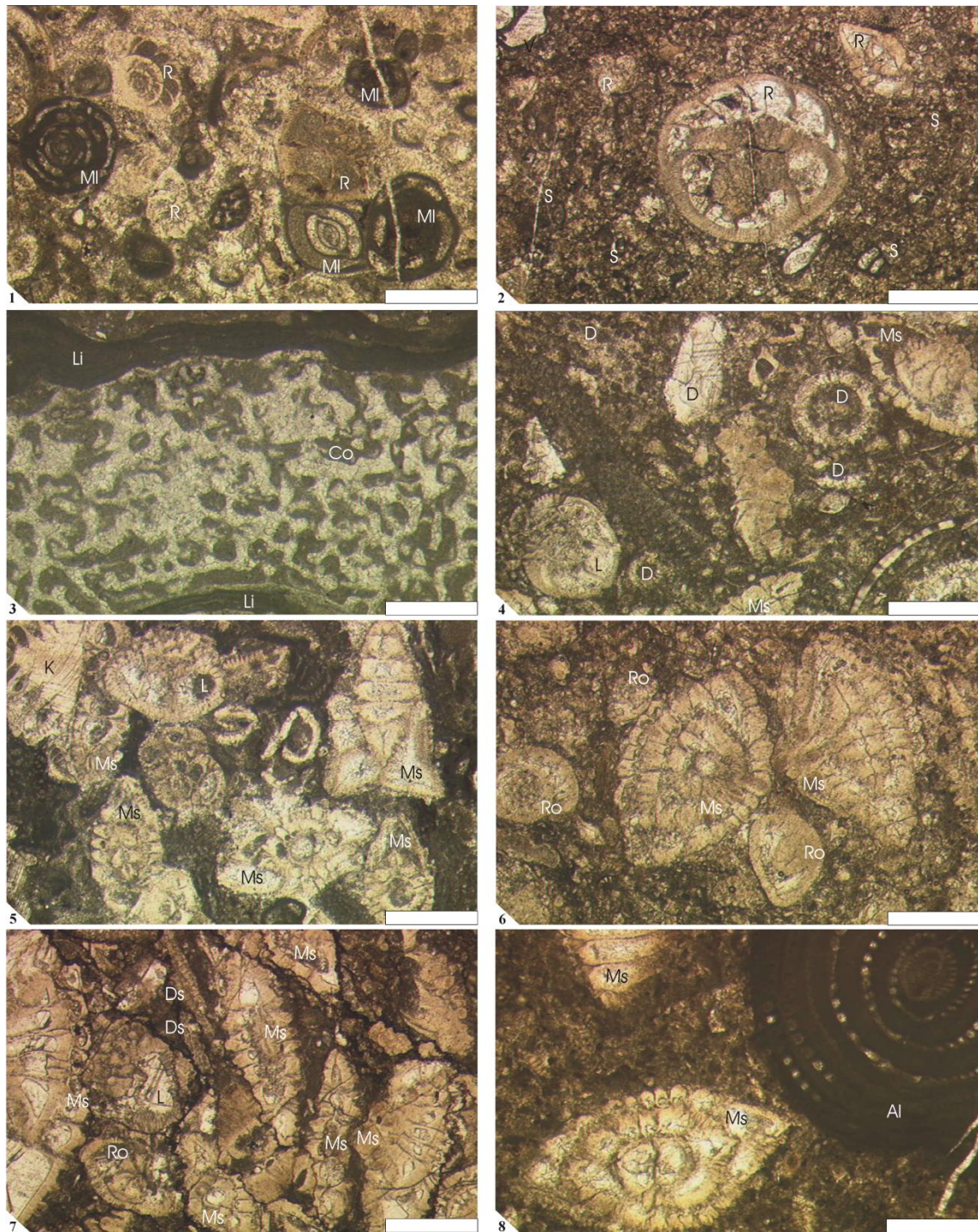


**Plate 2.** Late Paleocene-Early Eocene microfacies and palaeoecological associations. 1. Smaller miliolid and rotaliid foraminifer wackestone-packstone (MFT9), defined by association of miliolid (MI), rotaliid (R) benthic foraminifera, sample ZRD38. 2. Rotaliid (R) and smaller benthic (S) foraminifer packstone-grainstone (MFT10), sample KL42. 3. Coral, bioclastic boundstone (MFT11), note encrustation of framework coral (Co) by *Lithothamnion* coralline algae (Li), sample KL45. 4. Dasycladacean algae and smaller rotaliid foraminifer packstone-grainstone (MFT12), showing association of dasycladacean algae (D), *Lockhartia* (L) and smaller *Miscellanea* (Ms), sample 4471.89. 5. Smaller miscellanid and rotaliid foraminifer packstone (MFT 13),

assemblage of smaller *Miscellanea* (Ms), *Lockhartia* (L) and *Kathina* (K), sample ZRD28. 6. Large miscellanid and rotaliid foraminifer wackstone (MFT14), characterized by association of large megalospheric *Miscellanea* (Ms) and rotaliid (R), sample ZRD16. 7. Larger miscellanid and smaller discocyclinid foraminifer packstone (MFT15), defined by association of microspheric *Miscellanea* (Ms) and smaller *Discocyclina* (Ds), other forms commonly present include *Rotalia* (Ro) and *Lockhartia* (L), sample 4468.3. 8. Large miscellanid foraminifer packstone-grainstone (MFT16), showing large megalospheric *Miscellanea* (Ms) and *Alveolina* (Al), sample ZRD6. Scale for all images is 900µm.

assemblages including conical agglutinated, miliolid, glomalveolinid and various smaller benthic foraminifera with infrequent smaller rotaliid foraminifera, echinoderms, molluscs and ostracods (Figs 4, 7). Thus, environments with unfavourable living conditions for many normal-marine benthic organisms (especially LBFs) are likely due to increased salinity, irradiation and increased nutrient levels and/or decreased oxygen as indicated by the palaeoecological assemblages (e.g. Hallock & Glenn 1986; Hottinger 1997; Geel 2000; Romero *et al.* 2002; Barattolo *et al.* 2007; Zamagni *et al.* 2008).

Open lagoon/inner ramp environments are recognized in the stratigraphically higher part of the succession (equivalent to the upper part of the SBZ3 Biozone), suggesting a deepening marine trend, giving way to comparatively diverse facies belts and benthic communities (Fig. 7). Shallow, high-energy water regimes formed a foraminiferal shoal/bar (MFT10) that consisted of different smaller benthic and rotaliid foraminifera, whereas lower energy parts of the open lagoon favoured small patch reefs (MFT11) dominated by frame-building corals with subordinate calcareous algae (coralline and dasycladacean), echinoderms and molluscs (Figs 2, 7). These coral and foraminiferal shoal bodies probably acted as barriers, producing protected to partly restricted environments, promoting meso-oligotrophic palaeoecological assemblages dominated by glomalveolinids, miliolids and smaller benthic and rotaliid foraminifera

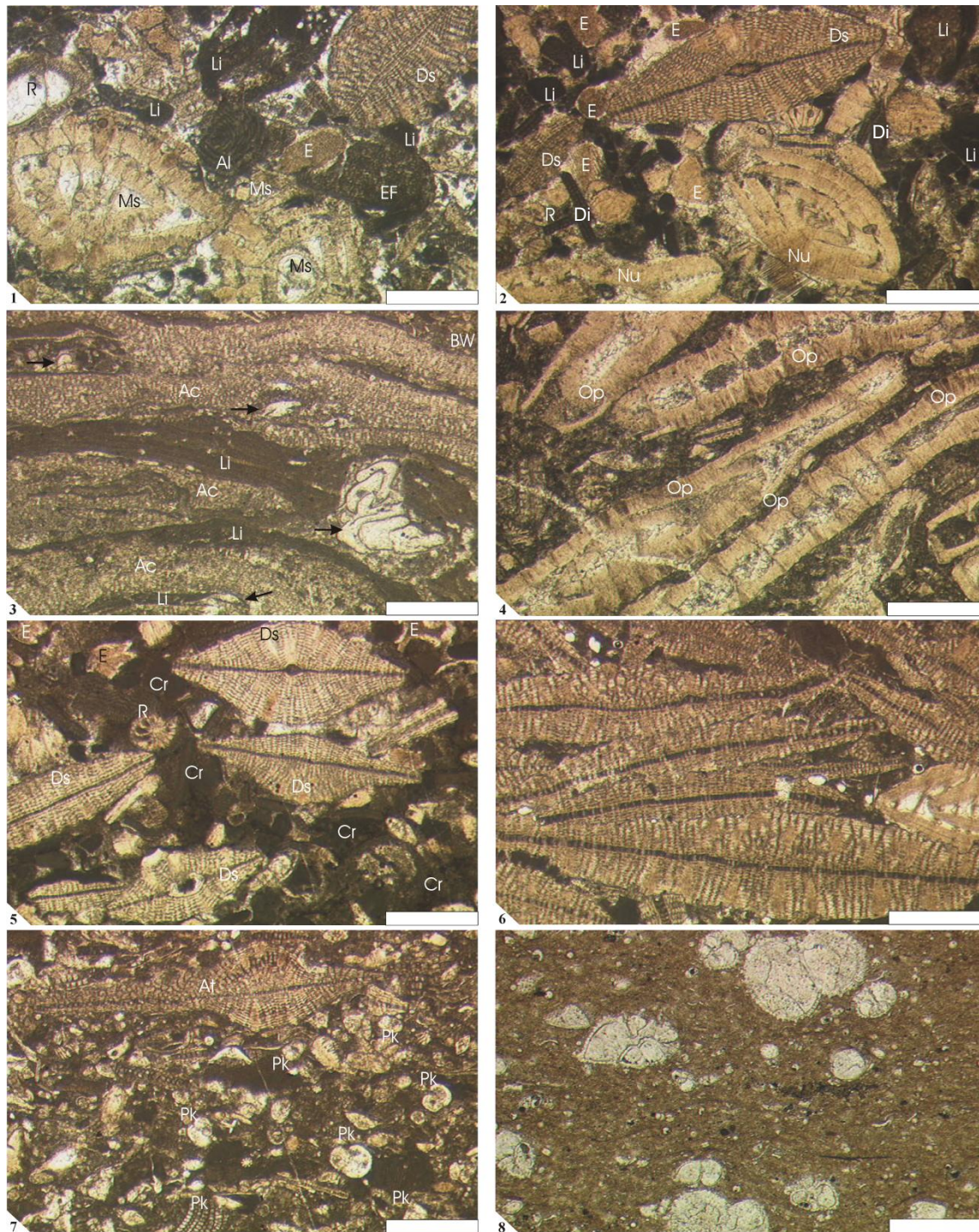


**Plate 3.** Early Eocene microfacies and palaeoecological assemblages. 1. Large miscellanid, smaller miliolid and rotaliid foraminifer grainstone (MFT17), showing large megalospheric *Miscellanea* (Ms), rotaliid (R) and discoidal *Discocyclina* (Ds) with fragmented *Alveolina* (Al), echinoderms, *Lithothamnion* coralline algae (Li) and encrusting foraminifera (EF), sample BD5. 2. Orthopragminid and *Nummulites* foraminifer packstone to grainstone (MFT18), characterized by *Discocyclina* (Ds) and *Nummulites* (Nu) associated with fragmented *Lithothamnion* (Li) and *Distichoplax biserialis* (Di) coralline algae and echinoderms (E), sample BD15. 3. Encrusting foraminifer boundstone with bioclastic wackestone (MFT19), note the alternating crusts

of thick acervulinids (Ac) encrusting foraminifera and thin *Lithothamnion* (Li) with embedded few other forms of encrusting foraminifera (arrowed) and bioclastic wackestone (BW), sample BD11. 4. Large *Operculina* and *Discocyclina* foraminifer packstone (MFT20), showing large flattened *Operculina* (Op), sample ZRD2. 5. Orthopragminid foraminifer and coralline red algal packstone (MFT21), composed of orthopragminid (shown here as *Discocyclina*-Ds) and fragmental coralline algae (Cr) with few rotaliid (R) and echinoderm fragments (E), sample BD19. 6. Orthopragminid foraminifer rudstone and packstone (MFT22), note orthopragminid tests in rock-building quantity forming packstone, dominated by large flattened tests, sample HLD20. 7. Orthopragminid and planktonic foraminifer packstone (MFT23), note common planktonic foraminifera (Pk), *Actinocyclina* (At) and abundant fragmented orthopragminid and coralline algae in fine micritic matrix, sample HLD21. 8. Planktonic foraminifer wackestone (MFT24), showing planktonic foraminifera in fine micritic matrix, sample 4299.3. Scale for figures 1-7 is 900µm and 300µm for figure 8.

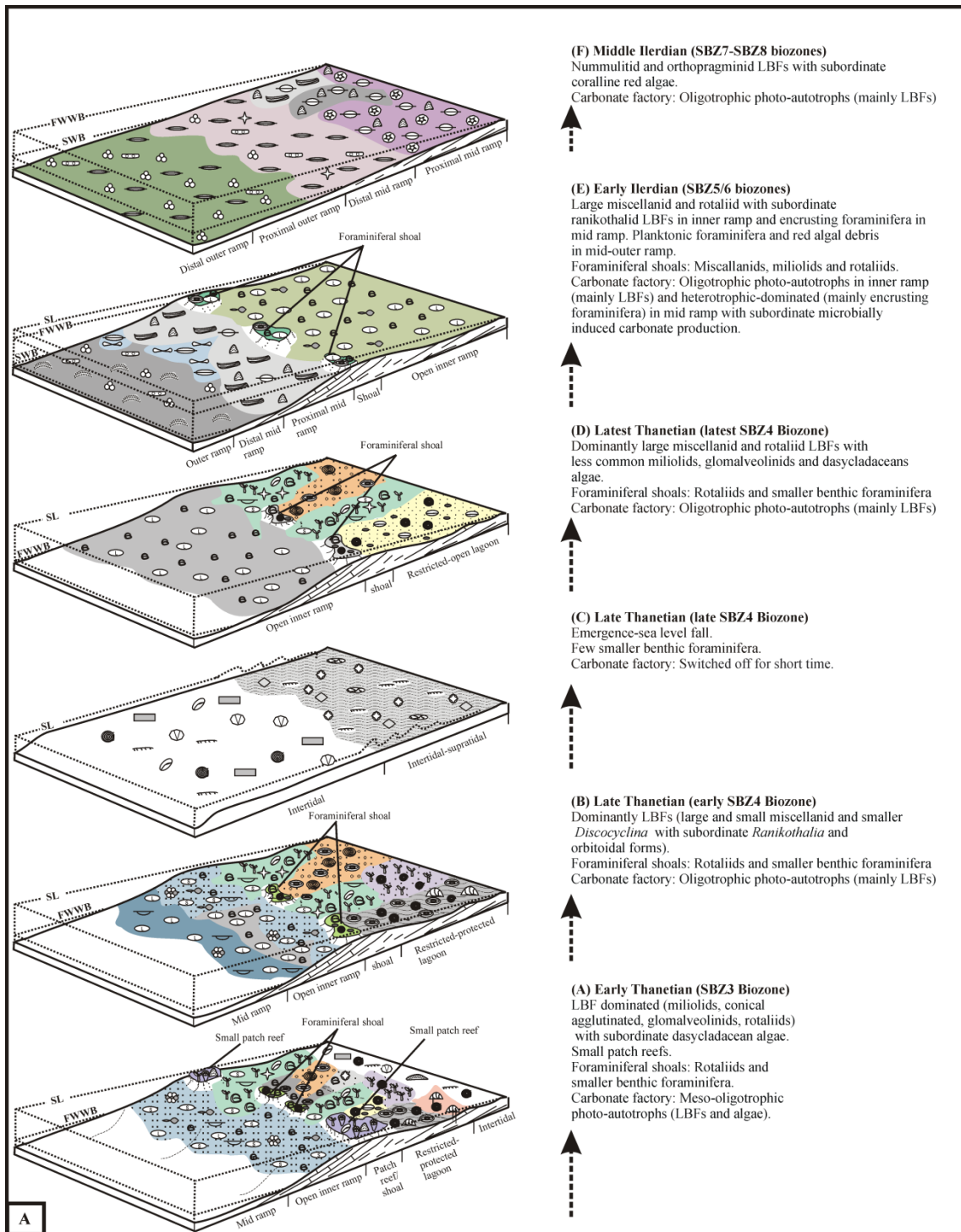
(e.g. MFT5, MFT7, MFT8, MFT9, Figs 2, 4, 7). A seagrass cover/ algal meadow within the open lagoon/backreef setting can be deduced from the high abundance and diversity of dasycladacean algae and benthic foraminifera (smaller rotaliids, miliolids, miscellanids, and other foraminifera) in association with ostracods, bivalves and echinoderms in MFT12. In relatively deeper, moderate-energy oligotrophic (low-light and nutrient deficient) lagoon/backreef settings, assemblages of smaller miscellanid and rotaliid foraminifera (e.g. MFT13) with very rare or no algae and macro-biota (e.g. molluscs, echinoderms) flourished (Fig. 7).

The latest Paleocene succession (SBZ4 Biozone) shows significant biotic and sedimentary changes, and is dominated by LBFs. Some palaeoecological assemblages of the earlier part of the succession (e.g. MFT12, MFT13) persisted, where they alternated with communities dominated by large miscellanid and smaller discocyclinid LBFs (MFT15), indicative of backreef/open lagoonal environments (Fig. 7). This time was characterized by diverse assemblages, with LBFs including *Operculina*, *Assilina*, *Ranikothalia* and orbitoidal forms particularly successful, associated with echinoderms, molluscs, brachiopods and bryozoans (e.g. MFT15). These diverse LBFs are indicative of stable, nutrient-deficient, low-light environmental conditions (Hottinger 1997; Geel

2000). No corals or coralline algae were recorded (Fig. 7). A prominent decrease in palaeo-water-depth is interpreted up-succession (at a level equivalent to the upper SBZ4 Biozone), when open ramp facies (MFT13, MFT14, MFT15) gradually regressed into restricted subtidal/lagoonal (MFT6, MFT7), and eventually intertidal-supratidal facies (MFT1), exposing the ramp in parts of the basin (e.g. desiccation cracks and evaporite formation in MFT1 of the Kotal Pass section, Fig. 7). Later, open lagoonal/backreef environments re-established (Fig. 7). However, a prominent decline in biotic diversity and abundance is recorded, large megalospheric miscellanids and robust rotaliids (e.g. MFT14) began to dominate inner ramp environments and occurrences of miliolids, glomalveolinids and calcareous algae (dasycladaceans) become more prevalent. This suggests a shift from oligotrophic environments of the lower SBZ4 to weakly oligotrophic-mesotrophic ramp conditions during the uppermost SBZ4 Biozone (Hallock *et al.* 1991; Hottinger 1997; Hallock 2000; Geel 2000). Sea level drop in the Indus Basin sections during the upper SBZ4 Biozone is consistent with data from the Atlantic and Tethys regions (e.g. Steurbaut *et al.* 2003; Pujalte & Schmitz 2006; Schmitz & Pujalte 2007; Egger *et al.* 2009), suggesting a eustatic effect.

### **Early Eocene**

The earliest Eocene (SBZ5/6 biozones) inner carbonate ramp represented in the Zranda section was dominated by low-diversity faunal assemblages of large megalospheric miscellanids and rotaliids with infrequent occurrences of other LBFs such as *Alveolina* and megalospheric *Ranikothalia*, *Assilina* and *Discocyclusina* (e.g. MFT16, Figs 4, 7, Pl. 2). This suggests stressed environmental conditions, likely shallow turbulent water, with high-light and increased nutrients and/or temperatures as indicated by the scarcity of oligotrophic communities (i.e. non-diverse LBFs, no corals etc.), though some taxa



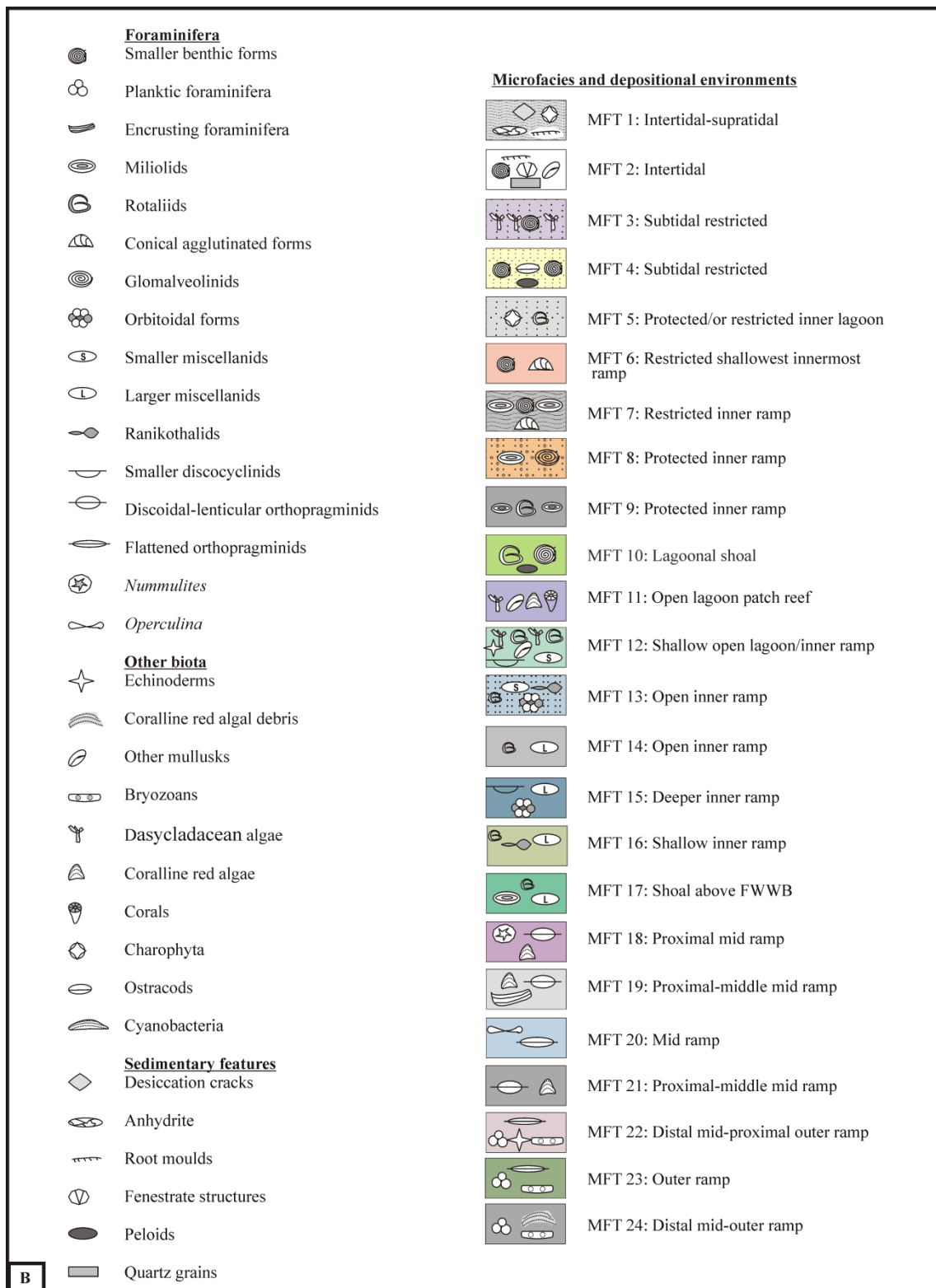


**Figure 7A-B.** Palaeoenvironmental evolution of major facies and biota of the Indus Basin through the Late Paleocene-Early Eocene. Not to scale. SL, sea level; FWWB, fair weather wave base; SWB, storm wave base.

could tolerate these conditions (e.g. large *Miscellanea* and rotaliids). Megalospheric-dominated LBF communities can be a result of apogamic schizogony (repetitive asexual reproduction resulting in successive generations of megalospheric schizonts, Dettmering *et al.* 1998), possibly reflecting stressed environmental conditions (e.g. increases in food supply, or rapid population increase in marginal habitats, after mortality events or during colonization of new areas) (Lipps 1982; Beavington-Penney & Racey 2004).

A high-energy foraminiferal shoal/bar (MFT17) developed close to FWWB at the inner carbonate ramp margin, mixing paleoecological assemblages of varied environments (e.g. inner ramp smaller miliolids, rotaliids and miscellanid foraminifera and mid ramp coralline algae, echinoderms, large-sized deeper LBFs etc.) (Figs 6-7). The environment was hydrodynamically active under constant current action (as indicated by grainstone textures with very little micritic mud) and demonstrates meso-oligotrophic conditions (as shown by the abundance of miliolids and smaller benthic foraminifera, Hallock & Glenn 1986; Geel 2000). Laterally, mid ramp environments below FWWB were dominated by bioconstructing communities such as encrusting foraminifera with subordinate coralline algae (MFT19) associated with a few large LBFs (*Discocyclina*, *Operculina* and *Assilina*) and grazers and filter-feeders (e.g. echinoderms, molluscs etc; see Fig. 7). During the Early Eocene, encrusting foraminifera built monospecific ‘reefs’ in carbonate environments of the Tethyan realm as a consequence of coral decline (Plaziat & Perrin 1992). The widespread occurrences of encrusting foraminifera and coralline red algae indicate increased nutrients in the water column (Hottinger 1983; Perrin 1992; Mutti & Hallock 2003). The presence of grazers and filter-feeding biota and scarcity of LBFs support this interpretation, though some LBFs probably could tolerate eutrophication, as indicated by the modern *Assilina ammonoides* (Langer & Hottinger, 2000). Fine-grained muddy facies with common

planktonic foraminifera dominated distal mid to outer ramp environments, indicative of low-water energy, with high-nutrient levels and conditions of very low-/or no light (as indicated by the scarcity/absence of photo-dependent fauna such as LBFs and algae) (Fig. 7). Occasional sea-bottom storms could be responsible for the transportation and redistribution of nutrients into deeper waters (e.g. Bassi 2005), which prevented oligotrophic communities (such as LBFs) from occupying these niches. The oligotrophic (low-nutrient and low-light) conditions were achieved in the stratigraphically higher part of the succession (SBZ5/6 biozones; e.g. MFT20 in the Zranda section), where large, flattened symbiont-bearing oligotrophic LBFs (*Discocyclina* and *Operculina*) thrived in mid ramp environments (Fig. 7).

During the SBZ7-SBZ8 biozones, palaeoenvironmental conditions were optimal for oligotrophic communities. For example, typical oligotrophic orthopragminid- and *Nummulites*-dominated assemblages (MFT18) together with orthopragminids and coralline red algal communities (MFT21) flourished in mid ramp environments below FWWB (Fig. 7). Deeper mid to outer ramp environments were occupied by highly oligotrophic benthic communities including larger, flattened and thin-walled orthopragminid LBF assemblages (MFT22, Fig. 7). Orthopragminid LBFs in these environments were dominated by microspheric forms (B-form, sexually produced). Large shell sizes together with microspheric generations in LBFs indicate a longer lifetime, produced by sexual reproduction in ecologically optimal and stable environments (Hottinger 2000). Therefore, palaeoenvironmental conditions were highly stable for the growth of these oligotrophic communities (Reiss & Hottinger 1984; Hottinger 1997; Langer & Hottinger 2000; Yordanova & Hohenegger 2002; Čosović *et al.* 2004). Orthopragminids and planktonic foraminifera (MFT23) and planktonic foraminifera (MFT24) were the dominant palaeoecological communities in outer ramp

and upper slope environments respectively, suggesting environmental settings below SWB (Hallock *et al.* 1991; Geel 2000, Fig. 7).

## **Discussion**

### **Comparison of the shallow marine benthic biota of the Indus Basin with other Tethyan carbonate successions**

Palaeoecological trends for the Indus Basin carbonate ramp can be sub-divided temporally into the following four stages, each characterized by varied biotic and facies patterns. In addition, a pan-Tethyan comparison of facies and biotic assemblages is presented (Fig. 8).

Stage 1. The early Thanetian (SBZ3 Biozone) in the Indus Basin corresponds with Tethyan Platform stage I (i.e. Scheibner & Speijer 2008a and references therein). All these studies indicated that solitary and colonial corals together with coralline algae and miliolid and rotaliid foraminifera dominated carbonate environments in low to mid-latitudes (Fig. 8). However, in the Indus Basin, India and Tibet, LBFs were the dominant biota with coralgal communities (corals and coralline algae) subordinate (Scheibner & Speijer 2008a, 2008b, Fig. 8).

Stage 2. The Indus Basin late Thanetian (SBZ4 Biozone) is equivalent to Tethyan platform stage II (Scheibner & Speijer 2008a). LBF dominated facies in the Indus Basin are comparable with other low-latitude Tethyan sites such as NE India (Jauhri & Agarwal 2001; Jauhri *et al.* 2006; Tewari *et al.* 2010), Tibet and the Galala area of Egypt (Scheibner & Speijer 2008a) (Fig. 8). However, mixed coralgal reef/corals-coral debris and LBF facies were sparse in low-mid latitude carbonate environments (e.g. NW India, NW Somalia, Oman, Egypt, Libya, Adriatic Platform, Scheibner & Speijer 2008a; Zamagni *et al.* 2009, Fig. 8). Coralgal reefs were still the

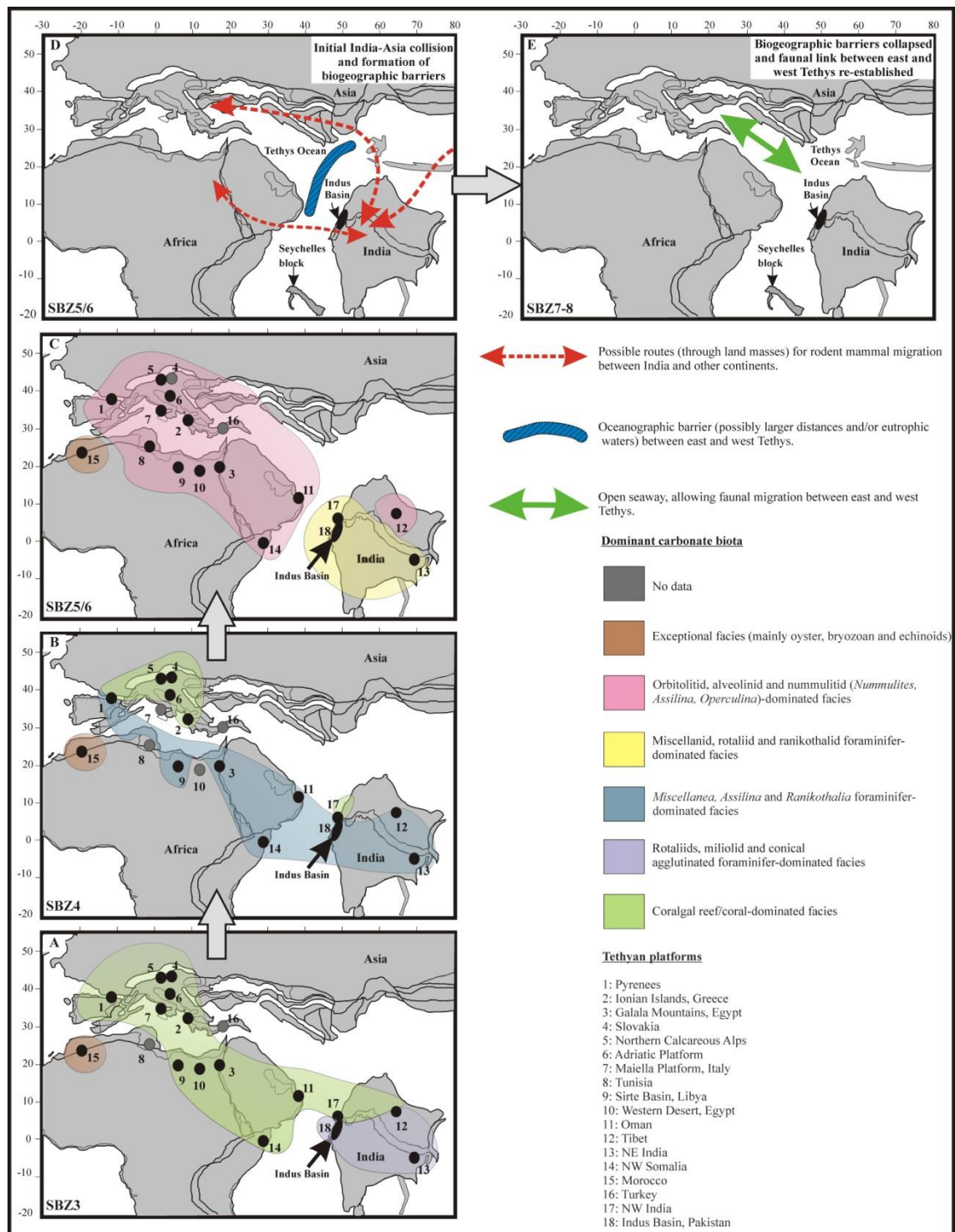


**Figure 8.** Late Paleocene-Early Eocene evolution of Tethyan shallow marine carbonate biota (modified from Scheibner & Speijer 2008a). Palaeogeographic reconstruction for Figures A-E is based on Hay *et al.* (1999) with additional data from Smith *et al.* (1994), Gaetani & Garzanti (1991) and Gingerich *et al.* (1997) for Figures D-E. SBZ, shallow benthic biozones.

main carbonate biota in the mid-latitudes (e.g. N. Calcareous Alps, W. Carpathians, Maiella, Ionian Islands, see Scheibner *et al.* 2008a for summary, Fig. 8).

Stage 3. The early Ilerdian (SBZ5/6 biozones) of the Indus Basin coincides with the base of the earliest Eocene and Tethyan platform stage III (Scheibner & Speijer 2008a). In the Tethyan realm, this period started with widespread LBF dominance of shallow marine carbonate environments and a major decline in coral-reef communities in low-mid latitudes, with carbonate environments nearly barren of, or only with scarce, corals (Scheibner & Speijer 2008a, 2008b, Fig. 8). During this time, the rapid radiation of *Alveolina*, *Nummulites* and orbitolitids in inner-middle platforms replaced typical latest Paleocene LBF assemblages (e.g. *Miscellanea*, *Ranikothalia*) (larger foraminifera turnover, LFT of Orue-Etxebarria *et al.* 2001), whereas *Operculina*, *Assilina* and *Discocyclina* dominated middle-outer platform environments (Scheibner *et al.* 2005; Scheibner & Speijer 2008a). However, in contrast, the Indus Basin, like carbonate successions in India (Jauhri & Agarwal 2001; Jauhri *et al.* 2006; Scheibner & Speijer 2008; Tewari *et al.* 2010), showed unusual faunal compositions, where typical latest Paleocene LBFs (e.g. *Miscellanea*, *Ranikothalia*) still dominated, while Orbitolitids and *Alveolina* were rare and *Nummulites* absent (Fig. 8).

Stage 4. The biotic communities of the Indus Basin during the middle Ilerdian time (SBZ7-SBZ8 biozones) are comparable with other Early Eocene Tethyan carbonate biota of this age (e.g. Racey 1995; Hottinger 1997, 2001; Geel, 2000; Nebelsick *et al.* 2005; Adabi *et al.* 2008).

### **Environmental changes and evolution of carbonate factories in the Indus Basin**

According to Schlager (2003), the space and processes that lead to carbonate production are known as a carbonate factory. Schlager (2000, 2003) described three main benthic

carbonate factories: (1) the tropical factory, (2) the cool-water factory and (3) the mud-mound factory. The pathways and products of marine carbonate production in these factories are very diverse and are grouped into three basic categories: abiotic (e.g. ooids), biotically induced (microbial, cyanobacterial mats) and biotically controlled (photo-autotrophic or heterotrophic organisms) (Schlager 2000, 2003).

The Indus Basin was located in a tropical setting (approximately 5°N) throughout the Late Paleocene-Early Eocene and therefore a hot, humid tropical climate would be expected, promoting a tropical carbonate factory (Fig. 8). The tropical factory operates in warm, sunlit waters high in oxygen (constant equilibration with the atmosphere) and low in nutrients because of intense competition between occupying organisms (Schlager 2003). The distribution of shallow marine carbonate factories in time and space are characterized by local and global environmental changes (i.e. nutrients, temperatures, atmospheric CO<sub>2</sub>, sea water chemistry etc.; see Pomar & Hallock 2008). The mechanisms of environmental changes and transitions between carbonate factories in the Indus Basin through the Late Paleocene to Early Eocene are evaluated below.

During the Paleocene SBZ3 Biozone, the major carbonate factory operated in shallow upper photic zone environments (restricted to open lagoons), characterized by mesotrophic LBFs (miliolids, glomalveolinids, smaller rotaliids) with subordinate dasycladacean algae (Fig. 7). Elevated temperatures, high-salinities, high nutrients and high-light conditions were controlling factors for carbonate production in these environments as indicated by palaeoecological assemblages (Murray 1991; Hallock 2000; Aguirre & Riding 2005). Heterotrophic organisms such as molluscs and echinoderms were less important whilst conical agglutinated LBFs (MFT6) dominated the shallowest inner ramp settings. The micritic/mud-dominated MFTs (e.g. MFT1 and

MFT2), with common fenestrate and cyanobacterial fabrics in tidal environments, probably suggest abiotic or biotically induced carbonate precipitation (Yates & Robbins 1999; Thompson 2001). Nutrifaction, high intensities of sunlight and significant fluctuations in temperature and salinity in shallow waters can be assumed for carbonate production by cyanobacteria (e.g. He *et al.* 2002; Hallock 2005). However, the coralgall-reef communities which were the main carbonate producers during the SBZ3 Biozone in other low-mid latitude Tethyan carbonate environments (see Scheibner & Speijer 2008, Fig. 8) did not succeed in the Indus Basin and are poorly represented by small patch-reefs (Fig. 7). The reason for this might be local paleoecological conditions (i.e. elevated nutrients and temperatures and abnormal salinities) and/or a latitudinal temperature gradient (Sewall *et al.* 2004).

A shift from mesotrophic- to oligotrophic-dominated photo-autotrophic carbonate factory production occurred during the uppermost SBZ3-SBZ4 biozones, when low-light dependant LBFs (miscellanids, rotaliids, orbitoidal forms, *Ranikothalia*, *Discocyclusina*, MFT14, MFT15) became the dominant carbonate producers in open inner ramp environments (Fig. 7). Other photo-autotrophic carbonate producers such as calcareous algae were significantly reduced, and coral-reefs were absent; biotically/abiotic induced carbonate production was also absent. The shallowing and continental influx/brackish water incursions related to short term sea level drop in late SBZ4 Biozone times switched off photo-autotrophic-dominated carbonate factory production for a short time (Figs 2, 4, 7). Later, in latest SBZ4 times, photo-autotrophic-carbonate production resumed and was dominated by LBFs, which continued into the earliest Eocene (Fig. 2, 4, 7).

The earliest Eocene (SBZ5/6 biozones) was represented by a benthic foraminiferal factory (miscellanids, rotaliids, miliolids, MFT16 and MFT17) in the

inner ramp and shoals. However, on the shoals, heterotrophic (echinoderms and molluscs) and biotically induced (i.e. as micrite coating of bioclasts) carbonate precipitation was also recorded. In the mid-ramp, a heterotrophic-dominated (mainly encrusting foraminifera, MFT19) factory operated, whilst the contribution of photo-autotrophic organisms (LBFs and red algae) was limited (Figs 5-7). In deeper, mid and outer ramp settings, carbonate production was dominated by fine-grained micrite (e.g. MFT24) with skeletal carbonates rarely deposited (Figs 6-7). Heterotroph-dominated carbonate production is typical for cool-water, higher latitude factories (Schlager 2003). Tropical-to-cool-water transitions occur in shallow tropical waters where upwelling brings cool, nutrient-rich waters to the surface, hampering the function of the tropical factory because its photo-autotrophic communities (especially LBFs) are adapted to low-nutrient environments (Hallock 1987; James 1997). In modern oceans, the tropical factory is largely driven by skeletal production; however, microbially induced precipitation of carbonate (fine-grained micrite) can co-occur (e.g. Tahiti and Great Barrier Reef, Reitner *et al.* 1995). The typical environment for microbially induced precipitation of carbonate in the Phanerozoic is dysphotic or aphotic, nutrient-rich waters low in oxygen but not anoxic (Neuweiler *et al.* 1999; Stanton *et al.* 2000).

The tropical to cool-water-microbially induced carbonate factory transition in the Indus Basin coincides with a global temperature rise (4-5°C in low-latitudes) and eutrophic conditions (continental influx by increased precipitation) caused by the Paleocene-Eocene Thermal Maximum (PETM) at the P-E boundary. This likely hindered oligotrophs in shallow ramp environments (Scheibner *et al.* 2005). Like hermatypic corals, perforate larger benthic foraminifera contain different photosynthetic symbionts that restrict them to the photic zone (Falkowski *et al.* 1990; Lee & Anderson 1991). Excessive nutrients may have reduced water clarity by creating plankton blooms

which can hamper oligotroph growth (both corals and larger benthic foraminifera; see Hallock 2001). Probably as a consequence, the photo-autotrophic communities (LBFs and coralgall biota) dramatically reduced in abundance in certain ramp niches (e.g. mid ramp) whilst more opportunist assemblages (e.g. encrusting foraminifera) were flourished.

By the SBZ7-SBZ8 biozones, stable oligotrophic conditions on the carbonate ramp were re-established, which promoted photo-autotrophic carbonate production (Figs 5-6). In the mid-outer ramp (up to the lowest photic zone), LBFs such as nummulitids and orthopragminids dominated the skeletal factory with subordinate coralline red algae (Figs 5-6). Heterotrophic skeletal production (e.g. echinoderms, molluscs etc.) was insignificant.

### **Biotic and environmental changes through the Late Paleocene-Early Eocene**

The long-term warming, high CO<sub>2</sub> levels and/or low Mg/Ca ratios in the early Paleogene may have decreased aragonite saturation in surface waters, which favoured calcitic organisms such as LBFs over aragonitic corals (Stanley & Hardie 1998; Kleypas *et al.* 1999; Pearson *et al.* 2001; Hallock 2005). Present day coral growth is high under reduced nutrients and increased water clarity; excessive nutrients and elevated temperatures can hinder coral growth, whereas LBFs unlike corals are much less susceptible to increased temperatures and mesotrophic conditions (Hallock 2000, 2005; Wilson & Vecsei 2005; Pomar & Hallock 2008).

During the Late Paleocene (SBZ3 Biozone), coral reefs were still important carbonate contributors in Tethyan shallow marine environments (especially in west Tethys, Scheibner & Speijer 2008a, 2008b, Fig. 8). Later, during the latest Paleocene (SBZ4 Biozone), LBFs experienced an increase in generic diversity (global maturity

community maturation cycle phase 2 of Hottinger 2001, 2006) giving rise to k-strategists (adapted to low-light and low nutrients, with a long life span, e.g. *Miscellanea* and *Ranikothalia*). These gradually supplanted corals from low to mid latitudes in response to continued long-term warming of the early Paleogene (platform stage II, Scheibner & Speijer 2008a). In addition to the trend of long-term warming, the latest Paleocene (SBZ4 Biozone) in Tethys appears to have been characterized by increased continental run-off (Speijer & Wagner 2002). This enhanced productivity in surface waters (Egger *et al.* 2003) and caused intermittent blooms of the heterotrophic dinoflagellate *Apectodinium*, that began several thousand years before the PETM CIE (Sluijs *et al.* 2007). The rise of k-strategy in acarininid and morozovellid planktonic foraminifera in the open oceans (Hallock *et al.* 1991; Boersma *et al.* 1998; Petrizzo 2007) during the Late Paleocene is thought to reflect a transition from a warm, relatively well-mixed Early Paleocene ocean to a warmer, poorly mixed global ocean during the Late Paleocene to Middle Eocene (Boersma *et al.* 1998). Consequently, this short-term eutrophication of ocean waters may also have played an important role in the rise of k-strategist LBFs in the Tethyan realm.

In contrast to west Tethys, corals are scarce/or nearly absent (particularly during the SBZ4 Biozone) in the Indus Basin and other low-latitude east Tethys (India and Tibet) sites (see Scheibner & Speijer 2008a), where carbonate environments were dominated by LBFs throughout the Late Paleocene (SBZ3-SBZ4 biozones) (Figs 2-8). In the early Paleogene sea-surface temperature (SST) model of Sewall *et al.* (2004), the east Tethys was characterized by higher temperatures than west Tethys. If this model provides realistic SST estimates, then LBF-dominated ramps in east Tethys were likely influenced by the latitudinal SST gradient; however, local paleoecological conditions

(e.g. high-nutrients, abnormal salinities and elevated temperatures etc.) may also have been significant.

The earliest Eocene coincides with a short-term climatic perturbation (PETM CIE) (Hallock *et al.* 1991; Zachos *et al.* 2003) which caused simultaneous and severe environmental changes including global warming related to emission of greenhouse gases into the atmosphere, eutrophication of tropical seawater by increased chemical weathering and runoff on land, and a general rise in oceanic carbonate compensation depth (Zachos *et al.* 2001; Thomas *et al.* 2002; Schmitz & Pujalte 2007). These environmental perturbations had a major impact on shallow marine carbonate environments, leading to a decline in aragonitic coral reefs and the rise of calcitic larger foraminifers (Orue-Etxebarria *et al.* 2001; Pujalte *et al.* 2009; Scheibner *et al.* 2005; Scheibner & Speijer 2008a, Fig. 8). A major faunal turnover in LBFs was recorded during this time, with typical latest Paleocene extreme k-strategist LBFs (e.g. *Miscellanea*, *Ranikothalia*) replaced by Eocene orbitolitids, *Alveolina* and *Nummulites* (LFT of Orue-Etxebarria *et al.* 2001) in Tethyan carbonate environments (Scheibner *et al.* 2005; Scheibner & Speijer 2008a). Consequently, larger benthic foraminifera in conjunction with red algae remained the main carbonate producers in shallow-marine settings in the Tethyan realm whereas aragonitic coral reefs did not recover until the end of the Middle Eocene (Perrin 2002; Scheibner & Speijer 2008).

Nevertheless, significant biotic and facies changes in the Indus Basin were recorded during the earliest Eocene (SBZ5/6 biozones), such as a reduction in diversity and abundance of some well-adapted k-strategist LBFs (e.g. orbitoidal forms, *Discocyclina*), but unlike west Tethys, *Nummulites* are absent and Orbitolitids and *Alveolina* are rare (Fig. 8). The inner ramp carbonate environments of the Indus Basin were still dominated by large megalospheric miscellanid-rotaliids with subordinate

ranikothalid LBF assemblages (e.g. MFT15), and smaller rotaliid and miliolid-dominated shoal (MFT16) areas. In general, LBFs were scarce and only dominated carbonate production in shallow inner ramp environments, while mid-outer ramp settings were dominated by a heterotrophic (encrusting foraminifera, MFT19) skeletal factory and microbially induced carbonate (e.g. MFT24) precipitation. Such biotic and facies development in the Indus Basin are remarkably different from the west Tethys (Fig. 8), and suggest the influence of other geological processes, in addition to the PETM.

The stratigraphical (e.g. shallowing in marine deposition, unconformities and continental sedimentation, Afzal *et al.* 2009) and paleontological (e.g. presence of Asian land mammals and freshwater gastropods on the Indian sub-continent, Clyde *et al.* 2003; Sahni 2006; Köhler & Glaubrecht 2007) evidence suggests that the Indo-Pakistan plate was subject to subduction and orogenic processes at about the P-E boundary (Najman 2006; Copley *et al.* 2010). Most recently, Afzal *et al.* (in press) suggest that the unusual and low-diversity LBF assemblage (i.e. *Nummulites* absent and *Alveolina* rare) of the Indus Basin during earliest Eocene time may have been influenced by the early collision of India with Asia. They argued that India-Asia collision possibly generated biogeographic barriers (geographic and oceanographic) between east (India and Pakistan) and west (Europe, North Africa) Tethys, preventing migration of certain LBFs (e.g. species of *Nummulites* and *Alveolina*), between these regions, resulting in reduced LBF diversity in the Indus Basin and enhancing the survival of existing lineages (e.g. *Miscellanea* and *Ranikothalia*) in East Tethys (Fig. 8). They also postulated that the LFT was not an instantaneous and synchronous event across the whole of the Tethyan region caused only by the PETM, but was a gradual process primarily driven by long-term evolutionary patterns (Palaeogene GCM cycle) of LBFs

(Hottinger 2001) and other factors, like local palaeoecological conditions, eco-space competition between fauna, and local tectonics. Collision between India and Asia may have played a major role in altering drainage patterns of major rivers (Brookfield 1998), ocean water chemistry and currents (Raymo *et al.* 1988; Richter *et al.* 1992), and regional climate (Raymo & Ruddiman 1992).

The abundance of megalospheric (product of repetitive asexual reproduction) *Miscellanea Ranikothalia* and *Discocyclina* in the Indus Basin during the earliest Eocene is indicative of stressed environmental conditions (Lipps 1982; Beavington-Penney & Racey 2004) such as reduced light, high-nutrients and shallower depths. MFT analysis suggests that these LBFs occupied shallower environments (i.e. MFT15) during the earliest Eocene than in the Late Paleocene (Pignatti 1994; Hottinger 1997). LBFs are considered k-strategists (Hottinger 1983, 1998) and are therefore, the first to disappear during a breakdown or interruption of stable oligotrophic conditions (Hottinger 1983) and the PETM represents just such an interruption (Scheibner & Speijer 2008a). However, the community structure of symbiont-bearing benthic foraminifera (k-strategists) in euphotic zone depths is a function of nutrient flux, and species can respond to some loss of water transparency (a function of plankton densities and fluvial influx of dissolved organic matter and suspended sediments) by compressing their depth ranges (Hallock 1987, 1988). On the other hand, if water transparency is reduced too much, most will probably disappear, especially if less specialised species are present (Hallock 1987).

Thus, I postulate that a large megalospheric generation in LBF assemblages and their occurrences in shallower depths in the Indus Basin was an adaptative strategy in response to the PETM and possibly India-Asia collision related environmental stresses (e.g. increased nutrients from land run-off and higher sea temperatures). These

increased temperatures and nutrients in surface waters may have increased plankton densities resulting in reduction in the depth of the photic zone (Zingonea & Enevoldsen 2000; Mutti & Hallock 2003). Therefore, some LBFs (e.g. *Miscellanea* and *Ranikothalia* in inner ramp environments) responded to reduced light conditions by partially compressing their depth range to shallower parts of the inner ramp. Furthermore, the absence of *Nummulites* and rarity of orbitolitids and *Alveolina* facilitated the survival of these LBFs by reducing eco-space competition in inner ramp environments (Afzal *et al.* in press). However, environmental conditions in mid-outer ramp settings were beyond the adaptative scope of LBFs due to increased nutrients and very low-light conditions, but were suitable for heterotrophic (encrusting foraminifera, MFT19) organisms. Similar biotic patterns can be found in Mesozoic warming events, for example during the Triassic/Jurassic and Pliensbachian/Toarcian events, coral-rich photozoan assemblages were replaced by heterozoan assemblages due to eutrophication of shallow water environments (Cobianchi & Picotti 2001; Lathuiliere & Marchal 2009). The Aptian Oceanic Anoxic Event 1 was characterized by a heterotrophic mode (mainly agglutinated orbitolinid foraminifera) of carbonate production replacing the photozoan (corals and rudistids) carbonate producers (Wissler *et al.* 2003; Fölmi & Gainon 2008). Similarly, during the Cenomanian/Turonian Oceanic Anoxic Event 2 (i.e. marked by thermal instability), most extreme oligotrophic larger foraminifera become extinct, allowing the survival of those capable of tolerating mesotrophic conditions (Parente *et al.* 2008).

From all the evidence, it is here concluded that India-Asia tectonics at the P-E boundary possibly created more severe environmental conditions (increased continental run off) superimposed on PETM related stresses, and thus caused a regional biotic reaction different from those of tectonically stable and solely climatically driven

environmental changes (i.e. PETM) in west Tethys carbonate environments. It is envisaged that, by preventing migration of certain LBFs (typical for inner-mid ramp environments) between east and west Tethys, the India-Asia collision facilitated the rise of opportunistic forms (e.g. encrusting foraminifera) in mid-ramp environments on the one hand, but also decreased competition for LBFs in inner ramp settings on the other.

The Early Eocene (SBZ7-SBZ8 biozones) was comparatively more environmentally stable (i.e. post PETM, Zachos *et al.* 2001) and was characterized by foraminiferan size-increase and further diversification of successful LBF lineages in the Tethyan realm (Hottinger 2001). In the Indus Basin, heterotrophic organisms were gradually replaced by highly oligotrophic/stable biota (mainly LBFs) and these began to occupy different niches of the mid-outer ramp. Later (SBZ8 Biozone), LBFs became the dominant carbonate producers, comparable to west Tethys, showing an increase in diversity and prominent morphological changes (such as size increase), with new lineages appearing such as the first *Nummulites* and *Actinocyclus*.

## Conclusions

The study of Late Paleocene-Early Eocene carbonate successions and associated biota of the Indus Basin has concluded that:

1. A total of 24 carbonate microfacies types are identified, suggesting a ramp dominated depositional system. Carbonate production was dominated by non-framework building, light-dependent biota such as LBFs and calcareous algae.

2. During the early Thanetian, meso-oligotrophic biotic communities (LBFs and dasycladacean algae) occupied ramp environments in the Indus Basin. This is different from the coralgall dominated west Tethys carbonate successions and may have been

related to the latitudinal SST gradient from west to east Tethys and local palaeoecological conditions (e.g. high-nutrients, abnormal salinities and temperatures).

3. The late Thanetian (SBZ4 Biozone) ramp environments in the Indus Basin were dominated by oligotrophic LBFs (mainly miscellanids-ranikothalids-rotaliids), comparable to the west and other low-mid latitude Tethyan biotas. This may indicate a regional biotic reaction to the early Paleogene warming.

4. The ramp environments in the Indus Basin during the earliest Eocene (SBZ5/6 biozones) were characterized by unusual low diversity assemblages (typical Paleocene *Miscellanea*, *Ranikothalia*, rotaliids and encrusting foraminifera), while typical west Tethyan elements were absent (e.g. *Nummulites*) or scarce (i.e. orbitolitids and *Alveolina*). It is postulated that the superimposition of India-Asia collision and PETM may have generated this biotic difference by creating biogeographical barriers (preventing faunal exchange) between east and west Tethys and extreme environmental conditions (increased nutrients and temperatures).

5. Later, during the Early Eocene (SBZ7-SBZ8 biozones), environmental conditions became stable and highly oligotrophic and cosmopolitan LBF communities (i.e. orthopragminids and nummulitids) appeared in the Indus Basin ramp environments.

---

## Chapter 6

---

Stable isotope ( $\delta^{18}\text{O}$  and  $\delta^{13}\text{C}$ ) analysis of latest Paleocene-Early Eocene carbonates, Indus Basin, Pakistan

---

## **Chapter 6: Stable isotope ( $\delta^{18}\text{O}$ and $\delta^{13}\text{C}$ ) analysis of latest Paleocene-Early Eocene carbonates, Indus Basin, Pakistan**

### **Abstract**

The stable carbon and oxygen isotope signature of selected latest Paleocene-Early Eocene carbonates of the Indus Basin of Pakistan are assessed in order to determine diagenetic and primary signals. By detailed petrographic analysis four carbonate preservational types are identified: 1) well preserved carbonates showing no or minimal diagenetic alteration; 2) carbonates altered by marine phreatic diagenesis; 3) carbonates altered by meteoric diagenesis; and 4) carbonates affected by burial diagenesis. A diagenetic history is reconstructed with the following three stages: 1) well preserved carbonates which likely retain some primary seawater isotope signal have  $\delta^{18}\text{O}$  values between  $-4.12\text{‰}$  and  $-4.25\text{‰}$  and  $\delta^{13}\text{C}$  between  $+2.10\text{‰}$  and  $+2.16\text{‰}$ ; 2) carbonates with marine phreatic diagenesis show negative  $\delta^{18}\text{O}$  ratios ( $-4.40\text{‰}$  to  $-5.00\text{‰}$ ); and 3) meteoric and burial diagenesis show  $\delta^{18}\text{O}$  with values more negative than  $-5.00\text{‰}$ .  $\delta^{13}\text{C}$  values were less affected by diagenesis and show little variability compared to  $\delta^{18}\text{O}$ . Temperature reconstructions using the  $\delta^{18}\text{O}$  values ( $-4.12\text{‰}$  and  $-4.25\text{‰}$ ) of the best preserved carbonates suggest seawater temperatures of between  $32^{\circ}\text{C}$  to  $33.5^{\circ}\text{C}$  for the earliest Eocene of the Indus Basin. Positive  $\delta^{13}\text{C}$  values for these carbonates are consistent with microfacies data that indicate increased productivity in the east Tethys.

### **Introduction**

The Late Paleocene-Early Eocene succession of the Lower Indus Basin in the Sulaiman Range is characterized by shallow marine carbonates of the Dungan Formation (Fig. 1).

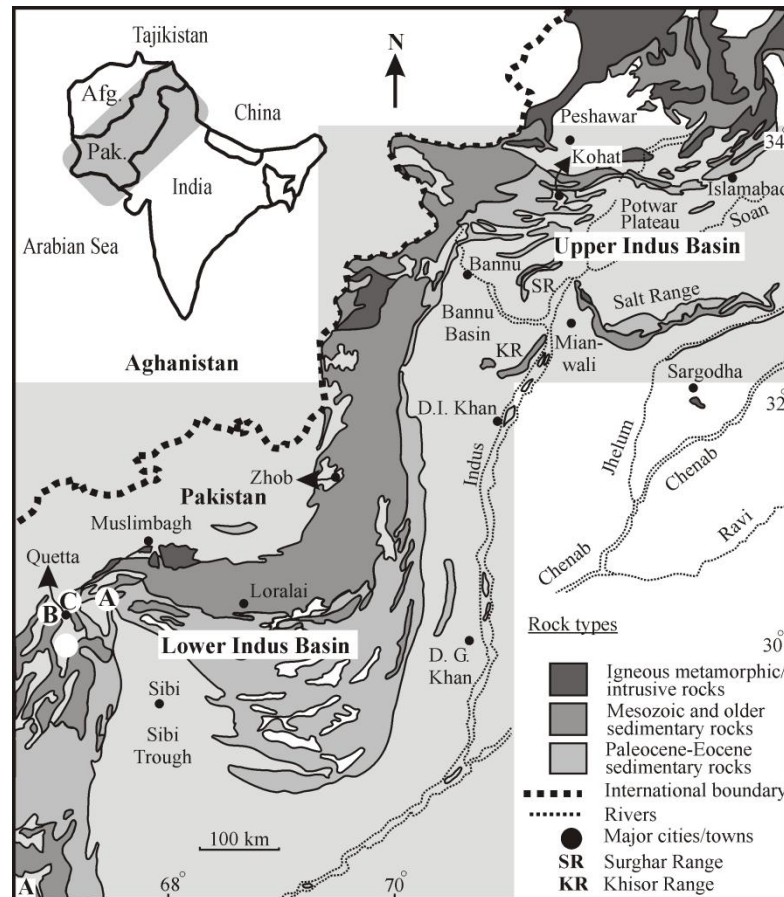


**Figure 1.** Map of the Upper Indus Basin and parts of the Lower Indus Basin showing position (A-C) of studied sections (modified after Afzal *et al.* in press). A, Zranda section; B, Muree Brewery section; C, Hanna Lake section.

Recent work has provided the first unified scheme for biostratigraphical correlation of the Palaeogene succession (see Afzal *et al.* 2009, in press). This chapter examines stable carbon and oxygen isotope data from 14 different carbonate microfacies types in the latest Paleocene-Early Eocene part of the Dungan Formation (Fig. 1) is an attempt to provide additional palaeoenvironmental data: for the stratigraphical implications of the isotope data see Chapter 4. The main objectives of this chapter are to identify the degree of diagenetic alteration in carbonate microfacies and its impact on isotopic variability; and, where material is identified as nearly pristine, attempt to reconstruct Palaeoenvironmental conditions through the latest Paleocene-Early Eocene interval.

## Materials and methods

The Paleogene sections analysed are situated in the western Sulaiman Mountain Range of the Lower Indus Basin (Fig. 1). The carbonates were deposited in the east Tethys Ocean. The geological and stratigraphical settings of the Indus Basin are described in Afzal *et al.* (2009, and Afzal *et al.* in press). For stable isotope analyses, a total of 58 limestone samples were selected from the Late Paleocene-Early Eocene Dungan Formation, comprising of 17 samples from the Zranda section, 20 from the Muree Brewery section and 21 from the Hanna Lake section. The biostratigraphical setting of these sections has been discussed in Afzal *et al.* (in press) and the stratigraphic nomenclature follows Afzal *et al.* (2009).

Determination of carbonate microfacies types in the Dungan Formation is based on visual examination and quantitative-semi-quantitative (see appendices 1-5) analysis of lithology, grain types (biogenic or abiogenic), textures, fossil assemblages and bioclasts in thin section (Wilson 1975; Flügel 1982, 2004). All samples were investigated for evidence of diagenesis using the petrographic microscope in order to classify various degrees of alteration.

For  $\delta^{13}\text{C}$  and  $\delta^{18}\text{O}$  isotopes, limestone bulk materials were ground in agate and equivalent of 10 mg of carbonate was reacted with anhydrous phosphoric acid *in vacuo* overnight at a constant 25°C. The  $\text{CO}_2$  liberated was separated from water vapour under vacuum and collected for analysis. Measurements were made on a VG Optima mass spectrometer. Overall analytical reproducibility for these samples is normally better than 0.2‰ for  $\delta^{13}\text{C}$  and  $\delta^{18}\text{O}$  ( $2\sigma$ ). Isotope values ( $\delta^{13}\text{C}$ ,  $\delta^{18}\text{O}$ ) are reported as per mil (‰) deviations of the isotopic ratios ( $^{13}\text{C}/^{12}\text{C}$ ,  $^{18}\text{O}/^{16}\text{O}$ ) calculated to the VPDB scale using a within-run laboratory standard calibrated against NBS standards.

### **Microfacies**

Fourteen microfacies (F1-F14) types (MFTs) are identified in the limestone of the latest Paleocene-Early Eocene Dungan Formation. Carbonate production was dominated by non-framework building, light-dependent biota such as larger benthic foraminifera (LBFs) and calcareous algae with rare heterotrophic, filter and grazer feeding biota. The stratigraphic distribution of MFTs is given in figures 2-4 and a depositional models in Figure 5. Detailed descriptions of these microfacies are given in Chapter 5 and Appendix 6.

The carbonate microfacies of the Dungan Formation record a complex history of sea level change, beginning with an open ramp/deep inner ramp setting succeeded by regressive microfacies of lagoon and intertidal carbonates, and in the latest Paleocene a return to more open marine ramp facies which continued into the earliest Eocene.

### **Petrographic assessment of the limestones**

In order to determine whether the isotope signatures reflect primary environmental parameters of the seawater in which they formed, the possible effects of diagenesis have been assessed. Overall, four preservational types are identified: 1) well preserved carbonates; 2) marine phreatic diagenesis; 3) carbonates with evidence of meteoric diagenesis; and 4) burial diagenesis. Examples of these different types of diagenesis are presented in Plate 1 and their isotopic compositions with respect to microfacies types are plotted in Figures 6-8.

*Well preserved carbonates:* Parts of the succession (especially in mid-outer ramp settings) show well-preserved carbonate with little or no diagenetic alteration . The mid ramp heterozoan-dominated facies (F9) of the Hanna Lake section (e.g. samples HLD3,

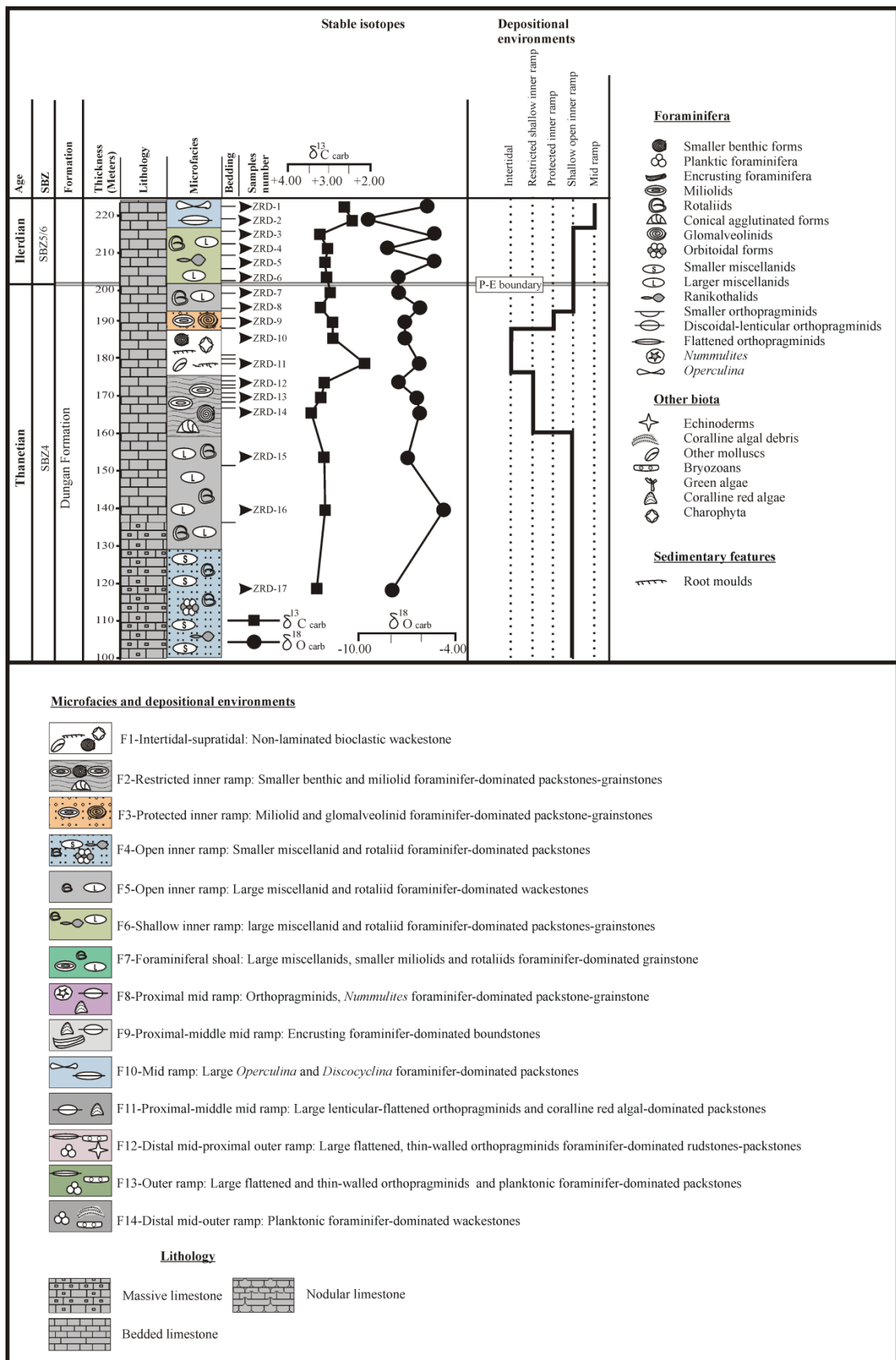


**Figure 2.** Lithostratigraphy, stratigraphic distribution of microfacies, depositional environments and  $\delta^{18}\text{O}$  and  $\delta^{13}\text{C}$  data for the latest Paleocene-Early Eocene Dungan Formation in the Zranda section, Lower Indus Basin. Larger benthic foraminiferal biozones (SBZ) after Afzal *et al.* (in press). Note that the numbering of the microfacies has changed from chapter 5 in order to conform with the analysis presented here. But the microfacies types are exactly the same.

5) suggest least/or no alteration. These are composed of encrusting foraminifera with a fine micritic matrix, showing well-preserved morphologies with very little or no sign of secondary calcite alteration. Similarly, in parts of the deeper mid-outer ramp facies F12 (samples HLD19, 21) and F13 (e.g. sample HLD21), well preserved LBFs (mainly orthopragminids) and planktonic foraminifer with unaltered fine micritic matrix also show little or no diagenetic alteration.

*Marine phreatic diagenesis:* Micritization (Tucker 1993) of bioclasts, isopachous microcrystalline calcite cement and ‘micritic envelopes’ are frequently observed and are likely formed by a combination of boring endolithic algae and precipitation where the ambient waters are supersaturated by calcium carbonate (Hook *et al.* 1984). Micritization of echinoderm and mollusc bioclasts and some LBF shells are common features in shoal-proximal mid ramp (i.e. F7, F8) and outer ramp (F13, F14) microfacies. Thin isopachous microcrystalline calcite cement around echinoderm and red algal fragments are also frequent in mid ramp microfacies F8 and F11 and some parts of F9 (samples BD8-10, HLD6), which represents early marine cement lost by dissolution, later followed by recrystallization, probably formed during seafloor diagenesis (Marshall & Davis 1981; Melim *et al.* 2001).

*Meteoric diagenesis:* This type is characterised by neomorphism, leaching/dissolution, root casts, microspar and drusy/blocky calcite precipitation (Flügel 1982; Melim *et al.*

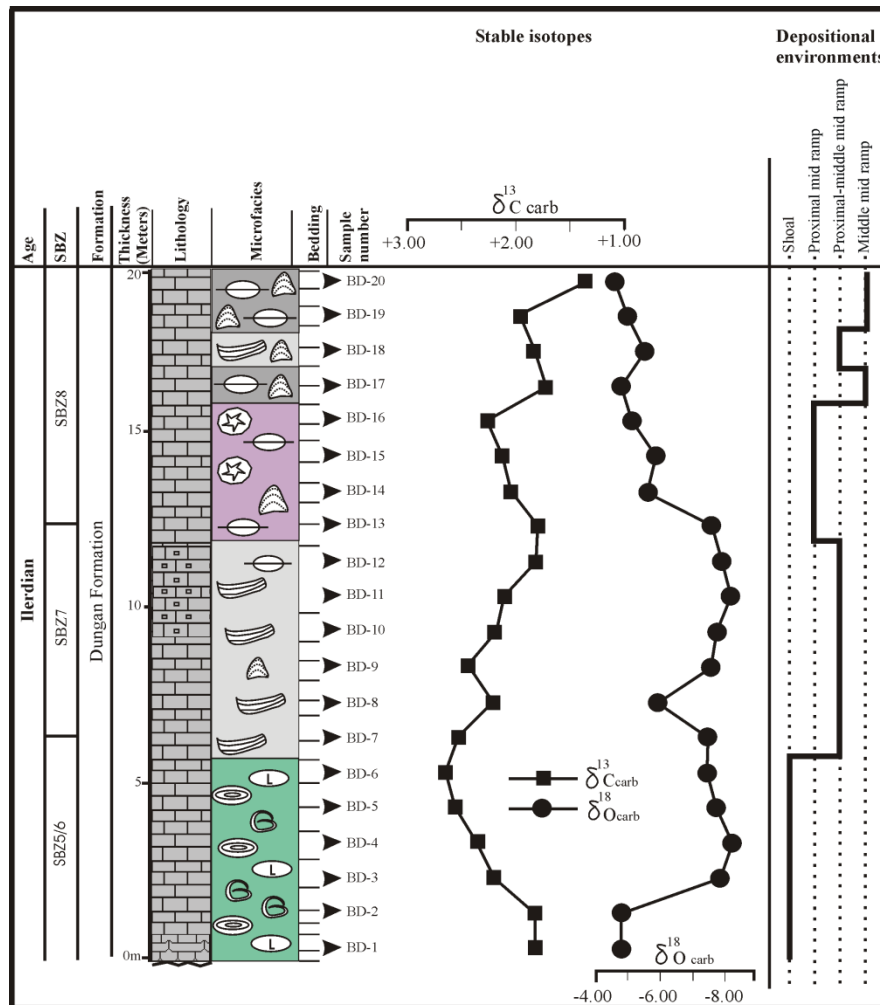


**Figure 3.** Lithostratigraphy, stratigraphic distribution of microfacies, depositional environments and  $\delta^{18}\text{O}$  and  $\delta^{13}\text{C}$  data for the Early Eocene Dungan Formation in the Muree Brewery section, Lower Indus Basin. Shallow benthic biozones (SBZ) after Afzal *et al.* (in press). Key same as Figure 2.

2001). Dissolution/leaching of mollusc and echinoderm bioclasts, replacement of fine micritic groundmass by microspar-coarse blocky calcite and common drusy/blocky calcite infilling of inter-skeletal cavities between LBF tests are frequently recorded features in the carbonates of restricted lagoonal and shallow open inner ramp facies (F2-6) of the Dungan Formation. Intertidal facies (F1) are characterized by root casts, and by leached and neomorphic bioclasts (mainly LBF fragments). Neomorphism indicates in-situ transformations, by solution-re-precipitation, between one mineral and itself or a

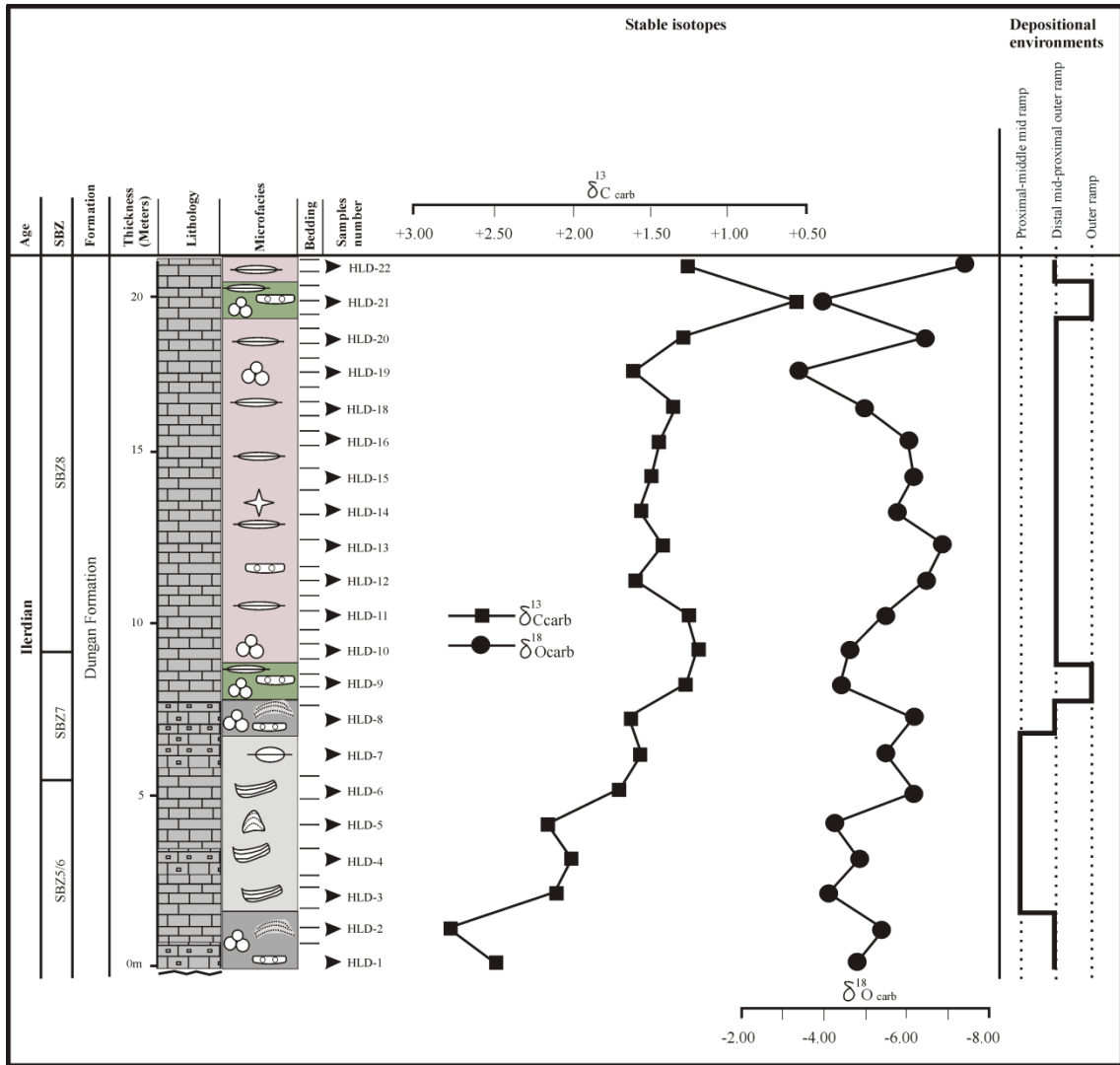


**Figure 4.** Lithostratigraphy, stratigraphic distribution of microfacies, depositional environments and  $\delta^{18}\text{O}$  and  $\delta^{13}\text{C}$  data for the latest Paleocene-Early Eocene Dungan Formation in the Hanna Lake section, Lower Indus Basin. Key same as Figure 2.

polymorph (Folk 1965). Foraminiferal shoal facies (F7) at the margin of the inner ramp show blocky calcite filled inter-skeletal cavities of LBF shells and rare neomorphism of echinoderm fragments. Deeper facies of the mid and outer ramp are rarely or not affected by meteoric diagenesis.

*Burial diagenesis:* Biogenic grain suture contacts, broken and deformed biogenic grains, stylolites and coarse calcite crystals infilling microfractures are identified as

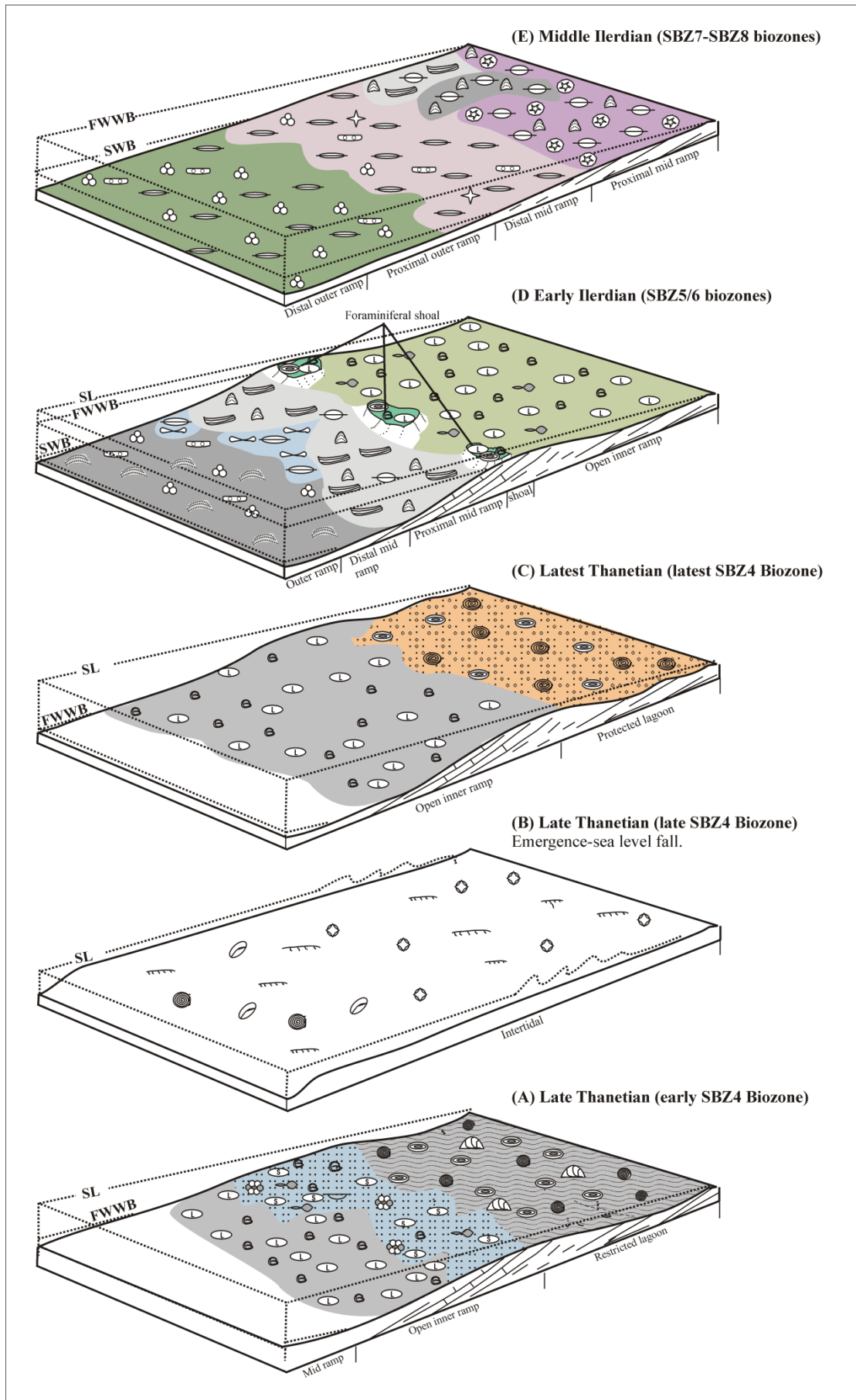


**Figure 5.** Depositional models for carbonate microfacies of the latest Paleocene-Early Eocene Dungan Formation in the Zranda, Muree Brewery and Hanna Lake sections. Key same as Figure 2. See Chapter 5 and Appendix 6 for detail description of microfacies types. Shallow benthic biozones (SBZ) after Afzal *et al.* (in press).

burial diagenetic features (Flügel 1982; Choquette & James 1987). Non-fabric-selective stylolites and coarse calcite crystals infilling microfractures are common in inner ramp microfacies F4 (e.g. sample ZRD17). Microfractures filled by coarse blocky calcite are commonly recorded in foraminifer shoal microfacies (F7, samples BD3-6), mid ramp microfacies (F8-9 and F10, samples BD7, 9-13, HLD6, 8, ZRD2). Grain suture contacts and broken and deformed biogenic grains with rare calcite-filled microfractures are prominent features in distal mid-outer ramp facies F12 (e.g. in sample HLD12-13, 15-16, 20). Two types of fractures can be recognized. The first type is fabric-selective (compare Flügel 1982), while the second type is non-fabric-selective, both filled by coarse blocky cements. Non-fabric selective fractures can cross-cut the first fracture type. It is likely that cementation of coarse calcite crystals infilling microfractures resulted from physical compaction, during which they were filled by sparitic calcite during early phases of burial diagenesis (Choquette & James 1987).

### **Stable isotope results**

$\delta^{18}\text{O}$  and  $\delta^{13}\text{C}$  values in each sample for the three studied sections are given in tables 1-3 and their stratigraphic distribution with respect to microfacies types and depositional environment are shown in figures 2-4. Temporal distribution with respect to ramp carbonate environments and facies is discussed below. In general,  $\delta^{13}\text{C}$  ratios of the latest Paleocene (SBZ4) part of the succession show a range from +2.26‰ to +3.47‰.  $\delta^{13}\text{C}$  ratios from the open inner ramp facies (F4-5) plot between +2.97‰ and +3.31‰. Protected/restricted marine microfacies types (F2-F3) exhibit values between +2.90‰

and +3.47‰. The range of  $\delta^{13}\text{C}$  in the intertidal facies (F1) ranges from +2.26‰ to +2.89‰. For  $\delta^{18}\text{O}$  ratios, a wide range of variation, regardless of microfacies types are observed and values vary between -4.66‰ and -8.02‰.

In the earliest Eocene (SBZ5/6 biozones),  $\delta^{13}\text{C}$  values in inner ramp facies (F6) show values from +3.08‰ to +3.23‰ and in the shoal facies (F7) at the margin of the inner ramp, values fluctuate between +2.20‰ and +2.65‰. Mid ramp facies (F9-10) are characterized by  $\delta^{13}\text{C}$  ratios of +1.69‰ to +2.63‰ and mid-outer ramp facies by a range of +2.49‰ to +2.78‰.  $\delta^{18}\text{O}$  ratios in these microfacies vary between -4.12‰ and -9.65‰.

Later, in the Early Eocene (SBZ7-SBZ8 biozones),  $\delta^{13}\text{C}$  values in the proximal-middle mid ramp facies (F8-9, F11) ranges from +1.36‰ to +2.53‰ and  $\delta^{18}\text{O}$  values vary between -4.64‰ and -8.11‰. In the distal mid-outer ramp facies (F12-14),  $\delta^{13}\text{C}$  ratios oscillate between +0.55‰ and +1.62‰ and  $\delta^{18}\text{O}$ ‰ values between -3.36‰ and -7.35‰.

## **Discussion**

### **Diagenetic overprint and isotopic interpretation**

The  $\delta^{18}\text{O}$  of carbonate is dependent on the isotopic composition, salinity and temperature of the water in which it precipitated, whereas  $\delta^{13}\text{C}$  reflects the source of carbon (Leeder 1982; Shackleton 1984).  $\delta^{18}\text{O}$  and  $\delta^{13}\text{C}$  can be influenced by regionally distinct water masses in shallow marine carbonate environments (e.g. Patterson & Walter 1994; Holmden *et al.* 1998) and the composition of skeletal grains can be influenced by differences in isotopic fractionation during biocalcification by organisms (e.g. Spero *et al.* 1997). Specific variations in  $\delta^{18}\text{O}$  and  $\delta^{13}\text{C}$  in shallow-marine carbonates are also related to global change in oceanographic and environmental

conditions and have been widely used as proxies to reconstruct palaeoenvironmental conditions (e.g. Mutti *et al.* 2006; Parente *et al.* 2007). However, stable isotopes in shallow marine carbonates are particularly susceptible to post-depositional diagenetic processes (Veizer *et al.* 1997), which generally leads to systematic bias in interpretation. Thus, the reliability of  $\delta^{18}\text{O}$  and  $\delta^{13}\text{C}$  data of the Indus Basin has been evaluated here with respect to diagenetic and microfacies changes.  $\delta^{13}\text{C}$  and  $\delta^{18}\text{O}$  ratios of the studied carbonate facies are shown in tables 1-3 and plots in figures 6-8. Diagenetic observations and its impact on isotopic composition are discussed in the following section.

Based on petrographic and stable isotopic analysis, the diagenetic history of the studied sections can be divided into 3 stages.

Stage-1: This is characterized by least/or no diagenetic alteration as represented by the Early Eocene mid-outer ramp facies F9, F12 and F13, comprising  $\delta^{18}\text{O}$  ratios between -3.36‰ and -4.25‰ and  $\delta^{13}\text{C}$  between +0.55‰ and +2.16‰ (Fig. 8). These ratios in the Indus Basin are comparable with those recorded elsewhere in Early Eocene tropical carbonates (i.e.  $\delta^{18}\text{O}$  [-0.5‰ to -4.70‰] and  $\delta^{13}\text{C}$  [-0.02‰ and +2.00‰], Western India, Saraswati *et al.* 1993; Shatsky Rise, ODP Leg 198, Kaiho *et al.* 2006; Bass River, Zachos *et al.* 2007; Eastern Alps (Austria), Egger *et al.* 2009). However, compared to Early Eocene tropical, well-preserved open marine planktonic foraminiferal  $\delta^{18}\text{O}$  and  $\delta^{13}\text{C}$  ratios (e.g. Zachos *et al.* 2007; Pearson *et al.* 2007), the  $\delta^{13}\text{C}$  values of the Indus Basin are more positive, and the  $\delta^{18}\text{O}$  ratios more negative. The well-preserved carbonate facies (especially F12-13) of the Indus Basin are dominantly composed of photoautotrophic biota (i.e. symbiont-bearing LBFs, Hottinger 1997; Ćosović *et al.*

2004; Bassi 2005), therefore the impact of photosynthesis and the growth-rate of foraminifera on the carbon isotopic composition of neighbouring water may have pushed values more positive (Reiss & Hottinger 1984). However, heterozoan-dominated facies (F9) are expected to show no or little photosynthesis effect on isotope ratios (Reiss & Hottinger 1984; Waelbroeck *et al.* 2005).

Stage-2: The first phase of diagenetic alteration started with marine diagenesis, resulting in more negative stable O isotopic ratios.  $\delta^{18}\text{O}$  values do not show any relationship with facies changes and vary between  $-4.40\text{‰}$  to  $-5.00\text{‰}$  (Figs 6-8). However,  $\delta^{13}\text{C}$  ratios suggest a link with microfacies transitions such as heavier values ( $+3.12\text{‰}$  to  $+3.23\text{‰}$ ) in inner ramp facies and relatively lighter ratios ( $+1.18\text{‰}$  to  $+2.26\text{‰}$ ) in mid-outer ramp facies (Figs 7-8). Moreover,  $\delta^{13}\text{C}$  values do not covary with  $\delta^{18}\text{O}$ , suggesting that marine diagenetic alteration of these carbonates occurred in a system with a low water/rock ratio for carbon, and a high ratio for oxygen (Veizer 1999). Marine diagenesis was probably frequent in all ramp facies (based on petrographic observations), however meteoric-burial diagenesis likely obscured the original marine signal in most of the studied samples.

Stage-3: The most advanced phase of diagenetic alteration in Indus Basin carbonates is characterized by meteoric and burial diagenesis, resulting in very negative  $\delta^{18}\text{O}$  values ( $-5.16\text{‰}$  or lower) (Figs 6-8). Meteoric waters rich in  $^{16}\text{O}$  and elevated temperatures during burial diagenesis permanently altered the primary  $\delta^{18}\text{O}$  values towards negative values (Land 1995; Veizer *et al.* 1997; Longinelli *et al.* 2003). Periodic emergence, such as suggested by tidal microfacies F1, introduced freshwater, which can also lower  $\delta^{18}\text{O}$  and  $\delta^{13}\text{C}$  values (Swart & Eberli 2005) (Figs 2, 5). Late burial diagenesis often (but not

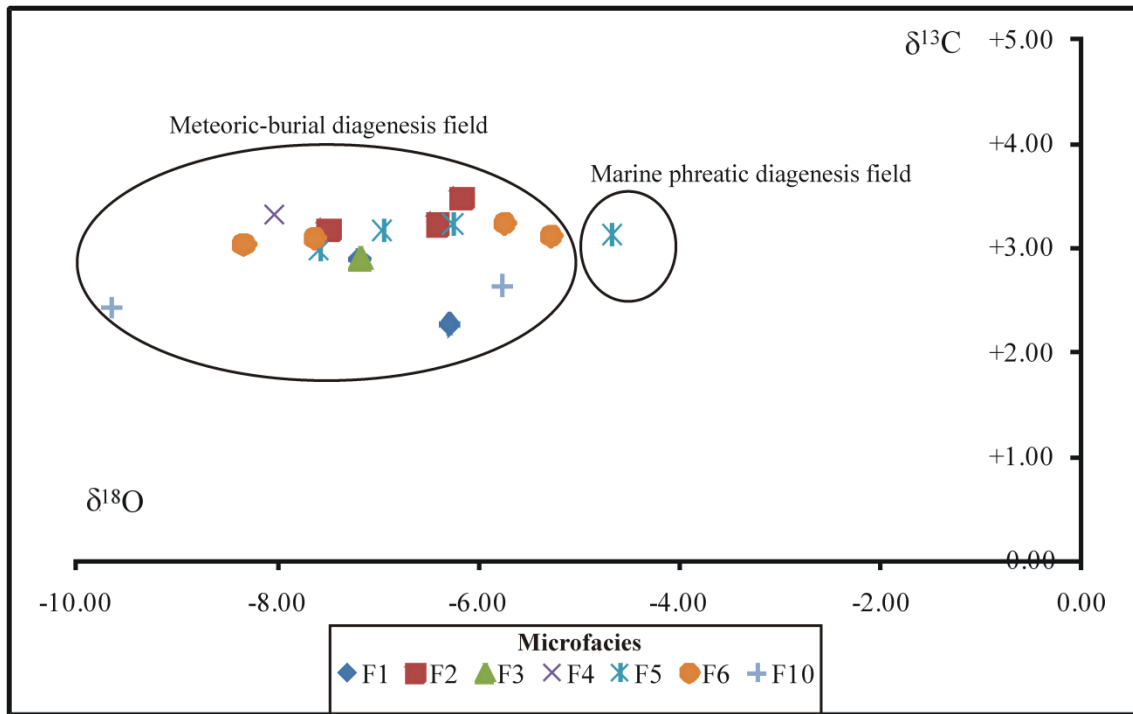


**Figure 6.**  $\delta^{18}\text{O}$  and  $\delta^{13}\text{C}$  values for diagenetic fields for carbonate microfacies of the Dungan Formation in the Zranda section. Diagenetic fields are determined from petrographic (and not isotope) analysis.

exclusively) results in more negative  $\delta^{13}\text{C}$  due to the breakdown of organic matter at depth and the incorporation of light carbon in burial precipitates (e.g. Schneider *et al.* 2008). The  $\delta^{13}\text{C}$  values of studied samples have shown more negative values associated with meteoric diagenesis (e.g. in facies F1). Compared to the highly variable  $\delta^{18}\text{O}$  values, the impact of burial diagenesis on  $\delta^{13}\text{C}$  ratios is, however, minimal, showing low variability (Figs 6-8). This may be due to the fact that burial diagenetic alteration commonly leads to a reduction of  $\delta^{13}\text{C}$  variations and homogenization of carbon isotopes (e.g. Algeo *et al.* 1992) or local effects of the carbon cycle.

### Palaeoenvironmental interpretation

The carbonate facies of the Indus Basin underwent various degrees of diagenetic alteration which obscured the primary isotopic signal.  $\delta^{18}\text{O}$  values show high variability



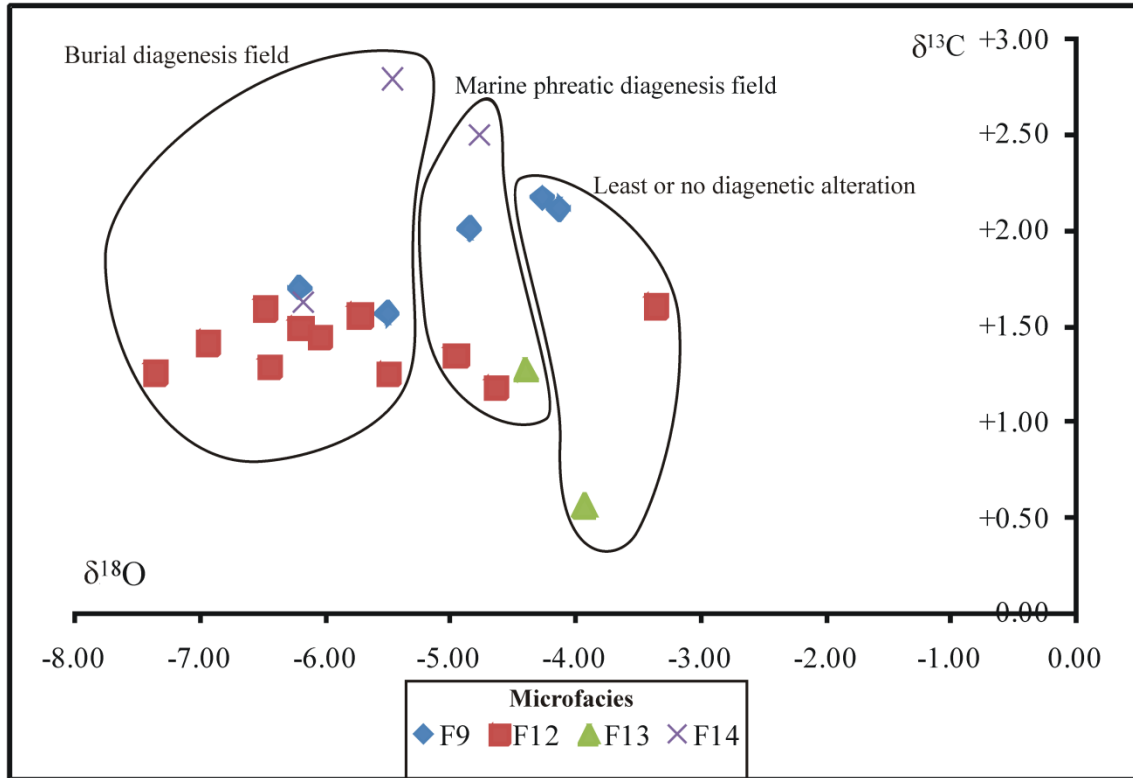


**Figure 8.**  $\delta^{18}\text{O}$  and  $\delta^{13}\text{C}$  values for diagenetic fields for carbonate microfacies of the Dungan Formation in the Hanna Lake section. Diagenetic fields are determined from petrographic (and not isotope) analysis.

Pearson *et al.* 2007), calculated palaeotemperatures from the  $\delta^{18}\text{O}$  of these carbonates range from 32°C to 33.5°C. This is in the upper range of those recorded for Early Eocene tropical sea surface temperatures (SST) elsewhere (i.e. 28°C to 34°C; see Pearson *et al.* 2007; Tripathi *et al.* 2003). However, based on microfacies analysis, the earliest Eocene microfacies (F9) represent lower photic zone depositional settings (Perrin 1992; Plaziat & Perrin 1992). These would be expected to show lower than surface seawater tropical temperatures. Thus, the high temperatures from the  $\delta^{18}\text{O}$  of the Indus Basin carbonates may be result of invisible diagenetic alteration or elevated temperatures in east Tethys. The later seems to be appropriate with the early Paleogene SST model of Sewall *et al.* (2004), which shows highest temperatures for the east Tethys tropical belt compared to west Tethys.

Sample	$\delta^{13}\text{C}\text{‰}$	$\delta^{18}\text{O}\text{‰}$	Microfacies	Sedimentary textures	Estimated diagenesis
ZRD-1	+2.63	-5.76	10	Packstone	Meteoric-burial diagenesis
ZRD-2	+2.42	-9.65	10	Packstone	Meteoric-burial diagenesis
ZRD-3	+3.23	-5.73	6	Packstone	Meteoric-burial diagenesis
ZRD-4	+3.03	-8.33	6	Packstone	Meteoric-burial diagenesis
ZRD-5	+3.11	-5.27	6	Grainstone	Meteoric-burial diagenesis
ZRD-6	+3.08	-7.63	6	Grainstone	Meteoric-burial diagenesis
ZRD-7	+2.97	-7.58	5	Wackstone	Meteoric-burial diagenesis
ZRD-8	+3.22	-6.25	5	Wackstone	Meteoric-burial diagenesis
ZRD-9	+2.90	-7.17	3	Wackstone	Meteoric-burial diagenesis
ZRD-10	+2.89	-7.19	1	Wackstone	Meteoric-burial diagenesis
ZRD-11	+2.26	-6.27	1	Wackstone	Meteoric-burial diagenesis
ZRD-12	+3.17	-7.48	2	Packstone	Meteoric-burial diagenesis
ZRD-13	+3.22	-6.41	2	Packstone	Meteoric-burial diagenesis
ZRD-14	+3.47	-6.16	2	Grainstone	Meteoric-burial diagenesis
ZRD-15	+3.16	-6.94	5	Wackstone	Meteoric-burial diagenesis
ZRD-16	+3.12	-4.66	5	Wackstone	Marine phreatic diagenesis
ZRD-17	+3.31	-8.02	4	Packstone	Meteoric-burial diagenesis

**Table 1.** Stable  $\delta^{18}\text{O}$  and  $\delta^{13}\text{C}$  values, carbonate microfacies types, sedimentary textures and estimated diagenetic alteration for the latest Paleocene-earliest Eocene Dungan Formation in the Zranda section, Lower Indus Basin, Pakistan.

The relatively positive  $\delta^{13}\text{C}$  values of these Early Eocene carbonates (F9) suggest either enhanced  $\text{C}_{\text{org}}$  burial and/or increased local productivity (Weissert 1989; Kurtz *et al.* 2003). These positive  $\delta^{13}\text{C}$  values are in good agreement with the microfacies data (Heterotroph-dominated assemblages), implying increased productivity likely linked with enhanced trophic levels in shallow marine environments of the Indus Basin. Heterotrophs (e.g. encrusting foraminifera of microfacies F9) replace photosymbiont-bearing communities (e.g. LBFs) when dissolved inorganic nutrients are more abundant than particulate organic matter (Hallock 1981). The post-PETM recovery of the oceanic carbonate system may have increased rates of marine or terrestrial organic carbon burial (Bains *et al.* 2000; Beerling 2000), through a feedback mechanism, involving increased productivity and/or by enhanced preservation of organic matter in the sediment (Weissert 1989). Moreover, a possible link between

Sample	$\delta^{13}\text{C}\%$	$\delta^{18}\text{O}\%$	Microfacies	Sedimentary textures	Estimated diagenesis
BD-1	+2.19	-7.77	7	Grainstone	Meteoric-burial diagenesis
BD-2	+2.18	-7.78	7	Grainstone	Meteoric-burial diagenesis
BD-3	+2.20	-7.81	7	Grainstone	Meteoric-burial diagenesis
BD-4	+2.34	-8.18	7	Grainstone	Meteoric-burial diagenesis
BD-5	+2.56	-7.71	7	Grainstone	Meteoric-burial diagenesis
BD-6	+2.65	-7.44	7	Grainstone	Meteoric-burial diagenesis
BD-7	+2.53	-7.44	9	Boundstone with wackstone	Meteoric-burial diagenesis
BD-8	+2.21	-5.92	9	Boundstone with wackstone	Burial diagenesis
BD-9	+2.44	-7.53	9	Boundstone with wackstone	Meteoric-burial diagenesis
BD-10	+2.19	-7.74	9	Boundstone with wackstone	Meteoric-burial diagenesis
BD-11	+2.10	-8.11	9	Boundstone with wackstone	Meteoric-burial diagenesis
BD-12	+1.82	-7.87	9	Boundstone with wackstone	Meteoric-burial diagenesis
BD-13	+1.79	-7.55	8	Packstone	Meteoric-burial diagenesis
BD-14	+2.05	-5.65	8	Grainstone	Burial diagenesis
BD-15	+2.12	-5.87	8	Packstone-grainstone	Burial diagenesis
BD-16	+2.26	-5.16	8	Packstone	Burial diagenesis
BD-17	+1.73	-4.81	11	Packstone	Marine phreatic diagenesis
BD-18	+1.84	-5.53	9	Boundstone with wackstone	Burial diagenesis
BD-19	+1.96	-5.00	11	Packstone	Marine phreatic diagenesis
BD-20	+1.36	-4.64	11	Packstone	Marine phreatic diagenesis

**Table 2.** Stable  $\delta^{18}\text{O}$  and  $\delta^{13}\text{C}$  values, carbonate microfacies types, sedimentary textures and estimated diagenetic alteration for the Early Eocene Dungan Formation in the Muree Brewery section, Lower Indus Basin, Pakistan.

rising sea level and positive C isotope anomalies has been suggested (Weissert 1989; Jenkyns 1996). However, if any of these processes were responsible for more positive  $\delta^{13}\text{C}$  ratios in the Indus Basin, then it should be a global signal and would be recorded elsewhere synchronously and heterozoan-dominated carbonates would be widespread. The heterozoan-dominated carbonates of the Indus Basin are in marked contrast with symbiont-bearing LBF-dominated (mainly nummulitids, alveolinids) shallow-marine carbonates of the west Tethys (e.g. Perrin 2002; Scheibner & Speijer 2008). Thus, the role of the local/regional C cycle and palaeoecological conditions seems to be more important.

Sample	$\delta^{13}\text{C}\text{‰}$	$\delta^{18}\text{O}\text{‰}$	Microfacies	Sedimentary textures	Estimated diagenesis
HLD-1	+2.49	-4.76	24	Wackstone	Marine phreatic diagenesis
HLD-2	+2.78	-5.46	24	Wackstone	Burial diagenesis
HLD-3	+2.10	-4.12	19	Boundstone with wackstone	Least or no diagenetic alteration
HLD-4	+2.00	-4.83	19	Boundstone with wackstone	Marine phreatic diagenesis
HLD-5	+2.16	-4.25	19	Boundstone with wackstone	Least or no diagenetic alteration
HLD-6	+1.69	-6.21	19	Boundstone with wackstone	Burial diagenesis
HLD-7	+1.56	-5.50	19	Boundstone with wackstone	Burial diagenesis
HLD-8	+1.62	-6.17	24	Wackstone	Burial diagenesis
HLD-9	+1.27	-4.40	23	Packstone	Marine phreatic diagenesis
HLD-10	+1.18	-4.63	22	Packstone	Marine phreatic diagenesis
HLD-11	+1.25	-5.48	22	Packstone	Burial diagenesis
HLD-12	+1.59	-6.48	22	Rudstone	Burial diagenesis
HLD-13	+1.41	-6.93	22	Rudstone	Burial diagenesis
HLD-14	+1.56	-5.72	22	Rudstone	Burial diagenesis
HLD-15	+1.49	-6.19	22	Rudstone	Burial diagenesis
HLD-16	+1.44	-6.04	22	Rudstone	Burial diagenesis
HLD-18	+1.34	-4.95	22	Packstone	Marine phreatic diagenesis
HLD-19	+1.60	-3.36	22	Packstone	Least or no diagenetic alteration
HLD-20	+1.28	-6.44	22	Packstone	Burial diagenesis
HLD-21	+0.55	-3.93	23	Packstone	Least or no diagenetic alteration
HLD-22	+1.26	-7.35	22	Rudstone	Burial diagenesis

**Table 3.** Stable  $\delta^{18}\text{O}$  and  $\delta^{13}\text{C}$  values, carbonate microfacies types, sedimentary textures and estimated diagenetic alteration for the Early Eocene Dungan Formation in the Hanna Lake section, Lower Indus Basin, Pakistan.

### Conclusions

Analyses of  $\delta^{18}\text{O}$  and  $\delta^{13}\text{C}$  isotope ratios of the latest Paleocene-Early Eocene shallow marine carbonates (Dungan Formation) of the Lower Indus, Pakistan identifies the following carbonate preservation types:

- a) Well-preserved carbonate facies with little or no diagenetic alteration;
- b) Marine phreatic diagenesis characterized by micritization of bioclasts, isopachous microcrystalline calcite cement and micritic envelopes;
- c) Meteoric diagenesis identified by the presence of neomorphism, leaching/dissolution, root casts, microspar and drusy/blocky calcite precipitation;
- d) Burial diagenesis represented by biogenic grain suture contacts, broken and deformed biogenic grains, stylolites and coarse calcite crystals infilling microfractures.

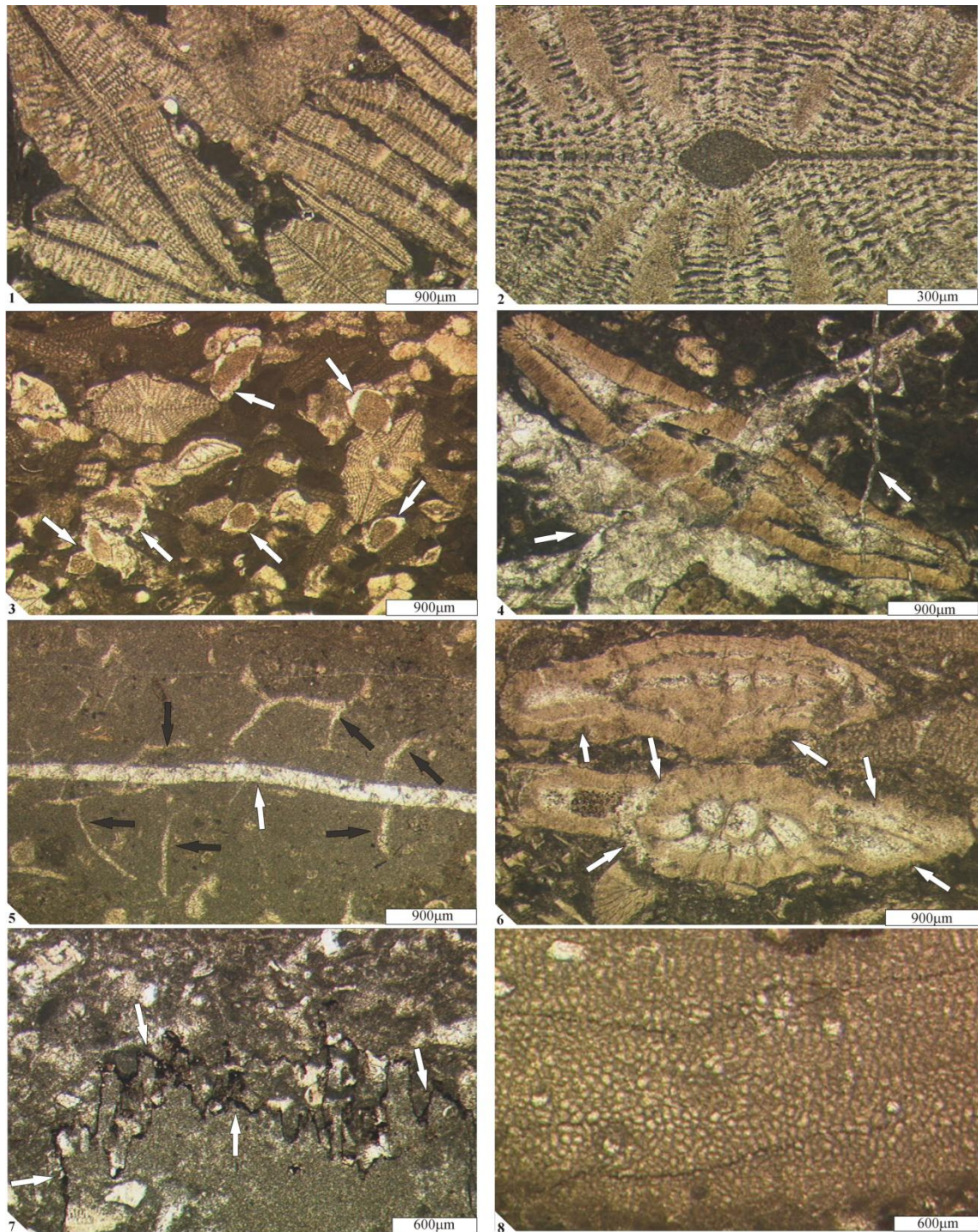


**Plate 1.** Facies and different preservation/diagenesis types for the Dungan Formation. 1. Orthopragminid foraminifer-dominated packstone (F12) showing well-preserved foraminifera and fine micritic matrix, sample HLD19. 2. Magnified view of well-preserved *Orbitoclypeus* foraminifer from orthopragminid foraminifer-dominated packstone (F12), sample HLD19. 3. *Discocyclina* and *Nummulites* foraminifer-dominated packstone (F8) with abundant isopachous microcrystalline calcite cement (white arrows) around echinoderm fragments, sample BD13. 4. Foraminiferal shoal facies (F7) showing coarse blocky calcite cement infilling of fractures, sample BD3. 5. Intertidal facies (F1) with root casts (black arrow) and coarse sparry calcite filled fracture (white arrow), sample ZRD10. 6. *Operculina* and *Discocyclina* foraminifera-

dominated packstones (F10) showing leached and coarse spary calcite filled foraminiferal test, sample ZRD2. 7. Inner ramp wackstone (F5) with stylolites and replacement of groundmass and skeletal fragments by microspar-coarse blocky calcite, sample ZRD15. 8. Heterozoan-dominated facies (F9) with encrusting foraminifera showing little or no diagenetic alteration, sample HLD5.

Based on an assessment of the  $\delta^{18}\text{O}$  values from the best preserved carbonates, sea temperatures of between 32°C to 33.5°C were calculated for the earliest Eocene East Tethys. Relatively positive  $\delta^{13}\text{C}$  values (+2.10‰ to +2.16‰) for these carbonates are consistent with microfacies data that suggest increased productivity in the east Tethys. Further research is required to test these results because the present dataset is small.

---

# Chapter 7

---

## Conclusions

---

## Chapter 7: Conclusions

The biotic responses of the Paleocene-Early Eocene shallow marine benthic communities (especially larger benthic foraminifera [LBF]) to early Paleogene environmental changes have been evaluated by combining palaeontological and sedimentological data together with stable isotope (Carbon and Oxygen) analyses of the shallow marine carbonates from east Tethys (Indus Basin, Pakistan). These studies have produced the following conclusions.

A detailed review of previously published bio- and lithostratigraphical data on the Paleocene-Eocene succession of the Indus Basin has provided a new stratigraphic nomenclature for the basin. The reinterpretation of stratigraphic data helped to resolve inter-basinal correlations between various lithostratigraphical units and to correlate with the global standard biostratigraphy and chronostratigraphy. In addition, the timing of India-Asia collision and resulting Tethys Sea retreat, and the land mammal migrations that are associated with this are correlated within the stratigraphy of the basin. The hiatus equivalent in time with planktonic foraminifera biozone P5-P7, and dramatic shifts in sedimentation (e.g. from marine to continental) has been linked with the initial collision of India-Asia at around the P-E boundary. These data indicate that the retreat of the Tethys Sea started in the early Lutetian in the north and was completed by Priabonian time in the south of the Indus Basin, resulting in a cessation of marine sedimentation in the region.

Taxonomic studies on LBFs from the newly collected Paleocene-Early Eocene sections (Kotal pass, Mughal Kot, Zranda, Muree Brewery and Hanna Lake) and a petroleum well (Shakardara Well-1) identify 45 species.

To assess the temporal evolution of LBFs in the east Tethys, I have constrained events by identifying eight foraminiferal biozones (SBZ1-SBZ8) coupled to a stable Carbon isotope record spanning the Paleocene to Early Eocene interval for the Indus Basin. The P-E boundary is marked by the first appearance of *Alveolina*. *Nummulites* which are characteristic of west Tethys in the earliest Eocene are absent in the Indus Basin and *Alveolina* are scarce. Moreover, typical Late Paleocene LBFs such as *Miscellanea* and *Ranikothalia* which were replaced by the adaptative radiation of *Nummulites* and *Alveolina* (known as the larger foraminifer turnover [LFT]) in the earliest Eocene of west Tethys remain the dominant forms in the earliest Eocene of east Tethys. The LFT in west Tethys has been related to the PETM climatic perturbation. Faunal differences between east and west Tethys were probably caused by the initial collision of India with Asia. The collision may have generated biogeographic barriers between east and west Tethys, which likely prevented migration of certain LBFs (e.g. *Nummulites*) from west to east. This may have facilitated the survival of existing LBFs (e.g. Late Paleocene *Miscellanea* and *Ranikothalia*) in the east, resulting in reduced eco-space competition between species and delaying the LFT. In addition, the persistence of Paleocene LBFs such *Miscellanea* and *Ranikothalia* in the east during the earliest Eocene suggests that the PETM did not affect these foraminifera severely and uniformly across Tethys and long-term LBF evolution, local palaeoecological conditions, eco-space competition between taxa, and local tectonics were also important factors for the timing of the LFT. The appearance of cosmopolitan LBFs later in the Early Eocene (SBZ7-SBZ8 biozones) suggests the collapse of biogeographic barriers between east and west Tethys.

Detailed palaeoecological (e.g. LBFs, algae) and sedimentological (carbonate microfacies) investigations of the Late Paleocene-Early Eocene carbonate successions of the Indus Basin document an important record of biotic responses to the regional and global environmental changes. Some 24 microfacies types with diverse palaeoecological assemblages are recorded, indicating inner-outer ramp environments. During the early Thanetian (SBZ3 Biozone) time, the inner ramp biotic assemblages of the Indus Basin were dominated by meso-oligotrophic LBFs and subordinate dasycladacean algae with rare coral-reef communities (only present as small patch-reefs). This is in marked contrast with the coral-algal dominated west Tethys, suggesting that local palaeoecological conditions (e.g. fluctuating nutrient levels, water energy etc.) in the Indus Basin as well as a latitudinal gradient in sea surface temperatures from west to east might be responsible for these biotic differences. The late Thanetian (SBZ4 Biozone) LBF-dominated facies (i.e. miscellanids, rotaliids and ranikothalids foraminifera) in the Indus Basin are comparable with those of west Tethys, indicating a wider-Tethyan biotic response to the long-term warming of the early Paleogene. The latest Paleocene eustatic change is recorded in the facies of the Indus Basin, resulting in partial exposure of the ramp and demise of carbonate production. During the earliest Eocene (SBZ5/6 biozones), when major faunal changes in LBFs (i.e. LFT) and decline of corals in low-mid latitudes are recorded in the west Tethys in response to the climatic perturbation of PETM, carbonate environments in the Indus Basin remain dominated by low-diversity LBF assemblages similar to those of the Paleocene (i.e. miscellanids and ranikothalids). Typical Tethyan earliest Eocene forms are either absent (e.g. *Nummulites*) or scarce (*Alveolina*, *Orbitolites*). Moreover, in the east, these LBFs were restricted to the shallow inner ramp environments, while mid-outer ramp settings were characterized by heterotroph-dominated (mainly encrusting

foraminifera) and micritic-rich planktonic foraminifer-bearing facies. The environmental (increased continental run off) and biogeographical consequences related to the India-Asia collision and PETM related stresses at the P-E boundary possibly created a significant regional impact on the shallow marine ecosystem in the east Tethys, resulting in biotic reactions different to those of the tectonically stable and climatically driven west Tethys carbonate environments. Later, in the Early Eocene (SBZ7-SBZ8 biozones), heterotroph-dominated facies were gradually replaced by LBF-dominated facies in the east, with cosmopolitan and highly oligotrophic forms (*Nummulites*, *Discocyclina*, *Orbitoclypeus* etc.), indicating stable environmental conditions.

Stable carbon and oxygen isotope analyses of the latest Paleocene-Early Eocene carbonate successions of the Indus Basin show diagenetic and primary signals. Detailed petrographic and stable isotopic analyses of these carbonates have shown three main groupings: 1) well preserved carbonates with  $\delta^{18}\text{O}$  values between -4.12‰ and -4.25‰; 2) carbonates showing marine phreatic diagenesis with  $\delta^{18}\text{O}$  ratios of -4.40‰ to -5.00‰; and 3) meteoric-burial diagenesis with more negative  $\delta^{18}\text{O}$  values (lower than -5.00‰).  $\delta^{13}\text{C}$  values show little variability compared to  $\delta^{18}\text{O}$ , suggesting that precipitation of these carbonates occurred in a system with a low water/rock ratio for carbon, and a high ratio for oxygen. The  $\delta^{18}\text{O}$  values (i.e. -4.12‰ and -4.25‰) from the best preserved carbonates (i.e. heterotroph-dominated facies) reconstruct seawater temperatures between 32°C to 33.5°C (using the O'Neil *et al.* 1969 equation, and a  $\delta^{18}\text{O}$  seawater of -0.75‰ after Pearson *et al.* 2007) for the earliest Eocene of the Indus Basin.  $\delta^{13}\text{C}$  values of these well-preserved carbonates are consistent with microfacies

data, indicating increased productivity and nutrient levels in the earliest Eocene seawater of the east Tethys.

---

# Appendices

---

---

## Appendices

**Appendix 1.** CD-Rom of a Excel file containing quantitative and semi-quantitative data for samples of the Late Paleocene Lockhart Formation in the Kotal Pass section, Upper Indus Basin, Pakistan.

**Appendix 2.** CD-Rom of a Excel file containing quantitative and semi-quantitative data for samples of the Lockhart and Patala formations in the Shakardara Well-1, Upper Indus Basin, Pakistan.

**Appendix 3.** CD-Rom of a Excel file containing quantitative and semi-quantitative data for samples of the Late Paleocene-Early Eocene Dungan Formation in the Zranda section, Lower Indus Basin, Pakistan.

**Appendix 4.** CD-Rom of a Excel file containing quantitative and semi-quantitative data for samples of the Early Eocene Dungan Formation in the Muree Brewery section, Lower Indus Basin, Pakistan.

**Appendix 5.** CD-Rom of a Excel file containing quantitative and semi-quantitative data for samples of the Early Eocene Dungan Formation in the Hanna Lake section, Lower Indus Basin, Pakistan.

**Appendix 6.** CD-Rom of a MS Word file containing detailed microfacies description of the Late Paleocene-Early Eocene carbonate succession of the Indus Basin, Pakistan.

**Appendix 7.** CD-Rom of a PDF file containing a research paper published in the Journal of Micropaleontology (Afzal, J., Williams, M. & Aldridge, R.J. 2009. Revised stratigraphy of the lower Cenozoic succession of the Greater Indus Basin in Pakistan. *Journal of Micropalaeontology*, **28**, 7-23).

**Appendix 8.** CD-Rom of a PDF file containing a research paper in press for *Lethaia* (Afzal, J., Williams, M., Leng, M.J., Aldridge, R.J. & Stephenson, M.H. In press. Evolution of Paleocene to Early Eocene larger benthic foraminifer assemblages of the Indus Basin, Pakistan. *Lethaia*).

**Appendix 9.** British Geological Survey (BGS), Keyworth, Nottingham repository numbers for studied samples of the Indus Basin, Pakistan. Sample No with KL are from Kotal Pass section; 4472.24-4299.3 from Shakardara Well-1; PD from Mughal Kot section; ZRD from Zranda section; BD from Muree Brewery section; HLD from Hanna Lake section.

Field No.	BGS No.						
KL-1	MPA60676	KL-51	MPA60726	PD-3	MPA60776	ZRD-33	MPA60826
KL-2	MPA60677	KL-52	MPA60727	PD-4	MPA60777	ZRD-34	MPA60827
KL-3	MPA60678	KL-53	MPA60728	PD-5	MPA60778	ZRD-35	MPA60828
KL-4	MPA60679	KL-54	MPA60729	PD-6	MPA60779	ZRD-36	MPA60829
KL-5	MPA60680	KL-55	MPA60730	PD-7	MPA60780	ZRD-37	MPA60830
KL-6	MPA60681	KL-56	MPA60731	PD-8	MPA60781	ZRD-38	MPA60831
KL-7	MPA60682	KL-57	MPA60732	PD-9	MPA60782	ZRD-39	MPA60832
KL-8	MPA60683	KL-58	MPA60733	PD-10	MPA60783	BD-1	MPA60833
KL-9	MPA60684	KL-59	MPA60734	PD-11	MPA60784	BD-2	MPA60834
KL-10	MPA60685	KL-60	MPA60735	PD-12	MPA60785	BD-3	MPA60835
KL-11	MPA60686	KL-61	MPA60736	PD-13	MPA60786	BD-4	MPA60836
KL-12	MPA60687	KL-62	MPA60737	PD-14	MPA60787	BD-5	MPA60837
KL-13	MPA60688	KL-63	MPA60738	PD-15	MPA60788	BD-6	MPA60838
KL-14	MPA60689	KL-64	MPA60739	PD-16	MPA60789	BD-7	MPA60839
KL-15	MPA60690	KL-65	MPA60740	PD-17/17A	MPA60790	BD-8	MPA60840
KL-16	MPA60691	KL-66	MPA60741	PD-18	MPA60791	BD-9	MPA60841

## Appendices

---

KL-17	MPA60692	KL-67	MPA60742	PD-19	MPA60792	BD-10	MPA60842
KL-18	MPA60693	KL-68	MPA60743	PD-20	MPA60793	BD-11	MPA60843
KL-19	MPA60694	KL-69	MPA60744	ZRD-1	MPA60794	BD-12	MPA60844
KL-20	MPA60695	KL-70	MPA60745	ZRD-2	MPA60795	BD-13	MPA60845
KL-21	MPA60696	KL-71	MPA60746	ZRD-3	MPA60796	BD-14	MPA60846
KL-22	MPA60697	KL-72	MPA60747	ZRD-4	MPA60797	BD-15	MPA60847
KL-23	MPA60698	KL-73	MPA60748	ZRD-5	MPA60798	BD-16	MPA60848
KL-24	MPA60699	KL-74	MPA60749	ZRD-6	MPA60799	BD-17	MPA60849
KL-25	MPA60700	KL-75	MPA60750	ZRD-7	MPA60800	BD-18	MPA60850
KL-26	MPA60701	KL-76	MPA60751	ZRD-8	MPA60801	BD-19	MPA60851
KL-27	MPA60702	KL-77	MPA60752	ZRD-9	MPA60802	BD-20	MPA60852
KL-28	MPA60703	KL-78	MPA60753	ZRD-10	MPA60803	BD-21	MPA60853
KL-29	MPA60704	4299.3	MPA60754	ZRD-11	MPA60804	HLD-1	MPA60854
KL-30	MPA60705	4299.6	MPA60755	ZRD-12	MPA60805	HLD-2	MPA60855
KL-31	MPA60706	4300.01	MPA60756	ZRD-13	MPA60806	HLD-3	MPA60856
KL-32	MPA60707	4300.31	MPA60757	ZRD-14	MPA60807	HLD-4	MPA60857
KL-33	MPA60708	4300.8	MPA60758	ZRD-15	MPA60808	HLD-5	MPA60858
KL-34	MPA60709	4301.17	MPA60759	ZRD-16	MPA60809	HLD-6	MPA60859
KL-35	MPA60710	4301.55	MPA60760	ZRD-17	MPA60810	HLD-7	MPA60860
KL-36	MPA60711	4468	MPA60761	ZRD-18	MPA60811	HLD-8	MPA60861

---

## Appendices

---

KL-37	MPA60712	4468.3	MPA60762	ZRD-19	MPA60812	HLD-9	MPA60862
KL-38	MPA60713	4468.61	MPA60763	ZRD-20	MPA60813	HLD-10	MPA60863
KL-39	MPA60714	4468.91	MPA60764	ZDR-21	MPA60814	HLD-11	MPA60864
KL-40	MPA60715	4469.21	MPA60765	ZRD-22	MPA60815	HLD-12	MPA60865
KL-41	MPA60716	4469.63	MPA60766	ZRD-23	MPA60816	HLD-13	MPA60866
KL-42	MPA60717	4469.98	MPA60767	ZRD-24	MPA60817	HLD-14	MPA60867
KL-43	MPA60718	4470.53	MPA60768	ZRD-25	MPA60818	HLD-15	MPA60868
KL-44	MPA60719	4470.78	MPA60769	ZRD-26	MPA60819	HLD-16	MPA60869
KL-45	MPA60720	4471.11	MPA60770	ZRD-27	MPA60820	HLD-17	MPA60870
KL-46	MPA60721	4471.58	MPA60771	ZRD-28	MPA60821	HLD-18	MPA60871
KL-47	MPA60722	4471.89	MPA60772	ZRD-29	MPA60822	HLD-19	MPA60872
KL-48	MPA60723	4472.24	MPA60773	ZRD-30	MPA60823	HLD-20	MPA60873
KL-49	MPA60724	PD-1	MPA60774	ZRD-31	MPA60824	HLD-21	MPA60874
KL50	MPA60725	PD-2	MPA60775	ZRD-32	MPA60825	HLD-22	MPA60875

---

## Note

The following paper was published just after completion and submission of this thesis.

The paper discusses the classification of the early Palaeogene nummulitid foraminifera from Oman and has implications for parts of Chapter 3 of this thesis.

Haynes, J.R., Racey, A. & Whittaker, J.E. 2010. A revision of the Early Palaeogene nummulitids (Foraminifera) from northern Oman, with implications for their classification. *In*: Whittaker, J.E. & Hart, M.B. (eds) *Micropalaeontology, Sedimentary Environments and Stratigraphy: A Tribute to Dennis Curry (1912-2001)*. *The Micropalaeontological Society, Special Publication*, **TMS004**, 29-89.

---

# References

---

---

## References

- Adabi, M.H., Zohdi, A., Ghabeishavi, A., & Amiri-Bakhtiyar, H. 2008. Applications of nummulitids and other larger benthic foraminifera in depositional environment and sequence stratigraphy: An example from the Eocene deposits in Zagros Basin, SW Iran. *Facies*, **54**, 499-512.
- Adams, C.G. 1970. A reconsideration of the East Indian letter classification of the Tertiary. *Bulletin of the British Museum (Natural History) Geology*, **19**, 1-137.
- Adams, C.G. 1987. On the classification of the Lepidocyclinidae (Foraminiferida) with redescription of the unrelated Palaeocene genera *Actinosiphon* and *Orbitosiphon*. *Micropaleontology*, **33**, 289-317.
- Adams, C.G. 1989. Foraminifera as indicators of geological events. *Proceedings of the Geologist Association*, **100**, 297-311.
- Afzal, J. 1996. Late Cretaceous to Early Eocene foraminiferal biostratigraphy of the Rakhi Nala area, Sulaiman Range, Pakistan. *Pakistan Journal of Hydrocarbon Research*, **8**, 1-24.
- Afzal, J. & Butt, A.A. 2000. Lower Tertiary planktonic biostratigraphy of the Salt Range, Northern Pakistan. *Neues Jahrbuch für Geologie und Paläontologie, Monatshefte*, **2000**, 721-747.
- Afzal, J. & Daniels, C.H.V. 1991. Foraminiferal biostratigraphy and paleoenvironmental interpretation of the Paleocene to Eocene Patala and Nammal Formations from Khairabad-East, Western Salt Range, Pakistan. *Pakistan Journal of Hydrocarbon Research*, **3**, 61-79.
- Afzal J., Khan F.R., Khan S.N., Alam S. & Jalal M. 2005. Foraminiferal biostratigraphy and paleoenvironments of the Paleocene Lockhart Limestone from Kotal Pass, Kohat, Northern Pakistan. *Pakistan Journal of Hydrocarbon Research*, **15**, 9-24.
- Afzal, J., Williams, M., & Aldridge, R.J. 2009. Revised stratigraphy of the lower Cenozoic succession of the Greater Indus Basin in Pakistan. *Journal of Micropalaeontology*, **28**, 7-23.
- Afzal, J., Williams, M., Leng, M.J., Aldridge, R.J. & Stephenson, M.H. in press. Evolution of Paleocene to Early Eocene larger benthic foraminifer assemblages of the Indus Basin, Pakistan. *Lethaia*.
- Aguirre, J. & Riding, R. 2005. Dasycladalean algal biodiversity compared with global variations in temperature and sea level over the past 350 Myr. *Palaios*, **20**, 581-588.
- Aguirre, J., Baceta, J.I. & Braga, J.C. 2007. Recovery of marine primary producers after the Cretaceous-Tertiary mass extinction: Paleocene calcareous red algae from the Iberian Peninsula. *Palaeogeography, Palaeoclimatology, Palaeoecology*, **249**, 393-411.
- Ahmad, N. & Ahmad, S. 2001. Petrography of the Dungan Formation eastern Sulaiman Range, Pakistan. *Geological Bulletin Punjab University*, **36**, 1-16.
- Ahmad, N. & Hudson, J.D. 2000. Diagenetic environments of the Dungan Formation, eastern Sulaiman Range, Pakistan. *Geological Bulletin Punjab University*, **35**, 21-36.
- Akhtar, M. & Butt, A.A. 1999. Lower Tertiary biostratigraphy of the Kala Chitta Range, northern Pakistan. *Revue de Paléobiologie, Genève*, **18**, 123-146.

- Akhtar, M. & Butt, A.A. 2000. Significance of *Miscellanea miscella* (D' Archiac & Haime) in the Early Palaeogene stratigraphy of Pakistan. *Revue de Paléobiologie, Genève*, **19**, 123-135.
- Akhtar, M. & Butt, A.A. 2001. The Paleogene of the Kala Chitta Range, northern Pakistan. *Neues Jahrbuch für Geologie und Paläontologie, Monatshefte*, **1**, 43-55.
- Algeo, T.J., Wilkinson, B.H. & Lohmann, K.C. 1992. Meteoric-burial diagenesis of Middle Pennsylvanian limestones in the Orogrande Basin, New Mexico: water/rock interactions and basin geothermics. *Journal of Sedimentary Petrology*, **62**, 652-670.
- Ali, J.R. & Aitchison, J.C. 2008. Gondwana to Asia: Plate tectonics, paleogeography and the biological connectivity of the Indian sub-continent from the Middle Jurassic through latest Eocene (166–35 Ma). *Earth-Science Reviews*, **88**, 145-166.
- Allan, J.R. & Matthews, R.K. 2006. Isotope signatures associated with early meteoric diagenesis. *Sedimentology*, **29**, 797-817.
- Arenillas, I., Molina, E., Ortiz, S. & Schmitz, B. 2008. Foraminiferal and d13C isotopic event-stratigraphy across the Danian–Selandian transition at Zumaya (northern Spain): chronostratigraphic implications. *Terra Nova*, **20**, 38-44.
- Aubry, M.P. & Ouda, K. 2003. Introduction to the Upper Paleocene-Lower Eocene of the Upper Nile Valley. In: Ouda, K. & Aubry, M.P. (eds) *Part I. Stratigraphy*, ii-iv. Micropaleontology Press, New York.
- Aubry, M.P., Berggren, W.A., Cramer, B., Dupuis, C., Kent, D.V., Ouda, K., Schmitz, B. & Steurbaut, E. 1999. Paleocene/Eocene boundary sections in Egypt. *1st International Conference on the Geology of Africa, Assiut, Egypt*, 1-11.
- Aubry, M.P., Ouda, K., Dupuis, C., Berggren, W.A., Van Couvering, J.A. & the Members of the Working Group on the Paleocene/Eocene Boundary 2007. Global Standard Stratotype-section and Point (GSSP) for the base of the Eocene Series in the Dababiya section (Egypt). *Episodes*, **30**, 271-286.
- Baceta J.I., Pujalte V. & Bernaola G. 2005. Paleocene Coralgial reefs of the Western Pyrenean basin, northern Spain: New evidence supporting an earliest Paleogene recovery of reefal ecosystems. *Palaeogeography, Palaeoclimatology, Palaeoecology*, **224**, 117-143.
- Bains, S., Norris, R.D., Corfield, R.M. & Faul, K.L. 2000. Termination of global warmth at the Palaeocene/Eocene boundary through productivity feedback. *Nature*, **407**, 171-174.
- Bannert, D. 1992. The structural development of the western fold belt. *Geologisches Jahrbuch*, **B80**, 3-60.
- Barattolo, F., Bassi, D. & Romano, R. 2007. Upper Eocene larger foraminiferal-coraline algal facies from the Knokova Mountain (southern continental Greece). *Facies*, **53**, 361-375.
- Bassi, D. 2005. Larger foraminiferal and coraline algal facies in an Upper Eocene storm-influenced, shallow-water carbonate platform (Colli Berici, north-eastern Italy). *Palaeogeography, Palaeoclimatology, Palaeoecology*, **226**, 17-35.
- Beavington-Penney, S.J. & Racey, A. 2004. Ecology of extant nummulitids and other larger benthic foraminifera: applications in palaeoenvironmental analysis. *Earth Science Reviews*, **67**, 219-265.
- Beavington-Penney, S.J., Wright, P.V. & Racey, A. 2005. Sediments production and dispersal on foramifera-dominated early Tertiary ramps: the Eocene El Garia Fm, Tunisia. *Sedimentology*, **52**, 537-569.
- Beck, R.A., Burbank, D.W., Sercombe, W.J., Riley, G.W., Barndt, J.K., Berry, J.R., Afzal, J., Khan, A.M., Jurgen, H., Metje, J., Cheema, A., Shafique, N.A.,

- Lawrence, R.D. & Khan, M.A. 1995. Stratigraphic evidence for an early collision between northwest India and Asia. *Nature*, **373**, 55-58.
- Beerling, D.J. 2000. Increased terrestrial carbon storage across the Palaeocene-Eocene boundary. *Palaeogeography, Palaeoclimatology, Palaeoecology*, **161**, 395-405.
- Berggren, W.A. & Pearson, P.N. 2005. A revised tropical to subtropical Palaeogene planktonic foraminiferal zonation. *Journal of Foraminiferal Research*, **35**, 279-298.
- Berggren, W.A., Kent, D.V., Swisher, C.C. & Aubry, M.P. 1995. A revised Cenozoic geochronology and chronostratigraphy. In: Berggren, W.A., Kent, D.V., Aubry, M.P. & Hardenbol, J.A. (eds) *Geochronology, Time Scales and Global Stratigraphic Correlations: A Unified Temporal Framework for an Historical Geology*. Society of Economic Paleontologists and Mineralogists, Special Volume, **54**, 129-212.
- Bignot, G. & Neumann, M. 1991. Les 'grands' foraminifères du Crétacé Terminal et du Palaeogene du Nord-Ouest Europeen: Recensement et extensions chronologiques. *Bulletin de la Information Geologique de Bass*, **28**, 13-29.
- Blanckenhorn, M. 1900. Neues zur Geologie und Paläontologie Aegyptens. II. Das Palaeogen. *Zeitschrift der Deutschen Geologischen Gesellschaft*, **52**, 403-479.
- Blanford, W.T. 1879. The geology of western Sind. *Memoir of the Geological Survey of India*, **17**, 1-197.
- Boersma, A., Premoli Silva, I. & Hallock, P. 1998. Trophic models for the well-mixed and poorly mixed warm oceans across the Paleocene/Eocene epoch boundary. In: Aubry, M.P., Lucas, S.G. & Berggren, W.A. (eds) *Late Paleocene–Early Eocene Climatic and Biotic Events in the Marine and Terrestrial Records*. Columbia University Press, New York, 204-213.
- Bolle, M.P. & Adatte, T. 2001. Palaeocene-early Eocene climatic evolution in the Tethyan realm: clay mineral evidence. *Clay Minerals*, **36**, 249-261.
- BouDagher-Fadel, M.K. 2008. The Cenozoic larger foraminifera: The Palaeogene. In: BouDagher-Fadel, M.K. (ed.) *Evolution and geological significance of larger benthic foraminifera (Developments in Palaeontology and Stratigraphy)*, **21**, 297-418. Elsevier, Amsterdam.
- Bowen, G.J., Koch, P.K., Gingerich, P.D., Norris, R.D., Bains, S. & Corfield, R.M. 2001. Refined isotope stratigraphy across the continental Paleocene-Eocene boundary on Polecat Bench in the Northern Bighorn Basin. In: Gingerich, P.D. (ed.) *Paleocene-Eocene Stratigraphy and Biotic Change in the Bighorn and Clarks Fork Basins, Wyoming*, **33**. University of Michigan Papers on Paleontology.
- Brady, H.B. 1882. Note on *Keramosphaera*, a new type of porcellanous foraminifera. *Annual Magazine of Natural History*, **5 (10)**, 1-245.
- Brady, H.B. 1884. Report on the Foraminifera dredged by H.M.S. Challenger, during the years 1873-1876. Report on the Scientific Results of the voyage of the H.M.S. Challenger during the years 1873-76. *Zoology*, **9**, 1-814.
- Brand, U. 2004. Carbon, oxygen and strontium isotopes in Paleozoic carbonate components: an evaluation of original seawater-chemistry proxies. *Chemical Geology*, **204**, 23-44.
- Bronn, H.G. 1825. *System der urweltlichen Pflanzenthiere*. Heidelberg, Germany, 1-76.
- Brönnimann, P. 1945. Zur Frage der verwandtschaftlichen Beziehungen zwischen *Discocyclus* s.s und *Asterocyclus*. *Eclogae geologicae Helvetiae*, **38**, 579-615.

- Brookfield, M.E. 1998. The evolution of the great river systems of southern Asia during the Cenozoic India-Asia collision: Rivers draining southward. *Geomorphology*, **22**, 285-312.
- Bruguère, J.G. 1792. Histoire naturelle des Vers. *Encyclopédie méthodique*, **1**, 345-757.
- Buonocunto, F.P., Sprovieri, M., Bellanca, A., D'Argenio, B., Ferreri, V., Neri, R. & Ferruzza, G. 2002. Cyclostratigraphy and high-frequency carbon isotope fluctuations in Upper Cretaceous shallow-water carbonates, southern Italy. *Sedimentology*, **49**, 1321-1337.
- Burchette, T.P. & Wright, V.P. 1992. Carbonate ramp depositional systems. *Sedimentary Geology*, **79**, 3-57.
- Butler, R. 1995. When did India hit Asia? *Nature*, **373**, 20-21.
- Butt, A.A. 1987. The Palaeogene stratigraphy of the Kala Chitta Range, Northern Pakistan. *Acta Mineralogica Pakistanica*, **3**, 97-110.
- Butt, A.A. 1991. *Ranikothalia sindensis* Zone in Late Paleocene biostratigraphy. *Micropaleontology*, **37**, 77-85.
- Butterlin, J. & Fourcade, E. 1989. Extension stratigraphique et distribution géographique du genre *Lockhartia* Davies, 1932 (foraminifère, rotaliidae). *Revue de Micropaléontologie*, **31**, 225-242.
- Carter, H.J. 1861. Further observations on the structure of Foraminifera and on the larger fossilized forms of Sind, etc., including a new genus and species. *Journal of the Bombay Branch of the Royal Asiatic Society*, **VI**, 31-96.
- Caudri, C.M.B. 1944. The larger foraminifera from San Juan de Los Morros, State of Guarico, Venezuela. *Bulletins of American Paleontology*, **28**, 355-405.
- Chapman, F. 1900. On a *Patellina* - limestone and another Foraminiferal Limestone from Egypt. *Geological Magazine*, **7**, 3-17.
- Checchia-Rispoli, G. 1909. La Serie nummulitica dei dintorni di TerminImerese II. *La Regione Cacasacco. Giornale di Scienze Naturali ed Economiche*, **27**, 183-212.
- Cheema, M.R., Raza, S.M. & Ahmad, H. 1977. Cainozoic. In: Shah, S.M.I. (ed.) *Stratigraphy of Pakistan*. Memoir of the Geological Survey of Pakistan, **12**, 1-138.
- Cherchi, A. & Schroeder R. 1997. Preliminary report on the keramosphaerinid foraminifers from the Thanetian (Paleocene) of South Tibet. *Zeitschrift für geologische Wissenschaften*, **25**, 643-647.
- Choquette, P.W. & James, N.P. 1987. Diagenesis in limestone: part 3, the deep burial environments. *Geoscience*, **14**, 3-35.
- Clyde, W.C., Khan, I.H. & Gingerich, P.D. 2003. Stratigraphic response and mammalian dispersal during initial India-Asia collision: Evidence from the Ghazij Formation, Balochistan, Pakistan. *Geological Society of America Bulletin*, **31**, 1097-1100.
- Cobianchi, M. & Picotti, V. 2001. Sedimentary and biological response to sea-level and paleoceanographic changes of a Lower-Middle Jurassic Tethyan platform margin (Southern Alps, Italy). *Palaeogeography, Palaeoclimatology, Palaeoecology*, **69**, 219-244.
- Cole, W.S. 1941. Stratigraphic and paleontologic studies of wells in Florida. *Bulletin Florida Geological Survey*, **19**, 1-91.
- Copley, A., Avouac, J.P. & Royer, J.Y. 2010. The India-Asia collision and the Cenozoic slowdown of the Indian plate; implications for the forces driving plate motions. *Journal of Geophysical Research*, **115**, B03410.

- Ćosović, V., Drobne, K. & Moro, A. 2004. Paleoenvironmental model for Eocene foraminiferal limestones of the Adriatic carbonate platform (Istrian peninsula). *Facies*, **50**, 61-75.
- Cotter, G. de P. 1933. The geology of the part of the Attock district, west of longitude 72° 45E. *Memoir of the Geological Survey of India*, **55**, 63-161.
- Crouch, E.M. & Brinkhuis, H. 2005. Environmental change across the Paleocene-Eocene transition from eastern New Zealand: a marine palynological approach. *Marine Micropaleontology*, **56**, 138-160.
- Crouch, E.M., Dickens, G.R., Brinkhuis, H., Aubry, M.P., Hollis, C.J., Rogers, K.M. & Visscher, H. 2003. The Apectodinium acme and terrestrial discharge during the Paleocene- Eocene Thermal Maximum: new palynological, geochemical and calcareous nannoplankton observations at Tawanui, New Zealand. *Palaeogeography, Palaeoclimatology, Palaeoecology*, **194**, 1-17.
- Cushman, J. A. 1917. A monograph of the North Pacific Ocean. Part 6, Miliolidae. *Bulletin United States National Museum*, **71**, 1-108.
- d'Orbigny, A. 1826. Tableau méthodique de la classe des Cephalopodes. *Annales des Sciences Naturelles*, **1**, 96-314.
- d'Orbigny, A. 1839. Foraminifères. In: Barker-Webb, P. and Berthelot, S. (eds) *Histoire Naturelle des Iles Canaries*, Zoologie, part 2. Bethune, Paris, 119-146.
- d'Archiac, E.J.A. & Haime, J. 1853. *Description des animaux fossiles du groupe nummulitique de l'Inde. Les Echinodermes*. Précédé dun Résumé Géologique et d'une Monographie des Nummulites, Gide et Bandry, Paris, 1-157.
- d'Archiac, E.J.A. 1850. Description des fossiles du groupe Nummulitique recueillis par M.S.P. Pratt et M. J. Delbos aux environs de Bayonne et de Dax. *Mémoires de la Société géologique de France*, **3**, 397-456.
- Danilchik, W. & Shah, S.M.I. 1987. Stratigraphy and coal resources of the Makarwal area, Trans-Indus Mountains, Mianwali District, Pakistan. *United States Geological Survey Professional Paper*, **1341**, 1-38.
- Davies, L.M. 1927. The Ranikot beds at Thal (North-West Frontier Ranges of India). *Quarterly Journal of the Geological Society of London*, **83**, 260-290.
- Davies, L.M. 1930. The fossil fauna of the Samana Range and some neighbouring areas, the Paleocene foraminifera. *Memoir of the Geological Survey of India, Paleontologia Indica*, **15**, 67-79.
- Davies, L.M. 1932. The genus *Dictyoconoides* Nuttall, *Lockhartia* nov. and *Rotalia* Lamarck. *Royal Society of Edinburgh Transactions*, **57**, 397-428.
- Davies, L.M. 1937. II. Paleontology. In: Davies, L.M. & Pinfold, E.S. (eds) *The Eocene beds of the Punjab Salt Range*. Memoirs of the Geological Survey of India, *Palaeontologia Indica*, **24**, 14-79.
- Davies, L.M. 1952. *Ranikothalia sahnii*, n.sp. and *R. savitriae*, n.sp., a possible link between the Paleocene faunas of the East and West Indies. *The palaeobotanist*, **1**, 155-158.
- Davies, L.M. & Pinfold, E.S. 1937. The Eocene beds of the Punjab Salt Range. *Memoir of the Geological Survey of India*, **24**, 1-79.
- de Blainville, H.M.D. 1825. *Dictionnaire des Sciences Naturelles, pin-plo*, vol. **41**. F.G. Levrault, Paris, 1-558.
- de Blainville, H.M.D. 1827. *Manuel de malacologie et de conchyliologie, Atlas*. F.G. Levrault, Paris, 1-664.
- De La Harpe, P. 1883. Étude des Nummulites de la Suisse et revision des especes éocenes des genres Nummulites et Assilina. 3<sup>ème</sup> partie. *Mémoires de la Société Paléontologique Suisse*, **X**, 141-180.

- de Sigoyer, J., Chavagnac, V., Blichert-Toft, J., Villa, I.M., Luais, B., Guillot, S., Cosca, M. & Mascle, G. 2000. Dating the Indian continental subduction and collisional thickening in the northwest Himalaya, multichronology of the Tso Moriri eclogites. *Geology*, **28**, 487-490.
- de Roissy, F. 1805. *Histoire naturelle, générale et particulière, des mollusques*, volume 5. Paris, Dufart, 1-480.
- Defrance, M. J.L. 1822. Lenticulites. In: Cuvier, M.F. (ed.) *Dictionnaire des Sciences naturelles*. F.G. Levrault, Paris, **25**, 425-453.
- Delage, Y. & Herouard, E. 1896. *Traité de Zoologie Concrète. Tome I. La Cellule et les Protozoaires*. Schleicher Frères, Paris, 1-584.
- Deloffre, R. & Hamaoui, M. 1969. De *Pseudobroeckinella soumoulouensis* n.gen., n.sp., Foraminifere du Cretace superieur D'Aquitaine. *Bulletin Du Centre De Recherches Pau-SNPA*, **3**, 5-31.
- Dettmering, C., Röttger, R., Hohenegger, J. & Schmaljohann, R. 1998. The trimorphic life cycle in foraminifera: observations from cultures allow new evaluation. *European Journal of Protistology*, **34**, 363-368.
- Dewey, J.F., Cande, S. & Pitman, W.C. 1989. Tectonic evolution of the India/Eurasia collision zone. *Eclogae Geologicae Helvetiae*, **82**, 717-734.
- Dickens, G.R. 1999. The blast in the past. *Nature*, **401**, 752-755.
- Doncieux, L. 1926. Catalogue descriptif des Fos siles Nummulitiques de l'Aude et de l'Hérault, 2e partie (fasc.III) : Corbières septentrionales. *Annuelle de University de Lyon*, **45**, 1-80.
- Douglass, R.C. 1960. Revision of the family orbitolinidae. *Micropaleontology*, **6**, 249-270.
- Douvillé, H. 1916. Les Cretace et L'Éocène du Tibet central. *Memoirs of the Geological Survey of India, Palaeontologia Indica, Calcutta*, **5**, 31-45.
- Douvillé, H. 1922. Révision des orbitoïdes. Deuxième partie: les orthophragmina du Danien et de l'Éocène. *Bulletin de la Société Géologique de France*, **4**, 55-100.
- Drobne, K., Čosović, V. & Robinson, E. 2002. Larger miliolids of the Late Cretaceous and Palaeogene seen through space and time. *Geologija*, **45**, 359-366.
- Dupuis, C., Aubry, M.P., Steurbaut, E., Berggren, W.A., Ouda, K., Magioncalda, R., Cramer, B.S., Kent, D.V., Speijer, R.P. & Heilmann-Clausen, C. 2003. The Dababiya Quarry Section: Lithostratigraphy, clay mineralogy, geochemistry and paleontology. *Micropaleontology*, **49**, 41-59.
- Eames, F.E. 1952. A contribution to the study of the Eocene in western Pakistan and western India; Part A. The geology of standard sections in the western Punjab and in the Kohat District. *Quarterly Journal of the Geological Society of London*, **107**, 159-171.
- Egger, H., Fenner, J., Heilmann-Clausen, C., Rögl, F., Sachsenhofer, R.F. & Schmitz, B. 2003. Paleoproductivity of the northwestern Tethyan margin (Anthering Section, Austria) across the Paleocene–Eocene transition. In: Wing, S.L., Gingerich, P.D., Schmitz, B. & Thomas, E. (eds) *Causes and Consequences of Globally Warm Climates in the Early Paleogene*. The Geological Society of America, Boulder, 133-146.
- Egger, H., Heilmann-Clausen, C. & Schmitz, B. 2009. From shelf to abyss: Record of the Paleocene/Eocene-boundary in the Eastern Alps (Austria). *Geologica Acta*, **7**, 215-227.
- Ehrenberg, C.G. 1839. *Die Infusionstierchen als volkonmene Organismen*. L. Voss (Leipzig), 1-547.
- Fagerstrom, J.A. 1987. *The Evolution of Reef Communities*. Wiley, New York, 1-600.

- Falkowski, P.G., Jokieli, P. & Kinzie, R. 1990. Irradiance and corals. In: Dubinsky, Z. (ed.) *Coral Reefs, in Ecosystems of the World*. Elsevier, Amsterdam, **7**, 89-107.
- Fatmi, A.N. 1974. Lithostratigraphic units of the Kohat-Potwar Range, Indus Basin, Pakistan. *Memoirs of the Geological Survey of Pakistan*, **10**, 1-80.
- Fermor, L.L. 1935. General report of the Geological Survey of India for the year 1934. *Records of the Geological Survey of India*, **69**, 1-108.
- Ferrandez-Canadell, C. 2002. New Paleocene orbitoidiform foraminifera from the Punjab Salt Range, Pakistan. *Journal of Foraminiferal Research*, **32**, 1-21.
- Flügel, E. 1982. *Microfacies Analysis of Limestone*. Springer, Berlin-Heidelberg, New York.
- Flügel, E. 2004. *Microfacies of Carbonate Rocks. Analysis, Interpretation and Application*. Springer, Berlin-Heidelberg, New York.
- Folk, R.L. 1965. Some aspects of recrystallization in ancient limestone. *Society of Economic Paleontologists Mineralogists Special Publication*, **13**, 14-48.
- Fölmi, K.B. & Gainon, F. 2008. Demise of the northern Tethyan carbonate platform and subsequent transition towards pelagic conditions: the sedimentary record of the Col de la Paline Morte area, central Switzerland. *Sedimentary Geology*, **205**, 142-159.
- Gaetani, M. & Garzanti, E. 1991. Multicyclic history of the northern India continental margin (northwestern Himalaya). *The American Association of Petroleum Geologists Bulletin*, **75**, 1427-1446.
- Galloway, J.J. 1928. A revision of the family Orbitoididae, *Journal of Paleontology*, **2**, 45-69.
- Gavrilov, Y.O., Shcherbinina, E.A. & Oberhänsli, H. 2003. Paleocene-Eocene boundary events in the northeastern Peri-Tethys. In: Wing, S.L., Gingerich, P.D., Schmitz, B. & Thomas, E. (eds) *Causes and Consequences of Globally Warm Climates in the Early Palaeogene*. The Geological Society of America, 147-168.
- Gee, E.R. 1934. The Saline Series of north-western India. *Current Science*, **2**, 460-463.
- Gee, E.R. 1945. The age of the Saline Series of the Punjab and of Kohat. *Proceedings of the National Academy of Science India*, **14**, 269-310.
- Geel, T. 2000. Recognition of stratigraphic sequences in carbonate platform and slope deposits: empirical models based on microfacies analysis of Paleogene deposits in southeastern Spain. *Palaeogeography, Palaeoclimatology, Palaeoecology*, **155**, 211-238.
- Gibbs, S.J., Bown, P.R., Sessa, J.A., Bralower, T.J. & Wilson, P.A. 2006. Nannoplankton extinction and origination across the Paleocene-Eocene Thermal Maximum. *Science*, **314**, 1770-1773.
- Gibson, T.G. 1990. Upper Paleocene foraminiferal biostratigraphy and paleoenvironments of the Salt Range, Punjab, Pakistan. *United States Geological Survey Bulletin*, **2078**, 1-13.
- Gill, W.D. 1953. Facies and fauna in the Bhadrans Beds of the Punjab Salt Range, Pakistan. *Journal of Paleontology*, **27**, 824-844.
- Gingerich, P.D. 2003. Stratigraphic and micropaleontologic constraints on the middle Eocene age of the mammal-bearing Kuldana Formation of Pakistan. *Journal of Vertebrate Paleontology*, **23**, 643-651.
- Gingerich, P.D., Abbas, S.G. & Arif, M. 1997. Early Eocene *Ouettacyon parachai* (Condylarthra) from the Ghazij Formation of Baluchistan (Pakistan): Oldest Cenozoic land mammal from South Asia. *Journal of Vertebrate Paleontology*, **17**, 629-637.

- Green, O.R., Searle, M.P., Corfield, R.I. & Corfield, R.M. 2008. Cretaceous-Tertiary Carbonate platform evolution and the age of the India-Asia collision along the Ladakh Himalaya (Northwest India). *The Journal of Geology*, **116**, 331-353.
- Grimsdale, T.F. 1952. Cretaceous and Tertiary foraminifera from the Middle East. *Bulletin of the British Museum (Natural History) Geology*, **1**, 221-248.
- Gümbel, C.W. 1870. Beiträge zur Foraminiferenfauna der nordalpinen Eozängebilde oder der kressenberger Nummuliten Schisten. *Abhandlungen der Mathematisch-Physikalischen Classe der Königlich Bayerischen Akademie der Wissenschaften*, **10**, 581-720.
- Gupta, A.K.S. 1963. A restudy of two common species of *Discocyclina* from India. *Micropaleontology*, **9**, 39-44.
- Hallock, P. 1981. Algal symbiosis: A mathematical analysis. *Marine Biology*, **62**, 249-255.
- Hallock, P. 1987. Fluctuation in the trophic resource continuum: a factor in global diversity cycles? *Paleoceanography*, **2**, 457-471.
- Hallock, P. 1988. Interoceanic differences in Foraminifera with symbiotic algae: a result of nutrient supplies? *Proceedings Sixth International Coral Reef Symposium Townsville, Australia*, **3**, 251-255.
- Hallock, P. 2000. Symbiont-bearing foraminifera: harbingers of global change. *Micropaleontology*, **46**, 95-104.
- Hallock, P. 2001. Coral Reefs, Carbonate Sedimentation, Nutrients, and Global Change. In: Stanley, G.D. (ed.) *The History and Sedimentology of Ancient Reef Ecosystems*. Kluwer Academic/Plenum Publishers, 387-427.
- Hallock, P. 2005. Global change and modern coral reefs: New opportunities to understand shallow-water carbonate depositional processes. *Sedimentary Geology*, **175**, 19-33.
- Hallock, P. & Glenn, E.C., 1986. Larger foraminifera: A Tool for Paleoenvironmental analysis of Cenozoic carbonate depositional facies. *Palaios*, **1**, 55-64.
- Hallock, P. & Pomar, L. 2008. Cenozoic Evolution of Larger Benthic Foraminifers: Paleooceanographic Evidence for Changing Habitats. *Proceedings of the 11th International Coral Reef Symposium, Ft. Lauderdale, Florida*, 16-20.
- Hallock, P., Lidz, B.H., Cockey-Burkhard, E.M. & Donnelly, K.B. 2003. Foraminifera as bioindicators in coral reef assessment and monitoring: The FORAM Index. *Environmental Monitoring and Assessment*, **81**, 221-238.
- Hallock, P., Premoli-Silva, I. & Boersma, A. 1991. Similarities between planktonic and larger foraminiferal evolutionary trends through Palaeogene paleoceanographic changes. *Palaeogeography, Palaeoclimatology, Palaeoecology*, **83**, 49-64.
- Hanzawa, S. 1937. Notes on some interesting cretaceous and tertiary foraminifera from the west Indies. *Journal of Paleontology*, **11**, 110-117.
- Haq, B.U., Hardenbol, J., & Vail, P.R. 1987. Chronology of fluctuating sea levels since the Triassic (250 million years ago to present). *Science*, **235**, 1156-1167.
- Haque, A.F.M.M. 1956. The Foraminifera of the Ranikot and the Laki of the Nammal Gorge, Salt Range. *Pakistan Geological Survey, Paleontologia Pakistanica*, **1**, 1-300.
- Hardenbol, J.A., Thierry, J., Farley, M.B., Jacquin, T., de Graciansky, P.-C. & Vail, P.R. 1998. Mesozoic and Cenozoic sequence chronostratigraphic framework of European basins. In: de Graciansky, P.C., Hardenbol, J.A., Jacquin, T. & Vail, P.R. (eds) *Mesozoic and Cenozoic Sequence Stratigraphy of European Basins*. Society for Sedimentary Geology, Special Publication, **60**, 3-29.

- Harrington, G.J. & Jaramillo, C.A. 2007. Paratropical floral extinction in the Late Palaeocene-Early Eocene. *Journal of the Geological Society, London*, **164**, 323-332.
- Haynes, J.R. 1988. Massively chordate nummulitids (Foraminifera) at the Paleocene/Eocene boundary in Tethys. *Indian Journal of Geology*, **60**, 215-247.
- Haynes, J.R. & Whittaker, J.E. 1990. The status of *Rotalia* Lamarck (Foraminifera) and the Rotaliidae Ehrenberg. *Journal of Micropalaeontology*, **9**, 95-106.
- He, Y.Y., Klisch, M. & Hader, D.P. 2002. Adaptation of cyanobacteria to UV-B stress correlated with oxidative stress and oxidative damage. *Photochemical and Photobiological Sciences*, **76**, 188-96.
- Hemphill, W.R. & Kidwai, A.H. 1973. Stratigraphy of the Bannu and Dera Ismail Khan areas, Pakistan. *United States Geological Survey Professional Paper*, **716-B**, 1-36.
- Henson, F.R.S. 1948. *Larger Imperforate Foraminifera of South-Western Asia. Families Lituolidae, Orbitolinidae and Meandropsinidae*. British Museum (Natural History), London, 1-127.
- Hodges, K.V. 2000. Tectonics of the Himalayan and southern Tibet from two perspectives. *Geological Society of America Bulletin*, **112**, 324-350.
- Hohenegger, J. 2000. Coenoclines of larger foraminifera. *Micropaleontology*, **46**, 127-151.
- Hohenegger, J. 2004. Depth coenoclines and environmental considerations of western pacific larger foraminifera. *Journal of Foraminiferal Research*, **34**, 9-33.
- Hohenegger, J. & Yordanova, E. 2001. Displacement of larger foraminifera at the western slope of Motobu Peninsula (Okinawa, Japan). *Palaios*, **16**, 53-72.
- Holmden, C., Creaser, R.A., Muehlenbachs, K., Leslie, S.A. & Bergstrom, S.M. 1998. Isotopic evidence for geochemical decoupling between ancient epeiric seas and bordering oceans: Implications for secular curves. *Geology*, **26**, 567-570.
- Hook, J.E., Golubic, S. & Milliman, J.D. 1984. Micrite cement in microborings is not necessarily a shallow-water indicator. *Journal of Sedimentary Petrology*, **54**, 425-431.
- Hottinger, L. 1960. Recherches sur les Alvéolines du Paléocène et de l'Eocène. *Schweizerische Palaeontologische Abhandlungen*, **75/76**, 1-243.
- Hottinger, L. 1962. Recherches sur les Alvéolines du Paléocène et de l'Eocène. *Mémoires Suisses de Paléontologie*, **75/76**, 1-243.
- Hottinger, L. 1971. Larger foraminifera common to Mediterranean and Indian Paleocene and Eocene formations. *Annals of the Geological Institute, Hungary*, **54**, 145-151.
- Hottinger, L. 1983. Processes determining the distribution of larger foraminifera in space and time. *Utrecht Micropaleontological Bulletins*, **30**, 239-253.
- Hottinger, L. 1997. Shallow benthic foraminiferal assemblages as signals for depth of their deposition and their limitations. *Bulletin de la Société Géologique de France*, **168**, 491-505.
- Hottinger, L. 1998. Shallow Benthic Foraminifera at the Paleocene-Eocene Boundary. *Strata Serie*, **19**, 61-64.
- Hottinger, L. 2000. Functional morphology of benthic foraminiferal shells, envelopes of cells beyond measure. In: Lee, J.J. & Muller, P.H. (eds) *Advances in the Biology of Foraminifera*. Micropaleontology, Special Publication, **46**, 57-86.
- Hottinger, L. 2001. Learning from the past? In: Box, E. & Pignatti, J. (eds) *The Living World*. Academic Press, San Diego, **IV**, 449-477.
- Hottinger, L. 2006. Illustrated glossary of terms used in foraminiferal research. *Carnets de Géologie Memoir*, **2**, 1-126.

- Hottinger, L. 2009. The Paleocene and earliest Eocene foraminiferal Family Miscellaneidae: neither nummulitids nor rotaliids. *Carnets de Géologie / Notebooks on Geology*, **CG2009/A06**, 1-41.
- Hottinger, L. & Drobne, K. 1980. Early Tertiary conical imperforate foraminifera. *Razprave IV. Razreda SAZU*, **22**, 186-276.
- Hottinger, L., & Drobne, K. 1988. Tertiary Alveolinids: problems linked to the conception of species. *Revue Palaeobiologie (Benthos '86)*, **2**, 665-681.
- Hottinger, L., Lehmann, R. & Schaub, H. 1964. Données actuelles sur la biostratigraphie de Nummulitique Méditerranéen. *Mémoires du Bureau de Recherches géologiques et minières*, **28**, 611-652.
- Hottinger, L., Sameeni J. & Butt, A.A. 1998. Emendation of *Alveolina vredenburgi* Davies & Pinfold 1937 from the Surghar Range, Pakistan. *Dela Sazu, Ljubljana*, **34**, 155-163.
- Hunting Survey Corporation Ltd. 1960. *Reconnaissance geology of part of West Pakistan (a Colombo Plan Cooperative Project)*. Government of Canada, Toronto, 1-550.
- Inan, N., Tasli, K. & Inan, S. 2005. *Laffitteina* from the Maastrichtian-Paleocene shallow marine carbonate successions of the Eastern Pontides (NE Turkey): biozonation and microfacies. *Journal of Asian Earth Sciences*, **25**, 367-378.
- James, N.P. 1997. The cool-water carbonate depositional realm. In: James, N.P. & Clarke, J.A.D. (eds) *Cool-water carbonates*. Society of Sedimentary Geology, Special Publication, **56**, 1-20.
- Jauhri, A.K. 1998. *Miscellanea* Pfender, 1935 (foraminiferida) from the South Shillong region, N.E. India. *Journal of the Palaeontological Society of India*, **43**, 73-83.
- Jauhri, A.K., Agarwal, K.K. 2001. Early Palaeogene in the south Shillong Plateau, NE India: local biostratigraphic signals of global tectonic and oceanic changes. *Palaeogeography, Palaeoclimatology, Palaeoecology*, **168**, 187-203.
- Jauhri, A.K., Misra, P.K., Kishore, S. & Singh, S.K. 2006. Larger foraminiferal and calcareous algal facies in the Lakadong Formation of the South Shillong Plateau, NE India. *Journal of the Palaeontological Society of India*, **51**, 51-61.
- Jenkyns, H.C. 1996. Relative sea-level change and carbon isotopes: data from the upper Jurassic (Oxfordian) of central and Southern Europe. *Terra Nova*, **8**, 75-85.
- Johnson, E.A., Warwick, P.D., Roberts, S.B. & Khan, I.H. 1999. Lithofacies, Depositional Environments, and Regional Stratigraphy of the Lower Eocene Ghazij Formation, Balochistan, Pakistan. *U.S. Geological Survey Professional Paper*, **1599**, 1-76.
- Jones, R.W. 1997. Aspects of the Cenozoic stratigraphy of the Northern Sulaiman Ranges, Pakistan. *Journal of Micropalaeontology*, **16**, 51-58.
- Kaever, M. 1970. Die alttertiären Grossforaminiferen Südost-Afghanistans unter besonderer Berücksichtigung der Nummulitiden-Morphologie, Taxonomie und Biostratigraphie. *Münsterische Forschungen zur Geologie und Paläontologie, Münster, Heft*, **16/17**, 1-400.
- Kaiho, K., Arinobu, T., Ishiwatari, R., Morgans, H.E.G., Okada, H., Takeda, N., Tazaki, K., Zhou, G., Kajiwarra, Y., Matsumoto, R., Hirai, A., Niitsuma, N. & Wada, H. 1996. Latest Paleocene benthic foraminiferal extinction and environmental changes at Tawanui, New Zealand. *Paleoceanography*, **11**, 447-465.
- Kaiho, K., Takeda, K., Petrizzo, M.R. & Zachos, J.C. 2006. Anomalous shifts in tropical Pacific planktonic and benthic foraminiferal test size during the Paleocene-Eocene thermal maximum. *Palaeogeography, Palaeoclimatology, Palaeoecology*, **237**, 456-464.

- Kassi, A.M., Kakar, D.M., Khan, A.S., Umar, M. & Khan, A.T. 1999. Lithostratigraphy of the Cretaceous-Paleocene succession in Quetta region, Pakistan. *Acta Mineralogica Pakistanica*, **10**, 1-9.
- Kassi, A.M., Kelling, G., Kasi, A.K., Umar, M. & Khan, A.S. 2009. Contrasting Late Cretaceous–Palaeocene lithostratigraphic successions across the Bibai Thrust, western Sulaiman Fold-Thrust Belt, Pakistan: Their significance in deciphering the early-collisional history of the NW Indian Plate margin. *Journal of Asian Earth Sciences*, **35**, 435-444.
- Kazmi, A.H. 1995. Sedimentary sequence. In: Bender, F.K. & Raza, H.A. (eds) *Geology of Pakistan*. Stuttgart, Berlin, Gebruder Borntraeger, 162-181.
- Kelly, D.C., Bralower, T.J., Zachos, J.C., Premoli-Silva, I. & Thomas, E. 1996. Rapid diversification of planktonic foraminifera in the tropical Pacific (ODP Site 865) during the Late Paleocene thermal maximum. *Geology*, **24**, 423-426.
- Kemal, A., Balkwill, H.R. & Stoakes, F.A. 1992. Indus basin hydrocarbon plays. In: Ahmad, G., Kemal, A., Zaman, A.S.H. & Humayon, M. (eds) *New Directions and strategies for accelerating petroleum exploration and production in Pakistan*. Oil and Gas Development Corporation, Islamabad, 78-105.
- Khan, A.M. & Srivastava, S.K. 2006. The paleogeographic significance of Aquilapollenites occurrences in Pakistan. *Journal of Asian Earth Sciences*, **28**, 251-258.
- Khan, S.N. & Ahmad, W. 1966. Geology of Langrial iron ore, Hazara District. *Memoirs Geological Survey of Pakistan*, **25**, 1-15.
- Khan, S.R., Khan, M.A., Nawaz, R. & Karim, T. 1990. Stratigraphic control for the age of Peshawar plain magmatism, northern Pakistan. *Geological Bulletin, University of Peshawar*, **23**, 253-263.
- Kiessling, W. 2002. Secular variations in the Phanerozoic reef ecosystem. In: Kiessling, W., Flügel, E. & Golonka, J. (eds) *Phanerozoic Reef Patterns*, 625-690. Society for Sedimentary Geology, Tulsa.
- Kleypas, J.A., Buddemeier, R.W., Archer, D., Gattuso, J.P., Langdon, C., Opdyke, B.N. 1999. Geochemical consequences of increased atmospheric carbon dioxide on coral reefs. *Science*, **284**, 118-120.
- Klootwijk, C.T., Gee, J.S., Peirce J.W. & Smith, G.M. 1991. Constraints on the India-Asia convergence: Paleomagnetic results from Ninetyeast Ridge. *Proceedings of the Ocean Drilling Program, Scientific Results*, **121**, 777-881.
- Koch, P.L., Zachos, J.C. & Gingerich, P.D. 1992. Correlation between Isotope Records in marine and Continental Carbon Reservoirs near the Paleocene Eocene Boundary. *Nature*, **358**, 319-322.
- Köhler, F. & Glaubrecht, M. 2007. Out of Asia and into India - On the molecular phylogeny and biogeography of the endemic freshwater gastropod *Paracrostoma* Cossmann, 1900 (Caenogastropoda: Pachychilidae). *Biological Journal of the Linnean Society of London*, **91**, 627-651.
- Köthe, A., Khan, A.A. & Ashraf, M. 1988. Biostratigraphy of the Surghar Range, Salt Range, Sulaiman Range and the Kohat area, Pakistan, according to Jurassic through Paleogene calcareous nannofossils and Paleogene dinoflagellates. *Geologisches Jahrbuch*, **B71**, 1-87.
- Kump, L.R. 2001. Chill taken out of the tropics. *Nature*, **413**, 470-471.
- Kureshy, A.A. 1978. Tertiary larger foraminiferal zones of Pakistan. *Revista española de micropaleontología*, **X**, 467-483.

- Kurtz, A.C., Kump, L.R., Arthur, M.A., Zachos, J.C. & Paytan, A. 2003. Early Cenozoic decoupling of the global carbon and sulfur cycles. *Paleoceanography*, **18**, 1090, doi:10.1029/2003PA000908.
- Lamarck, J.B. 1801. *Système des animaux sans vertèbres*. Paris, 1-432.
- Lamarck, J. B. 1804. Suit des mémoires sur les fossiles environs de Paris. *Annales Muséum National d'Histoire Naturelle, Paris*, **5**, 179-188.
- Lamarck, J.B. 1804. Suite des Memoires sur les Fossiles des Environs de Paris. *Annales du Museum National d'Histoire Natirre/let*, **5**, 237-245.
- Land, L.S. 1995. Oxygen and carbon isotopic composition of Ordovician brachiopods: implications for coeval seawater: discussion. *Geochimica et Cosmochimica Acta*, **59**, 2843-2844.
- Langer, M.R. & Hottinger, L. 2000. Biogeography of selected “larger” foraminifera. *Micropaleontology*, **46**, 105-126.
- Lathuiliere, B. & Marchal, D. 2009. Extinction, survival and recovery of corals from the Triassic to Middle Jurassic time. *Terra Nova*, **21**, 57-66.
- Latif, M.A. 1964. Variations in abundance and morphology of pelagic Foraminifera in the Paleocene-Eocene of the Rakhi Nala, West Pakistan. *Geological Bulletin of Punjab University*, **4**, 29-100.
- Latif, M.A. 1970. Explanatory notes on the geology of southeastern Hazara to accompany the revised geological map. *Jahrbuch der Geologischen Bundesanstalt, Sonderband*, **15**, 5-20.
- Latif, M.A. 1976. Stratigraphy and micropaleontology of the Galis Group of Hazara, Pakistan. *Geological Bulletin of Punjab University*, **13**, 1-64.
- Le Fort, P. 1996. Evolution of the Himalaya. In: Yin, A. & Harrison, M. (eds), *The Tectonic Evolution of Asia*. Cambridge University Press, Cambridge, 95-109.
- Le Pichon, X., Fournier, M. & Jolivet, J. 1992. Kinematics, topography, shortening and extrusion in the India-Asia collision. *Tectonics*, **11**, 1085-1098.
- Lee, J.L. & Anderson, O.R., 1991. Symbiosis in Foraminifera. In: Lee, J.L. & Anderson, O.R. (eds) *Biology of Foraminifera*. Academic Press, London, 157-220.
- Leeder, M.R. 1982. *Sedimentology: process and product*. George Allen and Unwin, London, 344.
- Leppig, U. 1988. Structural analysis and taxonomic revision of *Miscellanea*, Paleocene larger Foraminifera. *Eclogae Geologicae Helvetiae, Basel*, **81**, 689-721.
- Less, Gy. & Kovács, L.O. 2009. Typological versus morphometric separation of orthophragminid species in single samples – a case study from Horsarrieu (upper Ypresian, SW Aquitaine, France). *Revue de Micropaleontologie*, **52**, 267-288.
- Less, Gy., Özcan, E., Báldi-Beke, M. & Kollányi, K. 2007. Thanetian and early Ypresian Orthophragmines (Foraminifera: Discocyclinidae and Orbitoclypeidae) from the Central Western Tethys (Turkey, Italy and Bulgaria) and their Revised Taxonomy and Biostratigraphy. *Rivista Italiana di Paleontologia e Stratigrafia*, **113**, 419-448.
- Leymerie, A. 1846. Mémoire sur le terrain à Nummulites (épicrotécé) des Corbières et de la Montagne Noire. *Mémoires de la Société géologique de France*, **1** (2), 5-41.
- Linne, C. 1758. *Systema Naturae*, Volume 1, 10<sup>th</sup> edition, Holmiae. Stockholm.
- Lipps, J.H. 1982. Biology/paleobiology of foraminifera. In: Broadhead, T.W. (ed.) *Foraminifera, Notes for a Short Course*. Palaeontological Society, University of Tennessee, 37-50.
- Loeblich, A.R. & Tappan, H. 1988. *Foraminiferal Genera and their Classification*. Van Nostrand Reinhold, New York, 1-1728.

- Loeblich, A.R. & Tappan, H. 1964. Foraminiferal Classification and Evolution. *Journal of the Geological Society of India*, **5**, 5-39.
- Lohmann, K.C. 1988. Geochemical patterns of meteoric diagenetic systems and their application to studies of paleokarst. In: James, N.P. & Choquette, P.W. (eds) *Paleokarst*. Springer-Verlag, New York, 58-80.
- Longinelli, A., Wierzbowski, H. & Di Matteo, A. 2003.  $\delta^{18}\text{O}$  ( $\text{PO}_4^{3-}$ ) and  $\delta^{18}\text{O}$  ( $\text{CO}_3^{2-}$ ) from belemnite guards from Eastern Europe: implications for palaeoceanographic reconstructions and for the preservation of pristine isotopic values. *Earth and Planetary Science Letters*, **209**, 337-350.
- Loucks, R.G., Moody, R.T., Bellis, J.K. & Brown, A.A. 1996. Regional depositional setting and pore network of the El Garia Fm. (Metlaoui Group, Lower Eocene), Offshore Tunisia. *Abstracts of the Fifth Tunisian Petroleum Exploration Conference, Tunis*, 147-171.
- Loucks, R.G., Moody, R.T.J., Bellis, J.K. & Brown, A.A. 1998. Regional depositional setting and pore network systems of the El Garia formation (Metlaoui Group, Lower Eocene), Offshore Tunisia. In: MacGregor, D.S., Moody, R.T.J. & Clark-Lowes, D.D. (eds) *Petroleum Geology of North Africa*. Special Publication Geological Society London, **132**, 355-374.
- Luterbacher, H.P., Ali, J.R., Brinkhuis, H., Gradstein, F.M., Hooker, J.J., Monechi, S., Ogg, J.G., Powell, J., Röhl, U., Sanfilippo, A. & Schmitz, B. 2004. The Paleogene Period. In: Gradstein, F., Ogg, J. & Smith, A. (eds.), *A Geological Timescale 2004*. Cambridge University Press, 384-408.
- Magioncalda, R., Dupuis, C., Smith, T., Steurbaut, E. & Gingerich, P.D. 2004. Paleocene-Eocene carbon isotope excursion in organic carbon and pedogenic carbonate: Direct comparison in a continental stratigraphic section. *Geology*, **32**, 553-556.
- Mangin, J.P. 1954. Description d'un nouveau genre de foraminifere: *Fallotella alavensis*. *Bulletin scientifique de Bourgogne*, **14**, 209-219.
- Marie, P. 1945. Sur *Laffitteina bibensis* et *Laffitteina monodi*, nouveau genre et nouvelles especes de foraminifères du Montien. *Bulletin de la Société Géologique de France* **5**, 419-434.
- Marshall, F.F. & Davis, P.J. 1981. Submarine lithification on windward reef slopes: Capricorn-Bunker Group, Southern Great Barrier Reef. *Journal of Sedimentary Petrology*, **51**, 953-960.
- Martin, K. 1890. Untersuchungen über den Bau von Orbitolina (Patellina auct) von Borneo. *Leiden, Sammlungen des Geologischen Reichs- Museums*, **1**, 209-231.
- Martini, E. 1971. Standard Cenozoic and Quaternary calcareous nannoplankton zonation. *Proceedings of the Second International Conference on Planktonic Microfossils Rome*, **2**, 739-777.
- Mathur, N.S., Juyal, K.P. & Kumar, K. 2009. Larger foraminiferal biostratigraphy of lower Palaeogene successions of Zaskar Tethyan and Indus-Tsangpo Suture Zones, Ladakh, India in the light of additional data. *Himalayan Geology*, **30**, 45-68.
- Matsumaru, K. & Kimora, K. 1989. Larger foraminifera from the Eocene Shimizu and Miocene Misaki formations in Tosa Shimizu City, Kochi prefecture, Shikoku, Japan. *Transactions of Palaeontological Society of Japan*, **156**, 255-269.
- Meissner, C. R., Hussain, M., Rashid, M.A. & Sethi, U.B. 1975. Geology of the Parachinar quadrangle, Pakistan. *United States Geological Survey Professional Paper*, **716-F**, 1-24.

- Meissner, C.R., Master, J.M., Rashid, M.A. & Hussain, M. 1968. Stratigraphy of the Kohat quadrangle. *United States Geological Survey, Project Report*, **PK-20**, 1-86.
- Meissner, C.R., Master, J.M., Rashid, M.A. & Hussain, M. 1974. Stratigraphy of the Kohat quadrangle, West Pakistan. *United States Geological Survey Professional Paper*, **716-D**, 1-75.
- Melim, L.A., Swart, P.K. & Maliva, R.G. 2001. Meteoric and marine burial diagenesis in the subsurface of the Great Bahama Bank. In: Ginsburg, R.N. (ed.), *Subsurface Geology of a Prograding Carbonate Platform Margin, Great Bahama Bank*. Society for Sedimentary Geology, Special Publication, **70**, 137-162.
- Michelin, H. 1846. *Iconographie zoöphytologique*. P. Bertrand, Paris, 1-348.
- Middlemiss, C.S. 1896. The geology of Hazara and Black Mountain. *Memoir of the Geological Survey of India*, **26**, 1-302.
- Moullade, M. 1965. Contribution au probleme de la classification des Orbitolinidae (Foraminiferida, Lituolacea). *Comptes Rendus Hebdomadaires des Seances, Academie des Sciences, Paris*, **260**, 4031-4034.
- Moussavian, E. 1984. Die Gosau- und Alttertiär-Geröll der Angerberg-Schichten (Höheres Oligozän, Unterinntal, Nördliche Kalkalpen). *Facies*, **10**, 1-86.
- Munier-Chalmas, E. 1887. Sur la Cyclolina et trois nouveaux genres de foraminiferes de couches a Rudistes: Cyclopsina, Dicyclina et Spirocyclina, Compte Rendu des Seances. *Societe Geologique de France*, **1887**, 30-31.
- Murray, J.W. 1991. *Ecology and Palaeoecology of benthic foraminifera*. Longman Scientific and Technical, New York.
- Mutti, M. & Hallock, P. 2003. Carbonate systems along nutrient and temperature gradients: Some sedimentological and geochemical constraint. *International Journal of Earth Science*, **92**, 465-475.
- Mutti, M., John, C.M. & Knoerich, A.C. 2006. Chemostratigraphy in Miocene heterozoan carbonate settings: applications, limitations and perspectives. In: Pedley, H.M. & Carannante, G. (eds) *Cool-Water Carbonates: Depositional Systems and Palaeoenvironmental Controls*. Geological Society London Special Publication, **255**, 311-322.
- Nagappa, Y. 1959a. Note on operculinoids Hanzawa 1935. *Palaeontology*, **2**, 21-23.
- Nagappa, Y. 1959b. Foraminiferal biostratigraphy of the Cretaceous-Eocene succession in the India-Pakistan, Burma region. *Micropaleontology*, **5**, 145-192.
- Najman, Y. 2006. The detrital record of orogenesis: a review of approaches and techniques used in the Himalayan sedimentary basins. *Earth Science Review*, **74**, 1-72.
- Nebelsick, J.H., Rasswer, M. & Bassi, D. 2005. Facies dynamic in Eocene to Oligocene Circumalpine carbonates. *Facies*, **51**, 197-216.
- Nebelsick, J.H., Stingl, V. & Rasser, M. 2001. Autochthonous facies and allochthonous debris flows compared: Early Oligocene carbonate facies patterns of the Lower Inn Valley (Tyrol, Austria). *Facies*, **44**, 1-45.
- Nekola, J.C. & White, P.S. 1999: The distance decay of similarity in biogeography and ecology. *Journal of Biogeography*, **26**, 867-878.
- Neuweiler, F., Gautret, P., Thiel, V., Lange, R., Michaelis, W. & Reitner, J. 1999. Petrology of Lower Cretaceous carbonate mud mounds (Albian, N Spain): insight into organomineralic deposits of the geological record. *Sedimentology*, **46**, 837-859.
- Newberry, D., Cambell, E.F.J., Proctor, J. & Still, M.J. 1996. Primary lowland dipterocarp forest at Danum Valley, Sabah, Malaysia. Species composition and patterns in the understory. *Vegetatio*, **122**, 193-220.

- Nuttall, W.L.F. 1925. The stratigraphy of the Laki Series (Lower Eocene) of parts of Sind and Baluchistan (India); with a description of the larger foraminifera contained in those beds. *Quarterly Journal of the Geological Society*, **81**, 337-373.
- Nuttall, W.L.F. 1926. The larger foraminifera of the Upper Ranikot Series (Lower Eocene) of Sind, India. *Geological Magazine*, **63**, 112-121.
- Oldham, R.D. 1890. Report on the geology and economic resources of the country adjoining the Sind-Pishin railway between Sharigh and Spintangi, and of the country between it and Khattan. *Records of the Geological Survey of India*, **23**, 93-109.
- O'Neil, J.R., Clayton, R.N. & Mayeda, T.K. 1969. Oxygen isotope fractionation in divalent metal carbonates. *Journal of Chemical Physics*, **51**, 5547-58.
- Orue-Etxebarria, X., Pujalte, V., Bernaola, G., Apellaniz, E., Baceta, J.I., Payros, A., Nunez-Betelu, K., Serra-Kiel, J. & Tosquella, J. 2001. Did the Late Paleocene Thermal Maximum affect the evolution of larger foraminifers? Evidence from calcareous plankton of the Campo Section (Pyrenees, Spain). *Marine Micropaleontology*, **41**, 45-71.
- Özgen-Erdem, N. & Akyazi, M. 2001. The benthic foraminifera of Thanetian of Padriciano (Italy), Sopada (Slovenia) and Western Pontids (Turkey). *Bulletin of Earth Sciences Application and Research Centre of Hacettepe University*, **23**, 87-98.
- Özgen-Erdem, N., Inan, N., Akyazi, M. & Tunoglu, C. 2005. Benthonic foraminiferal assemblages and microfacies analysis of Paleocene-Eocene carbonate rocks in the Kastamonu region, Northern Turkey. *Journal of Asian Earth Sciences*, **25**, 403-417.
- Özgen-Erdem, N., Akyazi, M. & Karabaşoğlu, A. 2007. Biostratigraphic interpretation and systematics of Alveolina assemblages from the Ilerdian–Cuisian limestones of Southern Eskioehir, Central Turkey. *Journal of Asian Earth Sciences*, **29**, 911-927.
- Pak, D.K. & Miller, K.G. 1992. Paleocene to Eocene benthic foraminiferal isotopes and assemblages: implications for deep water circulation. *Paleoceanography*, **7**, 405-422.
- Palmer, D.K. 1934. Some large fossil foraminifera from Cuba. *Memorias de la Sociedad Cubana de Historia Natural*, **8**, 235-265.
- Pannacciulli, F.G., Bishop, J.D.D. & Hawkins, S.J. 1997. Genetic structure of populations of two species of *Chthamalus* (Crustacea: Cirripedia) in the north-east Atlantic and Mediterranean. *Marine Biology*, **128**, 73-82.
- Parente, M., Frijia, G. & Di Lucia, M. 2007. Carbon-isotope stratigraphy of Cenomanian-Turonian platform carbonates from the southern Apennines (Italy): a chemostratigraphic approach to the problem of correlation between shallow-water and deep-water successions. *Journal of the Geological Society*, **164**, 609-620.
- Parente, M., Frijia, G., Di Lucia, M., Jenkyns, H.C., Woodfine, R.G. & Baroncini, F. 2008. Stepwise extinction of larger foraminifers at the Cenomanian-Turonian boundary: a shallow-water perspective on nutrient fluctuations during Oceanic Anoxic Events 2 (Bonarelli Event). *Geology*, **36**, 715-718.
- Pascoe, E.H. 1920. Petroleum in the Punjab and North West Frontier Range. *Memoir of the Geological Survey of India*, **40**, 341-493.
- Pascoe, E.H. 1963. A manual of the geology of India and Burma. *Government of India Press, Calcutta*, **3**, 2073-2079.

- Patterson, W.P. & Walter, L.M. 1994. Depletion of  $^{13}\text{C}$  in seawater  $\Sigma\text{CO}_2$  on modern carbonate platforms: significance for the carbon isotopic record of carbonates. *Geology*, **22**, 885-888.
- Pearson, P.N., Ditchfield, P.W., Singano, J., Harcourt-Brown, K.G., Nicholas, C.J., Olsson, R.K., Shackleton, N.J. & Hall, M.A. 2001. Warm tropical sea surface temperatures in the Late Cretaceous and Eocene epochs. *Nature*, **413**, 481-487.
- Pearson, P.N., van Dongen, B.E., Nicholas, C.J., Pancost, R.D., Schouten, S., Singano, J.M. & Wade, B.S. 2007. Stable warm tropical climate through the Eocene Epoch. *Geology*, **35**, 211-214.
- Perrin, C. 1992. Signification écologique des foraminifères acervulinidés et leur rôle dans la formation de faciès récifaux et organogènes depuis le Paléocène. *Geobios*, **25**, 725-751.
- Perrin, C. 2002. Tertiary: the emergence of modern reef ecosystems. In: Kiessling, W., Flügel, E. & Golonka, J. (eds) *Phanerozoic Reef Patterns*. Society of Sedimentary Geology Special Publication, Tulsa, **72**, 587-621.
- Petrizzo, M.R. 2007. The onset of the Paleocene-Eocene Thermal Maximum (PETM) at Sites 1209 and 1210 (Shatsky Rise, Pacific Ocean) as recorded by planktonic foraminifera. *Marine Micropaleontology*, **63**, 187-200.
- Pfender, J. 1935. À propos de *Siderolites vidali* et de quelques autres. *Bulletin de la Société géologique de France*, **4**, 225-236.
- Pignatti, J. 1994. Paleobiogeography of Palaeogene Larger Foraminifera from the Mediterranean Tethys to the Western Pacific Using Parsimony Analysis: a Preliminary Attempt. *Bollettino Della Società Paleontologica Italiana*, **2**, 243-252.
- Pignatti, J., Di Carlo M., Benedetti, A., Bottino, C., Briguglio, A., Falconi, M., Matteucci, R., Perugini, G. & Ragusa, M. 2008. SBZ 2-6 larger foraminiferal assemblages from the Apulian and Pre-Apulian Domains. *Atti del Museo civico di storia naturale di Trieste*, **53**, 131-146.
- Pinfold, E.S. 1918. Notes on structure and stratigraphy in NW Punjab. *Records of the Geological Survey of India*, **49**, 138-161.
- Plaziat, J.C. & Perrin, C. 1992. Multikilometer-sized reefs built by foraminifera (Solenomeris) from the early Eocene of the Pyrenean domain (S. France, N. Spain): Palaeoecologic relations with coral reefs. *Palaeogeography, Palaeoclimatology, Palaeoecology*, **96**, 195-231.
- Pomar, L. & Hallock, P. 2008. Carbonate factories: a conundrum in sedimentary geology. *Earth Science Reviews*, **87**, 134-169.
- Pujalte, V. & Schmitz, B. 2006. Abrupt climatic and sea level changes across the Paleocene-Eocene boundary, as recorded in an ancient coastal plain setting (Pyrenees, Spain). In: Caballero, F., Apellaniz, E., Baceta, J.I., Bernaola, G., Orue-Etxebarria, X., Payros, A. & Pujalte, V. (eds.) *Climate and Biota of the Early Paleogene*. Volume of abstracts, Bilbao, Spain, 103.
- Pujalte, V., Baceta, J.I., Schmitz, B., Orue-Etxebarria, X., Payros, A., Bernaola, G., Apellaniz, E., Caballero, F., Robador, A., Serra-Kiel, J. & Tosquella, J. 2009a. Redefinition of Ilerdian Stage (early Eocene). *Geologica Acta*, **7**, 177-194.
- Pujalte, V., Schmitz, B., Baceta, J.I., Orue-Etxebarria, X., Bernaola, G., Dinares-Turell, J., Payros, A., Apellaniz, E. & Caballero, F. 2009b. Correlation of the Thanetian-Ilerdian turnover of larger foraminifera and the Paleocene-Eocene thermal maximum: confirming evidence from the Campo area (Pyrenees, Spain). *Geologica Acta*, **7**, 161-175.

- Qayyum, M., Niem, A.R. & Lawrence, R.D. 2001. Detrital modes and provenance of the Paleogene Khojak Formation in Pakistan: implications for early Himalayan orogeny and unroofing. *Geological Society of America Bulletin*, **133**, 320-332.
- Racey, A. 1995. Lithostratigraphy and larger foraminiferal (nummulitid) biostratigraphy of the Tertiary of Northern Oman. *Micropaleontology*, **41**, 1-123.
- Rahaghi, A. 1983. Stratigraphy and faunal assemblage of Paleocene-Lower Eocene in Iran. *National Iranian Oil Company, Geological Laboratories, Teheran*, **10**, 1-73.
- Rao, S.R.N. 1940. On *Orbitosiphon*, a new genus of orbitoidal foraminifera from the Ranikot beds of the Punjab Salt Range (N. W. India). *Current Science, Bangalore*, **9**, 414-415.
- Rao, S.R.N. 1944. A revision of some foraminifera described by Douvillé from the Kampa system of Tibet. *Proceedings of the National Academy of Science of India*, **14**, 93-101.
- Rasser, M.W. & Nebelsick, J.H. 2003. Provenance analysis of Oligocene autochthonous and allochthonous coralline algae: a quantitative approach towards reconstructing transported assemblages. *Palaeogeography, Palaeoclimatology, Palaeoecology*, **201**, 89-111.
- Raymo, M.E. & Ruddiman, W.F. 1992. Tectonic forcing of the Late Cenozoic climate. *Nature*, **359**, 117-122.
- Raymo, M.E., Ruddiman, W.F. & Froelich, P.N. 1988. Influence of late Cenozoic mountain building on ocean geochemical cycles. *Geology*, **16**, 649-653.
- Raza, S.M. 2001a. The Eocene red beds of the Kala Chitta Range (Northern Pakistan) and its stratigraphic implications on the Himalayan Foredeep Basin. *Geological Bulletin, University of Peshawar*, **34**, 83-104.
- Raza, S.M. 2001b. Stratigraphic chart of Pakistan. *Geological Survey of Pakistan, Quetta*, 1 sheet.
- Reichel, M. 1937. Etude sur les alvéolines. *Mémoires de la Société Paléontologique Suisse*, **57/59**, 1-147.
- Reiss, Z. & Hottinger, L. 1984. *The Gulf of Aqaba: ecological micropaleontology*. Springer, New York, 1-354.
- Reitner, J., Neuweiler, F., Dingle, P., Flajs, G., Gautret, P., Hensen, C., Hüssner, H., Kaufmann, B., Keupp, H., Leinfelder, R.R., Meischner, D., Paul, J., Schäfer, P., Vigener, M., Warnke, K. & Weller, H. 1995. Mud mounds: a polygenetic spectrum of fine-grained carbonate buildups. *Facies*, **32**, 1-70.
- Renema, W. & Troelstra, S.R. 2001. Larger foraminifera distribution on a mesotrophic carbonate shelf in SW Sulawesi (Indonesia). *Palaeogeography, Palaeoclimatology, Palaeoecology*, **175**, 125-147.
- Renema, W. 2008. Habitat selective factors influencing the distribution of large benthic Foraminifera assemblages over the Kepulauan Seribu. *Marine Micropaleontology*, **68**, 286-298.
- Renema, W., Bellwood, D.R., Braga, J.C., Bromfield, K., Hall, R., Johnson, K.G., Lunt, P., Meyer, C.P., McMonagle, L.B., Morley, R.J., O'Dea, A., Todd, J.A., Wesselingh, F.P., Wilson, M.E. & Pandolfi, J.M. 2008. Hopping Hotspots: Global Shifts in Marine Biodiversity. *Science*, **321**, 654-657.
- Richter, F.M., Rowley, D.B. & Depaolo, D.J. 1992. Sr isotope evolution of seawater: the role of tectonics. *Earth and Planetary Science Letters*, **109**, 11-23.
- Romero, J., Caus, E. & Rossel, J. 2002. A model for the palaeoenvironmental distribution of larger foraminifera based on Late Middle Eocene deposits on the margin of the south Pyrenean basin (SE Spain). *Palaeogeography, Palaeoclimatology, Palaeoecology*, **179**, 43-56.

- Rose, K.D., Smith, T., Rana, R.S., Sahni, A., Singh, H., Missiaen, P. & Folie, A. 2006. Early Eocene (Ypresian) continental vertebrate assemblage from India, with description of a new anthracobunid (mammalia, tethytheria). *Journal of Vertebrate Paleontology*, **26**, 219-225.
- Rowley, D.B. 1996. Age of initiation of collision between India and Asia; a review of stratigraphic data. *Earth and Planetary Science Letters*, **145**, 1-13.
- Sahni, A. 2006. Biotic response to the India-Asia collision. *Palaeontographica Abteilung A –Stuttgart*, **278**, 15-26.
- Sahni, A. & Jolly, A. 1993. Eocene mammals from Kalakot, Kashmir Himalaya: community structure, taphonomy and palaeobiogeographical implications. *Kaupia, Darmstädter Beiträge zur Naturgeschichte*, **3**, 209-222.
- Samanta, B.K. 1965. *Discocyclina* from the Upper Eocene of Assam, India. *Micropaleontology*, **11**, 415-430.
- Samanta, B.K. 1969. Taxonomy and stratigraphy of the Indian species of *Discocyclina* (foraminifera). *Geological Magazine*, **106**, 115-129.
- Samantha, B.K. 1973. Planktonic foraminifera from the Paleocene-Eocene succession in the Rakhi Nala, Sulaiman Range, Pakistan. *Bulletin of the British Museum (Natural History), Geology*, **22**, 421-482.
- Samanta, B. K. & Lahiri, A. 1985. The occurrence of *Discocyclina* Gumbel in the middle Eocene Fulra limestone of Cutch, Gujarat, Western India, with notes on species reported from the Indian region. *Bulletin of Geological Mining and Metallurgical Society of India*, **52**, 211-295.
- Sameeni, S. J. & Butt, A. A. 2004. Alveolinid biostratigraphy of the Salt Range succession, Northern Pakistan. *Revue de Paléobiologie, Genève*, **23**, 505-527.
- Saraswati, P.K., Ramesh, R. & Navada, S.V. 1993. Paleogene isotopic temperatures of western India. *Lethaia*, **26**, 89-98.
- Schaub, H. 1981. Nummulites et Assilines de la Téthys paléogène, taxinomie, phylogenèse et biostratigraphie. *Schweizerische Palaeontologische Abhandlungen*, **104-106**, 1-236.
- Scheibner, C. & Speijer, R.P. 2008a. Late Paleocene-early Eocene Tethyan carbonate platform evolution -A response to long- and short-term paleoclimatic change. *Earth-Science Reviews*, **90**, 71-102.
- Scheibner, C. & Speijer, R.P. 2008b. Decline of Coral Reefs during Late Paleocene to Early Eocene Global Warming. *eEarth*, **3**, 19-26.
- Scheibner, C. & Speijer, R.P. 2009. Recalibration of the Tethyan Shallow-Benthic Zonation Across the Paleocene-Eocene Boundary; the Egyptian Record. *Geologica Acta*, **7**, 195-214.
- Scheibner, C., Rasser, M.W. & Mutti, M. 2007. The Campo section (Pyrenees, Spain) revised: implications for changing carbonate assemblages across the Paleocene–Eocene boundary. *Palaeogeography, Palaeoclimatology, Palaeoecology*, **248**, 145-168.
- Scheibner, C., Speijer, R.P. & Marzouk, A.M. 2005. Larger foraminiferal turnover during the Paleocene/Eocene Thermal Maximum and paleoclimatic control on the evolution of platform ecosystems. *Geology*, **33**, 493-496.
- Schlager, W. 2000. Sedimentation rates and growth potential of tropical, cool-water and mud-mound carbonate systems. *Geological Society of London, Special Publication*, **178**, 217-227.
- Schlager, W. 2003. Benthic carbonate factories in the Phanerozoic. *International Journal of Earth Sciences*, **92**, 445-464.
- Schlotheim, E.F. 1820. *Die Petrefactenkunde*. Gotha, Germany, 1-100.

- Schlumberger, C. 1903. Troisième note sur les Orbitoides. *Bulletin de la Société géologique de France*, **4**, 273-289.
- Schlumberger, C. 1904. Quatrième note sur les Orbitoides. *Bulletin de la Société géologique de France*, **4**, 119-135.
- Schlumberger, C. 1905. Deuxième note sur les Miliolidées trématophorées. *Bulletin de la Société géologique de France*, **5**, 115-134.
- Schlumberger, C. & Munier-Chalmas, E. 1884. Note sur les Miliolides trématophores. *Bulletin de la Société géologique de France*, **3**, 629-630.
- Schmitz, B. & Pujalte, V. 2007. Abrupt increase in extreme seasonal precipitation at the Paleocene-Eocene boundary. *Geology*, **35**, 215-218.
- Schmitz, B., Asaro, F., Molina, E., Monechi, S., von Salis, K. & Speijer, R.P. 1997. High-resolution iridium,  $\delta^{13}\text{C}$ ,  $\delta^{18}\text{O}$ , foraminifera and nannofossil profiles across the latest Paleocene benthic extinction event at Zumaya, Spain. *Palaeogeography, Palaeoclimatology, Palaeoecology*, **133**, 49-68.
- Schmitz, B., Pujalte, V. & Núñez-Betelu, K. 2001. Climate and sealevel perturbations during the Initial Eocene Thermal Maximum: evidence from siliciclastic units in the Basque Basin (Ermua, Zumaia and Trabakua Pass), northern Spain. *Palaeogeography, Palaeoecology, Palaeoclimatology*, **165**, 299-320.
- Schneider, J., Bakker, R.J., Bechstädt, T. & Littke, R. 2008. Fluid evolution during burial diagenesis and subsequent orogenic uplift: the La Vid Group (Cantabrian Zone, Northern Spain). *Journal of Sedimentary Research*, **78**, 282-300.
- Scholle, P.A. & Ulmer-Scholle, D.S. 2003. A Color Guide to the Petrography of Carbonate Rocks. *American Association of Petroleum Geologists Memoir*, **77**, 141-177.
- Schwager, C. 1876. Saggio di una classificazione dei Foraminiferi avuto riguardo alle loro famiglie naturali. *Bolletino R. Comitato Geologico d'Italia*, **7**, 475-485.
- Schwager, C. 1877. Quadro del proposto sistema di classificazione dei foraminiferi con guscio. *Bolletino R. Comitato Geologico d'Italia*, **8**, 18-27.
- Schwager, C. 1883. Die foraminiferen aus den Eocaenablagerungen der libyschen Wüste und Aegyptiens. *Palaeontographica*, **30**, 79-154.
- Searle, M.P., Windley, B.F., Coward, M.P., Cooper, D.J.W., Rex, A.J., Rex, D., Tingdong, L.X.X., Jan, M.Q., Thakur, V.C. & Kumar, S. 1987. The closing of Tethys and tectonics of the Himalayas. *Geological Society of America Bulletin*, **98**, 678-701.
- Serra-Kiel, J., Hottinger, L., Caus, E., Drobne, K., Fernandez, C., Jauhri, A.K., Less, G., Pavlovec, R., Pignatti, J., Samsó, J.M., Schaub, H., Sirel, E., Strougo, A., Tambareau, Y., Tosquella, Y. & Zakrevskaya, E. 1998. Larger foraminiferal biostratigraphy of the Tethyan Paleocene and Eocene. *Bulletin de la Société Géologique de France*, **169**, 281-299.
- Sewall, J.O., Huber, M. & Sloan, L.C. 2004. A method for using a fully coupled climate system model to generate detailed surface boundary conditions for paleoclimate modelling investigations: an early Paleogene example. *Global and Planetary Change*, **43**, 173-182.
- Shackleton, N.J. & Hall, M.A. 1984. Carbon isotope data from Leg 74 sediments. In: Moore, T.C., Rabinowitz, P.D., Boersma, A., Borella, P.E., Chave, A.D., Duee, G., Futterer, D.K., Jiang, M.J., Kleinert, K., Lever, A., Manivit, H., O'Connell, S., Richardson, S.H. & Shackleton, N.J. (eds) *Initial reports of the deep sea drilling project*, **74**, 613-619.
- Shah, S.M.I. 1977. Stratigraphy of Pakistan. *Memoirs of the Geological Survey of Pakistan*, **12**, 1-137.

- Shah, S.M.I. 1990. Coal resources of Baluchistan. *In: Kazami, A.H. & Siddiqui, R.A.* (eds) *Significance of the coal resources of Pakistan*. Geological Survey of Pakistan/United States Geological Survey, Quetta/ Reston, 63-93.
- Shinn, E. 1983. Tidal flats. *In: Scholle, P.A., Bebout, D.G. & Moore, C.H.* (eds.) *Carbonate Depositional Environments*. American Association of Petroleum Geologists Memoir, **33**, 171-210.
- Siddiqui, Q.A. 2006. The ostracod genus *Paijenborchella* and some of its species in the Early Tertiary of Pakistan. *Journal of Micropalaeontology*, **25**, 165-72.
- Silvestri, A. 1907. Fossili d'orioniani dei dintorni di Termini- Imerese (Palermo). *Atti della Pontificia Accademia dei Nuovi Lincei*, 1-60.
- Silvestri, A. 1939. Foraminiferi dell' Eocene della Somalia. *Palaeontographica italica*, **32**, 1-102.
- Sirel, E. 1969. Rotaliidae familyasina ait yeni bir cins *Orduina* n. gen. Ve türü hakkında. *Maden Tetkik ve Arama Enstitü sü Dergisi*, **73**, 160-162.
- Sirel, E. 1976. Polatli (GB Ankara) güneyinde bulunan *Alveolina*, *Nummulites*, *Ranikothalia* ve *Assilina* cinslerinin sistematik incelemeleri. *Türkiye Jeoloji Kurumu Bülteni*, **19**, 89-102.
- Sirel, E. 1994. *Orduina* erki 1969 renamed as *Laffitteina* erki (Sirel) from the Thanetian of Ordu and Burdur (Turkey). *Maden Tetkik ve Arastirma Enstitüsü Dergisi (foreign edition)*, **116**, 47-48.
- Sirel, E. 1996. Description and geographic, stratigraphic distribution of the species of *Laffitteina* Marie from the Maastrichtian and Paleocene of Turkey. *Revue de Paléobiologie*, **15**, 9-35.
- Sirel, E. 1997a. *Karsella*, a new complex orbitolinid (Foraminiferida) from the Thanetian limestone of the Van region (East Turkey). *Micropaleontology*, **43**, 206-210.
- Sirel, E. 1997b. The species of *Miscellanea* Pfender, 1935 (Foraminiferida) in the Thanetian-Ilerdian sediments of Turkey. *Revue de Paléobiologie, Genève*, **16**, 77-99.
- Sirel, E. 1998. Foraminiferal description and biostratigraphy of the Paleocene-Lower Eocene shallow-water limestones and discussion on the Cretaceous-Tertiary boundary in Turkey. *General Directorate of the Mineral Research and Exploration, Monographs Series*, **2**, 1-117.
- Sirel, E. & Gündüz, H. 1985. *Vania*, a new foraminiferal genus from the Thanetian of the Van region (East Turkey). *Bulletin of the Mineral Research and Exploration Institute (MTA) of Turkey*, **101/102**, 20-24.
- Sluijs, A., Brinkhuis, H., Schouten, S., Bohaty, S.M., John, C.M., Zachos, J.C., Reichert, G.J., Crouch, E.M. & Dickens, G.R. 2007. Environmental precursors to rapid light carbon injection at the Palaeocene/Eocene boundary. *Nature*, **450**, 1218-1221.
- Smith, A.G., Smith, D.G. & Funnell, B.M. 1994. *Atlas of Mesozoic and Cenozoic Coastlines*. Cambridge University Press, 1-112.
- Smout, A.H. 1954. Lower Tertiary foraminifera of the Qatar Peninsula. *Bulletin of the British Museum (Natural History)*, **9**, 1-80.
- Smout, A.H. & Haque. A.F.M.M. 1956. A note on the larger foraminifera and ostracoda of the Ranikot from the Nammal Gorge, Salt Range, Pakistan. *In: Haque, A. F. M. M.* (ed.) *Shorter contributions to the Geology of Pakistan*. Records of the Geological Survey of Pakistan, **8**, 49-60.

- Sowerby, J.C. 1840. Systematic list of organic remains. Appendix to Grant C.W.: Memoir to illustrate a geological map of Cutch. *Transaction Geological Society*, **5**, 327-329.
- Speijer, R.P. & Wagner, R. 2002. Sea-level changes and black shales associated with the late Paleocene Thermal Maximum; organic-geochemical and micropaleontologic evidence from the southern Tethyan margin (Egypt-Israel). *In: Koeberl, C. & MacLeod, K.G. (eds) Catastrophic Events & Mass Extinctions: Impacts and Beyond*. Geological Society of America Special Paper, 533-549.
- Speijer, R.P., Schmitz, B. & van der Zwaan, G.J. 1997. Benthic foraminiferal extinction and repopulation in response to latest Paleocene Tethyan anoxia. *Geology*, **25**, 683-686.
- Spero, H.J., Bijma, J., Lea, D.W. & Bemis, D.E. 1997. Effect of seawater carbonate concentration on foraminiferal carbon and oxygen isotopes. *Nature*, **390**, 497-500.
- Springer, V.G. 1982. Pacific plate biogeography with special reference to shore fishes. *Smithsonian Contributions to Zoology*, **367**, 1-182.
- Stanley, S.M. & Hardie, L.A. 1998. Secular oscillations in the carbonate mineralogy of reef-building and sediment-producing organisms driven by tectonically forced shifts in seawater chemistry. *Palaeogeography, Palaeoclimatology, Palaeoecology*, **144**, 3-19.
- Stanton, R.J., Jeffery, D.L. & Guillemette, R.N. 2000. Oxygen minimum zone and internal waves as potential controls on location and growth of Waulsortian Mounds (Mississippian, Sacramento Mountains, New Mexico). *Facies*, **42**, 161-176.
- Steinhauser, N. 1969. *Recherches stratigraphiques dans le Crétacé inférieur de la Savoie occidentale (France)*. PhD thesis, University of Genève, Suisse, 1-287.
- Steurbaut, E., Magioncalda, R., Dupuis, C., Van Simaëys, S., Roche, E. & Roche, M. 2003. Palynology, paleoenvironments, and organic carbon isotope evolution in lagoonal Paleocene-Eocene boundary settings in North Belgium. *In: Wing, S.L., Gingerich, P., Schmitz, B. & Thomas, E. (eds) Causes and Consequences of Globally Warm Climates in the Early Paleogene*. Geological Society of America, Special Paper, **369**, 291-317.
- Swart, P.K. & Eberli, G. 2005. The nature of the  $\delta^{13}\text{C}$  of periplatform sediments: implications for stratigraphy and the global carbon cycle. *Sedimentary Geology*, **175**, 115-129.
- Tewari, V.C., Kumar, K., Lokho K. & Siddaiah, N.S. 2010. Lakadong limestone: Paleocene-Eocene boundary carbonates sedimentation in Meghalaya, northeastern India. *Current Science*, **98**, 88-95.
- Thiry, M., Milnes, A.R., Rayot, V. & Simon-Coincon, R. 2006. Interpretation of paleoweathering features and successive silicifications in the Tertiary regolith of inland Australia. *Journal of the Geological Society*, **163**, 723-736.
- Thomas, D.J., Zachos, J.C., Bralower, T.J., Thomas, E. & Bohaty, S. 2002. Warming the fuel for the fire: Evidence for the thermal dissociation of methane hydrate during the Paleocene-Eocene thermal maximum. *Geology*, **30**, 1067-1070.
- Thomas, E. 2007. Cenozoic mass extinctions in the deep sea: what perturbs the largest habitat on Earth? *In: Monechi, S., Coccioni, R. & Rampino, M.R. (eds) Large Ecosystem Perturbations: Causes and Consequences*. *The Geological Society of America Special Paper*, **424**, 1-24.
- Thompson, J.B. 2001. Microbial whitings. *In: Riding, R.E. & Awramik, S.M. (eds) Microbial sediments*. Springer, Berlin Heidelberg New York, 250-269.

- Todal, A. & Edholm, O. 1998. Continental margin off western India and Deccan large igneous province. *Marine Geophysical Research*, **20**, 273-291.
- Tosquella, J., Serra-Kiel, J., Ferràndez-Cañadell, C. & Samsó, J.M. 1998. Las biozonas de nummulítidos del Paleoceno Superior -Eoceno Inferior de la Cuenca Pirenaica. *Acta Geologica Hispanica*, **31**, 23-36.
- Tripati, A.K & Elderfield, H. 2004. Abrupt hydrographic changes in the equatorial Pacific and subtropical Atlantic from foraminiferal Mg/Ca indicate greenhouse origin for the Thermal Maximum at the Paleocene-Eocene boundary. *Geochemistry Geophysics Geosystems*, **5**, Q02006.
- Tripati, A.K., Delaney, M.L., Zachos, J.C., Anderson, L.D., Kelly, D.C. & Elderfield, H. 2003. Tropical sea-surface temperature reconstruction for the early Palaeogene using Mg/Ca ratios of planktonic foraminifera. *Paleoceanography*, **18**, 1101.
- Tucker, M.E. 1993. Carbonate diagenesis and sequence stratigraphy. *Sedimentary Reviews*, **1**, 51-72.
- Vaughan, T.W. 1929. *Actinosiphon semmesi* a new genus and species of orbitoidal Foraminifera, and *Pseudorbitoides trechmanni* H. Douvillé. *Journal of Paleontology*, **3**, 163-169.
- Vaughan, T.W. 1933. The Biogeographic Relations of the Orbitoid Foraminifera. *Proceeding of National Academy of Sciences*, **19**, 922-938.
- Vecchio, E. & Hottinger, L. 2007. Agglutinated conical foraminifera from the Lower-Middle Eocene of the Trentinara Formation (southern Italy). *Facies*, **53**, 509-533.
- Veizer, J. 1999. Comment on “ $\delta^{18}\text{O}$  of mudrocks: more evidence for an  $^{18}\text{O}$  buffered ocean,” by L. S. Land & F. L. Lynch Jr. *Geochimica et Cosmochimica Acta*, **63**, 2309-2310.
- Veizer, J., Buhl, D., Diener, A., Ebner, S., Podlaha, O.G., Bruckschen, P., Jasper, T., Korte, C., Schaaf, M., Ala, D. & Azmy, K. 1997. Strontium isotope stratigraphy: Potential resolution and event correlation. *Palaeogeography, Palaeoclimatology, Palaeoecology*, **132**, 65-77.
- Vredenburg, E.W. 1906. *Nummulites douvillei*, an undescribed species from Kachh with remarks on the zonal distribution of Indian *Nummulites*. *Records of the Geological Survey of India*, **34**, 79-95.
- Waagen, W. & Wynne, A.B. 1872. The geology of Mount Sirban in the upper Punjab. *Memoir of the Geological Survey of India*, **9**, 331-350.
- Waelbroeck, C., Mulitza, S., Spero, H., Dokken, T., Kiefer, T. & Cortijo, E. 2005. A global compilation of late Holocene planktonic foraminiferal  $\delta^{18}\text{O}$ : relationship between surface water temperature and  $\delta^{18}\text{O}$ . *Quaternary Science Reviews*, **24**, 853-868.
- Wakefield, M.I. & Monteil, E. 2002. Biosequence stratigraphical and palaeoenvironmental findings from the Cretaceous through Cenozoic succession, Central Indus Basin, Pakistan. *Journal of Micropalaeontology*, **21**, 115-130.
- Wandrey, C.J., Law, B.E. & Shah, H.A. 2004. Sembar Goru/Ghazij Composite Total Petroleum System, Indus and Sulaiman-Kirthar Geologic Ranges, Pakistan and India. *United States Geological Survey Bulletin*, **1**, 1-20.
- Warraich, M.Y. & Nishi, H. 2003. Eocene planktonic foraminiferal biostratigraphy of the Sulaiman Range, Indus Basin, Pakistan. *Journal of Foraminiferal Research*, **33**, 219-236.
- Warraich, M.Y., Ogasawara, K. & Nishi, H. 2000. Late Paleocene to Early Eocene planktonic foraminiferal biostratigraphy of the Dungan Formation, Sulaiman Range, Central Pakistan. *Paleontological Research*, **4**, 275-301.

- Warwick, P.D. & Shakoor, T. 1993. *Lithofacies and depositional environments of the coal-bearing Paleocene Patala Formation, Salt Range coal field, northern Pakistan*. Geological Survey of Pakistan, Project Report (IR) PK-109.5, 1-52.
- Warwick, P.D., Javed, S., Mashhadi, S.T.A., Shakoor, T., Khan, A.M. & Khan, A.L. 1993. Lithofacies and palynostratigraphy of some Cretaceous and Paleocene Rocks, Surghar and Salt Range Coal Fields, Northern Pakistan. *United States Geological Survey Bulletin*, **2096**, 1-33.
- Weiss, W. 1993. Age assignments of larger foraminiferal assemblages of Maastrichtian to Eocene age in northern Pakistan. *Zitteliana*, **20**, 223-252.
- Weissert, H. 1989. C-isotope stratigraphy, a monitor of paleoenvironmental change: a case study from the early Cretaceous. *Surveys in Geophysics*, **10**, 1-61.
- White, M.R. 1992. On species identification in the foraminiferal genus *Alveolina* (Late Paleocene-Middle Eocene). *Journal of Foraminiferal Research*, **22**, 52-70.
- White, M.R. 1997. A new species of *Somalina* (*Somalina hottingeri*) with partially vacuolated lateral walls from Middle Eocene of Oman. *Journal of Micropalaeontology*, **16**, 131-135.
- Wiesner, H. 1920. Zur systematik der Miliolideen. *Zoologisches Anzeiger*, **51**, 13-20.
- Williams, M.D. 1959. Stratigraphy of the Lower Indus Basin, West Pakistan. Section 1, paper 19. *Proceedings of the 5th World Petroleum Congress, New York*, 377-394.
- Wilson, J.L. 1975. *Carbonate Facies in Geological History*. Springer, Berlin-Heidelberg, New York.
- Wilson, M.E.J. & Evans, M.E.J. 2002. Sedimentology and diagenesis of Tertiary carbonates on the Mangkalihat Peninsula, Borneo: implications for subsurface reservoir quality. *Marine and Petroleum Geology*, **19**, 873-900.
- Wilson, M.E.J. & Vecsei, A. 2005. The apparent paradox of abundant foramol facies in low latitudes: Their environmental significance and effect on platform development. *Earth Science Reviews*, **69**, 133-168.
- Wissler, L., Funk, H. & Weissert, H. 2003. Response of Early Cretaceous carbonate platforms to changes in atmospheric carbon dioxide levels. *Palaeogeography, Palaeoclimatology, Palaeoecology*, **200**, 187-205.
- Wolanski, E., Colin, P., Naithani, J., Deleersnijder, E. & Golbuu, Y. 2004. Large amplitude, leaky, island-generated internal waves around Palau, Micronesia. *Estuarine, Coastal and Shelf Science*, **60**, 705-716.
- Wray, J.L. 1977. *Calcareous algae*. Elsevier Scientific Publishing, Amsterdam, Oxford, New York, 1-185.
- Wynne, A.B. 1873. Memoir on the geology of Kutch. *Memoir of the Geological Survey of India*, **9**, 1-294.
- Wynne, A.B. 1874. Observations on some features in the physical geology of the Outer Himalayan Region of the Upper Punjab, India. *Quarterly Journal of the Geological Society of London*, **30**, 61-80.
- Yaseen, A., Munir, M., Rehman, O.U. & Mirza, K. 2007. Microfacies analysis of the Middle Eocene Kohat Formation, Shekhan Nala, Kohat Basin, Pakistan. *Geological Bulletin Punjab University*, **42**, 15-24.
- Yates, K.K. & Robbins, L.L. 1999. Radioisotopic tracer studies of inorganic carbon and Ca in microbially derived CaCO<sub>3</sub>. *Geochim Cosmochim Acta*, **63**, 129-136.
- Yordanova, E.K. & Hohenegger, J. 2002. Taphonomy of larger foraminifera: relationships between living individuals and empty tests on flat reef slopes (Sesoko Island, Japan). *Facies*, **46**, 169-204.
- Zachos, J.C. 1994. Evolution of early Cenozoic marine temperatures. *Paleoceanography*, **9**, 353-387.

- Zachos, J.C., Bohaty, S.M., John, C.M., McCarren, H., Kelly, D.C. & Nielsen, T. 2007. The Paleocene-Eocene Carbon Isotope Excursion: Constraints from Individual Shell Planktonic Foraminifer Records. *Royal Society Philosophical Transactions*, **365**, 1829-1842.
- Zachos, J.C., Pagani, M., Sloan, L., Thomas, E. & Billups, K. 2001. Trends, rhythms, and aberrations in global climate 65 Ma to present. *Science*, **292**, 686-693.
- Zachos, J.C., Röhl, U., Schellenberg, S.A., Sluijs, A., Hodell, D.A., Kelly, D.C., Thomas, E., Nicolo, M., Raffi, I., Lourens, L.J., McCarren, H. & Kroon, D. 2005. Rapid acidification of the ocean during the Paleocene–Eocene Thermal Maximum. *Science*, **308**, 1611-1615.
- Zachos, J.C., Wara, M.W., Bohaty, S., Delaney, M.L., Petrizzo, M.R., Brill, A., Bralower, T.J. & Premoli-Silva, I. 2003. A transient rise in tropical sea surface temperature during the Paleocene-Eocene Thermal Maximum. *Science*, **302**, 1551-1554.
- Zamagni, J. 2009. *Responses of a shallow-water ecosystem to the early Palaeogene greenhouse environmental conditions*. PhD thesis, University of Potsdam, Germany, 1-109.
- Zamagni, J., Košir, A., & Mutti, M. 2009. The first microbialite - coral mounds in the Cenozoic (Uppermost Paleocene) from the Northern Tethys (Slovenia): Environmentally-triggered phase shifts preceding the PETM? *Palaeogeography, Palaeoclimatology, Palaeoecology*, **274**, 1-17.
- Zamagni, J., Mutti, M. & Košir, A. 2008. Evolution of shallow benthic communities during the Late Paleocene-earliest Eocene transition in the Northern Tethys (SW Slovenia). *Facies*, **54**, 25-43.
- Zingonea, A. & Enevoldsen, H.O. 2000. The diversity of harmful algal blooms: a challenge for science and management. *Ocean and Coastal Management*, **43**, 725-748.